



University  
of Glasgow

Cunningham, Madeleine Elizabeth (2015) *The motor nerve terminal is a novel regulator of anti-ganglioside antibodies in mouse models of autoimmune neuropathy*. PhD thesis.

<http://theses.gla.ac.uk/6368/>

Copyright and moral rights for this thesis are retained by the author

A copy can be downloaded for personal non-commercial research or study, without prior permission or charge

This thesis cannot be reproduced or quoted extensively from without first obtaining permission in writing from the Author

The content must not be changed in any way or sold commercially in any format or medium without the formal permission of the Author

When referring to this work, full bibliographic details including the author, title, awarding institution and date of the thesis must be given

# The motor nerve terminal is a novel regulator of anti-ganglioside antibodies in mouse models of autoimmune neuropathy

Madeleine Elizabeth Cunningham BSc (Hons), MRes.

A thesis submitted in fulfilment of the requirements of the  
University of Glasgow for the degree of Doctor of  
Philosophy

Institute of Infection, Immunity and Inflammation

College of Medical, Veterinary and Life Sciences  
University of Glasgow

January 2015

## Abstract

Autoimmune neuropathies are a group of conditions resulting from inflammatory attack of the peripheral nervous system (PNS). Guillain-Barré syndrome (GBS), an acute autoimmune neuropathy, presents in both axonal and demyelinating forms. Axonal forms of GBS are caused by autoantibodies which target gangliosides on peripheral nerves. Here, they cause axonal damage via activation of the complement pathway. In *ex vivo* preparations, anti-ganglioside antibodies have been shown to cause complement-mediated injury to the node of Ranvier and the motor nerve terminal. Of these two vulnerable sites, the motor nerve terminal has recently been shown to be able to internalise anti-ganglioside antibody while the node of Ranvier does not. Rabbit models have demonstrated that immunisation with ganglioside results in a motor axonal neuropathy but no such model currently exists in mice. This is partially due to the fact that wildtype mice respond poorly when immunised with ganglioside and partially due to the requirement of an exogenous complement source to cause injury. This laboratory has recently developed GalNAcT<sup>-/-</sup>-*Tg(neuronal)* and GalNAcT<sup>-/-</sup>-*Tg(glial)* mice with complex ganglioside expression restricted to neurons and glia, respectively. This thesis aimed to develop a mouse model of GBS by actively immunising these mice with ganglioside liposomes. Subsequently, the aims were expanded to look at the clearance of the antibodies by membranes which express their ganglioside target. To complete these aims, wildtype, GalNAcT<sup>-/-</sup>, GalNAcT<sup>-/-</sup>-*Tg(neuronal)* and GalNAcT<sup>-/-</sup>-*Tg(glial)* mice were compared.

Following immunisation with liposomes containing GD1b, wildtype mice responded poorly as demonstrated by low presence of immunoglobulin in their sera. Conversely, GalNAcT<sup>-/-</sup> mice, which lack complex gangliosides, showed high presence of immunoglobulin in their sera. GalNAcT<sup>-/-</sup>-*Tg(neuronal)* and GalNAcT<sup>-/-</sup>-*Tg(glial)* mice showed intermediate levels. This was assumed to be due to varying levels of tolerance to “self” lipids among the mice. However, when normal human serum was introduced, GalNAcT<sup>-/-</sup>-*Tg(neuronal)* and GalNAcT<sup>-/-</sup>-*Tg(glial)* mice did not show any complement-mediated injury. Based upon evidence from ELISpots from the splenocytes of these mice, there did not appear to be any major differences in anti-GD1b antibody-producing cells among genotypes. The possibility that the antibodies produced by these mice were being removed by internalisation was investigated at the NMJ *ex vivo* and *in vivo*. *Ex vivo*, antibodies against complex gangliosides were demonstrated to be cleared in a receptor-dependent and activity-dependent manner. Following passive immunisation with pathogenic monoclonal antibody *in vivo*, serum levels of the antibody were cleared rapidly in wildtype mice but remain elevated at 7 days in GalNAcT<sup>-/-</sup> mice. GalNAcT<sup>-/-</sup>-*Tg(neuronal)* mice cleared antibody at an intermediate rate. Non-pathogenic antibodies were not cleared from the circulation over the 7 days from any of the three genotypes.

These results have demonstrated that levels of anti-ganglioside antibody can be regulated by receptor-dependent internalisation, especially at the motor nerve terminal. These studies have highlighted this structure as a novel regulator of anti-ganglioside antibody *in vivo*. The clearance of antibody is also dependent on the ability of the antibody to bind to living tissue; therefore antibodies detected in patient serum may not represent pathogenic, disease-causing antibodies. These factors may profoundly influence host vulnerability to antibody-mediated disease by affecting circulating levels of pathological antibodies.

## **Dedication**

I dedicate this thesis to my parents and grandparents

## Acknowledgements

I would like to start by thanking Professor Hugh Willison, who probably didn't realise that the Master's student who emailed him one day "choosing" his lab for her 6 month project would end up spending the next four years there. I am grateful for his advice when I was stumped, his patience when I was slow on the up-take and his encouragement when I was lacking in confidence. Most of all I thank him for going above and beyond to give me every opportunity to pursue experiments to complete my body of work.

Next, to the other members of the Willison lab both past and present: I'm so happy to have got to spend my PhD with you guys. I've had such a great time and feel so lucky that "going to work" for the last 4 years has also meant "getting to see my friends". Rhona, you have my eternal gratitude for putting up with my incessant stupid questions, being calm and understanding when I did something entirely moronic and most of all for reading this entire thesis and not tearing it to shreds! Jen, thank you also for patiently answering all the questions I have come at you with over the years and for all the help you've given me with dissections, ELISAs, antibodies...the list is endless! Sue, thank you for all your advice on experiments and presentations - especially about how to handle the nerves. I'd also like to thank Denggao for all his work on breeding our wonderful mice and the great amount of PCR which comes along with it, Ruth for her help with the ELISpot protocol, Eddie Rowan and his group for their help with the stimulation experiments and the staff of the CRF for all their help over the years, especially Dougie for keeping my mice going.

I'd especially like to thank Gavin, for being there for me both in and out of work. I'm so glad we got to do our PhD together! I don't know what I'd have done if I had to make trips to the basement, the vending machine or the shops by myself (boring). Thank goodness for the friend clause! I am really grateful for all the help you've given me, even if some was in exchange for ELISA plate washes or TS dissections.

To the rest of the GBRC: Mark Williams, Katie Chapple, the Barnetts, the Liningtons and the Goodyears - thanks to everyone who has been around for a laugh, a chat, a drink, a cinema trip...oh and for all the help with science too of course!

To Craig: Thank you for inspiring me to do a PhD in the first place and for putting up with multiple presentation practices, complaints about failed experiments and crises of confidence during the last few years - especially since you were going through the same thing and handling it with a bit more grace! I also want to thank you for encouraging me not to just come home and vegetate and actually do something productive with my free time!

To Pipkin, who will never read this because she is a rabbit, thanks for letting me pat you when I came home all stressed out!

Finally, I'd like to thank my family, especially my parents and grandparents to whom this thesis is dedicated. Thank you for encouraging me to do this and for all of your positivity, support and love over the years. You'll be glad to know I'm finally ready to not be a student anymore!

## Declaration of authorship

All experiments are the work of the author unless specifically stated otherwise.

A handwritten signature in black ink, appearing to read 'M. Cunningham', written in a cursive style.

Madeleine Elizabeth Cunningham BSc (Hons), MRes

University of Glasgow

January 2015

# Contents

Abstract .....	ii
Dedication .....	iii
Acknowledgements .....	iv
Declaration of authorship .....	v
Contents .....	vi
List of figures and tables .....	xv
Figures .....	xv
Tables .....	xix
Abbreviations .....	xx
1 Introduction .....	1
1.1 Guillain-Barré syndrome .....	1
1.1.1 Discovery .....	1
1.1.2 Clinical presentation and diagnosis .....	1
1.1.3 GBS Subtypes .....	3
1.1.3.1 Acute Inflammatory Demyelinating Polyneuropathy .....	4
1.1.3.2 Acute Motor Axonal Neuropathy (AMAN) .....	5
1.1.3.3 Miller Fisher Syndrome (MFS) .....	5
1.1.4 Chronic autoimmune neuropathies .....	6
1.1.5 Molecular mimicry .....	7
1.1.6 Anti-ganglioside antibodies .....	8

1.1.7	Pathophysiology of GBS .....	10
1.2	Complement.....	13
1.2.1	Classical complement pathway.....	13
1.2.2	Alternative and lectin complement pathways.....	14
1.2.3	Complement-mediated injury and its role in GBS .....	15
1.3	Gangliosides .....	17
1.3.1	Nomenclature, .....	18
1.3.2	Ganglioside synthesis .....	18
1.3.3	Ganglioside cycling .....	19
1.3.4	Ganglioside function: animal models .....	20
1.3.5	Complex ganglioside rescue mice .....	21
1.4	The peripheral nervous system .....	23
1.4.1	Axon .....	23
1.4.2	Nodes of Ranvier.....	24
1.4.3	The neuromuscular junction .....	25
1.4.3.1	Motor nerve terminal and synaptic cleft.....	25
1.4.3.2	Perisynaptic Schwann cells.....	27
1.4.3.3	Kranocytes.....	27
1.5	Plasma membrane .....	28
1.5.1	Lipid rafts.....	28
1.5.2	Caveolae .....	30
1.5.3	Ganglioside organisation in the plasma membrane.....	31

1.6	Endocytosis at the motor nerve terminal .....	34
1.6.1	Trafficking of vesicles.....	34
1.6.2	Bacterial toxins targeting gangliosides .....	36
1.6.3	Uptake of anti-ganglioside antibody .....	37
1.6.4	Retrograde trafficking of immunoglobulins.....	39
1.6.5	The neonatal Fc receptor .....	40
1.7	Animal models of Guillain-Barré syndrome .....	41
1.7.1	Experimental Allergic Neuritis.....	41
1.7.2	Rabbit model of AMAN .....	42
1.7.3	Mouse models of Guillain-Barré syndrome .....	42
1.8	Aims of thesis .....	44
2	Methods .....	46
2.1	Materials .....	46
2.1.1	Antibodies and tissue stains.....	46
2.1.2	Commonly used lipids.....	48
2.1.3	Commonly Used reagents.....	48
2.1.4	Preparation of commonly used buffers.....	48
2.1.4.1	Ringer's Solutions.....	48
2.1.4.2	Phosphate buffered saline (PBS) .....	49
2.2	Animals.....	49
2.2.1	Genotypes .....	49
2.2.2	Fluorescent mice .....	50

2.2.3	Genotyping .....	50
2.2.3.1	Polymerase chain reaction .....	50
2.2.3.2	Gel electrophoresis.....	52
2.2.4	Fluorescent Phenotyping .....	52
2.3	Production of monoclonal antibodies from hybridoma cell lines. ....	52
2.4	Purification of monoclonal antibody supernatant .....	54
2.5	Labelling of monoclonal antibody.....	54
2.6	<i>In vivo</i> procedures.....	55
2.6.1	Nerve crush.....	56
2.6.2	Gait analysis.....	56
2.6.3	Passive Immunisation of anti-ganglioside antibody for injury.....	58
2.6.3.1	Protocol .....	58
2.6.3.2	Rotarod testing.....	58
2.6.3.3	Whole body plethysmography.....	59
2.6.4	Active immunisation of mice with GD1b liposomes .....	59
2.6.4.1	Liposome preparation.....	59
2.6.4.2	Protocol .....	60
2.6.4.3	Latency to Platform .....	62
2.6.4.4	Grip strength .....	62
2.6.4.5	Blood samples .....	62
2.6.4.6	Splenocyte isolation.....	62
2.6.5	Serum clearance of monoclonal antibody.....	62

2.7	Dissections.....	63
2.7.1	Triangularis sterni preparation .....	63
2.7.2	Diaphragm dissection .....	63
2.7.3	Sciatic and tibial nerve dissection .....	64
2.7.4	Lumbrical dissection .....	64
2.7.5	Spinal cord dissection.....	64
2.8	Resin processing and staining for light microscopy .....	64
2.9	Lumbrical analysis.....	65
2.10	Antiganglioside antibody studies.....	65
2.10.1	Muscle sections .....	65
2.10.2	Whole mount, live triangularis sterni staining.....	66
2.10.3	Uptake of antibody at the NMJ.....	66
2.11	Anti-ganglioside antibody-mediated injury.....	67
2.12	Activity dependent uptake experiments.....	67
2.12.1	High potassium stimulation in TS .....	67
2.12.2	Stimulation of intercostal nerves .....	67
2.13	Staining of diaphragm sections from immunised mice .....	68
2.14	Spinal cord staining.....	68
2.15	Topical complement assay.....	68
2.16	Microscopy .....	69
2.16.1	Light microscopy .....	69
2.16.2	Fluorescent microscopy .....	69

2.16.3	Fluorescent intensity at the nerve terminal .....	70
2.16.4	Percentage coverage of Nfil at the nerve terminal.....	70
2.16.5	CFP counts .....	71
2.17	ELISpots.....	72
2.18	ELISAs .....	73
2.19	Glycoarray.....	74
2.20	Statistics and display of data.....	74
3	Rescue of complex ganglioside in neuronal and glial membranes.....	75
3.1	Introduction .....	75
3.2	Comparison of binding profiles of different antibodies in mice with restored neuronal complex ganglioside expression .....	76
3.2.1	MOG3 staining .....	76
3.2.2	DG2 staining .....	77
3.2.3	DG1 staining .....	78
3.2.4	MOG35 staining .....	79
3.2.5	Summary .....	80
3.3	Illustrative binding profiles of GalNAcT <sup>-/-</sup> - <i>Tg(neuronal)</i> and GalNAcT <sup>-/-</sup> - <i>Tg(glial)</i> mice.....	81
3.4	Comparison of gait parameters between wildtype, GalNAcT <sup>-/-</sup> and rescue mouse strains .....	84
3.5	Comparison of axon regeneration in wildtype, GalNAcT <sup>-/-</sup> and GalNAcT <sup>-/-</sup> - <i>Tg(neuronal)</i> mice .....	86
3.5.1	Lumbrical re-innervation .....	86
3.5.2	Sciatic and tibial nerve light morphometry.....	87

3.6	Discussion .....	88
4	Development of an active immunisation model of GBS .....	93
4.1	Introduction .....	93
4.2	Passive immunisation of mice with anti-GD1b antibody .....	93
4.2.1	Behaviour and plethysmography.....	94
4.2.2	Tissue analysis .....	97
4.3	Active immunisation of mice with GD1b-containing liposomes.....	99
4.3.1	Immune response .....	99
4.3.1.1	IgM response.....	100
4.3.1.2	IgG response.....	101
4.3.2	Behavioural testing and plethysmography .....	103
4.3.3	Tissue analysis .....	105
4.3.4	Topical complement assay .....	107
4.3.5	ELISpots .....	108
4.4	Discussion .....	111
5	Ability of the NMJ to clear anti-GD1b antibody.....	117
5.1	Introduction .....	117
5.2	<i>Ex vivo</i> uptake of anti-GD1b antibody.....	117
5.2.1	Fate of antibody at the nerve terminal .....	123
5.2.2	Autophagy inhibition in GalNAcT <sup>-/-</sup> -Tg(glial) mice .....	124
5.3	<i>In vivo</i> uptake of anti-GD1b antibody .....	125
5.3.1	Serum levels of anti-GD1b antibody .....	125

5.3.2	Tissue analysis .....	126
5.4	Discussion .....	131
6	Ability of the NMJ to clear anti-GM1 antibody .....	138
6.1	Introduction .....	138
6.2	Ex vivo uptake of anti-GM1 antibody .....	138
6.2.1	Autophagy inhibition in GalNAcT <sup>-/-</sup> -Tg(neuronal) mice .....	144
6.2.2	Fate of antibody following disappearance at the NMJ .....	145
6.3	In vivo uptake of anti-GM1 antibody.....	149
6.3.1	Serum levels of anti-GM1 antibody .....	149
6.3.2	Tissue analysis .....	152
6.4	Discussion .....	153
7	Uptake of anti-GD1b antibody is activity dependent .....	158
7.1	Introduction .....	158
7.2	Stimulation of nerve terminals with KCl .....	158
7.3	Electrical stimulation of intercostal nerves .....	163
7.4	Discussion .....	166
8	Discussion.....	170
8.1	Main findings .....	171
8.1.1	Receptor-dependent internalisation can affect circulating levels of anti-ganglioside antibody .....	173
8.1.2	Motor nerve terminal is a major site of activity dependent antibody clearance .....	175
8.1.3	Uptake may result in spinal cord trafficking .....	177

8.1.4	Antibodies in patient serum may not be pathogenic .....	178
8.2	Additional insight and future work.....	179
8.2.1	Parallel studies supporting the concept of antibody internalisation 179	
8.2.2	Future work .....	181
8.2.2.1	Active immunisation model of GBS .....	181
8.2.2.2	Investigation of antibody uptake at places other than the motor nerve terminal .....	182
8.2.2.3	Retrograde transport and trans-synaptic spread of antibody ..	183
8.2.2.4	Can exercise increase the clearance of antibody from the circulation? .....	183
8.3	Concluding remarks .....	184
	List of Publications .....	187
	Papers .....	187
	Abstracts .....	187
	References.....	188

## List of figures and tables

### Figures

Figure 1.1: The major pathogenic mechanisms in GBS. ....	4
Figure 1.2. Postulated mechanisms of GBS pathogenesis. ....	12
Figure 1.3: Classical and alternative complement activation pathways. ....	15
Figure 1.4: The biosynthesis pathway of gangliosides. ....	18
Figure 1.5: Schematic showing the trafficking of gangliosides to the membrane and their subsequent endocytosis along with anti-ganglioside antibodies. ....	20
Figure 1.6: Restoration of complex ganglioside expression in <i>GalNAcT<sup>-/-</sup>-Tg(neuronal)</i> and <i>GalNAcT<sup>-/-</sup>-Tg(glial)</i> mice. ....	22
Figure 1.7: Structure of a peripheral nerve. ....	24
Figure 1.8: Schematic showing the gross anatomy and organisation of the NMJ. ....	26
Figure 1.9: Organisation of lipid raft domains. ....	30
Figure 1.10: Ligand binding to gangliosides can be altered by presence of surrounding gangliosides. ....	33
Figure 1.11: Schematic of synaptic vesicle exo-and endocytosis at the motor nerve terminal. ....	35
Figure 1.12: The motor nerve terminal, but not the node of Ranvier has the ability to internalise antibody within 60 minutes at physiological temperatures. ....	38
Figure 1.13: Antisera against nerve terminal glycoproteins are retrogradely transported to the spinal cord. ....	40
Figure 1.14: Immunisation with ganglioside and OVA-containing liposomes induces anti-ganglioside antibodies more effectively in mice which lack endogenous antigen. ....	43

Figure 2.1: Protocols used for active immunisations. ....	61
Figure 2.2: Measurement of fluorescent intensity overlying the endplate. ....	70
Figure 2.3: Measurement of percentage NFil coverage. ....	71
Figure 2.4: Illustrative examples of CFP presence at the NMJ. ....	72
Figure 3.1: Anti-GD1b staining at the nerve terminal in various muscles in wildtype, GalNAcT <sup>-/-</sup> , NFLTg and Thy1Tg (line 112 and 115) mice (n=3 per group). ....	77
Figure 3.2: DG2 staining at the nerve terminal in various muscles in wildtype, GalNAcT <sup>-/-</sup> , NFLTg and Thy1Tg (line 112 and 115) mice (n=3 per group).....	78
Figure 3.3: DG1 staining at the nerve terminal in various muscles in wildtype, GalNAcT <sup>-/-</sup> , NFLTg and Thy1Tg (line 112 and 115) mice (n=3 per group).....	79
Figure 3.4: MOG35 staining at nerve terminals in various muscles in wildtype, GalNAcT <sup>-/-</sup> , NFLTg and Thy1Tg (line 112 and 115) mice (n=3 per group).....	80
Figure 3.5: Binding pattern in TS muscles of mouse monoclonal antibodies in four mouse strains. ....	83
Figure 3.6: Comparison of gait parameters between 4 mouse strains. ....	85
Figure 3.7: Comparison of axon regeneration in wildtype, GalNAcT <sup>-/-</sup> and GalNAcT <sup>-/-</sup> -Tg( <i>neuronal</i> ) mice (n=3 per group).....	87
Figure 3.8: Comparison of myelinated fibre presence among wildtype, GalNAcT <sup>-/-</sup> and GalNAcT <sup>-/-</sup> -Tg( <i>neuronal</i> ) mice 8 weeks following sciatic nerve crush. ....	88
Figure 4.1: <i>In vivo</i> analysis of injury in wildtype, GalNAcT <sup>-/-</sup> , GalNAcT <sup>-/-</sup> -Tg( <i>neuronal</i> ) and GalNAcT <sup>-/-</sup> -Tg( <i>glial</i> ) mice following MOG1 + NHS mediated injury. ....	96
Figure 4.2: <i>Ex vivo</i> analysis of diaphragm injury in wildtype, GalNAcT <sup>-/-</sup> , GalNAcT <sup>-/-</sup> -Tg( <i>neuronal</i> ) and GalNAcT <sup>-/-</sup> -Tg( <i>glial</i> ) mice following MOG1 + NHS mediated injury. ....	99
Figure 4.3: IgM reactivity in GD1b-immunised mice.....	101

Figure 4.4: IgG reactivity in GD1b-immunised mice.....	102
Figure 4.5: Rotarod and plethysmography data from immunised mice both before and after NHS injection.....	104
Figure 4.6: Analysis of diaphragm from actively immunised mice following NHS injection. ....	107
Figure 4.7: Serum from actively immunised mice does not result in MAC deposition in wildtype diaphragm. ....	108
Figure 4.8: Immune reactivity of various mouse strains to GD1b liposomes. ....	110
Figure 4.9: ELISpot analysis of spleen B cell reactivity to GD1b liposome. ....	111
Figure 5.1: Internalisation of anti-GD1b antibody occurs at the nerve terminal after 30 minutes at 37°C in wildtype mice. ....	119
Figure 5.2: Internalisation of anti-GD1b antibody occurs at the nerve terminal after 30 minutes at 37°C in GalNAcT <sup>-/-</sup> -Tg( <i>neuronal</i> ) mice.....	120
Figure 5.3: Internalisation of anti-GD1b antibody occurs at the nerve terminal after 30 minutes at 37°C in GalNAcT <sup>-/-</sup> -Tg( <i>glial</i> ) mice. ....	122
Figure 5.4: Internalisation of anti-GD1b antibody does not occur at nerve terminals lacking GD1b ganglioside. ....	123
Figure 5.5: Inhibition of vesicle acidification does not increase presence of MOG1 in GalNAcT <sup>-/-</sup> -Tg( <i>glial</i> ) mouse perisynaptic Schwann cells following incubation at physiological temperatures. ....	124
Figure 5.6: MOG1 serum presence by ELISA over 7 days. ....	126
Figure 5.7: Presence of IgG3 antibody in the cervical cord 7 days after injection. ....	127
Figure 5.8: Antibody found in the ventral horn of GalNAcT <sup>-/-</sup> -Tg( <i>neuronal</i> ) mice does not co-localise with MAP2 or synaptophysin. ....	128
Figure 5.9: Presence of IgG3 in cervical cord 1 day following injection of 1 mg of MOG1. ....	130

Figure 5.10: Antibody was only occasionally co-localised with Lamp-2 in ventral horn neurons. ....	131
Figure 6.1: Anti-GM1 antibody is cleared from the nerve terminal after 60 minutes at 37°C in wildtype mice. ....	140
Figure 6.2: Anti-GM1 antibody is cleared from the nerve terminal after 60 minutes at 37°C in GalNAcT <sup>-/-</sup> - <i>Tg(neuronal)</i> mice. ....	141
Figure 6.3: Anti-GM1 antibody does not bind at the NMJ in GalNAcT <sup>-/-</sup> - <i>Tg(glial)</i> mice, but binds the myelin sheath and terminal myelinating SC. ....	142
Figure 6.4: Internalisation of anti-GM1 antibody does not occur at nerve terminals lacking GM1 ganglioside. ....	143
Figure 6.5: Pilot study indicates inhibition of vesicle acidification increases DG2 presence following incubation at physiological temperatures. ....	144
Figure 6.6: Testing of labelled DG2 antibody on glycoarray and in whole mount TS tissue. ....	145
Figure 6.7: Binding of DG2-488 in wildtype TS muscle following 0, 30 and 60 minutes at physiological temperatures. ....	147
Figure 6.8: Binding of DG2-488 in GalNAcT <sup>-/-</sup> - <i>Tg(neuronal)</i> TS muscle following 0, 30 and 60 minutes at physiological temperatures. ....	148
Figure 6.9: Difference in tissue-binding ability of DG1 and DG2 affects their clearance from serum in wildtype mice. ....	150
Figure 6.10: DG1 and DG2 serum presence by ELISA over 7 days in wildtype, GalNAcT <sup>-/-</sup> and GalNAcT <sup>-/-</sup> - <i>Tg(neuronal)</i> mice. ....	152
Figure 6.11: Anti-ganglioside antibodies detectable in patient sera by ELISA do not necessarily represent the disease-causing antibodies. ....	156
Figure 7.1: Internalisation of anti-GD1b antibody is accelerated by K <sup>+</sup> induced nerve terminal stimulation. ....	160

Figure 7.2: Accelerated internalisation of anti-GD1b antibody by K <sup>+</sup> induced nerve terminal stimulation does not reduce MAC deposition at motor nerve terminals.....	163
Figure 7.3: Electrical stimulation of intercostal nerves increases the uptake of anti-GD1b antibody at wildtype TS motor nerve terminals. ....	164
Figure 7.4: Accelerated internalisation of anti-GD1b antibody by intercostal nerve stimulation results in reduced MAC deposition at motor nerve terminals and increased presence of healthy NMJs. ....	165
Figure 8.1: MOM8 serum presence by ELISA over 7 days.....	180
Figure 8.2: Schematic representation of the hypothesis of anti-ganglioside antibody internalisation. ....	186

## Tables

Table 1.1: Diagnostic criteria for typical Guillain-Barré syndrome as taken from Asbury and Cornblath, (1990).....	2
Table 1.2: Fulfilment of the criteria of GBS as caused by molecular mimicry. ...	8
Table 2.1: Primary antibodies used throughout this thesis. ....	47
Table 2.2: Mouse monoclonal anti-ganglioside antibodies used throughout this thesis, their predominant targets by ELISA and their immunoglobulin subtype..	53
Table 2.3: Examples of gait parameters generated by the Digigait™ which can be used to assess function after injury (Taken from Berryman et al., 2009) .....	58

## Abbreviations

<b>ACh</b>	acetylcholine
<b>ACP</b>	acute flaccid paralysis
<b>AIDP</b>	acute inflammatory demyelinating polyneuropathy
<b>AMAN</b>	acute motor axonal neuropathy
<b>ANOVA</b>	analysis of variance
<b>APC</b>	antigen presenting cell
<b>BBE</b>	Bickerstaff's brainstem encephalitis
<b>BNB</b>	blood-nerve barrier
<b>BSA</b>	bovine serum albumin
<b>BTx</b>	$\alpha$ -bungarotoxin
<b>CFP</b>	cyan fluorescent protein
<b>CIDP</b>	chronic inflammatory demyelinating neuropathy
<b>CSF</b>	cerebrospinal fluid
<b>Cy5</b>	cyanine-5
<b>DC</b>	dendritic cell
<b>ELISA</b>	enzyme-linked immunosorbent assay
<b>FcRn</b>	neonatal Fc receptor
<b>FCS</b>	foetal calf serum
<b>fH</b>	factor H
<b>FITC</b>	fluorescein isothiocyanate
<b>FOV</b>	field of view
<b>GalNAcT</b>	b1, 4-N- acetylgalactosamineyltransferase
<b>GBS</b>	Guillain-Barré syndrome
<b>GD3s</b>	Sial-T2
<b>GFP</b>	green fluorescent protein
<b>HRP</b>	horse radish peroxidase
<b>IgG</b>	immunoglobulin G
<b>IgM</b>	immunoglobulin M
<b>KO</b>	knock-out
<b>LOS</b>	lipooligosaccharides
<b>MAC</b>	membrane attack complex
<b>MFS</b>	Miller-Fisher syndrome
<b>MMN</b>	multifocal motor neuropathy

<b>MPLA</b>	monophosphoryl lipid A
<b>nAChR</b>	nicotinic acetylcholine receptor
<b>NFil</b>	neurofilament
<b>NFL</b>	neurofilament light
<b>NHS</b>	normal human serum
<b>NMJ</b>	neuromuscular junction
<b>OD</b>	optical density
<b>OVA</b>	ovalbumin
<b>PBS</b>	phosphate buffered saline
<b>PFA</b>	paraformaldehyde
<b>PLP</b>	proteolipid protein
<b>PNS</b>	peripheral nervous system
<b>pSC</b>	perisynaptic Schwann cell
<b>rpm</b>	revolution per minute
<b>ROI</b>	region of interest
<b>SC</b>	Schwann cell
<b>TRITC</b>	tetramethylrhodamine isothiocyanate
<b>TS</b>	triangularis sterni

# 1 Introduction

## 1.1 Guillain-Barré syndrome

Autoimmune neuropathies are a group of conditions resulting from inflammatory attack of the peripheral nervous system (PNS) which can present in both chronic and acute forms. Guillain-Barré syndrome (GBS) is an acute form of such a disorder, affecting around 1000 people per year in the United Kingdom (McGrogan et al., 2009). Although a rare condition, approximately 10% of GBS cases are fatal and 10-30% leave the patient with some form of disability (Bersano et al., 2006; Soysal et al., 2011; Vedeler et al., 1997). For this reason, GBS remains a problem both in the UK and worldwide, where it is now recognised as the leading cause of acute flaccid paralysis (AFP), accounting for over 50% of AFP cases following the eradication of poliomyelitis (Olive et al., 1997).

### 1.1.1 *Discovery*

The first mention of the condition now known as GBS was in 1859, when Jean Landry described an ascending symmetric muscular paralysis in a cohort of 10 patients (Landry, 1859). However, it was not until the early 20<sup>th</sup> century that the recently developed lumbar puncture technique allowed further characterisation of the disorder. This technique allowed three army physicians, Georges Guillain, Jean Barré and André Strohl, to describe two patients who had a paralysis similar to that of poliomyelitis, suffering from both ataxia and areflexia (Guillain et al., 1916). Analysis of the cerebrospinal fluid (CSF) revealed elevated albumin and an absence of pleocytosis which allowed a diagnostic distinction to be made between this acute condition and poliomyelitis. This significant finding led people to refer to the condition as Guillain-Barré syndrome.

### 1.1.2 *Clinical presentation and diagnosis*

During the period following its first description, GBS cases became more commonly recognised and there began a discussion over diagnostic criteria. Guillain-Barré syndrome is characterised by ascending symmetric muscular paralysis. The condition is rapid in onset, presenting with ataxia and areflexia.

This can progress to complete paralysis of the affected muscles, with around 25% of patients requiring artificial ventilation (Eldar and Chapman, 2014). Generally the illness will reach its nadir at around 4 weeks following its onset, with recovery time ranging from weeks to months. Around 10% of GBS patients cannot walk independently within 6 months of disease onset, with some individuals taking over a year to complete such a task unaided (Hiraga et al., 2005).

Diagnostic criteria were set down by the National Institute of Neurological and Communicative Disorders and Stroke (NINCDS), in response to the increased rate of GBS cases following the swine flu outbreak in 1976-1977 (Asbury, 1978). The vaccine provided for this outbreak is thought to have triggered autoimmune responses leading to the disease. The criteria were again updated in 1990, adding more detail (Asbury and Cornblath, 1990). Current diagnostic criteria are detailed below in Table 1.

**Table 1.1: Diagnostic criteria for typical Guillain-Barré syndrome as taken from Asbury and Cornblath, (1990)**

Diagnostic Criteria for typical Guillain-Barré Syndrome
<p><b>I. Features Required for Diagnosis</b></p> <p><b>A.</b> Progressive motor weakness of more than one limb. The degree ranges from minimal weakness of the legs, with or without mild ataxia, to total paralysis of the muscles of all four extremities and the trunk, bulbar and facial paralysis, and external ophthalmoplegia.</p> <p><b>B.</b> Areflexia (loss of tendon jerks). Universal areflexia is the rule, though distal areflexia with definite hyporeflexia of the biceps and knee jerks will suffice if other features are consistent.</p> <p><b>II. Features Strongly Supportive of the Diagnosis</b></p> <p><b>A.</b> Clinical features (ranked in order of importance)</p> <ol style="list-style-type: none"> <li>1. Progression. Symptoms and signs of motor weakness develop rapidly but cease to progress by four weeks into the illness. Approximately 50% will reach the nadir by two weeks, 80% by three weeks, and more than 90% by four weeks.</li> <li>2. Relative symmetry. Symmetry is seldom absolute, but usually, if one limb is affected, the opposite is as well.</li> <li>3. Mild sensory symptoms or signs.</li> <li>4. Cranial nerve involvement. Facial weakness occurs in approximately 50% and is frequently bilateral. Other cranial nerves may be involved, particularly those innervating the tongue and muscles of deglutition, and sometimes the extraocular motor nerves. On occasion (less than 5%), the neuropathy may begin in the nerves to the extraocular muscles or other cranial nerves.</li> <li>5. Recovery. It usually begins two to four weeks after progression stops. Recovery may be delayed for months. Most patients recover functionally.</li> <li>6. Autonomic dysfunction. Tachycardia and other arrhythmias, postural hypotension, hypertension, and vasomotor symptoms, when present, support the diagnosis. These findings may fluctuate. Care must be exercised to exclude other bases for these symptoms, such as pulmonary embolism.</li> <li>7. Absence of fever at the onset of neuritic symptoms.</li> </ol> <p><i>Variants (not ranked)</i></p> <ol style="list-style-type: none"> <li>1. Fever at onset of neuritic symptoms.</li> <li>2. Severe sensory loss with pain.</li> <li>3. Progression beyond four weeks. Occasionally, a patient's disease will continue to progress for many weeks longer than four or the patient will have a minor relapse.</li> <li>4. Cessation of progression without recovery or with major permanent residual deficit remaining.</li> <li>5. Sphincter function. Usually the sphincters are not affected, but transient bladder paralysis may</li> </ol>

occur during the evolution of symptoms.

6. Central nervous system involvement. Ordinarily, Guillain-Barre syndrome is thought of as a disease of the peripheral nervous system. Evidence of central nervous system involvement is controversial. In occasional patients, such findings as severe ataxia interpretable as cerebellar in origin, dysarthria, extensor plantar responses, and ill-defined sensory levels are demonstrable, and these need not exclude the diagnosis if other features are typical.

**B. Cerebrospinal fluid features strongly supportive of the diagnosis**

1. CSF protein. After the first week of symptoms, CSF protein is elevated or has been shown to rise on serial lumbar punctures.

2. CSF cells. Counts of 10 or fewer mononuclear leukocytes/mm<sup>3</sup> in CSF.

*Variants*

1. No CSF protein rise in the period of one to ten

2. Counts of 11 to 50 mononuclear leukocytes/mm<sup>3</sup>

**C. Electrodiagnostic features strongly supportive of the diagnosis**

Approximately 80% will have evidence of nerve conduction slowing or block at some point during the illness. Conduction velocity is usually less than 60% of normal, but the process is patchy and not all nerves are affected. Distal latencies may be increased to as much as three times normal. Use of F-wave responses often gives good indication of slowing over proximal portions of nerve trunks and roots. Up to 20% of patients will have normal conduction studies. Conduction studies may not become abnormal until several weeks into the illness.

**III. Features Casting Doubt on the Diagnosis**

1. Marked, persistent asymmetry of weakness.

2. Persistent bladder or bowel dysfunction.

3. Bladder or bowel dysfunction at onset.

4. More than 50 mononuclear leukocytes/mm<sup>3</sup> in CSF.

5. Presence of polymorphonuclear leukocytes in CSF.

6. Sharp sensory level.

**IV. Features That Rule Out the Diagnosis**

1. A current history of hexacarbon abuse (volatile solvents; n-hexane and methyl n-butyl ketone). This includes huffing of paint lacquer vapours or addictive glue sniffing.

2. Abnormal porphyrin metabolism indicating a diagnosis of acute intermittent porphyria. This would manifest as increased excretion of porphobilinogen and 6-aminolevulinic acid in the urine.

3. A history or finding of recent diphtheritic infection, either faucial or wound, with or without myocarditis.

4. Features clinically consistent with lead neuropathy (upper limb weakness with prominent wrist drop; may be asymmetrical) and evidence of lead intoxication.

5. The occurrence of a purely sensory syndrome.

6. A definite diagnosis of a condition such as poliomyelitis, botulism, hysterical paralysis, or toxic neuropathy (e.g., from nitrofurantoin, dapsone, or organophosphorus compounds), which occasionally may be confused with Guillain-Barre syndrome.

### 1.1.3 GBS Subtypes

Several subtypes of GBS have now been described, with differing clinical presentation and pathology, however all subtypes appear to conform to two major mechanisms of pathology: demyelination or axonal damage (Figure 1.1).

The incidence of these subtypes also appears to vary between different parts of the world.

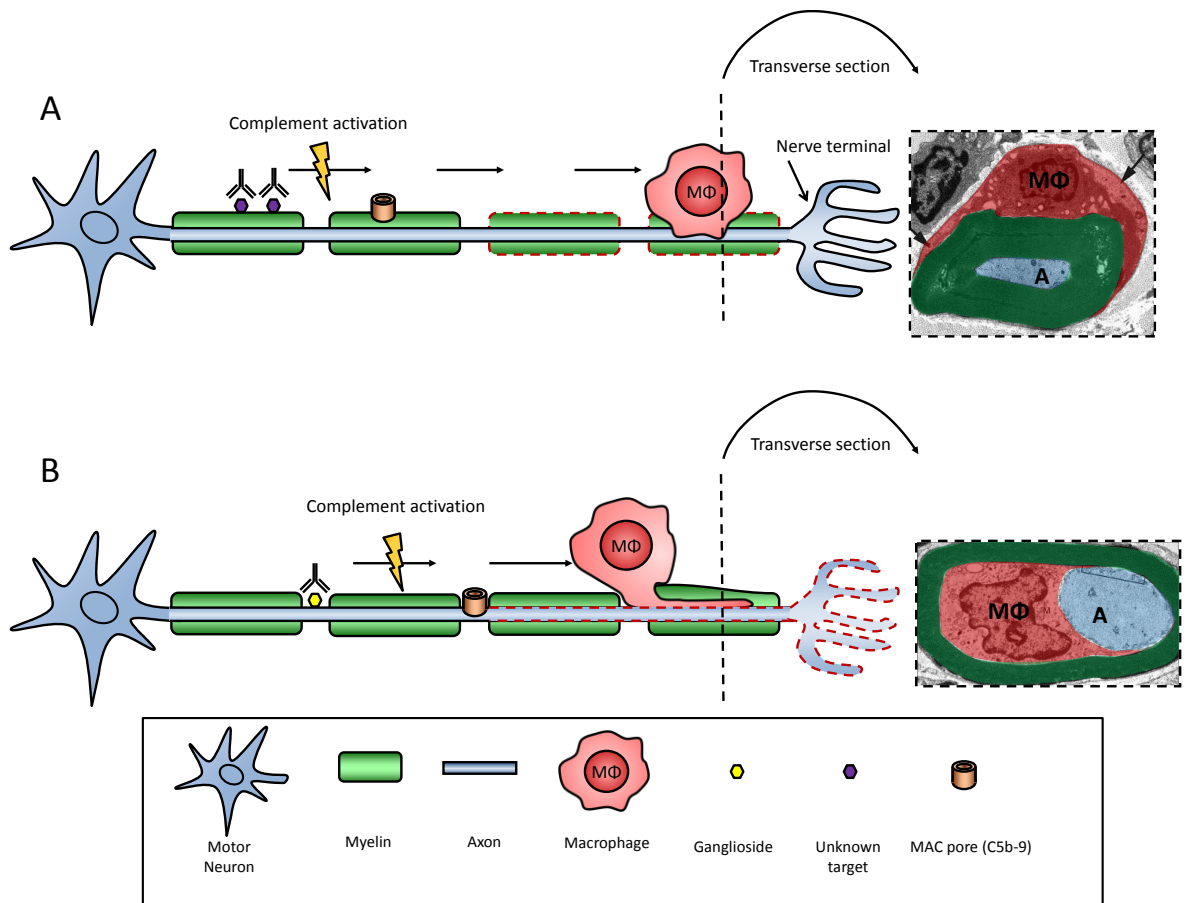


**Figure 1.1: The major pathogenic mechanisms in GBS. A:** Demyelination caused by antibody binding to an unknown antigen, causing complement activation and subsequent myelin injury. This can be followed by clearance of myelin debris by macrophages. **B:** Motor axonal damage caused by anti-ganglioside antibody binding to nodes of Ranvier, followed by complement activation and nodal injury via MAC pore formation. This may be followed by axonal degeneration and clearance of axon debris by macrophages. Electron microscopy images in A and B taken with permission from Hughes, (1990) and Griffin et al., (1996) respectively.

### 1.1.3.1 Acute Inflammatory Demyelinating Polyneuropathy

In Western countries such as Europe and North America, the predominant form of GBS is by far acute inflammatory demyelinating polyneuropathy (AIDP), representing around 70% of GBS cases (Hadden et al., 1998). This subtype is much less common (around 30% of cases) in Asian and Latin American countries (Ho et al., 1995; Islam et al., 2010; Nachamkin et al., 2007). Initially, AIDP represented the “classical” picture of GBS pathogenesis: the demyelination of the peripheral motor nerves, by two possible mechanisms. Firstly, macrophages may be targeted towards the Schwann cell (SC) membrane or myelin sheath, resulting in the denuding of the axon. Alternatively, antibodies may be directed against SC membrane or myelin sheath, resulting in complement-mediated

membrane lysis. Macrophage infiltration in this instance would be as a consequence of this preceding event (Hughes, 1990). Identifying precisely which SC or myelin targets these macrophages or antibodies are directed at in AIDP has proven difficult and currently remains unresolved.

#### **1.1.3.2 Acute Motor Axonal Neuropathy (AMAN)**

Initially all GBS cases were thought to be demyelinating (potentially with only secondary bystander axonal damage). Soon however, cases began to emerge which had electrophysiological signs of axonal damage (Albers et al., 1985). Following an investigation of a cohort of Chinese patients by McKhann et al, who initially named this condition Chinese paralytic syndrome, it became clear that this was indeed a subtype of GBS, and was termed acute motor axonal neuropathy (AMAN) (McKhann et al., 1991). This subtype of GBS is very common in Asia and Latin America (40-70% of GBS cases) (Ho et al., 1995;Islam et al., 2010;Nachamkin et al., 2007). Commonly referred to as axonal GBS, AMAN is a result of axonal damage mediated by antibodies which bind to the axolemma and are followed by complement activation, most likely at nodes of Ranvier (NoR) or at the nerve terminal, where the axon membrane is exposed (Hafer-Macko et al., 1996a). At the node, this can also be followed by macrophage infiltration into the nodal gap. These insert beneath the myelin sheath to target the axon, causing transection and subsequent Wallerian degeneration (Griffin et al., 1996). However, as many patients with AMAN recover rapidly, it is likely that these patients have only localised nerve terminal degeneration (Ho et al., 1997;Rupp et al., 2012) or reversible conduction block caused by antibody binding to the NoR, or localised Node of ranvier damage caused by antibody binding plus complement (Ho et al., 1997;McGonigal et al., 2010;Susuki et al., 2007b;Takigawa et al., 1995)

#### **1.1.3.3 Miller Fisher Syndrome (MFS)**

First described in 1956 by Charles Miller-Fisher, the syndrome which bears his name is recognised by the three cardinal symptoms of ophthalmoplegia, ataxia and areflexia, targeting mainly the muscles of the face (Fisher, 1956). This subtype of GBS has been shown to overlap with GBS as Miller-Fisher syndrome (MFS) patients can also show limb weakness and respiratory involvement.

Similarly, patients presenting with typical GBS can also have some ophthalmic involvement. Three such GBS patients were also described by Miller-Fisher, one of which died of respiratory failure, allowing him to show that the oculomotor symptoms were due to myelin destruction. An overlapping syndrome, Bickerstaff's brainstem encephalitis (BBE), also presents with the three cardinal symptoms of MFS, but with additional brainstem involvement, resulting in drowsiness and even, in extreme cases, coma (Shahrizaila and Yuki, 2013). These CNS symptoms are thought to be due to a transient inflammatory injury to the brainstem.

#### ***1.1.4 Chronic autoimmune neuropathies***

In 1958, James Austin described a group of recurring polyneuropathies which also present with elevated CSF protein count and progressive motor weakness progressing over a much longer time course than GBS and relapsing months to years after the initial recovery phase (Austin, 1958). The presence of conduction block and the improvement of disease in response to steroid treatment led to this chronic GBS-like disease being termed chronic inflammatory demyelinating neuropathy (CIDP). This condition may present as pure motor or motor-sensory and has a variety of subvariants (Eldar and Chapman, 2014).

Multifocal motor neuropathy (MMN), a purely motor form of autoimmune neuropathy, was described most recently, by Lewis et al, when he was presented with patients who had multifocal asymmetric weakness and conduction block in motor nerves only (Lewis et al., 1982). Initially thought to be a variation of CIDP, the term MMN was coined in 1988 by Pestronk et al who delineated the differences seen between two patients with this condition and other immune-mediated demyelinating neuropathies (Pestronk et al., 1988). These were namely the multifocal, asymmetric nature of the condition, the predominant involvement of the upper limbs, the pure motor involvement, the normal or only slightly elevated CSF protein count and the finding of antibodies against nerve glycosphingolipids called gangliosides. Again MMN is chronic and generally progresses slowly and is associated with a demyelinating pathology.

### **1.1.5 Molecular mimicry**

GBS is an acute post-infectious disease, normally manifesting 2-3 weeks following infection or other causative agent. Many triggering factors have been associated with GBS, including H1N1 vaccination (Salmon et al., 2013) and respiratory and gastrointestinal infections (Leneman, 1966; McGrogan et al., 2009). The most frequently noted infection preceding GBS is that of *Campylobacter jejuni* (*C. jejuni*) (McCarthy and Giesecke, 2001; Tam et al., 2007), a gram-negative bacterium found in the faeces of many animal species. Indeed when AMAN was first described, it was one of the first studies demonstrating a clear link between *C. jejuni* infection and GBS and giving an explanation to the somewhat seasonal pattern of AMAN in China, where it coincided with summer epidemics of *C. jejuni* infection (McKhann et al., 1991). This form of disease was found to be predominant in children, presumably due to the poor hygiene of children in these areas, and their increased likelihood of contracting antecedent *C. jejuni* infections (McKhann et al., 1991; McKhann et al., 1993; Nachamkin et al., 2007; Liu et al., 2003).

One particular serotype of *C. jejuni*, O:19, appeared to be more common in patients who developed GBS than in other gastrointestinal infection cases (Fujimoto et al., 1992; Kuroki et al., 1993). A great step in GBS research was made when it was discovered that the core oligosaccharides of O:19 which can cause GBS were similar in structure to the saccharide moiety of gangliosides GM1 and GD1a (Aspinall et al., 1994; Yuki et al., 1993b). Animal models of disease have provided further evidence of the link between molecular mimicry, especially that of *C. jejuni*, and GBS (see section 1.6). Thus, GBS fulfils all of the criteria which must be fulfilled for a disease to be autoimmune in origin, triggered by molecular mimicry (see table 1.2).

**Table 1.2: Fulfilment of the criteria of GBS as caused by molecular mimicry.** Criteria are set out in Ang et al based on Witebsky's postulates on criteria for autoimmune disease (Ang et al., 2004;Witebsky et al., 1957).

Criteria	Fulfilment	References
Association with infectious agent	Associated with <i>C. jejuni</i> and other infections	(Salmon et al., 2013;Leneman, 1966;McGrogan et al., 2009;McCarthy and Giesecke, 2001;Tam et al., 2007)
Presence of T cell or antibodies directed against self-antigen	Autoantibodies directed against gangliosides	(Ilyas et al., 1988b;Ilyas et al., 1988a)
Microbial target antigen mimic of <i>C. jejuni</i> gangliosides	LOS mimic	(Aspinall et al., 1994;Yuki et al., 1993b)
Disease reproduced in animal model	Rabbits immunised with GM1 or GM1-like LOS develop AMAN-like disease	(Yuki et al., 2004;Yuki et al., 2001)

### 1.1.6 Anti-ganglioside antibodies

The first association made between anti-ganglioside antibodies and GBS was made by Ilyas and colleagues in 1988, when serum from patients was shown to react with gangliosides from peripheral nerves (Ilyas et al., 1988b;Ilyas et al., 1988a). This association between these antibodies, which are generally of the IgG subclass, and GBS is now well established. In some cases different GBS subtypes have been linked to specific anti-ganglioside antibody profiles. In the case of MFS, the primary target has been defined for a number of years. The complex ganglioside GQ1b was first seen to be associated with MFS by Chiba et al in 1992, when they found that 100% of patients they tested had IgG reactivity to GQ1b, with many subsequent studies confirming this link (Chiba et al., 1992;Ichikawa et al., 2002;Ohtsuka et al., 1998;Yuki et al., 1998). In addition, it

has been shown that the nerves controlling eye movement have a high GQ1b composition compared to other nervous system tissue, providing rationale for the anti-GQ1b antibody's localised pathogenesis in this disease (Chiba et al., 1993;Chiba et al., 1997). Already sharing all the symptoms of MFS plus the addition of brainstem involvement, it was later discovered that BBE is also associated with high titres of GQ1b antibody, providing further evidence that the two disorders are linked (Yuki et al., 1993a). It is hypothesised that in the case of BBE, the circulating anti-GQ1b antibodies which bind to the oculomotor nerve node of Ranvier and nerve terminal, also permeate the BBB and bind to regions of the brainstem (Shahrizaila and Yuki, 2013).

Motor axonal and sensory forms of GBS have been linked to anti-GM1, GD1a and GD1b antibodies (Ho et al., 1995;Kuwabara et al., 1998;Ogawara et al., 2000;Ilyas et al., 1988c;Ho et al., 1999;Yuki et al., 1992b;Kaida et al., 2000). The relative specificity of cholera toxin for binding GM1 ganglioside allowed early studies to show enrichment of GM1 at node of Ranvier and at motor nerve terminals, but not on the internodal SC surfaces (Hansson et al., 1977;Ganser et al., 1983). It is therefore unsurprising that antibodies to GM1 are often present in motor axonal but not demyelinating forms of GBS (Kuwabara et al., 1998;Yuki et al., 1999). Similarly, GD1a has been found to be enriched in motor nerve fibres (Gong et al., 2002) and in sensory and motor nerves, both GM1 and GD1a have been shown to be enriched in the axonal compared to the myelin fraction. This again indicates why antibodies against these gangliosides are associated with axonal forms of GBS (Ogawa-Goto et al., 1990).

Ganglioside GD1b is most classically associated with sensory forms of GBS. Antibodies binding to GD1b stain human dorsal root ganglia and bind well to sensory fibres in animal models (Gong et al., 2002;Kusunoki et al., 1997). However, GD1b can also be found in cases of AMAN (Ilyas et al., 1988c;Ogawara et al., 2000;Vriesendorp et al., 1993) and immunohistology has also shown that anti-GD1b antibodies bind motor fibres and motor nerve terminal (Gong et al., 2002) suggesting they may also contribute to motor axonal damage.

As first described by Pestronk in 1988, anti-GM1 antibodies are also associated with MMN, though these antibodies are exclusively IgM in nature (Pestronk et al.,

1988). Though not present in all MMN patients, the presence of anti-GM1 IgM antibodies is supportive of an MMN diagnosis and can help distinguish it from amyotrophic lateral sclerosis, for which it can often be misdiagnosed. The primary antigen in AIDP remains elusive. As AIDP symptoms are related to myelin damage, it is likely that the primary target for this disease is SC or myelin-associated. Thus far, no single ganglioside has been identified as a target in AIDP, leading many to look for protein targets, a few of which have been identified as potential candidates (Ng et al., 2012; Sawai et al., 2014). However, it is also now recognised that antibodies formed against gangliosides in GBS may in fact target new epitopes formed by the *cis*-interaction of two or more glycolipids in the membrane (Rinaldi et al., 2013). Thus, antibodies are expected to form against complexes of gangliosides, rather than single gangliosides alone. This novel concept may be the key to understanding why no single ganglioside or glycolipid AIDP target has been found. Using combinatorial lipid array technology, Rinaldi et al 2013 screened serum from AIDP patients against glycolipid complexes and found an increase in positivity versus single epitopes alone, though no particular complex was identified as a novel AIDP target (Rinaldi et al., 2013).

### **1.1.7 Pathophysiology of GBS**

Due to the high association of anti-ganglioside antibodies with Guillain-Barré syndrome, it was surmised that these antibodies may be a causative factor in disease pathogenesis. Although the mechanism of GBS pathology is not fully understood, many studies have added pieces to the puzzle, resulting in a general understanding of some of the factors involved. Using *C. jejuni* as an example, in response to infection, endothelial cells in the gut may first recruit antigen presenting cells (APCs) by secretion of a variety of cytokines and chemokines. In a patient who is not susceptible to GBS, this results in an inflammatory Th1 response which eliminates the bacteria by recruitment of macrophages, nitric oxide toxicity and B cell IgA antibody response (Willison and Goodyear, 2013). Although it is unknown why some individuals lack the robust tolerance normally seen to glycolipids, these people instead go on to develop IgM, IgA, IgG1 and IgG3 antibodies against ganglioside-like lipooligosaccharides (LOS) found on the *C. jejuni* coat (Willison and Veitch, 1994). These antibodies then bind to

gangliosides on peripheral nerves, driving complement-mediated pathology (Figure 1.2). Macrophages may also be activated as part of a Th1 response to directly target peripheral nerve. This type of response is increased when the bacterial LOS is disialylated (Bax et al., 2011). Though APCs such as dendritic cells (DCs) and neutrophils may directly activate B cells, the class switching seen in GBS indicates that T cell help must be involved, despite the exposed portion of the LOS/ganglioside being carbohydrate in nature. As yet the mechanisms behind glycolipid presentation and antibody production are unclear and research is still attempting to elucidate the underlying mechanisms, though evidence has been conflicting. Some studies have shown APCs to be able to present glycolipids to natural killer T cells by MHC class 1-like protein CD1 (Galli et al., 2003; Liu et al., 2009), which can help induce B-cell proliferation and antibody production. Other literature has shown that CD4<sup>+</sup> T cells have the ability to process polysaccharides and present them on MHC class II (Christiansen et al., 2011; Cobb et al., 2004). A new class of neutrophils, termed B cell helper neutrophils (iN<sub>BH</sub>s), has been shown to prime marginal zone B cells and induce non-classical class switching (Puga et al., 2012).

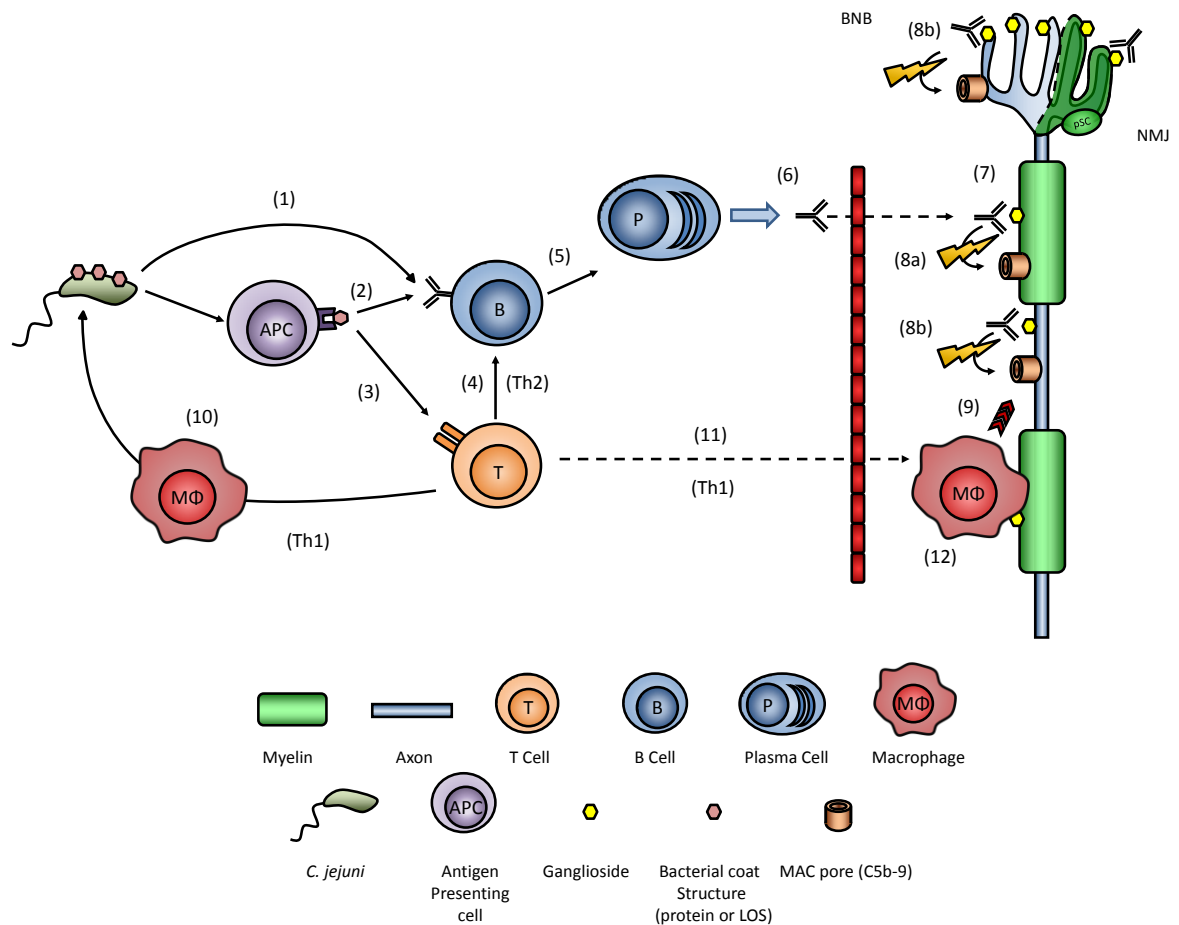


**Figure 1.2. Postulated mechanisms of GBS pathogenesis.** Bacteria such as *C.jejuni* present their LOS to B cells either directly (1), by cross-linking the B cell receptor, or via presentation by APCs such as B-cell helper neutrophils ( $iN_{BH}S$ ) (2). APCs may also present to T cells (3) which may then be able to present the antigen to B cells via the MHC class II pathway (4). The activated B cell differentiates into a plasma cell (5) which secretes antibodies which cross-react with gangliosides. These cross the BNB (6) and may bind ganglioside or related glycolipids on the peripheral nerve membranes (7). This may result in complement activation and MAC pore formation (see section 1.2) on glial (8a) or neuronal (8b) membranes, in particular, the nerve terminal and the node of Ranvier. Complement also attracts macrophages (9) which may be recruited to clear away debris from injured tissue. T cells, activated by antigen presentation by APCs, may also directly recruit macrophages via a Th1-type response, which results in pathogen clearance (10), but may also cross the BNB (11) to target myelin (12).

It remains uncertain why certain members of the population lack tolerance to glycolipids and develop auto-reactive anti-ganglioside antibodies in response to antecedent infection or vaccination. It has been postulated that Toll-like receptor (TLR) 4, a ligand for bacterial LOS found on APS such as macrophages and dendritic cells, may be a host factor which determines autoimmune reaction

to self-gangliosides, as it is known to be a potent enhancer of DC activation. However, a population study of 242 GBS patients and 210 healthy controls showed single nucleotide polymorphisms (SNPs) in the TLR4 gene do not increase susceptibility to GBS (Geleijns et al., 2004). Additionally human B cells do not express large amount of TLR4, making it less likely to be a major influencing factor in GBS development.

As an alternative to host mechanisms of susceptibility, the strain of *C. jejuni* infection may also play a role in the effectiveness of DC activation. Sialylated LOS, which are associated with GBS-causing *C. jejuni* strains, are more effective at promoting B cell responses than non-sialylated LOS. This enhancement has been shown to be due to an increase in cytokine TNF $\alpha$  and IFN $\beta$  released by dendritic cells in response to their activation by LOS (Huizinga et al., 2013).

## 1.2 Complement

One of the consequences of antibody binding is the triggering of a cascade of enzymatic reactions which cleave a specific collection of proteins, culminating in the insertion of a membranolytic pore into the cell membrane. This group of proteins, collectively called complement, is one of the primary means of humoral immunity. In the early 1890s, Hans Ernst August Buchner described an albuminoid substance in the blood which had bactericidal properties. He termed this substance alexin (Buchner, 1889). Further research by Jules Bordet showed that Buchner's alexin required a heat stable "sensitising" substance to produce its effects (Bordet, 1898). This heat stable "sensitising" substance is the antibody response, which binds to the invading microorganism. In later work on alexin, Paul Ehrlich coined the term "complement" due to its ability to complement the antibody response.

### 1.2.1 Classical complement pathway

Work in the 1920s began to show that the activity of complement is dependent on more than one serum fraction but it was not until the 1960s that all 11 serum proteins of the "classical", or antibody-dependent, complement activation pathway had finally been identified (Inoue and Nelson, Jr., 1965). These proteins

are named complement components and are termed C1-C9, with C1 being composed of 3 subunits, C1q, C1r and C1s. In this pathway, immune complexes containing complement-fixing IgG and IgM antibodies are recognised by the C1q portion of the C1 component which causes a conformational change, allowing C1r to cleave C1s. These two subunits then convert C2 to C2a and C2b and C4 to C4a and C4b. The C2b and C4a components combine to form C3 convertase, with the enzymatic capability to convert C3 into C3a and C3b. The resulting C3b joins the C2b/C4a complex to form C5 convertase. (Figure 1.2, red dashed box).

### ***1.2.2 Alternative and lectin complement pathways***

There are now 3 known pathways of complement activation, totalling around 20 serum proteins, plus an array of endogenous complement regulatory factors. The lectin binding pathway is activated by mannose-binding lectin directly binding to pathogen oligosaccharides, but progresses similarly to the classical pathway from C4 cleavage onwards (Ji et al., 1993). The alternative pathway is activated by the spontaneous conversion of C3 to C3a and C3b by hydrolysis. The released C3b forms a C3 convertase complex with factor Bb, which was cleaved from Factor B. This alternative C3 convertase complex (C3bBb) then cleaves C5 in the same manner as in the classical pathway. These two pathways can provide positive feedback to each other as the C3b released by the classical pathway can increase C3bBb, which in turn increases C5 cleavage and so on. The alternative pathway therefore serves to enhance the complement response generated by the classical complement pathway (Figure 1.2, blue dashed box).

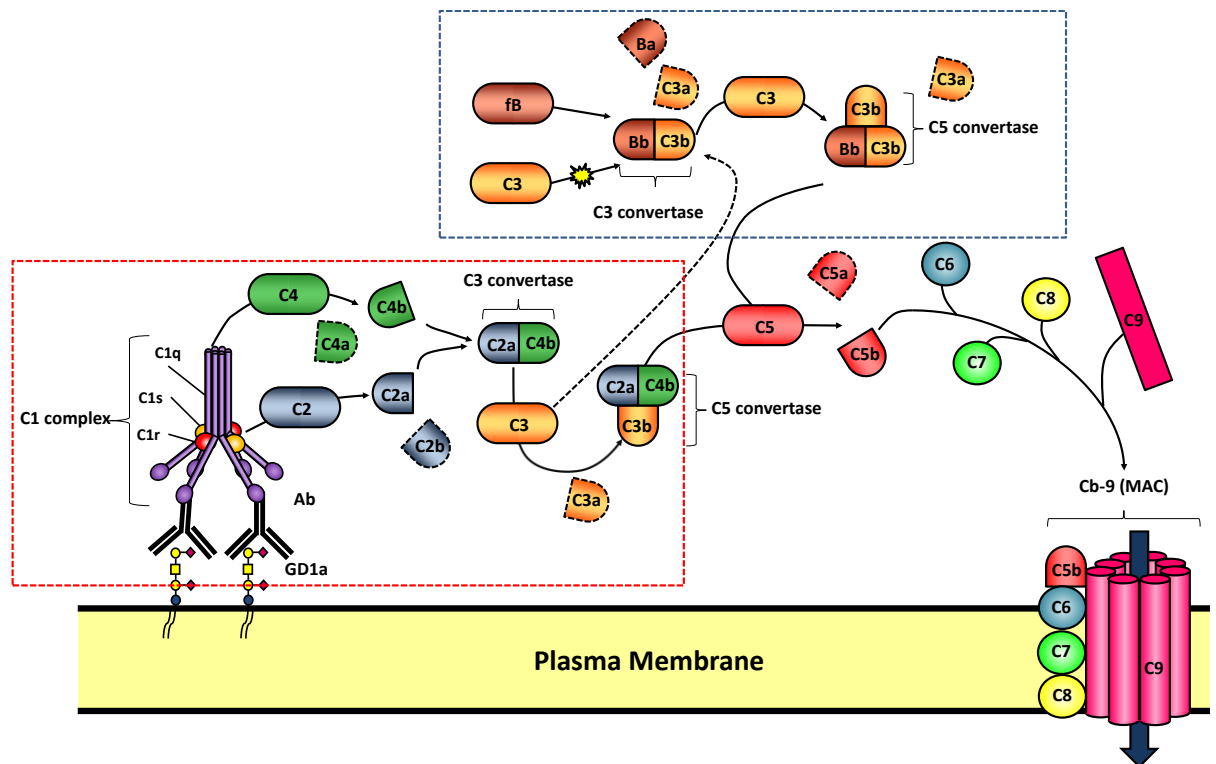


**Figure 1.3: Classical and alternative complement activation pathways.** The classical pathway (red dashed box) is activated by antibody-antigen interaction, in this case, ganglioside GD1a. The C1q protein recognises and binds the antibody-antigen complex, thus activating each of the C1r and C1s components. Subsequently, the activated C1 complex cleaves C2 and C4 into C2a and b and C4a and b. C2a and C4b combine to form a C3 convertase which converts C3 into C3a and C3b. The resulting C3b combines with C4b2a to form a C5 convertase. This cleaves C5, producing C5a and C5b. C5b, C6, C7, C8 and multiple C9 proteins then combine to form C5b-9 complex, which inserts into the membrane as a pore, allowing uncontrolled influx of extracellular fluid and ions. The alternative activation pathway (blue dashed box) occurs when C3 is naturally hydrolysed into C3a and b. An alternative C3 convertase is formed by C3b in combination with Bb, the result of factor B (fB) cleavage into Ba and Bb. The formation of this complex is enhanced by C3b formed by the classical pathway (dotted arrow). The C3bBb cleaves C3, producing more C3b, which combines to the complex to form a C5 convertase, C3bBb3b. This cleaves C5 in the same manner as the classical pathway. Cleaved components which are not involved in the complement cascade are outlined with dashed lines, though these have other inflammatory roles.

### 1.2.3 Complement-mediated injury and its role in GBS

The C5 convertases formed by all three complement pathways serve to cleave C5, forming C5a and C5b. The membrane-bound C5b joins with C6-8 and multiple C9 proteins to form the C5b-9 complex, also called membrane attack complex (MAC). All three complement pathways, if left unregulated, culminate in the insertion of MAC into the membrane. The multiple C9 proteins form a pore which inserts into the plasma membrane, allowing the uncontrolled influx of

extracellular fluid and ions into the cell, causing swelling and cell lysis. The first study showing that anti-ganglioside antibodies may require complement to cause neuronal damage was conducted in GM2-containing neuroblastoma cells, where anti-GM2 antibody positive patient serum required the presence of complement to cause injury (Yuki et al., 1992a). In GBS patients, complement components have been shown to be present in patient sera, deposited on nodal structures in early stages of AMAN and on SC and myelin structure in AIDP (Hafer-Macko et al., 1996a;Hafer-Macko et al., 1996b;Koski et al., 1987). In mouse models of GBS, many components of the classical complement cascade have been shown to overlap anti-ganglioside antibody deposition and to be necessary for damage to the nerve terminal, node of Ranvier and perisynaptic SCs (pSCs), as demonstrated by the reduction in injury in the presence of complement pathway inhibitors, or the denaturing of complement components by heat inactivation (Halstead et al., 2004;Halstead et al., 2005b;McGonigal et al., 2010;Fewou et al., 2012). The structural and mitochondrial damage which is seen in the neuronal structures has been shown to be due to the uncontrolled influx of calcium through the MAC pore, which results in release of neurotransmitter acetylcholine (ACh) from the synapse, injury to mitochondria, and the activation of the calcium-dependant protease calpain (McGonigal et al., 2010;O'Hanlon et al., 2003). Calpain activation results in the cleavage of many membrane bound receptors, cytoskeletal and nuclear proteins and cytosolic enzymes, resulting in a failure of the homeostatic control of cell processes, mitochondrial dysfunction, and failure of DNA transcription, among other neurotoxic consequences (Vosler et al., 2008).

In all mouse models of anti-ganglioside antibody and complement-mediated injury, it is necessary to add normal human serum (NHS) to see a pathogenic effect. This is because, though antibody deposition is clearly seen in *ex vivo* mouse muscle preparations and in *in vivo* passive antibody transfer models, no injury is seen with endogenous mouse complement alone (Fewou et al., 2012;Halstead et al., 2004;Rupp et al., 2012). This appears to be the case despite the observation that the anti-ganglioside antibodies used have the ability to fix mouse complement to the same degree as an anti-nicotinic ACh receptor (nAChR) antibody which is known to bind and induce complement-mediated injury at post synaptic membranes in mice (Willison et al., 2008). It was

considered that endogenous mouse complement regulators may be highly regulating complement activation at the presynaptic membrane. Despite the presence of CD59a, an endogenous inhibitor of mouse MAC assembly (Baalasubramanian et al., 2004), being detectable at nerve terminal and pSC membranes, CD59a deficient mice were still not able to demonstrate an anti-ganglioside antibody-mediated injury without exogenous NHS, though some C3c deposits are detected (Willison et al., 2008). Another complement regulator, factor H (fH), works by accelerating the breakdown of the C3 convertase C3Bb3b, and by complementing the breakdown of C3b, thus mediating the activation of the alternative complement pathway (reviewed in Ferreira et al., 2010). This complement regulator works in domains rich in sialic acid, therefore it is possible that at sites such as the ganglioside-rich presynaptic components of the NMJ, fH could prevent complement activation at “self” sites. Mouse fH has been demonstrated to be present at presynaptic membranes in mouse nerve-muscle preparations, but only in the additional presence of NHS to initially activate the complement cascade (Willison et al., 2008).

### **1.3 Gangliosides**

Ernst Klenk first discovered a new type of acidic glycolipid in 1935 and coined the term ganglioside 7 years later, due to its suspected localisation to ganglial cells in grey matter (Klenk, 1935). Since then it has become known that gangliosides are, in fact, ubiquitous, though are enriched in the nervous system. Gangliosides are amphiphilic, containing both a ceramide core, which inserts into the plasma membrane and an oligosaccharide domain, containing one or more sialic acid residues, which exists on the outer leaflet of the plasma membrane.

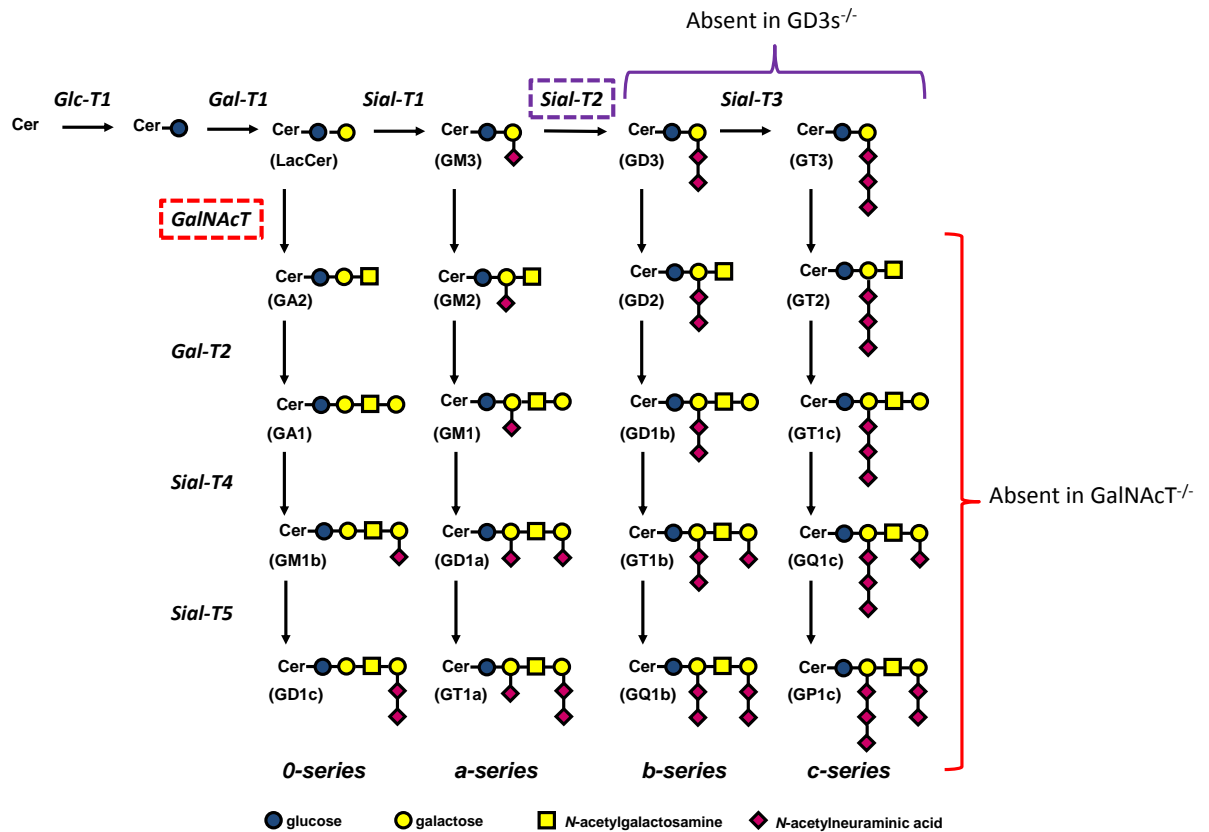


**Figure 1.4: The biosynthesis pathway of gangliosides.** From ceramide, each addition of oligosaccharide moiety requires a different glycosyltransferase enzyme (shown in italics). Complex gangliosides synthesis is initiated by the GalNAcT enzyme (red dashed box). Mice are available with disrupted GalNAcT. Due to the stepwise nature of ganglioside synthesis these mice therefore lack all complex gangliosides (see section 1.3.4). Similarly mice are available which lack Sial-T2 (purple dashed box), also called GD3 synthase (GD3s). These mice lack all b and c series gangliosides.

### 1.3.1 Nomenclature,

Ganglioside nomenclature was defined by Svennerholm to incorporate the number of sialic acid residues (indicated by the initial M, D, T and Q for mono, di, tri and tetra), the number of sugar groups (represented by 5 minus the chain length e.g. GM1 has 4 sugar groups) and the number of sialic acid residues on the inner galactose group (0=none, a=1, b=2 or c=3) (IUPAC-IUB Commission on Biochemical Nomenclature, 1977).

### 1.3.2 Ganglioside synthesis

Ceramide is formed in the endoplasmic reticulum and transported to the Golgi complex where it is converted to glucosylceramide (GlcCer) by UDP-Glc:

ceramide glucosyltransferase (Glc-T1). From GlcCer, lactosylceramide (LacCer) is formed by the addition of a galactose group by UDP-Gal: glucosylceramide galactosyltransferase (Gal-T1). Simple gangliosides are formed by the sequential addition of the sialic acid N-acetylneuraminic acid (NeuAc), to LacCer by sialyltransferase enzymes Sial-T1 (also called GM3 synthase or GM3s), Sial-T2 (GD3s) and Sial-T3. These simple gangliosides can be further converted to complex gangliosides of the a, b and c series, by the action of  $\beta$ 1,4-N-acetylgalactosamineyltransferase (GalNAcT), Gal-T2, Sial-T4 and Sial-T5, resulting in the addition of N-Acetylgalactosamine (GalNAc), galactose, and NeuAc respectively (Daniotti and Iglesias-Bartolome, 2011).

### ***1.3.3 Ganglioside cycling***

After their synthesis, gangliosides are transported inside vesicles from the Golgi complex to the plasma membrane, where they exist in cholesterol-enriched lipid rafts and caveolae. Once on the plasma membrane however, they can be endocytosed and sorted into early endosomes. This internalisation has been shown by the use of both fluorescent ganglioside analogues and antibodies to be clathrin-independent, instead being endocytosed via caveolae, a type of lipid raft in the form of an invagination in the plasma membrane (Crespo et al., 2008; Singh et al., 2003; Fewou et al., 2012). From both early and recycling endosomes, gangliosides may be recycled back to the plasma membrane, but they may also be transferred back into the Golgi complex, to undergo further glycosylation before returning to the plasma membrane (Chigorno et al., 1997; Riboni et al., 1993). Endocytosed gangliosides may also be sorted into lysosomes, where they are enzymatically broken down (reviewed in Daniotti and Iglesias-Bartolome, 2011; Simons and Ikonen, 1997) (Figure 1.5).

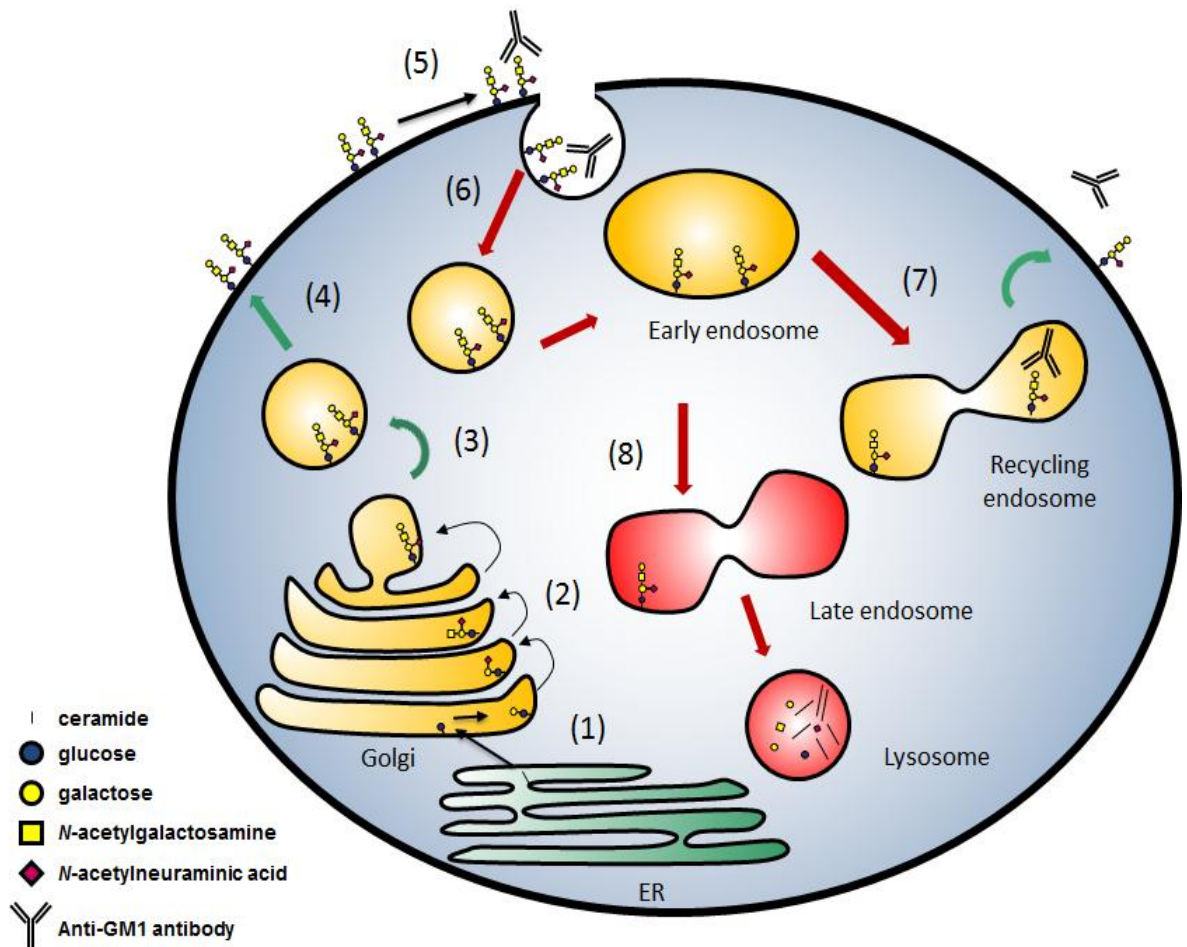


**Figure 1.5:** Schematic showing the trafficking of gangliosides to the membrane and their subsequent endocytosis along with anti-ganglioside antibodies. Ceramide is synthesised in the ER and transported to the Golgi complex (1). Here the stepwise addition of oligosaccharide groups forms the finished ganglioside (2). The gangliosides bud off into vesicles (3) and are transported to the plasma membrane (4). In the membrane they may be bound by anti-ganglioside antibodies (5). As part of normal ganglioside turnover, the gangliosides and any attached antibody may be endocytosed in a clathrin-independent manner (6) and sorted to early endosomes. From here, the fate of the ganglioside and the antibody is either sorting to recycling endosomes and subsequent return to the plasma membrane (7), or sorting to late endosomes and degradation in lysosomes (8).

### 1.3.4 Ganglioside function: animal models

The generation of mice with disrupted ganglioside synthesis enzymes has furthered the understanding of ganglioside function. Mice lacking GD3s, and therefore b and c series gangliosides, were generated by Okada et al. These mice develop normally, the only apparent deficits being impeded regeneration of hypoglossal nerve (Okada et al., 2002) and an enhanced sensitivity to insulin

(Yamashita et al., 2003). This near-normality suggests that b and c series gangliosides are either non-essential for normal nervous system development and maintenance, or that the consequential excess of a-series gangliosides which results from GD3s ablation can compensate.

Takamiya et al were the first to develop a mouse with a disrupted GalNAcT gene, which lack all complex gangliosides (Takamiya et al., 1996). Upon investigation of these GalNAcT<sup>-/-</sup> mice at 10 weeks old, the group found no morphological or behavioural abnormalities, with a decrease in neural conduction velocity being the only difference between them and their wildtype counterparts. Further studies have also demonstrated near-normal synaptic transmission (Kawai et al., 2001). It appeared therefore that complex gangliosides were not necessary for effective neuronal development and transmission. However, an age-dependent phenotype becomes clear in GalNAcT<sup>-/-</sup> mice. From about 12 weeks they develop spontaneous degenerative features in their sciatic nerves and dorsal horns and central dysmyelination (Sheikh et al., 1999; Sugiura et al., 2005; Susuki et al., 2007a) and a clinical phenotype, including a Parkinson-like tremor and abnormalities in hind-limb reflexes, balance, strength and gait (Chiavegatto et al., 2000). GalNAcT<sup>-/-</sup> mice also show delayed nerve regeneration following hypoglossal nerve transection compared with wildtype mice (Kittaka et al., 2008). However, these mice have no major abnormalities in neuromuscular transmission (Zitman et al., 2011a) and appear to regenerate motor nerve terminal and distal axons portions equally as well as wildtype counterparts (Rupp et al., 2013). Overall, these findings point to an important role for complex gangliosides in nervous system maintenance, however the widespread distribution of complex gangliosides, and the resulting over-expression of simple gangliosides, makes it difficult to pinpoint exactly where the expression of complex gangliosides is critical for nervous system integrity.

### ***1.3.5 Complex ganglioside rescue mice***

Recently, this lab has developed strains of transgenic mice which have restricted expression of the GalNAcT enzyme, and thus complex gangliosides, in neuronal or glial cells, two of which have been characterised in detail (Yao et al., 2014).

For neuronal-specific enzyme activity, the neurofilament light (NFL) promoter, active in mature neurons, was used while for glial-specific enzyme activity, the proteolipid protein (PLP) promoter, active in myelinating glia, was used. These mice were then backcrossed with  $\text{GalNAcT}^{-/-}$  mice, resulting in  $\text{GalNAcT}^{-/-}$ - $\text{Tg}(\text{neuronal})$  and  $\text{GalNAcT}^{-/-}$ - $\text{Tg}(\text{glial})$  mice, respectively. These mice only express the GalNAcT enzyme, and therefore complex gangliosides, on their neuronal and glial cells, respectively (Figure 1.6). In addition, a second neuronal transgenic mouse was created driven by the Thy1 promoter, which is also active in mature neurons.

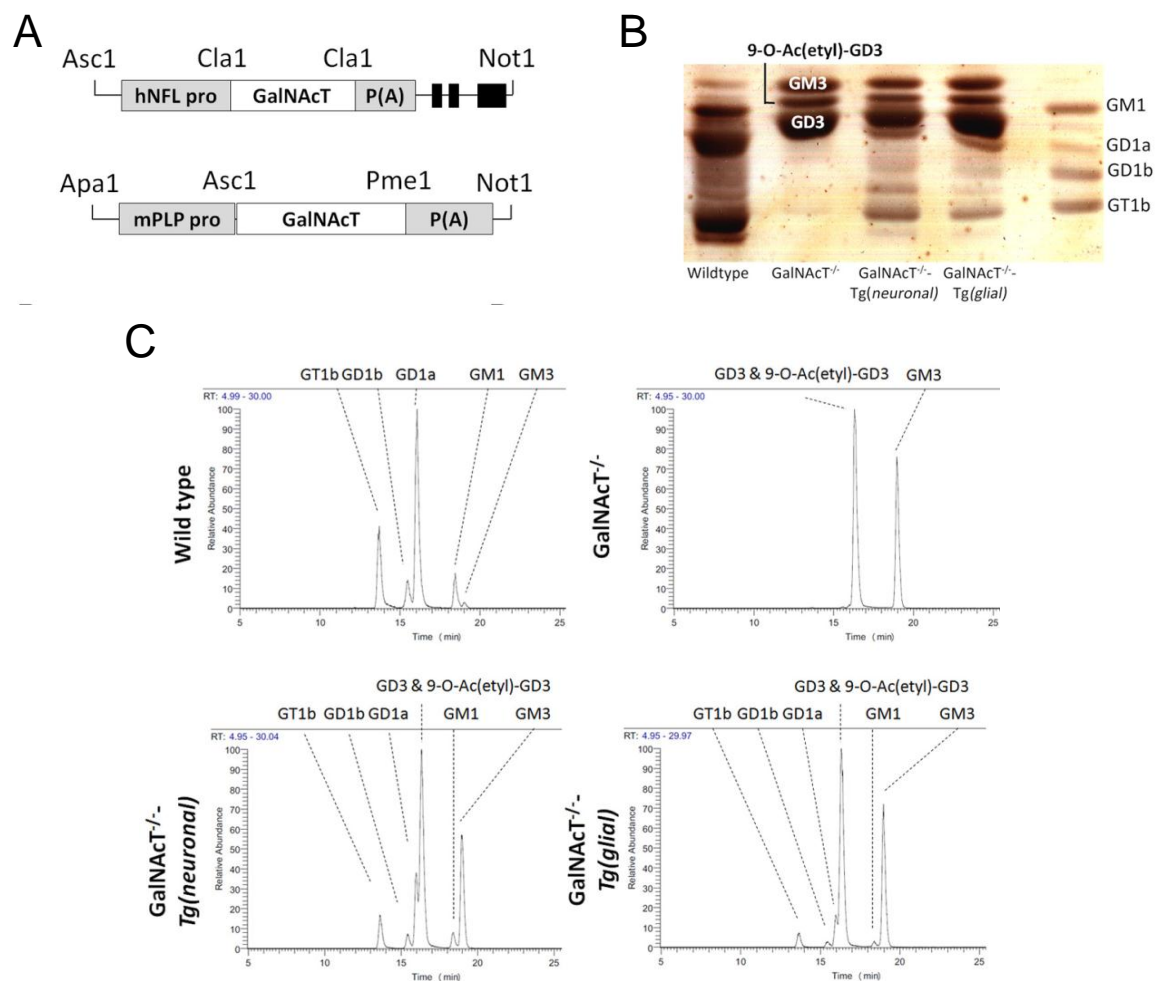


**Figure 1.6: Restoration of complex ganglioside expression in  $\text{GalNAcT}^{-/-}$ - $\text{Tg}(\text{neuronal})$  and  $\text{GalNAcT}^{-/-}$ - $\text{Tg}(\text{glial})$  mice.** **A.** GalNAcT enzyme driven by NFL and PLP promoter.  $\text{GalNAcT}^{-/-}$  mice lack complex gangliosides, whereas in  $\text{GalNAcT}^{-/-}$ - $\text{Tg}(\text{neuronal})$  and  $\text{GalNAcT}^{-/-}$ - $\text{Tg}(\text{glial})$  mice, their expression is restored as shown by **B**, TLC and **C**, mass spectrometry. Modified from Yao et al., (2014).

These mice were created for the purpose of ganglioside immunisations, however, they can also tell us about the importance of complex gangliosides in these different nervous system cell types. When GalNAcT is “rescued” in neuronal cells, the age-related phenotype seen in GalNAcT<sup>-/-</sup> mice is prevented. These mice are almost indistinct from wildtype mice by eye and perform equally well in behavioural tests even when over 12 months of age. In contrast, GalNAcT<sup>-/-</sup>-Tg(*glial*) mice show the characteristic tremors and impaired hind-limb clasping seen in GalNAcT<sup>-/-</sup> mice. GalNAcT<sup>-/-</sup>-Tg(*glial*) mice also perform much worse than wildtype and GalNAcT<sup>-/-</sup>-Tg(*neuronal*) mice in behavioural testing but are no different from GalNAcT<sup>-/-</sup> mice. The rescue in phenotype in GalNAcT<sup>-/-</sup>-Tg(*neuronal*) mice is also accompanied by a reduction in degenerate axon number and an increase in myelin volume, making them no different than wildtype mice. Nodal architecture in these mice was also similar to wildtype mice, with the exception of a lengthening of the paranode. The creation of these mice therefore demonstrated the importance of complex gangliosides in the neurons rather than glia.

## 1.4 The peripheral nervous system

In order to understand the effects of anti-ganglioside antibody and complement-mediated injury in the peripheral nervous system of GBS patients, it is important to understand the structure and function of the various components which have been shown to be affected in disease. These are namely the axon, the NoR, and the various components of the NMJ.

### 1.4.1 Axon

Lower motor neurons in the spinal cord are responsible for all voluntary muscle movement. From their location in the CNS, they extend axons outwith the protection of the blood-brain barrier (BBB). These axons are bundled within peripheral nerves, protected along with its myelinating SCs, by a layer of connective tissue called the endoneurium. This protective sheath also envelops the small capillaries, whose tight-junctioned epithelial cells form the blood-nerve barrier (BNB). The axons are also further bundled into fascicles, which contain variable numbers of fibres and larger blood vessels. Nerve fascicles are surrounded by the perineurium, a structure formed by multiple layers of

specialised perineurial cells and collagen. Perineurial cells form tight junctions with each other and work to maintain homeostatic control of the endoneurial environment (reviewed in Topp and Boyd, 2006). Nerves containing varying numbers and sizes of fascicles are surrounded by a layer of dense connective tissue called the epineurium, which serves to structurally protect the nerve as well as to adhere it to surrounding tissues (Figure 1.7).

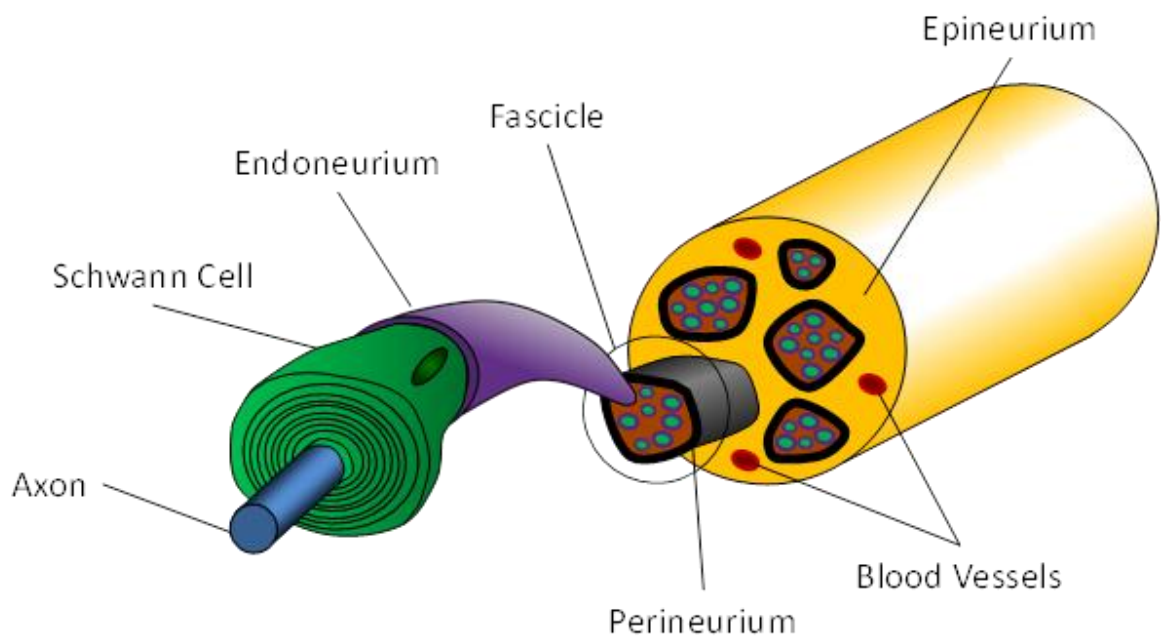


**Figure 1.7: Structure of a peripheral nerve.** The axon, surrounded by SC-derived myelin, is contained within protective endoneurium. Multiple axons are bundled together in fascicles, which in turn are surrounded by the perineurium. Fascicles are contained, along with blood vessels, within a layer of dense connective tissue called the epineurium.

Within the axon itself are neurofilament proteins, heteromeric cytoskeletal proteins composed of a combination of three subgroups named according to their relative sizes: light, medium and heavy.

#### **1.4.2 Nodes of Ranvier**

Along the axons lie nodes of Ranvier, specialised domains which facilitate the saltatory conduction of action potentials along the myelinated axon. These domains lie in the gaps between the myelinated portions of the axon (termed

the internodes) and are bordered on either side by the paranode and juxtaparanode, two distinct domains which are defined by specific proteins which contribute to the structural and functional integrity of the node. Peripheral NoRs are protected by the BNB, allowing it moderate protection from blood-borne substances, though not to the same degree as the BBB. Studies have shown that the node of Ranvier is susceptible to anti-ganglioside antibody and complement-mediated attack, especially at the very distal axons and at spinal roots (McGonigal et al., 2010).

### **1.4.3 The neuromuscular junction**

The neuromuscular junction (NMJ) is the tripartite interface between the axon and skeletal muscle. It comprises the terminal portion of the axon (the nerve terminal), the post synaptic muscle fibre and the non-myelinating pSC (Figure 1.8). Together these components are responsible for the efficient transmission of the electrochemical signalling resulting in muscle contraction. The NMJ is the most studied of all vertebrate synapses, from the first demonstration of chemical synaptic transmission (Dale et al., 1936), to the demonstration of synapse development (Greer et al., 1999), and to the entry of neuromuscular toxins studied for both their pathogenic and labelling properties (Ambache et al., 1948; Ambache, 1948; Stoeckel et al., 1977).

#### **1.4.3.1 Motor nerve terminal and synaptic cleft**

When the axon of a motor neuron reaches its destination at the muscle fibre, it forms a “pretzel” shape which lies outwith the protection of the BNB. This is the motor nerve terminal, the site of neurotransmitter release. Contained within this structure are pools of vesicles containing the neurotransmitter ACh, which fuse with the membrane and release their cargo in response to nerve activity (see section 1.6.1). Mitochondria are also present to fuel the energy-dependent process of packaging ACh into vesicles. The plasma membrane of the nerve terminal contains many transport proteins and receptors involved in the effective recycling and feedback of neurotransmitter, and the extracellular portion which opposes the post-synaptic domain is also rich in ganglioside, as evidenced by the binding of many anti-ganglioside antibodies (Fewou et al.,

2012;Goodfellow et al., 2005;Greenshields et al., 2009;Halstead et al., 2004;Halstead et al., 2005b;O'Hanlon et al., 1996).

Acetylcholine is released into the synaptic cleft, a space separating pre- and post-synaptic elements by around 50 nm (Fagerlund and Eriksson, 2009). The synaptic cleft contains ACh esterase (AChE), which breaks down ACh into its component parts following its activity on the post-synaptic membrane, thus terminating the neuromuscular transmission. This enzyme is tethered to an extracellular matrix called the basal lamina, which also has roles in maintaining synaptic organisation. Situated opposite the site of vesicle release, are the ionotropic nAChRs, which trigger muscle contraction by depolarising the post-synaptic membrane. This depolarisation is amplified by voltage-gated sodium channels which are present in invaginations between nAChR clusters (Figure 1.8).

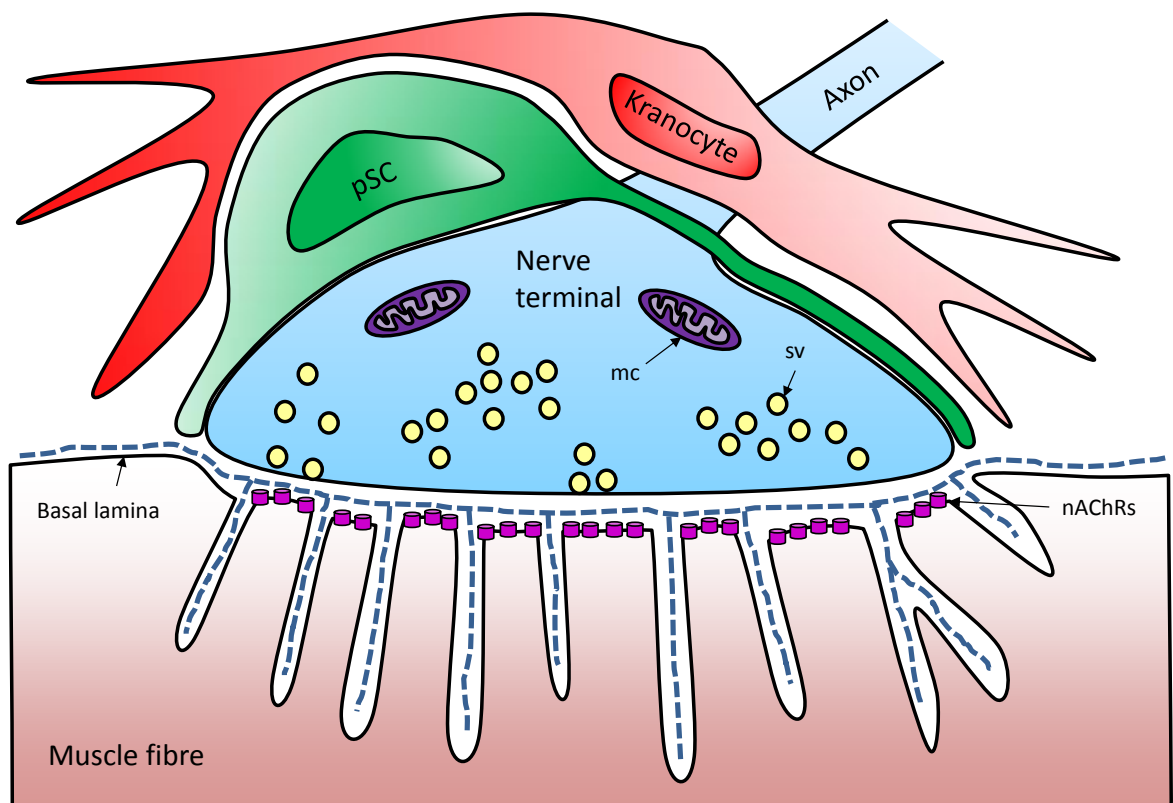


**Figure 1.8: Schematic showing the gross anatomy and organisation of the NMJ.** As the axon terminates it forms the nerve terminal which contains the machinery required for synaptic transmission, including mitochondria (mc) and pools of synaptic vesicles (sv), which fuse to the membrane, releasing ACh. Across from these release sites sit nAChRs, ligand-gated sodium channels, which trigger muscle fibre contraction. Within the synaptic cleft sits the basal lamina which holds the enzyme responsible for degrading ACh. Overlying the nerve terminal are pSCs, which maintain nerve terminal function and aid in regeneration in response to damage. Overlying both these structures is the kranocyte, a fibroblast-like cell which may also play important roles in NMJ maintenance.

### 1.4.3.2 Perisynaptic Schwann cells

Overlying the nerve terminal are the pSCs, non-myelinating SCs which extend processes which cap, rather than wrap, the nerve terminal. The function of these pSCs is manifold. Initial studies focussed on the role of these cells in reinnervation of damaged nerves. Upon nerve damage, pSCs enter an activated state and have not only been shown to remove nerve terminal debris (Miledi and Slater, 1970), but also to promote regeneration by extending processes which guide the regenerating axon back to its NMJ (Astrow et al., 1994a;Koirala et al., 2000;Reynolds and Woolf, 1992;Son et al., 1996;Son and Thompson, 1995a;Son and Thompson, 1995b;Astrow et al., 1994b). These cells also have a proposed modulatory role in synaptic transmission; pSCs can induce decreases in synaptic activity (Robitaille, 1998) in response to ACh release from the synapse, detected by muscarinic ACh and A1 adenosine receptors expressed on the pSC membrane (Jahromi et al., 1992;Robitaille et al., 1997;Rochon et al., 2001). At frog NMJs, ablation of pSCs does not immediately cause any perturbation of nerve terminal function, though after a week, nerve terminals begin to retract, suggesting a role in long-term NMJ maintenance of the nerve terminal. The various functions of pSCs are reviewed in detail by Auld and Robitaille (Auld and Robitaille, 2003).

Aside from their functions in synapse maintenance and repair, pSCs have also been shown to be targets of anti-ganglioside antibodies in a mouse model and are killed, often, but not always, in conjunction with damage to the nerve terminal (Halstead et al., 2004;Halstead et al., 2005b).

### 1.4.3.3 Kranocytes

Recently, a new cell type was described which closely caps the NMJ (Court et al., 2008). For this reason, they were termed kranocytes, meaning “helmet cell”. Kranocytes are positive for ganglioside GM1 and also show positive immunoreactivity to a variety of cell markers including ones for stem cells and fibroblasts. They also appear to activate in a similar manner to pSCs in response to denervation, by dividing and spreading from their empty endplate. This suggests a role for kranocytes in the maintenance and repair of the NMJ.

It is as yet unknown whether the kranocytes which the authors describe are, in fact, the same cells which had been previously noted at neuromuscular synapses, termed perisynaptic fibroblasts (Connor and McMahan, 1987; Gatchalian et al., 1989; Weis et al., 1991). These cells were also shown to proliferate in response to denervation, though appear to be less proximal to the NMJ than the kranocytes, with Weis et al describing the perisynaptic fibroblasts being 100-200  $\mu\text{m}$  from the NMJ, and Court et al showing the kranocytes to be within a proximity of 40  $\mu\text{m}$  (Court et al., 2008; Weis et al., 1991).

## **1.5 Plasma membrane**

The fluid mosaic model of the plasma membrane, first put forward by Singer and Nicholson (Singer and Nicolson, 1972) has become the classical model of the plasma membrane, where proteins and lipids float freely within a phospholipid bilayer. Although still generally relevant, many modifications have been made to the original theory. For example, Singer and Nicolson postulated that the membrane was uniform, with randomly distributed proteins, some of which form complexes in the membrane. In later modifications, it was proposed that more static domains may exist in the membrane, composed of ordered lipids (Nicolson, 1976).

### **1.5.1 Lipid rafts**

The domains of ordered lipids were formally described by Karnovsky et al who demonstrated the heterogeneity of the membrane and the importance of cholesterol to lipid packing (Karnovsky et al., 1982). These lipid microdomains are now referred to as lipid rafts. These rafts, so called because they are akin to a small platform of lipids and raft-associated proteins afloat on the fluidic lipid sea of the plasma membrane, are tightly packed, ordered domains of lipids which are rich in cholesterol and sphingolipids such as sphingomyelin and glycosphingolipids. Initially, rafts were defined as the detergent resistant part of the membrane, which were made detergent soluble if cholesterol was extracted. This definition caused controversies, leading to the refusal by many to accept the existence of lipid rafts and, due to the limitations in technology at the time, visualising rafts in the cell membrane was difficult. Using modern techniques such as single-molecule spectroscopy, novel microscopy techniques and

fluorescently tagged lipids, advances have been made in the visualisation of the structure and dynamics of lipid rafts in the membrane (reviewed in Simons and Gerl, 2010)).

Early work by Simons and van Meer demonstrated that following sorting in the Golgi complex, sphingolipids and cell surface proteins are sorted together in transport vesicles before movement to the apical surface of epithelial cells (Simons and van Meer, 1988). This led to the concept of lipid rafts as lipid and protein sorting and transport domains (Figure 1.9). The ability of lipid rafts to form stable domains in the membrane and to recruit specific proteins to these domains, has typified rafts as compartmentalised regions of cell signalling and lipid trafficking, which organise receptors and signalling molecules for efficient signal transduction (Simons and Ikonen, 1997).

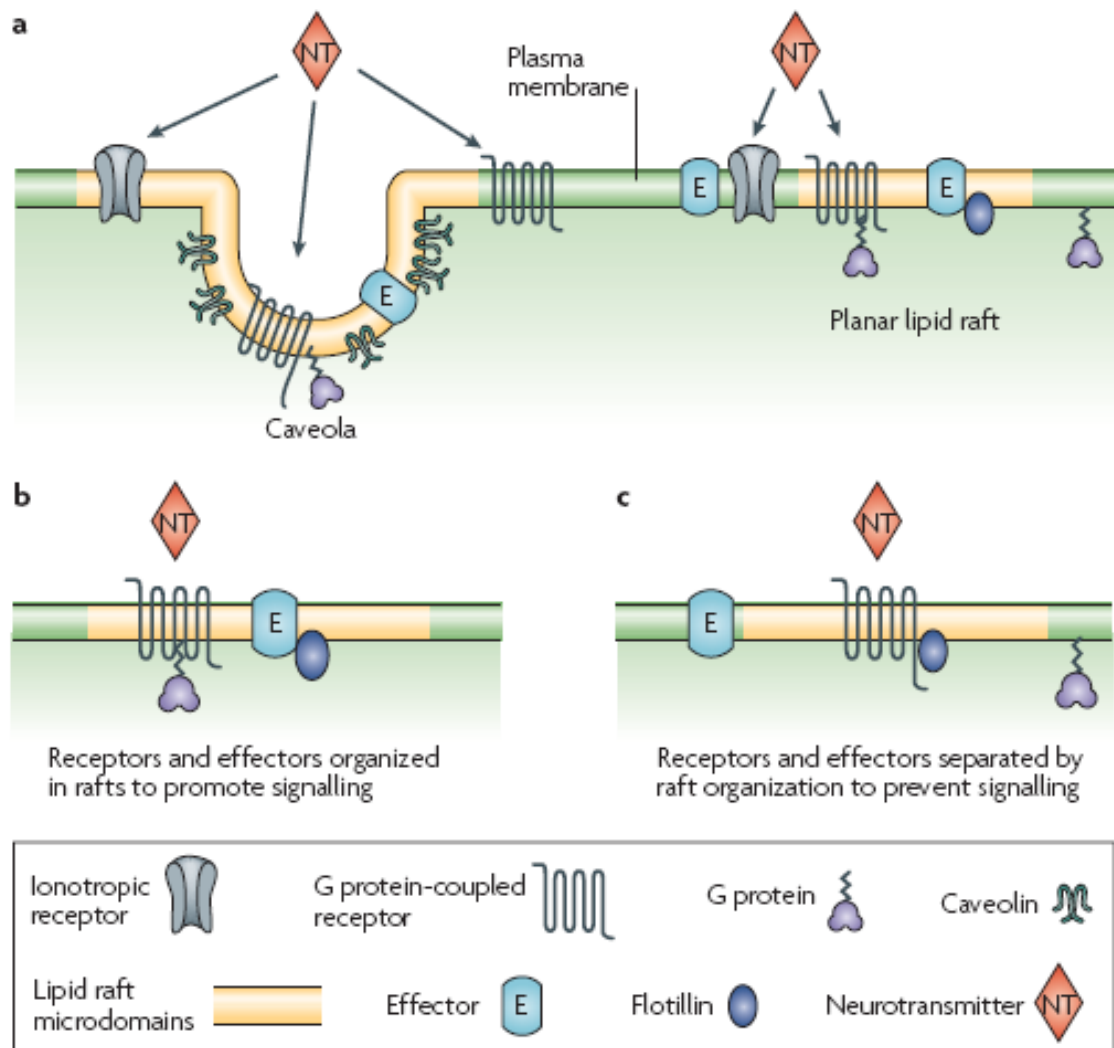


**Figure 1.9: Organisation of lipid raft domains.** Lipid rafts are cholesterol and sphingolipid rich domains in the plasma membrane **a**. Both caveolae and planar lipid rafts have roughly the same lipid composition, however, caveolae form flask-shaped invaginations in the membrane due to the association of caveolae-specific proteins caveolin and cavin, whereas planar lipid rafts are in line with the plasma membrane. **b**. Lipid rafts can cluster proteins to compartmentalise cell signalling cascades or **c**. prevent signalling responses by preventing interaction between signalling molecules. Taken with permission from Allen et al., (2007).

### 1.5.2 Caveolae

Caveolae, meaning “little caves”, are a subset of lipid rafts which form flask-like invaginations in the membrane. Caveolae are found in many mammalian cells, though are especially abundant in endothelial cells and adipocytes, and are absent in neurons (Bu et al., 2003; Trushina et al., 2006). As they are a type of lipid raft, these domains are also rich in sterol and sphingolipids, but are also associated with specialised proteins which are necessary for the formation of the

pit, namely caveolins and cavins (Lipardi et al., 1998; Park et al., 2002; Hill et al., 2008). Caveolins, of which there are three now known, were the first caveolae proteins to be discovered (Kurzchalia et al., 1992; Rothberg et al., 1992). Caveolin 1 is the predominant caveolin protein in most mammalian cells and appears in conjunction with caveolin 2 expression. In muscle cells, caveolin 3 appears to replace caveolin 1. Four cavin proteins have also now been discovered, which appear to form complexes specific to different tissue types (Bastiani et al., 2009), with cavin 4 having a similar tissue distribution to caveolin 3.

Caveolae have been suggested to have roles in cell signalling, lipid regulation and, more recently, have been implicated as protecting the membrane from over stretching, by flattening out in an accordion-like manner (Gustavsson et al., 1999; Siddiqui et al., 2011; Sinha et al., 2011). Caveolae also have a role in clathrin-independent endocytosis, where they have been shown to be involved in the internalisation of viruses, toxins and membrane surface lipids, including gangliosides (Montesano et al., 1982; Tran et al., 1987). Like clathrin-coated pits, caveolae are transiently associated with dynamin, which pinches off the caveolae from the membrane (Oh et al., 1998). It was initially thought that once internalised, caveolar vesicles merged with a distinct membrane organelle called a caveosome, which was described as a pH neutral endosome with no presence of clathrin proteins (Pelkmans et al., 2001). However in later years, these caveosomes were in fact shown to be late endosomes and lysosomes, indicating that the internalised caveolae can converge with clathrin-dependant endocytic pathways in early endosomes, (Hayer et al., 2010; Iglesias-Bartolome et al., 2009).

### ***1.5.3 Ganglioside organisation in the plasma membrane***

Though also found elsewhere, gangliosides usually concentrate in lipid rafts. As a consequence, gangliosides are often found tightly packed alongside other gangliosides and smaller lipid molecules such as cholesterol and sphingomyelin. Recent research has uncovered that this packing in the membrane can be crucial to the specificity of antibodies generated to gangliosides. Gangliosides had previously been shown to be “masked” by surrounding glycolipids and proteins,

which when stripped away improved antibody binding in tissue (Gregson et al., 1989; Kannagi et al., 1983). Crucially, Pestronk et al demonstrated that sera from MMN patients with no anti-GM1 IgM reactivity did show reactivity to a mixture of GM1, cholesterol and galactocerebroside, or GM1 cholesterol and sulphatide. In addition, they showed that in other GM1-lipid mixtures, even binding of sera with reactivity to GM1 alone was abolished, indicating that the lipid environment can affect antibody binding (Pestronk et al., 1997). Despite this observation, it was not until studies by Kaida and colleagues demonstrated that GBS patient sera may contain antibodies against not just a single ganglioside epitope, but against neopeptides formed by complexes of GD1a/GD1b that this idea truly garnered support (Kaida et al., 2004). Following their initial study, the group screened patient serum for antibodies to combinations of GM1, GD1a, GD1b and GT1b, finding 17% of GBS patients with antibodies against complexes and that certain anti-complex antibodies were associated with more severe clinical outcome (Kaida et al., 2007). Greenshields et al demonstrated that nearby gangliosides can alter the tissue binding ability of some populations of antibodies. Out of two mouse monoclonal antibodies which reacted to GM1 to a similar degree by enzyme-linked immunosorbent assay (ELISA), only one successfully bound mouse NMJs in live tissue preparations. Using a newly developed combinatorial glycoarray, where an array of lipid and lipid complexes is spotted onto PVDF membrane allowing easy antibody overlay, it was shown that the tissue-binding antibody (DG2) could bind GM1 equally well whether it was alone, or in complex with other gangliosides. In contrast, the non-tissue binding antibody (DG1) can bind GM1 alone, but its signal is attenuated when in complex with other gangliosides, in particular, GD1a. When tissue GD1a is removed with neuraminidase treatment to remove terminal sialic acid, DG1 is able to bind live tissue (Greenshields et al., 2009). This demonstrated that the pathogenicity of antibodies against GM1, but presumably also antibodies to other gangliosides, may be determined by the surrounding environment. With confirmation in further studies, using not only antibodies, but other ganglioside-binding ligands, the concept of three distinct types of ganglioside binding arose: those which bound to their target regardless of surrounding gangliosides; those which were inhibited by certain surrounding gangliosides and those whose binding to their target was enhanced by the presence of certain surrounding gangliosides (Rinaldi et al., 2010). These three populations of ligand binding are

termed complex-independent, complex-inhibited and complex-enhanced, respectively (Figure 1.8).

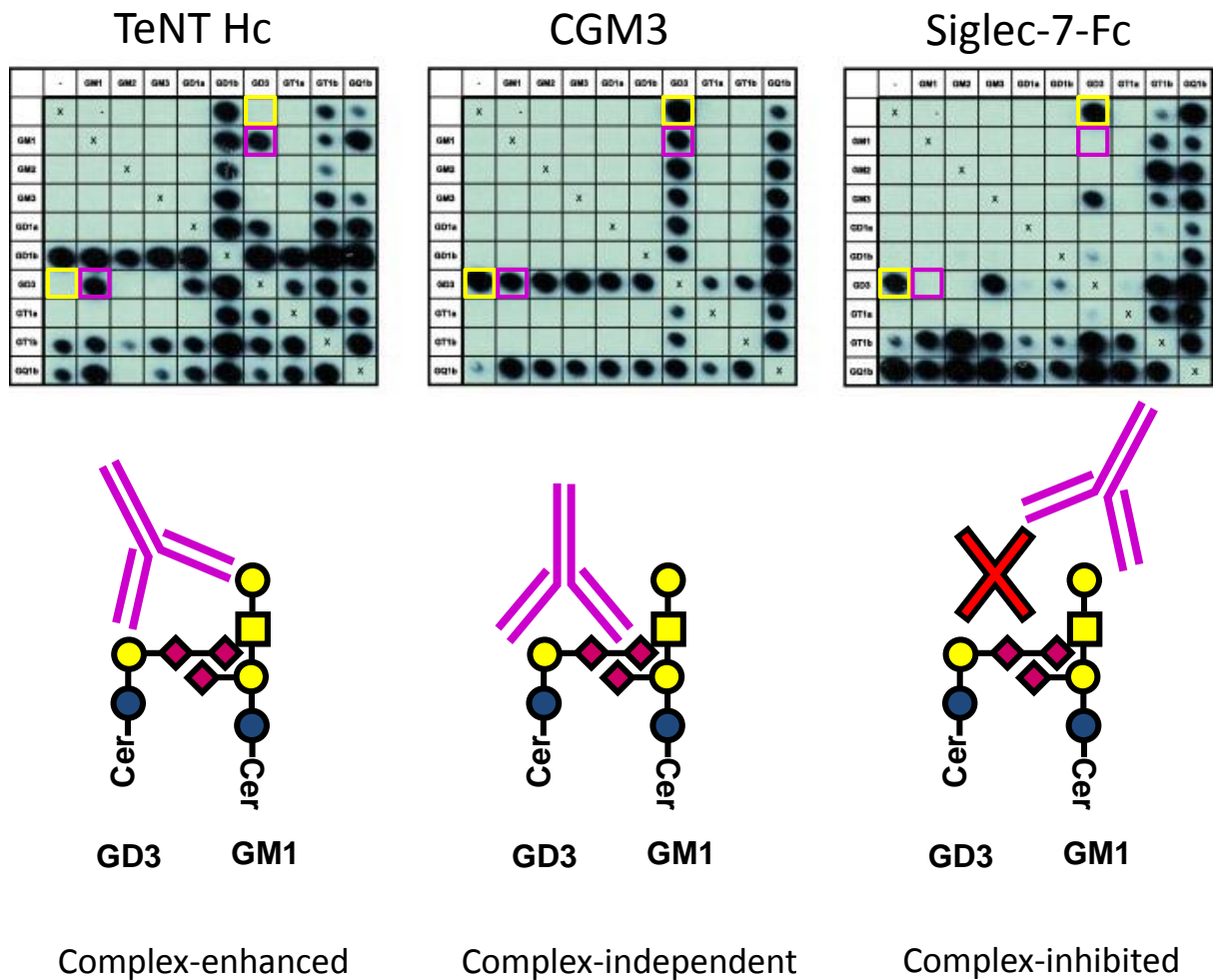


**Figure 1.10: Ligand binding to gangliosides can be altered by presence of surrounding gangliosides.** Glycoarray shows gangliosides, both alone or in complex, spotted onto PVDF membrane and probed with different GD3-binding ligands. Arrays are symmetrical along the blank methanol line marked by crosses. GD3 alone is marked in yellow boxes and GD3 in complex with GM1 is marked in pink boxes. Tetanus toxin neurofragment (TeNT Hc) does not bind to GD3 alone but does bind when GD3 is in complex with GM1 (complex-enhanced). CGM3, a mouse anti-GD3 antibody, binds to GD3 alone equally as well as when in complex with GM1 (complex-independent). Siglec-7-Fc, a sialic-acid binding lectin binds GD3 alone, but its binding is attenuated in the presence of GM1 (complex-inhibited). Diagrammatic representations of different types of *cis*-interactions are shown beneath each example. Modified with permission from Rinaldi et al., (2010).

Recent studies have shown that ganglioside binding can also be altered by *cis*-interactions by other surrounding lipids and glycolipids, confirming the data put forward by Pestronk in 1988, with particular interest in complexes of GM1 with galactocerebroside in MMN patient sera (Galban-Horcajo et al., 2012). The emergence of this data on antibodies against ganglioside-lipid complexes, and the effect that the plasma membrane microenvironment has on antibody

binding, has spurred new hope in identifying better biomarkers for disease and in finding the all-elusive AIDP antigen (Rinaldi et al., 2013).

## **1.6 Endocytosis at the motor nerve terminal**

### ***1.6.1 Trafficking of vesicles***

The motor nerve terminal is the site responsible for the release of neurotransmitter in response to the action potentials which are propagated along the axon from the motor neuron body. Within the motor nerve terminal lie pools of ACh-containing vesicles. Each vesicle contains around 10,000 ACh molecules, otherwise termed a quantum. When filled with neurotransmitter, the vesicles remain in a reserve pool until they are activated for release. In preparation for vesicle release, vesicles migrate to the “active zone” and form a releasable pool of vesicles. Around 20% of all motor nerve terminal vesicles are in the releasable pool at a given time, while 80% make up the reserve pool (Richards et al., 2003). At the active zone, vesicles dock to the presynaptic membrane by the interaction of the vesicle-associated synaptobrevin (also called vesicle associated membrane protein or VAMP) with the nerve terminal-associated SNAP-25 and syntaxin (Figure 1.11, inset). When an action potential reaches the synapse, the membrane becomes depolarised, causing the opening of voltage-gated calcium channels at the presynaptic membrane and the subsequent influx of extracellular calcium. Another vesicle-associated protein, synaptotagmin, is calcium-sensitive and allows the fusion of the synaptic vesicle to the nerve terminal membrane (Figure 1.10). Once the neurotransmitter has been released, the vesicle is endocytosed and recycled, however the mechanisms by which this recycling occurs are plastic and are dependent on the type of initial stimulus. It is generally accepted that vesicle recycling via clathrin-mediated endocytosis is one of the major methods of vesicle retrieval, especially during moderate stimulation (Granseth et al., 2007), where the retrieved vesicles are acidified and either recycle immediately, or via endosomes. Other methods include a direct recycling at the active zone, where the vesicles are immediately refilled and remain docked at the active zone and the “kiss and run” method, by which the vesicles are endocytosed in a clathrin independent manner and are acidified and recycled to the reserve pool (Figure 1.11).

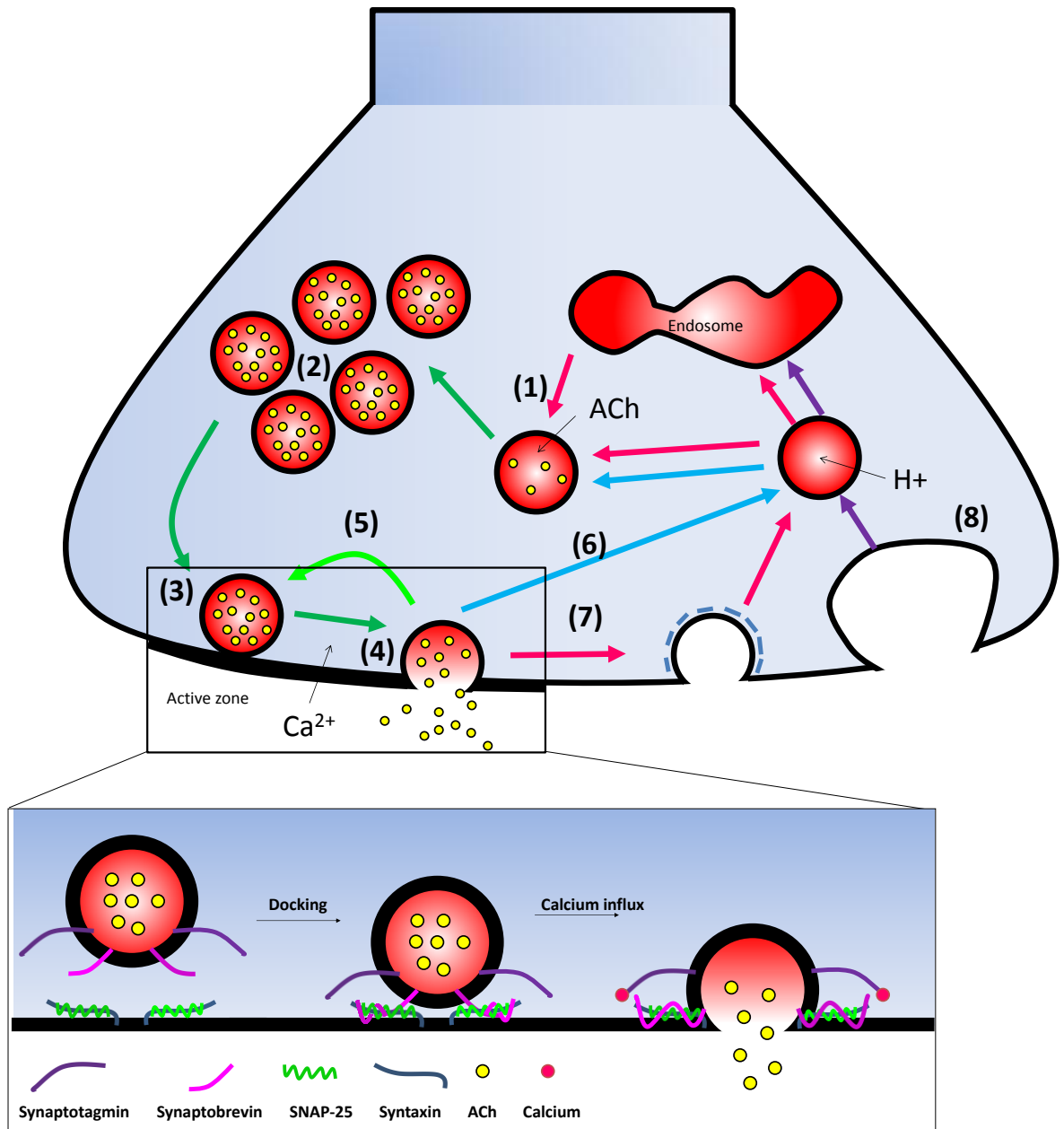


**Figure 1.11: Schematic of synaptic vesicle exo- and endocytosis at the motor nerve terminal.** Exocytic processes are shown by the dark green arrows, while the various endocytic pathways are displayed in other colours. ACh is synthesised locally in the nerve terminal and then transported into the synaptic vesicle (1). Filled vesicles abide in the reserve pool (2) or in the readily releasable pool at the active zone (3). Calcium influx via voltage gated calcium channels causes vesicle fusion (4) - insert shows the docking of vesicles to the membrane by interaction of vesicle-bound synaptobrevin and nerve terminal-bound syntaxin and SNAP-25. Calcium interacts with vesicle-bound synaptotagmin, causing vesicle fusion with the membrane and ACh release into the synapse. When vesicles have fused they may: (5) refill directly and remain bound to active zone, shown by light green arrow; (6) be endocytosed in a clathrin independent manner and undergo re-acidification and recycling to the reserve pool as shown by light blue arrow; (7) be endocytosed via clathrin-coated pits and either recycled directly or via endosomes; (8) be bulk endocytosed if membrane activity was strong, resulting in large vacuoles which are recycled via endosomes, shown by purple arrow.

### **1.6.2 Bacterial toxins targeting gangliosides**

As gangliosides can be endocytosed from the plasma membrane, it follows that any cargo which these gangliosides carry may also be internalised. The classic examples of this are bacterial toxins, many of which use gangliosides as a means of entering the cell in order to carry out their pathological effects. Examples of these toxins include the AB toxins pertussis and cholera which bind complex a-series gangliosides GD1a and GM1 respectively (Hausman and Burns, 1993; Holmgren et al., 1975). In contrast, clostridium toxins tetanus and botulinum both prefer complex b-series gangliosides. For instance botulinum toxin has a preference for GT1b and GD1b (Schiavo et al., 2000) and in GalNAcT<sup>-/-</sup> mice which lack complex ganglioside, its toxicity is greatly reduced (Peng et al., 2011). In addition, increased membrane activity and recycling increases botulinum toxin entry into cells implying that there is a high amount of endocytic recycling ongoing at the presynaptic membrane of the motor nerve terminal.

The endocytosis of toxins does not necessarily reflect the normal recycling of gangliosides however. The uptake of botulinum toxin is increased in response to membrane activity as it hijacks the synaptic vesicle recycling system by binding SNARE-proteins in addition to ganglioside ligand (Dong et al., 2003). Similarly, tetanus toxin has been shown to be internalised via clathrin-coated pits, independent of synaptic vesicle recycling. Its target ganglioside GD1b was not shown to be endocytosed along with it (Deinhardt et al., 2006). In addition, cholera toxin has been shown to be internalised by both clathrin-dependent and clathrin-independent pathways in different cell types and can switch between these methods if the cellular machinery required is low (Singh et al., 2003). In contrast to all of the above toxin entry, use of fluorescent glycosphingolipid analogues has shown that gangliosides are primarily internalised by clathrin-independent endocytosis (Iglesias-Bartolome et al., 2009; Singh et al., 2003). The use of antibodies against gangliosides as a means of labelling the gangliosides has also demonstrated their internalisation by clathrin-independent routes (Crespo et al., 2008; Iglesias-Bartolome et al., 2006; Iglesias-Bartolome et al., 2009). This is of interest in the context of GBS as these antibodies are pathogenic in this disease and their uptake opens a new perspective in which

disease may be mediated. The fact that they appear to be able to mark the normal trafficking of gangliosides logically implies that the antibodies may be able to undergo the same possible fates as endocytosed gangliosides (see Section 1.3.3.), i.e. recycling back to the plasma membrane, broken down into component parts to be used in new ganglioside synthesis, or degradation.

### ***1.6.3 Uptake of anti-ganglioside antibody***

In cell work, antibodies against GD3, GM1, GD1a and GD1b have been shown to be endocytosed via clathrin-independent pathways and sorted into early endosomes (Fewou et al., 2012; Iglesias-Bartolome et al., 2009). This uptake could be dramatically reduced by the reduction or ablation of caveolin-1 protein. Using a variety of cells, an antibody against GM1 was shown to be recycled back to the plasma membrane (Iglesias-Bartolome et al., 2009), while in CHO-K1 cells, anti-GD3 antibody was also shown to be recycled, rather than targeted to lysosomes. A separate GM1 antibody, along with antibodies against GD1b and GD1a showed co-localisation with recycling endosomes and also lysosomes in PC12 cells, indicating the possibility for both recycling and degradation (Fewou et al., 2012).

Having established that the antibodies associated with autoimmune attack of peripheral nerve membranes can be endocytosed, it became of interest to this laboratory to define whether this was relevant to the disease-specific sites and what effect this would have in the context of GBS. It was found that the motor nerve terminal, which is highly susceptible to attack by anti-ganglioside antibody in mouse nerve-muscle preparations (Goodyear et al., 1999; Greenshields et al., 2009; Halstead et al., 2004; Halstead et al., 2005b; Rupp et al., 2012; Rupp et al., 2013), can endocytose surface-bound anti-ganglioside antibody at physiological temperatures. This phenomenon protected the nerve terminals from complement-mediated damage and its prevention, by depletion of cholesterol, resulted in increased MAC deposition and nerve terminal injury (Fewou et al., 2012). The NoR, another site which is vulnerable to anti-ganglioside antibody attack (Hafer-Macko et al., 1996a; McGonigal et al., 2010; Susuki et al., 2007b; Susuki et al., 2012; Takigawa et al., 1995), was found not to share the same ability to internalise anti-ganglioside antibody, leaving it more vulnerable

to injury (Fewou et al., 2012). Mature nodes of Ranvier have been shown to be relatively stable, with slow turnover of membrane components (Zhang et al., 2012). This difference between membrane activity between the nerve terminal and the node of Ranvier may explain why nerve terminal damage has been difficult to show in patient tissue. The mechanism of internalisation at the motor nerve terminal is as of yet unknown. The normal caveolae-dependent route of uptake is less likely here as, although they can express caveolin proteins, neurons do not contain caveolae (Bu et al., 2003; Trushina et al., 2006).

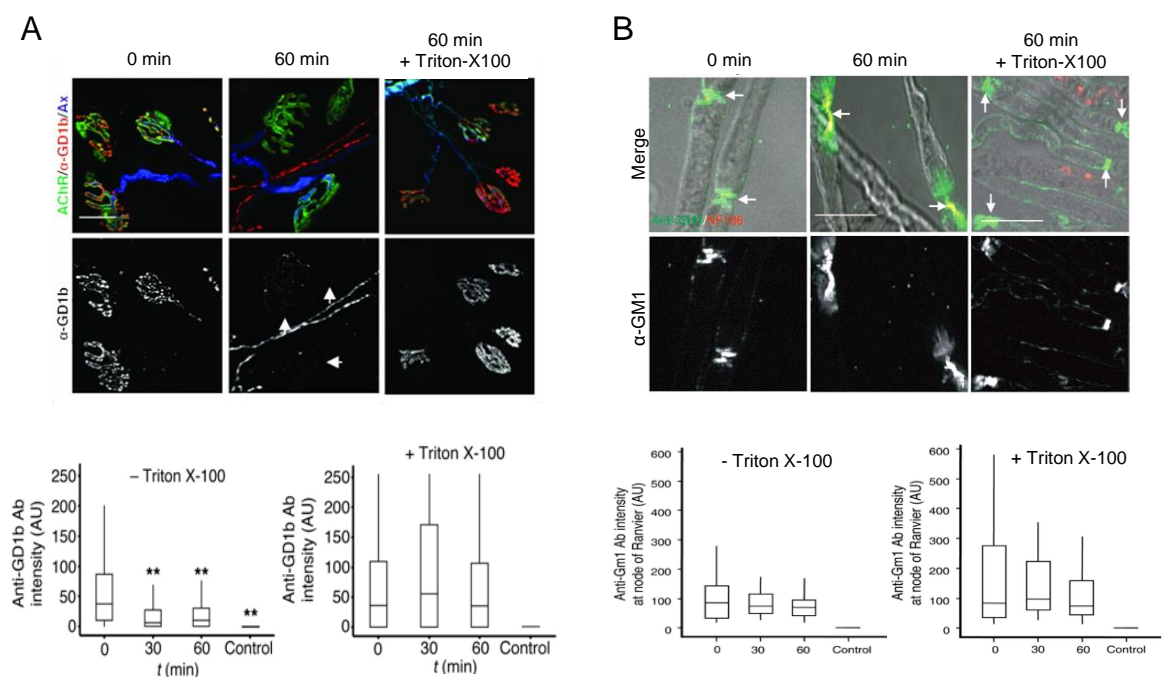


**Figure 1.12: The motor nerve terminal, but not the node of Ranvier has the ability to internalise antibody within 60 minutes at physiological temperatures. (A)** When mouse skeletal muscle is incubated *ex vivo* with anti-ganglioside antibody at 4°C before immediate fixation, strong binding is seen at the NMJ. If, before fixation, the antibody is washed and the tissue kept at physiological temperature for 30 or 60 minutes, the amount of surface-bound antibody at the nerve terminal is significantly reduced. Upon permeabilisation this antibody can be seen within the nerve terminal, leaving no significant difference between the antibody overlying the nerve terminal at any timepoint. **(B)** When the NoR is looked at under the same conditions, surface-bound antibody remains statistically similar after 30 and 60 minutes at physiological temperatures to that of 0 minutes. Modified with permission from Fewou et al., (2012).

#### ***1.6.4 Retrograde trafficking of immunoglobulins***

The fate of anti-ganglioside antibody which has been endocytosed at the nerve terminal is unknown, though it is possible that the antibody may be trafficked to the spinal cord, in a similar manner to some ganglioside-binding toxins. Though endocytosed in a different manner, cholera toxin and anti-ganglioside antibody have been shown to converge in early endosomes (Iglesias-Bartolome et al., 2009) and, while the toxic effects of cholera toxin are local, the B subunit responsible for docking to ganglioside on the plasma membrane, is retrogradely transported to the spinal cord (Angelucci et al., 1996). Tetanus toxin, also enters a retrograde transport pathway, resulting in its presence in the soma of motor neurons, from where it spreads trans-synaptically to inhibitory interneurons, preventing their action. These toxins are widely used as neuronal tracers, but it has also been known for some time that immunoglobulins which bind synaptic membrane components can be internalised by motor neurons and retrogradely transported to cell bodies in the spinal cord (Fabian and Ritchie, 1986; Fabian and Petroff, 1987; Fabian, 1988; Fabian, 1990; Ritchie et al., 1985; Ritchie et al., 1986; Wenthold et al., 1984). Although many papers described the phenomenon of intra-neuronal IgG and even IgM, no further work has been done to dissect the implications of this event. In one study, Ritchie et al found the apparent trans-synaptic spread of monoclonal antibodies following intramuscular injection and retrograde transport (Ritchie et al., 1986). In general, most studies have found that anti-sera and mono- or polyclonal antibodies which target synaptosome or nerve terminal membrane components were retrogradely transported, while control sera was not (Ritchie et al., 1985; Wenthold et al., 1984) (Figure 1.13). This implies that the uptake of these antibodies was at the nerve-terminal and was dependent on the binding of antibody to the nerve terminal membrane. In the context of GBS and the new concept of anti-ganglioside antibody internalisation, this implies that following its uptake into the nerve terminal, anti-ganglioside antibody may enter into a retrograde transport pathway and subsequently be present in the spinal cord. If this phenomenon occurs in patients it is unknown what kind of effect it may have within the motor neurons.

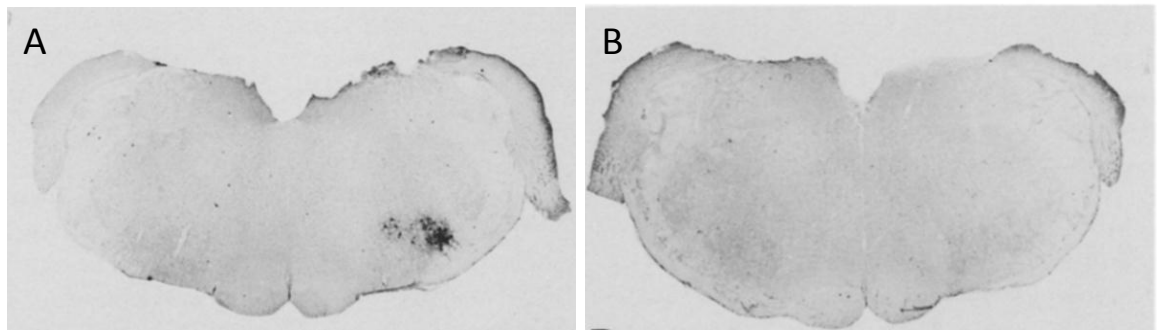


**Figure 1.13: Antisera against nerve terminal glycoproteins are retrogradely transported to the spinal cord.** This example shows the facial nucleus from rats injected with (A) guinea pig antisera against synaptic membrane glycoproteins and (B) unimmunised guinea pig serum. Immunoglobulins are detected in the facial nucleus of rats injected with antisera, but not in those who were injected with normal serum. Modified with permission from Wenthold et al., (1984).

### 1.6.5 The neonatal Fc receptor

The major method of antibody clearance from the serum is via non-specific pinocytosis. When internalised, the immunoglobulin is sorted into endosomes which are acidified and targeted to lysosomes for degradation (Mould and Sweeney, 2007). However, the expression of the neonatal Fc receptor (FcRn) can extend serum half-life of the IgG subclass by scavenging the endocytosed antibodies and return it to the cell surface (Lobo et al., 2004). This protein, originally named for its role in transportation of maternal antibodies to the foetal circulation, binds IgG molecules in acidified endosomes and protects the IgG from degradation by lysosomes. Instead, the IgG is sorted into recycling endosomes, returned to the cell surface and released back into the circulation. The effects of FcRn are demonstrated by the prolonged presence of IgG in the circulation. While in mice, IgM, IgA and IgE have a half-life of between 1 and 4 days, the various IgG subclasses can remain in the serum for between 3 and 10 days (Zuckier et al., 1989). In humans the effect is even more dramatic, with IgM, IgA, IgD and IgE half-lives ranging from 2-6 days, while IgG can remain in the serum for 23 days (Mould and Sweeney, 2007). Although expressed in other cell types, including immune cells (Zhu et al., 2001), FcRn is expressed to a high degree in the highly endocytically active cells of the vascular endothelium (Mould and Sweeney, 2007). The importance of the vascular endothelial FcRn's role in IgG homeostasis was shown by Montoyo et al in 2009 by its conditional

deletion in vascular endothelial cells. These mice showed a reduced serum half-life of IgG compared to het or wildtype controls, and levels of IgA were not affected (Montoyo et al., 2009).

## **1.7 Animal models of Guillain-Barré syndrome**

### ***1.7.1 Experimental Allergic Neuritis***

Animal models are important in gaining an integrated view of disease. The traditional model resembling GBS, experimental allergic neuritis (EAN) was described almost 60 years ago (Waksman and Adams, 1955). This rabbit model is characterised by a demyelinating pathology caused by an immune response against a sciatic nerve homogenate, and can be recreated using inoculation with p0 or p2 myelin protein in rabbits and rats. The immunised animals develop a nerve disease characterised by abnormal gait and posture and motor abnormalities (Waksman and Adams, 1955). These symptomatic changes are accompanied by the appearance of lesions in the dorsal and ventral roots, the dorsal root ganglion and the spinal nerve itself. The pathology of EAN is thought to be mainly driven by the actions of macrophages, though the appearance of other inflammatory cells such as neutrophils, mononuclear cells and lymphocytes is also observed. In the original paper, macrophages were seen to be involved in the disintegration of myelin, with remnant of fatty deposits observed inside these cells. This has led EAN to be a characteristic model of AIDP, the demyelinating form of GBS. Rat immunisations with p2 or PNS myelin by Hughes et al demonstrated that an anti-p2 antibody response is generated, but that this response did not appear to coincide with the development of neurological symptoms. In addition, the transfer of antisera to naïve animals failed to induce disease, whereas the transfer of lymph nodes from immunised animals did induce neurological symptoms (Hughes et al., 1981). This, plus evidence that elimination of T cells in rats frequently prevents development of EAN, led to the hypothesis that the pathology seen in EAN is cell-mediated (Brosnan et al., 1987). While EAN mimics AIDP symptoms and pathology, the induction mechanism of myelin attack does not translate to AIDP patients (Asbury and McKhann, 1997;Willison, 2012).

### **1.7.2 Rabbit model of AMAN**

With the emerging association of antibodies against gangliosides in GBS, particularly with the association of anti-GM1 antibodies in AMAN (Kuwabara et al., 1998; Vriesendorp et al., 1993; Yuki et al., 1990; Yuki et al., 1999), there came a study lending great credence to the concept that these antibodies may be pathological in nature. Japanese white rabbits were inoculated with a mixture of bovine brain gangliosides or GM1 alone along with complete Freund's adjuvant and keyhole limpet hemocyanin to act as a carrier protein. Immunised rabbits began to develop limb weakness or flaccid paralysis, accompanied by an increase in serum-reactivity to GM1 ganglioside (Yuki et al., 2001). Upon sacrifice, rabbits were shown to have invasion of macrophages into the periaxonal space and Wallerian degeneration of nerve fibres, with only rare demyelination. A follow up study where rabbits were injected with GM1-mimicking LOS from *C. jejuni*, resulted in similar outcomes, thus demonstrating that the anti-GM1 antibodies may be generated as a result of molecular mimicry from an antecedent infection (Yuki et al., 2004).

### **1.7.3 Mouse models of Guillain-Barré syndrome**

Currently there is no mouse model equivalent of EAN, or as eloquent a model of active immunisation as seen in the rabbit AMAN model. Creating animal models for GBS and related conditions has proven difficult due to the poorly understood mechanisms of lipid tolerance and the poor immunogenicity of glycolipid structures. To model disease in mice, which bestow the benefit of potential genetic manipulation, investigations have thus far focused on generating antibodies in glycosyltransferase knock-out (KO) mice. Unlike wildtype mice, GalNAcT<sup>-/-</sup> and GD3s<sup>-/-</sup> mice lack the tolerance to those gangliosides which they fail to synthesise (Bowes et al., 2002; Gong et al., 2002; Goodyear et al., 1999; Lunn et al., 2000; Townson et al., 2007). More recent immunisations in this laboratory have utilised liposomes as a method of antigen introduction, whereby the ganglioside or LOS antigens are displayed in a multilamellar membrane with other lipid raft proteins, to emulate a physiologically similar environment to naturally occurring gangliosides. Using this method alone however, these liposomes yield very little/no immune response in wildtype mice and so liposomes were created which encapsulated the non-self-protein ovalbumin

(OVA), found in chick egg white. This hapten-carrier style approach recruits T-cell help and induces a high increase in anti-ganglioside antibody specific IgM and IgG by ELISA, though in wildtype mice this response is still far lower than in mice which lack the target antigen (Bowes et al., 2002) (Figure 1.14).

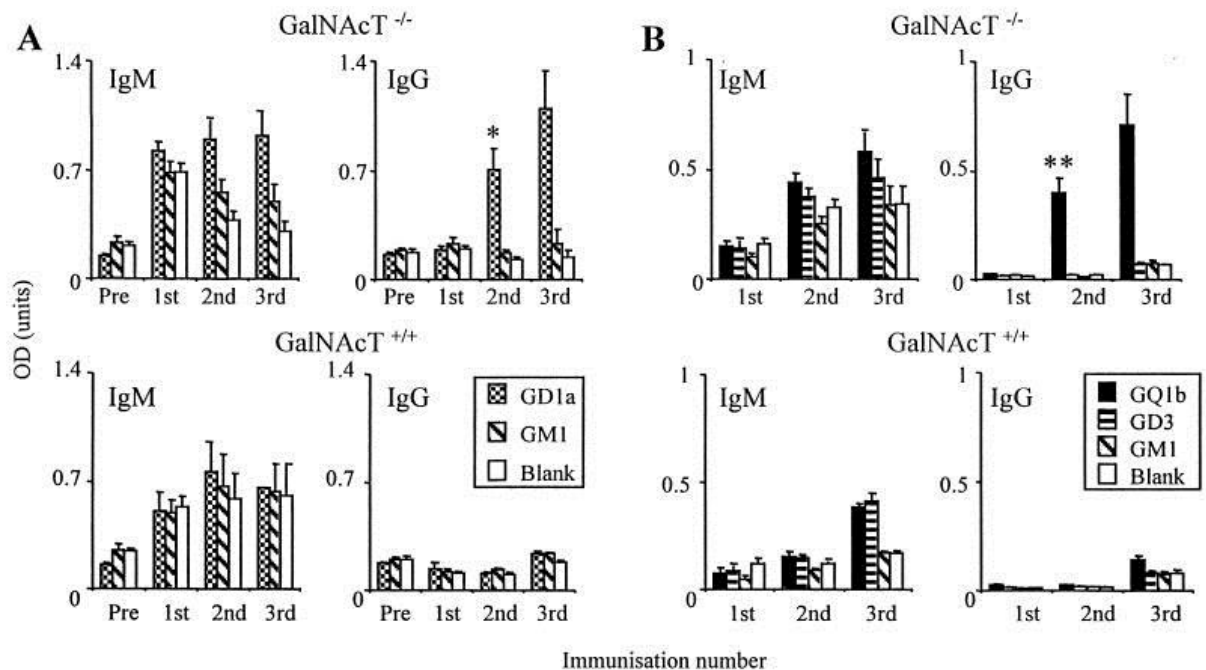


**Figure 1.14: Immunisation with ganglioside and OVA-containing liposomes induces anti-ganglioside antibodies more effectively in mice which lack endogenous antigen.** A. Anti-ganglioside IgM and IgG responses in wildtype and GalNAcT<sup>-/-</sup> mice immunised with GD1a liposomes. Immune response to GD1b is specific to this ganglioside and only occurs to a significant degree in GalNAcT<sup>-/-</sup> mice. B. Similarly, mice immunised with GQ1b liposomes also show a GQ1b-specific response which is only significant in GalNAcT<sup>-/-</sup> mice. Modified with permission from Bowes et al., (2002).

The antibodies produced in these mice can be purified and cloned and subsequently used to model anti-ganglioside-mediated injury both *in vivo* and *ex vivo* in studies designed both to understand disease pathogenesis and ultimately to test the effectiveness of therapeutics. These antibodies have been used to demonstrate the role of complement activation in AMAN and MFS, the effectiveness of complement inhibitors in preventing damage caused by MAC formation, and the role of complement and calpain in the injury of the node of Ranvier (Goodfellow et al., 2005; Greenshields et al., 2009; Halstead et al., 2004; Halstead et al., 2005a; Halstead et al., 2005b; Halstead et al., 2008; McGonigal et al., 2010). However the ultimate goal would be to create a

GBS model in which the antibodies are both generated and cause disease in the same animal. Due to the wildtype mice's inability to produce an effective response to ganglioside immunisation and the GalNAcT<sup>-/-</sup> mice's lack of target, this has thus far proved very difficult. The GalNAcT<sup>-/-</sup>-*Tg(neuronal)* and GalNAcT<sup>-/-</sup>-*Tg(glial)* mice described earlier were created for the purpose of active immunisations, where it was hoped that the restricted expression of complex gangliosides to neurons and glia would allow for a break in tolerance. This topic will be addressed as part of this thesis.

## 1.8 Aims of thesis

Generation of an active immunisation model of GBS in the mouse remains one of the major challenges in understanding the pathophysiology of GBS and for pre-clinical testing of novel therapies. One major historical hurdle to overcome is that the serum levels of antibody in wildtype mice immunised with ganglioside are low. This can be bypassed by immunising ganglioside deficient mice (GalNAcT<sup>-/-</sup> mice) as they lack immunological tolerance, seeing gangliosides as foreign; however they cannot themselves be injured as they lack the neural target for antibody attack. Consequently, in wildtype mice anti-ganglioside antibody levels are so low that injury does not occur, even with the addition of an exogenous source of complement. The generation of complex-ganglioside "rescue mice", which express GalNAcT (and therefore complex gangliosides) in only neurons or glia, may allow for such a model to be developed. In these mice, the restricted nature of ganglioside expression is anticipated to overcome the tolerance to ganglioside immunisation which is seen in wildtype mice. The creation of these mouse strains also affords the ability to investigate the importance of ganglioside expression and dynamics in these different membranes. The emergence of the novel concept of anti-ganglioside antibody internalisation at the motor nerve terminal, also allows these mice to be used for assessing the uptake of different anti-ganglioside antibodies at different membrane sites.

On this background, the aims of my thesis were to:

- Characterise the ganglioside expression in GalNAcT<sup>-/-</sup>-*Tg(neuronal)* mice and GalNAcT<sup>-/-</sup>-*Tg(glial)* rescue mice in comparison with wildtype and GalNAcT<sup>-/-</sup> mice.
- Determine whether the rescued expression of gangliosides could correct morphological and behavioural defects seen in GalNAcT<sup>-/-</sup> mice, thus investigating the importance of neuronal (and glial) ganglioside expression
- Optimise the conditions for achieving an active immunisation model of mouse GBS using neuronal and glial rescue mice.

The results of the active immunisation model led the project in a different direction by bringing up the issue of antibody internalisation. Therefore the aims of the thesis were expanded to:

- Investigate the uptake of anti-ganglioside antibody at the neuromuscular junction, exploiting the differences in ganglioside expression in the different mouse genotypes
- Determine how the uptake of anti-ganglioside antibody may affect its availability to bind and cause injury to neural membranes using *in* and *ex vivo* models of nerve injury.

## 2 Methods

### 2.1 Materials

#### *2.1.1 Antibodies and tissue stains*

Commonly used antibodies, manufacturers, stock concentrations (where applicable) and dilutions used are shown in Table 2.1. Controls are indicated throughout the thesis but were generally either secondary antibody alone, or a mouse lacking the receptor for the antibody.

Table 2.1: Primary antibodies used throughout this thesis.

Labelling reagent	Monoclonal /polyclonal	Manufacturer	Stock Concentration	Dilution
Rabbit anti-cow s100	Polyclonal	Dako, (Glostrup, Denmark)	4 mg/ml	1/200
Goat anti-mouse secondary antibodies: IgG, IgM, IgG2a, IgG2b, IgG3, IgG1 (TRITC, FITC and Cy5 conjugates)	Polyclonal	Southern Biotech, (Birmingham, AL, USA)	1 mg/ml	1/300 sections, 1/200 whole mount
Goat anti-rat IgG-Cy5	Polyclonal	Southern Biotech, (Birmingham, AL, USA)	1 mg/ml	1/300 sections
Goat anti-rabbit secondary antibodies: IgG, IgG1 (Alexa Fluor 555 and 647 conjugates)	Polyclonal	Molecular Probes, (Eugene, OR, USA)	2 mg/ml	1/500 sections 1/300 whole mount
Goat anti-mouse IgG, IgM (HRP conjugate)	Polyclonal	Southern Biotech, (Birmingham, AL, USA)	n/a	1/3000
Mouse anti-human C5b-9	Monoclonal	Dako, (Glostrup, Denmark)	50 µl /ml	1/50
Rabbit anti-human C3c-FITC	Polyclonal	Dako, (Glostrup, Denmark)	3 mg/ml	1/300 sections
Rabbit anti-mouse NeuN	Monoclonal	Millipore, (Billerica, MA, USA)	1 mg/ml	1/750 sections
Rabbit anti-mouse MAP-2	Polyclonal	Cell Signalling Technology, (Danvers, MA, USA)	n/a	1/100 sections
Rabbit 1211 (NF-H)	Polyclonal	Enzo Life Sciences (Exeter, UK)	n/a	1/200 whole mount

### **2.1.2 Commonly used lipids**

The gangliosides and lipids used for immunisations and glycoarray were purchased from Sigma Aldrich (*St Louis, MO, USA*), with the exception of sphingomyelin which was purchased from Carbosynth (*Newbury, UK*). For ELISpots, GD1b was also purchased from Carbosynth.

### **2.1.3 Commonly Used reagents**

Reagents, abbreviations, suppliers (and stock concentrations if required).

- Alpha-bungarotoxin (BTx) - Alexa Fluor 488, 555 and 647 conjugates, (*Molecular Probes, Eugene, OR, USA*)
- Bovine serum albumin (BSA), (*Sigma-Aldrich, St Louis, MO, USA*)
- Citifluor antifade (*Citifluor, Canterbury, UK*)
- Normal goat serum (NGS), (*Sigma-Aldrich, St Louis, MO, USA*)
- Normal human serum (NHS) (blood taken from one donor and serum removed and stored at  $-80^{\circ}\text{C}$ )
- Tissue Tek Optical cutting temperature compound (OCT) (*Sakura Finetek, Alphen aan den Rijn, Netherlands*)
- Triton X-100, (*Sigma-Aldrich, St Louis, MO, USA*)
- TWEEN-20, (*Sigma-Aldrich, St Louis, MO, USA*)
- Vectashield (with DAPI), (*Vector Laboratories, Burlington, Canada*)

### **2.1.4 Preparation of commonly used buffers**

All solutions were used at a pH of 7.3.

#### **2.1.4.1 Ringer's Solutions**

Ringer's was prepared to a final concentration of 116 mM NaCl, 4.5 mM KCl, 23 mM  $\text{NaHCO}_3$ , 1 mM  $\text{NaH}_2\text{PO}_4$ , 11 mM glucose, 1 mM  $\text{MgCl}_2$  and 2 mM  $\text{CaCl}_2$  in distilled water. Ringer's was bubbled with oxygen for 10 minutes prior to use.

For activity dependent internalisation experiments, a high potassium Ringer's solution was used. For this, KCl concentration was increased to 56 mM and NaCl

was reduced to 65 mM. For experiments inhibiting vesicle acidification, in some experiments, NaCl was replaced with NH<sub>4</sub>Cl.

#### **2.1.4.2 Phosphate buffered saline (PBS)**

Phosphate buffered saline (PBS) was used at a final concentration of 140 mM NaCl, 1.5mM KH<sub>2</sub>PO<sub>4</sub>, 2.7 mM KCl and 77 mM Na<sub>2</sub>HPO<sub>4</sub>.

## **2.2 Animals**

Male and female mice aged 4-12 weeks were used for all *in vivo* experiments. For *ex vivo* work, male and female mice ranged from 4-16 weeks. All mice were housed in the University central research facility under a 12 hour light/12 hour dark cycle and given food and water ad libitum. All animals were killed with a rising concentration of CO<sub>2</sub> as per Home Office regulation with either cardiac puncture or cervical dislocation to confirm death.

### **2.2.1 Genotypes**

The mice used throughout this thesis are referred to as wildtype, GalNAcT<sup>-/-</sup>, GalNAcT<sup>-/-</sup>-*Tg(neuronal)* and GalNAcT<sup>-/-</sup>-*Tg(glia)*. All of these mice are on a C57Bl/6 background (specifically C57Bl/6J01aHsd from Harlan Laboratories).

GalNAcT<sup>-/-</sup> mice, generated by the group of Koichi Furakawa, have disrupted GalNAcT synthesis (Takamiya et al., 1996), meaning they do not express complex gangliosides. Male GalNAcT<sup>-/-</sup> mice are sterile and therefore heterozygous male mice were bred with homozygous females. Subsequently, litters required genotyping.

GalNAcT<sup>-/-</sup>-*Tg(neuronal)* and GalNAcT<sup>-/-</sup>-*Tg(glia)* mice were created by crossing GalNAcT<sup>-/-</sup> mice with mice which carried a transgene expressing GalNAcT driven by either the NFL or PLP promoter respectively (Yao et al., 2014). The resulting GalNAcT<sup>-/-</sup>-*Tg(neuronal)* and GalNAcT<sup>-/-</sup>-*Tg(glia)* mice should have GalNAcT expression solely on their neurons and glia respectively. Like GalNAcT<sup>-/-</sup> mice, males were sterile and therefore heterozygous males were bred with homozygous females. The GalNAcT KO and the transgene insertion were confirmed by PCR (section 2.2.3).

### 2.2.2 Fluorescent mice

In some *ex vivo* experiments, B6.Cg-Tg(Thy1-CFP/S100B-GFP) transgenic mice, expressing green fluorescent protein (GFP) driven by the s100 promoter and cyan fluorescent protein (CFP) driven by the Thy1 promoter were used, allowing easy identification of Schwann cells and axons respectively (Feng et al., 2000; Zuo et al., 2004). These mice were gifted to the lab by Wesley Thompson but are now available commercially through Jackson laboratories. To make fluorescent varieties of all of the above transgenic mice in section 2.2.1, these mice were crossbred with B6.Cg-Tg(Thy1-CFP/S100B-GFP), making GalNAcT<sup>-/-</sup> x B6.Cg-Tg(Thy1-CFP/S100B-GFP), GalNAcT<sup>-/-</sup>-Tg(*neuronal*) x B6.Cg-Tg(Thy1-CFP/S100B-GFP) and GalNAcT<sup>-/-</sup>-Tg(*glial*) x B6.Cg-Tg(Thy1-CFP/S100B-GFP). However, for simplicity, throughout this thesis all fluorescent mice will be referred to as either wildtype, GalNAcT<sup>-/-</sup>, GalNAcT<sup>-/-</sup>-Tg(*neuronal*) or GalNAcT<sup>-/-</sup>-Tg(*glial*), and fluorescence will be indicated where appropriate.

### 2.2.3 Genotyping

#### 2.2.3.1 Polymerase chain reaction

Genotyping was done by polymerase chain reaction (PCR) to confirm in mice on a GalNAcT<sup>-/-</sup> background, the KO of the GalNAcT enzyme and, where appropriate, the incorporation of the transgene indicating restoration of GalNAcT synthesis tagged onto Thy1, PLP or NFL promoters. Genotyping of non-fluorescent GalNAcT<sup>-/-</sup> mice, GalNAcT<sup>-/-</sup>-Tg(*neuronal*) and GalNAcT<sup>-/-</sup>-Tg(*glial*) mice was carried out by Dr Denggao Yao.

DNA extraction was performed on ear or tail samples taken from mice. Briefly, the samples were incubated in 75 µl lysis buffer (25 mM NaOH, 0.2 mM EDTA, pH 12) for 1 hour at 95°C to extract DNA. The solution was neutralised with 75 µl neutralising buffer (40 mM TRIS, pH 5) and kept at 4°C.

The primers for GalNAcT KO used were:

PAG3: 5'-GCC TGC TTG CCG AAT ATC ATG GTG GAA AAT-3'

PES4: 5'-GAA GAA TTC AAG ACT GTC TGT GAA ATT CTG-3'

AK5: 5'-TCC CCC GTG AGA GTC ACT CCT GTT ACT TCC-3'

Flag primer was used to confirm GalNAcT transgene insertion:

P1: 5'-ACTTGGTTTCCTTCGTGTTG-3'

P59: 5'-CTTATCGTCGTCATCCTTGTAATC-3'

In autoclaved sample tubes the following volumes of reagents were added on ice:

DNA - 5  $\mu$ l

dH<sub>2</sub>O - 13.5  $\mu$ l

5X Green GoTaq® Reaction Buffer (*Promega, Madison, WI, USA*) -5  $\mu$ l

Primer (each) 0.5  $\mu$ l

dNTPs - 0.25  $\mu$ l

GoTaq® G2 DNA Polymerase (*Promega, Madison, WI, USA*) - 0.25  $\mu$ l

Samples were transferred immediately to a Veriti Thermal cycler (*Life Technologies, Thermo Fisher Scientific, MA, USA*). For confirmation of GalNAcT KO the following program was run:

- 3 minutes at 95°C
- 1 minute at 60°C.
- 2 minutes at 72°C
- 35 cycles of 1 minute at 90°C, 30s at 57°C, 1 minute at 72°C
- 10 minutes at 72°C,

For confirmation of the incorporation of the transgene, the program was as follows:

- 5 minutes at 95°C.
- 30 cycles of 30 s at 95°C, 30 s at 55°C, 1 minute 30 s at 72°C.

- 10 minutes at 72°C.

#### **2.2.3.2 Gel electrophoresis**

The DNA samples (20 µl) were run on an agarose gel (1.5% agarose in 1x Tris-acetate-EDTA buffer) containing ethidium bromide and DNA was imaged under UV light. A 1kb DNA marker was run alongside samples. GalNAcT<sup>-/-</sup> was confirmed by a 500bp band, wildtype a 350bp band and flag a 229bp band.

#### **2.2.4 Fluorescent Phenotyping**

The skin from mouse ear samples was peeled apart, mounted in Citifluor and coverslipped. Samples were then viewed under a Zeiss Axio Imager Z1 fluorescent microscope (*Carl Zeiss AG, Oberkochen, Germany*) to confirm presence of CFP in ear axons and GFP in S100 positive cells.

### **2.3 Production of monoclonal antibodies from hybridoma cell lines.**

Antibody-producing hybridoma cell lines (Table 2.2) were generated previously by immunisation of GalNAcT<sup>-/-</sup> mice or GD3s<sup>-/-</sup> mice with either liposomes containing ganglioside or with ganglioside-mimicking LPS using previously described immunisation protocols and hybridoma techniques (Bowes et al., 2002; Goodyear et al., 1999; Townson et al., 2007). Frozen stocks of previously purified antibodies were used where available but on occasion cell lines had to be grown and antibodies purified from hybridoma supernatant.

**Table 2.2: Mouse monoclonal anti-ganglioside antibodies used throughout this thesis, their predominant targets by ELISA and their immunoglobulin subtype.**

Mouse monoclonal antibody	Predominant targets	Immunoglobulin subtype
MOG1	GD1b	IgG3
MOG3	GD1b	IgG3
MOG16	GD1b	IgG3
MOG35	GD1a	IgG2b
DG1	GM1	IgG2b
DG2	GM1	IgG3

Non-adherent cells were grown in flasks suspended in RPMI supplemented with 10% foetal calf serum (FCS) at 37°C in 5% CO<sub>2</sub>. Once per week, cells were centrifuged at 1500rpm for 5 minutes and supernatant was collected and stored at -20°C. Cells were then resuspended in fresh media and split into 2 flasks. When >5 flasks were highly confluent, cells could be transferred to an Integra CELLline flask (*Integra Biosciences, MA, USA*), which are more efficient for antibody production than usual tissue culture flasks. To do this, firstly 10 ml of RPMI (20% FCS) was added to the cell compartment for 5 minutes. In this time, cells from 6 T175 flasks were spun down as above and resuspended in 15ml of RPMI (20% FCS). This was added to the cell compartment. The cells were grown in the cell compartment in RPMI (20% FCS), whereas the medium compartment still contained RPMI with the usual 10% FCS. Half the volume of medium from these cells were removed weekly and stored at -20°C until purification, and fresh media was applied. Similarly, 50% of the cell volume was removed each week and replaced with fresh 20% FCS.

## 2.4 Purification of monoclonal antibody supernatant

To purify IgG monoclonal antibodies, supernatant was spun down in Sorval centrifuge bottles (*Thermo Fisher Scientific, Waltham, MA, USA*) at 150000g for 30 minutes at 4°C. Supernatant was then dialysed overnight in 10x volume of binding buffer (0.2 M Na<sub>2</sub>H<sub>2</sub>PO<sub>4</sub>·2H<sub>2</sub>O, 0.2 M Na<sub>2</sub>HPO<sub>4</sub>). The supernatant was then collected, filtered through a 0.22 µm membrane and kept at 4°C. Binding buffer and 0.1 M glycine were also filtered before use. Binding buffer 10x column volume was run through a HiTrap Protein G HP column (*GE Healthcare, Little Chalfont, UK*) before the supernatant. Flow through was collected and stored at 4°C until antibody purification was confirmed. Binding buffer was run through the column and 10x 1 ml wash samples were collected. To remove the bound IgG from the column, 0.1 M glycine was run through the column and 10x 1 ml elutions were collected in centrifuge tubes containing 40 µl of 1 M Tris-HCl to neutralise the glycine. The IgG concentration in mg/ml of wash samples and elutions were measured using a NanoDrop 1000 spectrophotometer at an absorption wavelength of 280 nm (*Thermo Fisher Scientific, Waltham, MA, USA*).

## 2.5 Labelling of monoclonal antibody

To label anti-ganglioside antibodies, an Alexa Fluor 488 Protein labelling kit (*Molecular Probes, Eugene, OR, USA*) was used as per manufacturer's instructions. Briefly, purified monoclonal antibody from section 2.4, was prepared at 2 mg/ml (or as close as possible) and 0.5 ml of the antibody solution was added to 50 µl of 1 M sodium bicarbonate solution. The resulting solution was added to a vial of room temperature Alexa Fluor 488 reactive dye which contained a tiny stir bar. The solution was inverted to ensure all the dye was dissolved, and then reaction mixture was stirred for at least 1 hour at room temperature. While the mixture was stirring, the purification column was set up.

The column was positioned upright using a retort stand, using the provided foam holder to prevent the column being damaged. The provided purification resin (Bio-Rad BioGel P-30 Fine size exclusion purification resin, packaged in PBS) was stirred thoroughly before adding to the column, and allowing it to migrate downwards, with any excess PBS being collected in a small bijoux. The dye

reaction mixture was added to the column and allowed to enter into the resin. The provided PBS elution buffer 10x stock (0.1 M potassium phosphate, 1.5 M NaCl, 2 mM sodium azide) was diluted 1 in 10 and added to the column slowly, until the labelled antibody had been eluted. The eluted fractions were collected and retained and included buffer, dye-conjugated antibody, and unincorporated dye.

The final concentration of labelled antibody was once again calculated using a NanoDrop 1000 spectrophotometer (*Thermo Fisher Scientific, Waltham, MA, USA*). In addition to the concentration in mg/ml, the following equation was used to determine the molar concentration, accounting for dye absorption at 280 nm:

$$\text{protein concentration (M)} = \frac{[A_{280} - (A_{494} \times 0.11)]}{203,000}$$

where  $A_{280}$  is the absorption at 280 nm and  $203,000 \text{ cm}^{-1}\text{M}^{-1}$  is the molar extinction coefficient of an average IgG. The results were used to determine the degree of labelling using the following equation:

$$\text{moles dye per mole protein} = \frac{A_{494}}{71,000 \times \text{protein concentration (M)}}$$

where  $A_{494}$  is the absorption at 494 nm and  $71,000\text{cm}^{-1}\text{M}^{-1}$  is the approximate extinction coefficient of the dye at 494 nm.

Protein labelling was attempted using various dye incubation lengths. To test the binding and fluorescent intensity of the labelled antibodies following different incubation lengths, antibodies were tested by glycoarray first (see section 2.19), then, if successful binding was seen, in tissue (section 2.10.2).

## 2.6 *In vivo* procedures

All *in vivo* procedures were carried out in accordance with Home Office regulations and in accordance with both project (60/4493) and personal (60/12266) licences.

### **2.6.1 Nerve crush**

The sciatic nerve crush model is a well-established procedure for the study of peripheral nerve injury in rodents and is ideal for monitoring the regenerative capacity of the injured nerve (Bauder and Ferguson, 2012; Lehmann et al., 2007; Magill et al., 2007). To perform the nerve crush, anaesthesia was induced using an oxygen/isoflurane mixture (4%), and the hind leg on the crush side was shaved. The mice were transferred to a face mask and anaesthesia maintained at 1-2%. The notch of the pelvis was identified and the sciatic nerve was exposed by blunt dissection. Perpendicular to the notch of the pelvis, the sciatic nerve was crushed for 30 seconds with jeweller's forceps (size 5). Crush was confirmed immediately by the separation of proximal and distal parts of the nerve, and then post-recovery by identifying absence of toe stretching in mice held by their tails. The wound was closed using suture clips which were removed 1 week later.

Due to the likelihood of autotomy in mice, whereby their affected limb is bitten and chewed, measures were taken to prevent this behaviour. To provide a stimulating environment to distract and improve the mood of the mice, a tunnel, a wooden chew block and a pineapple-flavoured mineral block were provided in each cage. Additionally, to prevent swelling of the limb and provide low dose pain relief, carprofen was added to the animal's water (5ml in 250ml water). Mice were recovered for 8 weeks before sacrifice. Upon sacrifice, the legs of the mice were removed for lumbrical dissection (section 2.7.4), and the mice were perfusion fixed (perfused transcardially with saline, followed by 4% paraformaldehyde) and the sciatic and tibial nerves removed (section 2.7.3).

### **2.6.2 Gait analysis**

Information on gait differences between aged wildtype mice,  $\text{GalNACT}^{-/-}$ ,  $\text{GalNACT}^{-/-}\text{-Tg}(\text{neuronal})$  and  $\text{GalNACT}^{-/-}\text{-Tg}(\text{glial})$  mice was obtained using the Digigait™ imaging system (*Mouse Specifics Inc., Boston, MA*). This technology can automatically quantify gait dynamics of mice, rats and guinea pigs and consists of a motorized transparent treadmill with a high speed camera below to video capture the mice from the ventral side. The captured videos can then be analysed using the Digigait™ software which identifies the rodents' feet by and measures many parameters involved in the animals' gait including stride length,

stance width, stance duration, swing duration, braking duration, propulsion duration, stride frequency and paw angle (Table 2.3).

Wildtype, GalNacT<sup>-/-</sup>, GalNacT<sup>-/-</sup>-*Tg(neuronal)* and GalNacT<sup>-/-</sup>-*Tg(glial)* mice all between 12 and 18 months were given training on the Digigait™ prior to commencement of the study. This involved building up from placement in the testing chamber on a stopped treadmill to trial runs on the treadmill. This also allowed an optimal speed to be chosen where mice with the most severe phenotypes could still run while not being too slow for non-affected mice. Mice were placed in the Digigait™ and allowed to settle. The treadmill was started at 6cm/sec and increased to 16cm/sec as soon as the mouse began to walk. The treadmill was kept at this speed for approximately 10 seconds, unless the mouse stopped running. The videos captured were approximately 3 seconds long and roughly 10 videos were captured per animal.

Captured videos were analysed using Digigait™ software, which outputs the area of paw contact on the treadmill into graph form. The software allows manual correction of the calculated waveforms where the user can watch the videos in slow motion and ensure that for each limb, the software has interpreted the paw placement correctly. Videos with too many errors or errors which could not be resolved using the software were discarded. Animals were excluded if, when all corrections were done, they had fewer than 5 videos remaining. This left wildtype (n=4), GalNacT<sup>-/-</sup> (n=4), GalNacT<sup>-/-</sup>-*Tg(glial)* (n=3), GalNacT<sup>-/-</sup>-*Tg(neuronal)* (n=7). The software then calculates 38 parameters associated with gait based on the paw area graphs, examples of which are shown in Table 2.3. Analysis for the runs was averaged per animal and the mean values for each genotype were plotted.

**Table 2.3:** Examples of gait parameters generated by the Digigait™ which can be used to assess function after injury (Taken from Berryman et al., 2009)

<b>Gait Indices</b>	<b>Description</b>
1. Swing Time (sec)	The forward portion of the stride during which the paw is not in contact with the belt
2. Stance/Swing (ratio)	The ratio of Stance time to Swing time
3. Braking Time (sec)	The time between initial paw contact with the belt to the maximal paw contact
4. Stance Time (sec)	The portion of the stride in which the paw remains in contact with the belt
5. % Stance/Stride	The percent of time that the Stance Time contributes to one complete Stride cycle
6. Stride Length (cm)	The distance between initial contacts of the same paw in one complete stride
7. Stride Time (sec)	The amount of time to complete one complete stride for one limb
8. % Swing/Stride	The percent of time that the Swing Time contributes to one complete Stride cycle
9. % Propulsion/Stride	The percent of time that the Propulsion Time contributes to one complete Stride cycle
10. Paw Area at peak stance (cm <sup>2</sup> )	The maximal paw area in contact with the treadmill during the stance phase of the step cycle
11. Stance Width (cm)	The distance between the two front feet or the two hind feet as measured from the middle of the paw area

### ***2.6.3 Passive Immunisation of anti-ganglioside antibody for injury***

#### **2.6.3.1 Protocol**

Mice were injected with 1 mg monoclonal anti-GD1b antibody MOG1 via the intraperitoneal (i.p.) route. After 16 hours the mice were injected i.p. with 0.5 ml neat NHS. Mice were sacrificed following post-NHS plethysmography and behavioural analysis 3-4 hours later.

#### **2.6.3.2 Rotarod testing**

Prior to injection of antibody, mice underwent baseline rotarod analysis to assess their motor skills. The rotarod (*Ugo Basile, Gemonio, Italy*) is a rotating cylinder, 3 cm in diameter and forces motor movement in the mice, who need to move forward to stay on. Following 3 practice runs a day prior to baseline testing, mice were placed on a stopped rod which began rotating at 4.5 rpm and

increased at a rate of 0.12 rpm per second, up to 300 seconds, culminating in a speed of 40 rpm. Mice were given three trials on the rotarod with a 5 minute rest period in between. The latency to fall was recorded for each animal and each trial and the average of the three trials was calculated per mouse. This protocol was repeated 2 hours after NHS injection.

### **2.6.3.3 Whole body plethysmography**

Mice underwent whole body plethysmography (*Electro-Medical Measurement systems, Hampshire, UK*) to indicate changes in tidal volume and respiratory rate as a means of determining diaphragm function. Mice were acclimatised to the whole body chambers for 1 hour 1 day prior to baseline measurements. Chambers were calibrated according to the manufacturer's instructions. Before recording started, the mice were given a period of at least 20 minutes to acclimatise and longer if required. Breathing was recorded for 30 minutes at baseline before NHS injection, and for 2 hours after. The provided eDaq software outputs data averaged from 25 accepted breaths. An accepted breath was one which was over 0.01 ml tidal volume. At each timepoint, the first 25 outputs were averaged to provide a timepoint measurement. Some animals had such shallow breathing after injury that the software did not recognise any breaths in the entire 30 minute period between timepoints. The tidal volume of these animals was therefore marked as the minimum accepted tidal volume, 0.01 ml.

### **2.6.4 Active immunisation of mice with GD1b liposomes**

#### **2.6.4.1 Liposome preparation**

GD1b, cholesterol, sphingomyelin (SM) and dicetylphosphate (DCP) were dissolved in chloroform-methanol (1:1) and stored at -20°C. For liposomes, lipids were combined at a molar ratio of 1:5:4:1 with the optional addition of 200 µg/ml monophosphoryl lipid A (MPLA). Chloroform-methanol was removed by drying the suspension with nitrogen gas before resuspending lipids in PBS 5x the final volume and kept at 37°C. To encapsulate OVA within the liposomes, thereby promoting T-cell help in the immune response, PBS also contained OVA at 5 mg/ml. The mixture was vortexed briefly, then sonicated for 15 minutes at

room temperature before undergoing 5x freeze-thaw cycles in liquid nitrogen and a 37°C water bath. The solution was then centrifuged at 510 g for 20 minutes at room temperature. Following this, the supernatant was kept at 37°C and extruded 11X through a 0.4 µm polycarbonate filter using a mini extruder (*Avanti Polar Lipids Inc., AL, USA*). Liposomes were centrifuged at 109000 g for 1 hour at 16°C, supernatant discarded and the resulting pellet resuspended in PBS. Liposomes were stored at 4°C until used and kept for no longer than 5 days.

#### **2.6.4.2 Protocol**

Initial immunisations were carried out using previously a described protocol (Bowes et al., 2002) (Figure 2.1A). Briefly, on day 0, animals were given 100 µl OVA-alum (0.6 mg OVA per 1 ml aluminium hydroxide) i.p. to prime the immune response. On day 7, 14, 21 and 28, animals received a 100 µl i.p. injection of 1 mg/ml GD1b liposomes which did not contain MPLA (as per (Bowes et al., 2002)). On days 33, 34 and 35 animals received 50 µl of 200 µg /ml of these liposomes intravenously (i.v.) into the tail vein. In groups of 4 per day, mice were injected i.p. with 1 ml neat NHS on day 40, 41 or 42 and following behavioural analysis, were sacrificed. Blood samples were taken via tail vein venesection prior to injections on days 0, 7 and 14, 21, 28, 36 and upon sacrifice.

A modified protocol was employed to attempt to gain a similar immune response in a shorter period of time (Figure 2.1B). In this protocol, on day 0 animals were given 100 µl OVA-alum (0.6 mg OVA per 1 ml aluminium hydroxide) i.p. to prime the immune response. On day 7, 8, 11 and 12, animals received a 100 µl i.p. injection of 1 mg/ml GD1b liposomes containing the addition of MPLA. On days 19, 20 and 21 animals received 50 µl of 200 µg /ml GD1b liposomes intravenously (i.v.) into the tail vein. Blood samples were taken via tail vein venesection prior to injections on days 0, 19 and 22 and upon sacrifice. On the day of sacrifice, animals were given 1 ml of NHS i.p. to induce injury.

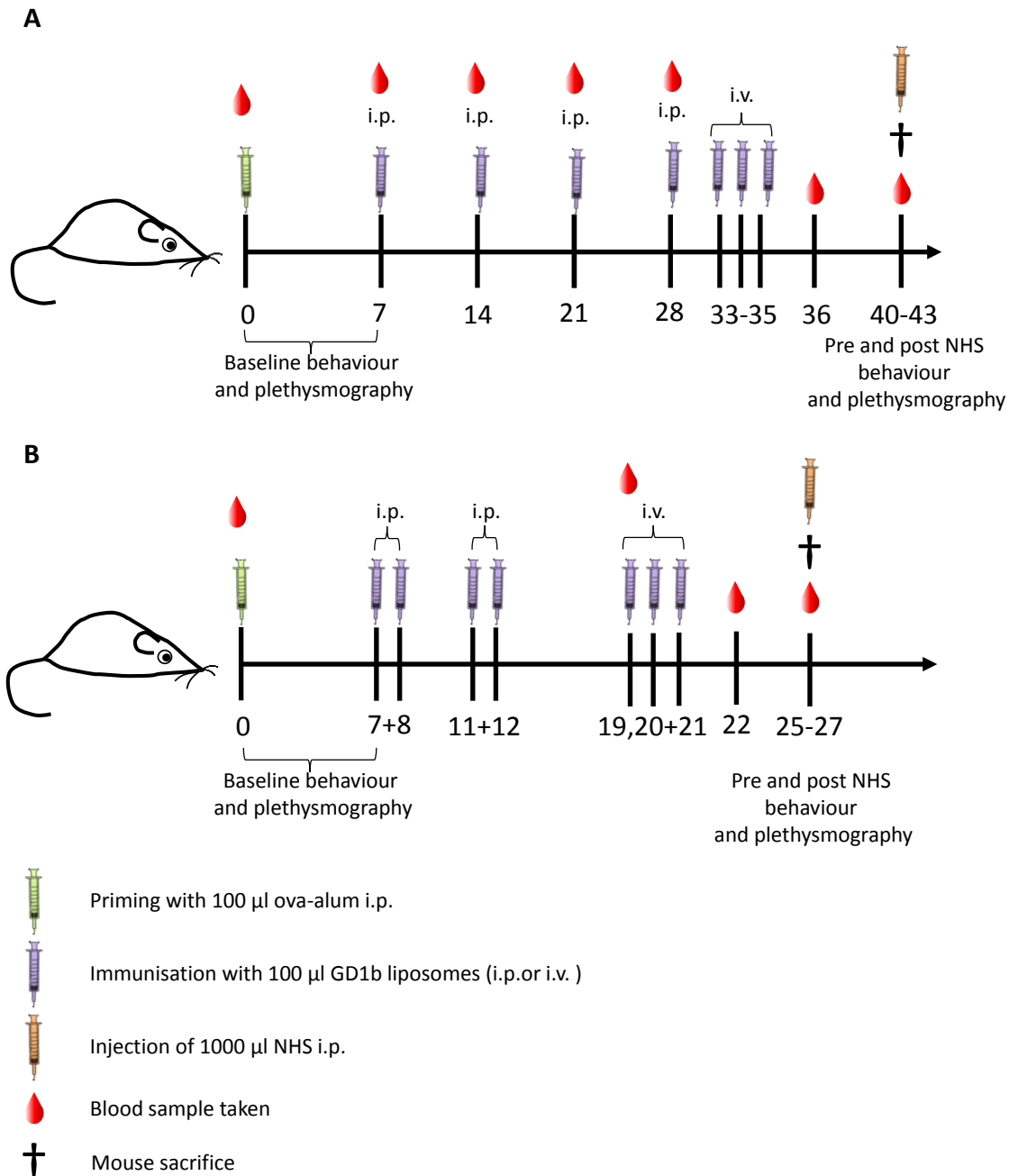


**Figure 2.1: Protocols used for active immunisations.** A. Initial immunisations were carried out using the protocol A. B. A modified protocol was employed for later immunisations.

Behavioural testing and plethysmography were carried out as in section 2.6.2.2 and 2.6.2.3, with the addition of the following behavioural tests:

#### **2.6.4.3 Latency to Platform**

To assess the mice's balance they were placed on a wooden beam 2 cm in diameter which was suspended 60 cm above a foam pillow. At either end of the beam was an enclosed platform. The time taken for the mice to reach this platform was recorded up to 60 seconds. If the mice failed to reach the platform they scored the maximum of 60 seconds. This was repeated 3 times per animal.

#### **2.6.4.4 Grip strength**

Both forelimb and total grip strength was scored using a Chatillon-Ametek digital Force Gauge model DFIS 2 (*Columbus Instruments, OH, USA*) as per manufacturer's instructions. Each animal was scored 6 times for both types of grip assessment.

#### **2.6.4.5 Blood samples**

Blood samples taken from mice were left to clot for 1 hour at room temperature, then centrifuged at 20000 g for 20 minutes at 4°C. Serum was removed and frozen in aliquots at -80°C.

#### **2.6.4.6 Splenocyte isolation**

Splenocytes from actively immunised mice were isolated under sterile conditions by homogenising mouse spleens with a tissue grinder in RPMI and passing through a 70 µm filter. Splenocytes were centrifuged for 10 minutes at 525 g, supernatant discarded and cells were resuspended in fresh RPMI. Cells were diluted 1 in 2 in Trypan blue to identify dead cells and counted using a haemocytometer. Cells were once again centrifuged for 10 minutes at 525 g and resuspended at  $1 \times 10^6$  cells/ml. Cells were either added to ELISpot plates immediately (see section 2.17), or kept in T25 tissue culture flasks for 7 days and supernatant removed and stored at 4°C.

#### **2.6.5 Serum clearance of monoclonal antibody**

A baseline blood sample was taken from mice 1 day before antibody injection. Mice were given 250 µg of monoclonal antibody i.p. on day 0 and further blood samples were taken by tail vein venesection on day 1, 3 and 6, with a terminal

blood sample taken on day 7 upon sacrifice. Spinal cord and diaphragm were harvested from these mice (section 1.7.2)

## **2.7 Dissections**

### ***2.7.1 Triangularis sterni preparation***

The triangularis sterni (TS) is a thin muscle sheet, densely innervated by branches of the third, fourth and fifth intercostal nerves and found on the inner surface of the ribcage. It is ideal for *ex vivo* imaging of distal motor axons and NMJs as it is easy to dissect, fewer than 5 muscle fibres thick, and has NMJs which lie parallel with the muscle. It can therefore be easily imaged whole mount giving clear images, and can be kept alive in a oxygenated physiological solution for several hours following dissection (McArdle et al., 1981).

The TS was isolated from the mice as described previously (Kerschensteiner et al., 2008). Briefly, the body cavity was opened and the rib cage isolated from all surrounding organs and connective tissue, dissected out and pinned flat, with the ventral surface of the ribs facing upwards, in an organ dish coated with Sylgard (*Dow-Corning, MI, USA*), in oxygenated Ringer's solution. The intercostalis internus muscles were removed carefully, revealing the TS below. A "window" of TS muscle with an external border of tissue was excised and pinned in a smaller Sylgard-coated organ dish filled with Ringer's solution.

For stimulation of the intercostal nerves which supply the TS, extra care was taken to ensure nerves were not damaged during dissection. The three nerves were carefully released from the surrounding muscle at the point they enter the ribcage.

### ***2.7.2 Diaphragm dissection***

Mice were pinned out on their backs and the ribcage exposed. The peritoneum was opened and the viscera moved downwards, exposing the diaphragm. For diaphragm sectioning, the diaphragm was cut out and snap frozen before cutting sections of 8  $\mu\text{m}$  using a cryostat (*Bright instruments, Cambridgeshire, UK*) and collecting onto Tissue Tek Adhesion slides (*Sakura Finetek, Alphen aan den Rijn, Netherlands*).

### ***2.7.3 Sciatic and tibial nerve dissection***

Sciatic and tibial nerves were exposed and removed by cutting through the skin overlying the pelvis and blunt dissecting through the overlying muscle. These nerves were pinned onto wax and stored in strong fix (4% PFA/5% glutaraldehyde) until resin processed (see section 2.8)

### ***2.7.4 Lumbrical dissection***

The legs were removed before perfusion fixation and the skin peeled back over the toes revealing the muscles below. The Achilles tendon was cut below the knee and carefully pulled back and removed along with the flexor digitorum brevis muscle and its associated tendons. The tendons of the flexor digitorum longus and the lumbrical muscles which arise in between these tendons were carefully removed. The tendons, with lumbricals still attached, were pinned down in Sylgard-coated dishes in oxygenated Ringer's solution. Lumbricals were stained and analysed as per section 2.9.

### ***2.7.5 Spinal cord dissection***

The skin along the spine was opened and the vertebrae exposed. Forceps were slipped between vertebra and cord and used to perform a laminectomy by simply breaking and peeling back the bones, exposing the spinal cord. Meninges were removed carefully and the cord was cut between the desired segments (as identified by the dorsal roots) and removed. Cord was fixed by storing in 4% PFA overnight then in 30% sucrose overnight. Cord was then embedded in OCT and stored at -80°C.

## **2.8 Resin processing and staining for light microscopy**

Sciatic and tibial nerves from animals that had undergone a sciatic nerve crush were removed from strong fix and washed in sodium cacodylate for 30 minutes in a fume hood. Cacodylate buffer was removed and replaced with 1% osmium tetroxide for two hours at room temperature. Nerves were washed again with sodium cacodylate for 30 minutes. Nerves were then incubated in increasing volumes of ethanol for 20 minutes each (50%, 70%, 80%, 90%, and 100%), followed by a final additional 30 minute incubation in 100% ethanol. Nerves were

then incubated with propylene oxide for 2x 20 minutes, and then left overnight in a 1:1 mixture of araldite:propylene oxide. The following day, this was replaced with a 3:1 mixture of araldite:propylene oxide overnight. Nerves were then oriented in araldite filled moulds and heated at 60°C for 4 days. The remainder of the protocol was kindly carried out in full by Jennifer Barrie: Once the araldite resin had hardened, tissue sections of 1 µm thickness were cut onto microscope slides and dried at 60°C. To stain sections for examination by light microscopy, a methylene blue/azur II stain (1% methylene blue, 1% azure II, 1% disodium tetraborate in dH<sub>2</sub>O) was added to the sections for 30-60 seconds then rinsed off with dH<sub>2</sub>O. Slides were mounted in DPX mounting media then coverslipped.

## 2.9 Lumbrical analysis

Lumbricals from mice which had undergone nerve crush were incubated with BTx-647, 2 µg/ml) in Ringer's for 30 minutes. The muscles were then rinsed with Ringer's and immersion fixed in 4% paraformaldehyde for 30 minutes at 4°C before sequential 10 minute rinses with PBS, 0.1M glycine then PBS. Tissue was then incubated in the anti-NFil antibody 1211, at a dilution of 1/200, overnight at 4°C with 1% Triton X-100. Following this, the tissue was rinsed 3x with PBS and incubated in TRITC-conjugated anti-rabbit IgG (5 µg/ml) for 3 hours at room temperature then rinsed with PBS, mounted and coverslipped. Lumbricals were viewed using a Zeiss Axiolmager Z1 microscope. A total of 100 NMJs were counted and scored as vacant, polyinnervated or monoinnervated. Innervation was determined by the presence or absence of NFil staining overlaying BTx signal and whether or not this staining entered the junction from one or more than one axonal branch.

## 2.10 Antiganglioside antibody studies

### 2.10.1 *Muscle sections*

For antiganglioside antibody binding studies in various muscles, the tissues to be investigated (sternomastoid, diaphragm, sternohyoid, lumbricals or triangularis sterni) were snap frozen before cutting sections of 8 µm using a cryostat (*Bright instruments, Cambridgeshire, UK*) and collecting onto Tissue Tek Adhesion slides

(Sakura Finetek, Alphen aan den Rijn, Netherlands). Monoclonal antiganglioside antibody was applied to slides at 40 µg/ml for 3 hours at 4°C. Appropriate secondary antibody (FITC conjugated) was applied at 3.3 µg/ml along with 1.33 µg/ml BTx-555. Sections were then washed 3x in PBS before coverslipping with Citifluor, sealing with clear nail varnish and storing at -20°C until imaged.

### **2.10.2 Whole mount, live triangularis sterni staining**

To determine the binding profile of monoclonal anti-ganglioside antibodies in live TS, the TS was incubated in 100 µg/ml of the desired antibody with BTx (488, 555 or 647 conjugate, 2 µg/ml) in Ringer's at 4°C for 30 minutes. Tissue was rinsed 3x with Ringer's then fixed in 4% PFA in PBS for 20 minutes at 4°C and rinsed with PBS, 0.1M glycine (dissolved in PBS) and PBS alone again for 10 minutes each. The TS was subsequently dissected away from any remaining excess tissue and then incubated with a subtype-specific FITC (or TRITC) conjugated secondary Ab (5 µg/ml) and 1% normal goat serum (NGS) in PBS overnight at 4°C. The muscle was then mounted on a glass slide, coverslipped with Citifluor, sealed with clear nail varnish and stored at -20°C until imaging.

### **2.10.3 Uptake of antibody at the NMJ**

To look at the uptake of anti-ganglioside antibody at the motor nerve terminal, the TS was incubated with antibody as per section 2.10.2. Following the 30 minute primary incubation and 3x Ringer's wash steps, tissue was either fixed as normal (0 minutes timepoint), or moved to 37°C for 30 or 60 minutes in Ringer's before fixation and secondary incubation. When TS had been imaged and quantified (see section 2.16.3), the coverslip was carefully removed, and the tissue then washed 3x in PBS, incubated in 0.5% Triton X-100 for 30 minutes at 4°C, washed again and incubated in secondary antibody as previously. The permeabilised tissue was then reimaged and requantified.

For some experiments, to determine the fate of antibody following internalisation, a labelled monoclonal antibody was used. For these experiments the labelled antibody was incubated for 30 minutes at 4°C. Preparations were washed and, as above, either left for 30 or 60 minutes in Ringer's at 37°C, or

fixed immediately. These preparations did not require permeabilisation and reimaging.

## **2.11 Anti-ganglioside antibody-mediated injury**

To demonstrate anti-ganglioside-mediated injury to the NT, TS muscle was incubated in a solution of anti-ganglioside antibody as above (see section 2.10.2), followed by a 3x rinse with Ringer's then a 30 minute incubation with 40% NHS in Ringer's at room temperature. The tissue was rinsed 3x with Ringer's. For MAC detection the tissue was incubated in anti-C5b-9 antibody (2.375 µg/ml in Ringers) for 1 hour at room temperature before fixing and rinsing as above. The fixed tissue was incubated again in anti-C5b-9 antibody (2.375 µg/ml in PBS) overnight at 4°C then rinsed 3x with PBS before applying the secondary antibody (5 µg/ml in PBS with 1% NGS) for 3 hours at 4°C. The tissue was then rinsed, coverslipped in Citifluor and stored as above.

## **2.12 Activity dependent uptake experiments**

### **2.12.1 *High potassium stimulation in TS***

To look at the effect of nerve terminal activity on the internalisation of antibodies, following the primary anti-ganglioside antibody incubation and wash steps (section 2.10.2), TS tissue was incubated for 10 minutes at room temperature in either standard Ringer's or high potassium Ringer's solution, then rinsed 3x with standard Ringer's solution. Tissue was then either fixed and incubated with secondary antibody as in section 2.10.2 to look for antibody presence, or incubated with 40% NHS in Ringer's at 37°C for 30 minutes, rinsed 3x with Ringer's then probed for MAC deposition as per section 2.11.

### **2.12.2 *Stimulation of intercostal nerves***

Again following the primary antibody incubation and wash steps (section 2.10.2), intercostal nerves were stimulated with a Grass SD9 square pulse stimulator (*Natus medical Inc., CA, USA*) using platinum electrodes. Live, whole mount TS preparations were stretched out so that successful muscle contraction would be evident. The intercostal nerves which innervate the TS were stimulated for 5 seconds at 10Hz, 30 Volts with a pulse duration of 0.3 ms. Stimulation was

confirmed by muscle twitching evoked by the nerves as opposed to direct muscle stimulation. For comparison of antibody binding, tissue was then fixed and incubated with secondary antibody as in section 2.10.2. For comparison of MAC deposition, TS muscle was incubated with 40% NHS in Ringer's at 37°C for 30 minutes, rinsed 3x with Ringer's then probed for MAC deposition as per section 2.11.

### **2.13 Staining of diaphragm sections from immunised mice**

Diaphragm sections which were previously exposed to antibody plus NHS *in vivo* were stained for presence of IgG or IgM, C3, MAC and NFil as follows. For C3 and IgG/IgM, tissue was incubated in mouse  $\alpha$ -human C3c-FITC (10  $\mu$ g/ml in PBS) or  $\alpha$ -mouse IgG or IgM-FITC (3.33  $\mu$ g/ml in PBS) for 3 hour at 4°C. MAC deposition was stained for by incubating tissue in mouse  $\alpha$ -human C5b-9 (2.375  $\mu$ g/ml in PBS) for 1 hour at 4°C then following 3x rinses in PBS, for 1 hour in  $\alpha$ -mouse IgG2a-FITC (3.33  $\mu$ g/ml in PBS) at 4°C. Each solution contained BTx-555 (1.33  $\mu$ g/ml). For NFil staining, tissue was incubated with BTx-555 for 1 hour at 4°C, then rinsed and incubated in 1/200 rabbit polyclonal 1211 overnight in 1% Triton and 1% NGS. Tissue was then rinsed and incubated in goat anti-rabbit-488 (4  $\mu$ g/ml in PBS) for 2 hours at 4°C. All tissue was rinsed in PBS before being mounted in Citifluor then coverslipped.

### **2.14 Spinal cord staining**

Transverse sections of spinal cord were cut at 15  $\mu$ m, air dried then stored at -20°C. Sections were first washed 3x with 0.5% Triton X-100/PBS then blocked for 1h at room temperature in 3% NGS/PBS. Primary antibodies were applied overnight at 4°C in 3% NGS/PBS at the dilutions or concentrations stated in Table 2.1. The following day, relevant secondary antibodies were applied for 3 hours at 4°C.

### **2.15 Topical complement assay**

Diaphragms from naïve wildtype mice were removed, snap frozen and stored at -80°C before being cut into 8  $\mu$ m sections. Serum from actively immunised mice was heat inactivated at 56°C for 30 minutes to inactivate complement proteins,

before adding neat to tissue sections for 2 hours at 4°C. Monoclonal antibody (20 µg/ml) was added as a positive control. Following a 3x rinse in PBS, sections were incubated with 4% NHS in Ringer's solution for 1 hour at 37°C. After another 3x PBS rinse, sections were incubated with anti-human C5b-9 (2.375 µg/ml) and BTx-555 (1.33 µg/ml) in PBS for 2 hours at 4°C. Tissue was rinsed 3x in PBS then incubated with anti-mouse IgG2a-Cy5 (3.33 µg/ml in PBS) for 1 hour at room temperature before rinsing and coverslipping.

## **2.16 Microscopy**

### **2.16.1 *Light microscopy***

Images of stained sciatic and tibial nerves were captured using a light microscope and the resulting images were analysed for presence of myelinated fibres in a 200 µm ROI. One image was taken per animal using a 20x objective.

### **2.16.2 *Fluorescent microscopy***

Images for analysis of fluorescent intensity (section 2.16.3) or percentage of NFil at the nerve terminal (section 2.16.4) were captured as single slices using an LSM 5 Pascal or LSM 510 microscope. The LSM 5 Pascal was used for tissue which had been stained with Rhodamine/555 conjugates and FITC/488 conjugates, whereas the LSM 510 allowed quantitative imaging of tissues which had been stained using cy5-conjugates or DAPI. For experiments where comparisons were being made between genotypes, tissue was coded and analysed blinded.

Pinhole size and amplifier gain were set at the beginning and kept consistent throughout each experiment. For analysis of diaphragm sections, each mouse/antibody to be analysed was imaged in triplicate using a 40x objective, with 15 images taken of each section of tissue with several NMJs in each image, so as to total over 100 NMJs imaged per animal/antibody.

For whole mount TS, at least 15 images were taken of each tissue, again with several NMJs per image. Although a thin muscle, TS is nonetheless thicker than sectioned tissue and therefore has superficial and deep NMJs. As any antibody was more likely to be uniformly present on the topmost layers, images were

taken of the superficial NMJs. This normally totalled around 50 NMJs imaged per animal.

Illustrative images of whole mount tissue were taken using a Zeiss AxioImager Z1 microscope with ApoTome attachment, which uses structured illumination to capture high resolution images. Images were captured as stacks and displayed as maximum intensity projections (MIPs). These are 2D renderings of the 3D image which are constructed using AxioVision 4.7.2 software.

### 2.16.3 *Fluorescent intensity at the nerve terminal*

To quantify the fluorescent intensity at the nerve terminal, the fluorescent intensity overlying the BTx signal was measured using ImageJ software (NIH, MD, USA). To do this, the BTx signal was thresholded between 50 and 255 pixels. Each area of BTx was then selected as a region of interest (ROI), and overlaid onto the channel of the antibody being measured. The mean intensity grey value was then measured in this ROI, generating a pixel value between 0 and 255 (Figure 2.2).

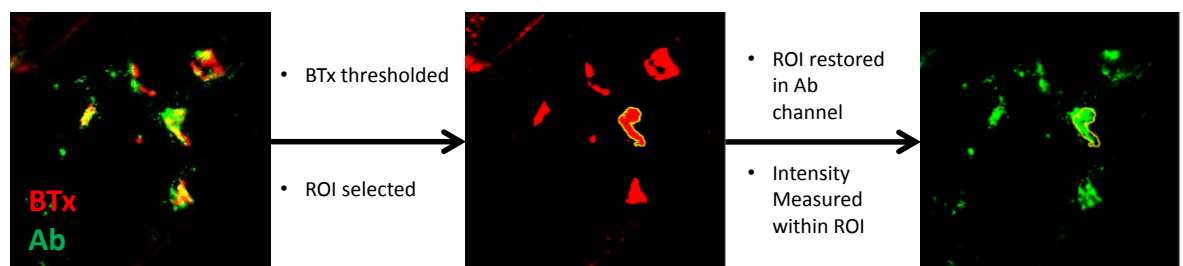


**Figure 2.2: Measurement of fluorescent intensity overlying the endplate.** The first image shows the merged signal from BTx (red) and antibody (green). Throughout the thesis this antibody may be against mouse anti-ganglioside antibodies, human C3 or human MAC. In the next image the BTx has been thresholded and one junction has been selected as a ROI (selection bordered by yellow line). This ROI is overlaid onto the antibody channel as shown in the third image and the mean pixel intensity is measured within the ROI. The process is repeated for all NMJs in the image.

### 2.16.4 *Percentage coverage of NFil at the nerve terminal*

To measure the extent damage to the nerve terminal structure, the percentage coverage of nerve terminal by NFil was calculated. Using ImageJ, both BTx and the NFil signals, were thresholded. Again the BTx was selected as a ROI and

overlaid onto the NFil channel. The % area coverage within this ROI was then measured (Figure 2.3).

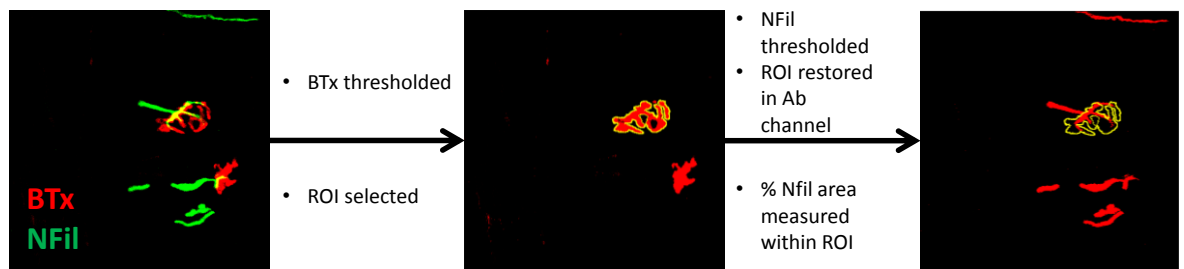


**Figure 2.3: Measurement of percentage NFil coverage.** The first image shows the merged signal from BTx (red) and NFil (green). In the next image the BTx has been thresholded and one junction has been selected as a ROI (selection bordered by yellow line). The third image shows the NFil channel which has also been thresholded (now shown in red). The ROI from the BTx channel is then overlaid onto the thresholded NFil channel and the % area of NFil within the ROI is measured.

Both of the above methods of quantification were performed using macros modified from ones originally generated by former lab member, Peter Humphries.

### 2.16.5 CFP counts

As an alternative to using percentage NFil coverage, in fluorescent mice, damage to nerve terminals could also be measured by manually assessing percentage of NMJs which contained CFP. A NMJ was scored as having CFP if CFP was present in a normal distribution overlying the BTx, regardless of intensity (Figure 2.4). One hundred NMJs were assessed per animal per condition.

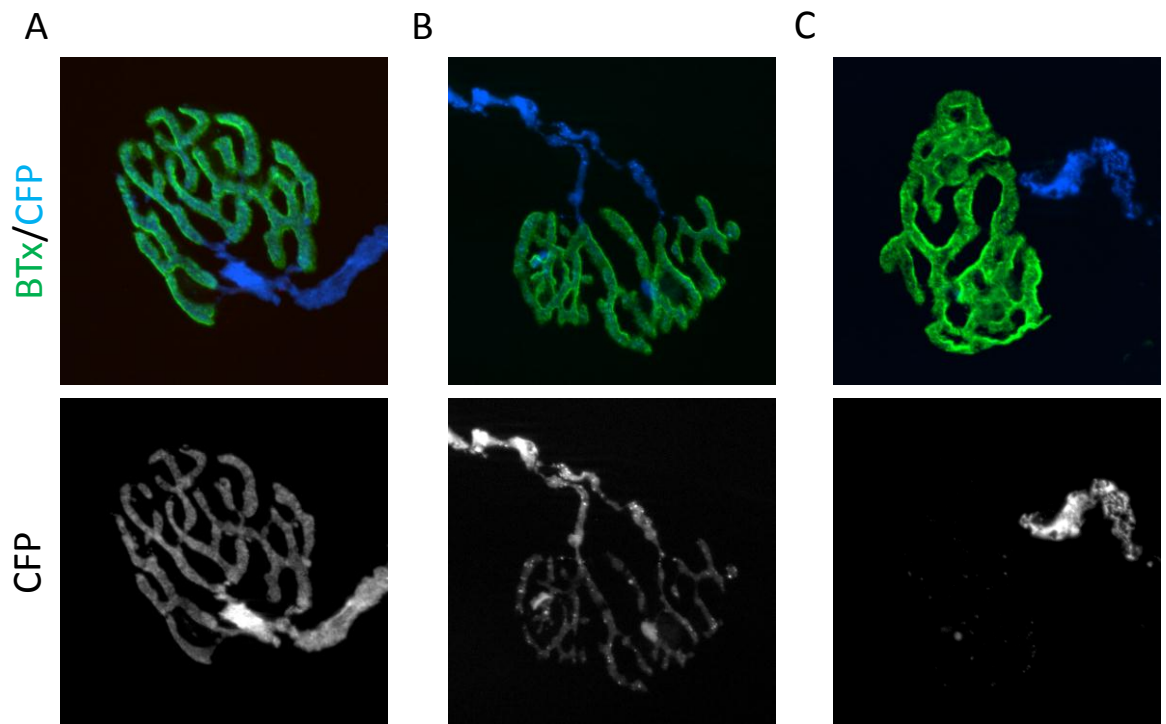


**Figure 2.4: Illustrative examples of CFP presence at the NMJ.** **A:** CFP in an undamaged nerve terminal. CFP follows the line of the BTx. **B:** CFP at a slightly injured nerve terminal. The CFP is less bright than in **A**, but is still present in a normal distribution overlying the BTx signal. **C:** A damaged nerve terminal with CFP present in the distal axon but not in the nerve terminal overlying the BTx. **A** and **B** are examples of nerve terminals which would be scored at “CFP present”, whereas **C** would be scored as “CFP absent”.

## 2.17 ELISpots

To quantitatively determine antigen-specific responses in mice which were immunised with ganglioside-containing liposomes, ELISpots were performed. MultiScreen-IP Filter Plates (*Merk Millipore, Billerica, MA, USA*) were activated with 35  $\mu$ l 35% ethanol for 30 seconds. Ethanol was discarded and plates coated with 100  $\mu$ l of 50  $\mu$ g/ml GD1b in 100% ethanol, or ethanol only for blank wells. When ethanol had evaporated, plates were blocked with RPMI with 10% FCS for 1 hour in a CO<sub>2</sub> incubator at 37°C. Block was discarded and 100  $\mu$ l previously isolated splenocytes (see section 2.6.3.6) were added at 10<sup>6</sup> cells per well, overnight in a CO<sub>2</sub> incubator at 37°C. The following day cells were discarded and plates washed 4x in PBS before incubating with secondary antibody (HRP conjugated goat anti-mouse IgG or IgM) for 1 hour at 4°C. Secondary was discarded and plates washed a further 4x in PBS. Plates were developed by

incubation with 3-Amino-9-ethylcarbazole (AEC) substrate. Solution was prepared by adding 1 AEC tablet (*Sigma-Aldrich, St Louis, MO, USA*) to 2.5 ml of *N,N*-dimethylformamide (DMF) in a fume hood. When tablet was fully dissolved, the 2.5 ml solution was added to 47.5 ml of 50 mM acetate buffer (14.8 mM  $C_2H_4O_2$ , 35.3 mM  $C_2H_3NaO_2$ ) and 25  $\mu$ l of 30%  $H_2O_2$  added immediately prior to use. The AEC substrate solution (100  $\mu$ l) was added to wells for around 20 minutes, or until spots began to develop. Reaction was stopped by washing wells with  $dH_2O$ . Wells were imaged using an AID ELISpot reader (*Autoimmun Diagnostika GmbH, Strassberg, Germany*) and spots were counted either manually or using the provided AID software.

## 2.18 ELISAs

To test for anti-ganglioside antibody reactivities, lipid ELISAs were performed. Immulon-2HB 96 well plates (*Thermo Fisher Scientific, MA, USA*), were coated with 200 ng of GD1b in methanol, or methanol only for blank wells. Plates were left to dry overnight at room temperature in a fume hood, then blocked with 200  $\mu$ l 2% bovine serum albumin (BSA)/PBS solution per well for 1 hour at 4°C. Block was discarded and mouse serum (1/100 in 0.1% BSA solution) or neat splenocyte supernatant (concentrated 5x) was added to both positive and negative wells. Monoclonal antibodies were used as positive controls and were used at 50  $\mu$ g/ml in 0.1% BSA and, if used as a standard, serial diluted 1 in 2. Each sample was run in triplicate. Plates were left overnight at 4°C then primary solution discarded. Plates were washed 3x in PBS then secondary antibody (goat anti-mouse IgG or IgM-HRP) was added at 30 ng/ml, in 0.1% BSA solution for 1 hour at 4°C. Plate was washed in PBS 3x then 100  $\mu$ l OPD substrate solution (30ml  $dH_2O$ , 16ml 0.2M  $Na_2HPO_4$ , 14ml 0.1M  $C_6H_8O_7$ , 1 OPD tablet and 20  $\mu$ l 30%  $H_2O_2$  added immediately prior to use) was added to each well. Plates were left to develop for 20 minutes at room temperature in the dark before addition of 50  $\mu$ l stop solution (4M  $H_2SO_4$ ) to each well. Plates were read at 492 nm on a Tecan Sunrise™ automated microplate reader (*Tecan Group Ltd, Männedorf, Switzerland*) using the provided Magellan™ software.

## 2.19 Glycoarray

Using combinatorial glycoarray (Rinaldi et al., 2009), serum and monoclonal antibodies were tested against single lipids and lipids complexes. Slides were pre-prepared by applying Immobilon-FL PVDF membrane (*Merk Millipore, Billerica, MA, USA*) to glass slides using photomount glue (*3M, MN, USA*). Once glue was dry, 0.1  $\mu$ l of each lipid or premixed lipid complex (100  $\mu$ g/ml for single lipid, 50  $\mu$ g/ml for each of the lipids in complex) was spotted using an automatic TLC sampler (*CAMAG, Muttenz, Switzerland*), onto the slides. Once spotted, slides were left overnight at 4°C then blocked with 2% BSA for 1 hour at room temperature. Serum (1/100 in 1% BSA) or monoclonal antibody (10  $\mu$ g/ml in 1% BSA) was applied to slides for 1 hour at 4°C. Following 2x 15 minute washes in 1% BSA, goat anti-mouse IgG or IgM 555 or 647-conjugated antibody was applied (2  $\mu$ g/ml in 1% BSA) for 1 hour at 4°C. Slides were washed 2x 30 minutes in 1% BSA, followed by 1x 5 minutes wash with PBS and 1x 5 minute wash with dH<sub>2</sub>O. Slides were left to dry overnight at 4°C then scanned using a ScanArray express microarray scanner (*Perkin-Elmer, Waltham, MA, USA*). Images from labelled DG2 antibody were taken on a Typhoon 8600 Variable Mode Imager (*GE Healthcare Life Sciences, Little Chalfont, UK*) as the ScanArray did not have a laser of the correct wavelength.

## 2.20 Statistics and display of data

All graphs were composed in GraphPad Prism 6 and all statistical tests were calculated using this software, using  $p < 0.05$  as the value of significance.

Immunohistological data on antibody intensity or NFil coverage (section 2.16.3 and 2.16.4) are considered to be nonparametric and as such, results from each NMJ are displayed as Tukey box and whisker plots. The horizontal line displays the median of the data, with the top and bottom of the box representing the 75<sup>th</sup> and 25<sup>th</sup> percentile respectively. Top whiskers denote the 75<sup>th</sup> percentile plus 1.5x the interquartile range (IQR). Bottom whiskers denote the 25<sup>th</sup> percentile minus 1.5x the IQR and any values outwith this range are plotted as individual points. Unless stated otherwise, ROUT analysis was conducted in

GraphPad Prism 6 to remove outliers caused by high background signal (maximum desired false discovery rate of 1%).

Bar graphs shown in this thesis show error bars representing the standard error of the mean from results from each animal tested. Statistical tests used for each figure are shown in the figure legends.

## **3 Rescue of complex ganglioside in neuronal and glial membranes**

### **3.1 Introduction**

The generation of complex ganglioside rescue mice driven by GalNAcT expression in neurons and glia is an important step in the generation of an animal model of GBS (Yao et al., 2014). This lab has developed three strains of mouse which have neuronal rescue of GalNAcT expression and one which has glial rescue. The three neuronal rescue strains have GalNAcT expression driven by the NFL promoter in one mouse strain and by the Thy1 promoter in the other two. Before using these mice as part of experimental paradigms, they needed to be characterised. Therefore this chapter focuses on the demonstration and localisation of ganglioside expression in these mice, which was also the basis for the selection of mouse strains, antibodies and antigens for future work. Additionally, this chapter includes some preliminary work characterising the phenotypic consequences of ganglioside rescue, including gait analysis differences and comparison of nerve regeneration. Wildtype mice have been shown to perform better than GalNAcT<sup>-/-</sup> mice in various behavioural tests from 4 months of age (Chiavegatto et al., 2000). This difference in behavioural phenotype is accompanied by neuronal degeneration as discussed in chapter 1, therefore it was expected that a neuronal reintroduction of complex ganglioside expression may result in an improvement in phenotype.

## 3.2 Comparison of binding profiles of different antibodies in mice with restored neuronal complex ganglioside expression

To demonstrate that the rescue mice generated had restored ganglioside expression, the nerve terminal antibody staining profile of 4 antibodies was compared in a number of different muscle sections from three different “neuronal rescue” mouse strains. The results were subsequently used to determine which antigen to concentrate on in future experiments. One such rescue mouse has GalNAcT enzyme expression driven by the NFL promoter and the other two driven by the Thy1 promoter. For this chapter only these mice will be referred to as NFLTg, Thy1Tg(112) and Thy1Tg(115) mice. The results of this section will also determine which of these three strains of “neuronal rescue” mouse to bring forward for use in future experiments. Nerve terminal antibody staining was calculated by measuring the antibody intensity overlying the BTx, representing the nerve terminal. Data were analysed by Kruskal-Wallis with Dunn’s multiple comparison test against wildtype mice, with GalNAcT<sup>-/-</sup> shown as negative controls. Three animals from each strain were analysed.

### 3.2.1 MOG3 staining

The anti-GD1b antibody MOG3 bound with high intensity to the nerve terminals of all muscle groups in each mouse strain, with the exception of the GalNAcT<sup>-/-</sup> mouse which lacks GD1b (Figure 3.1). This antibody binds strongly to wildtype nerve terminals in all muscles and staining is abolished in the GalNAcT<sup>-/-</sup> mice. In NFLTg mice, staining is rescued to levels akin to that of the wildtype in lumbricals and shows intensity levels higher than that of the wildtype in all other muscles. Similarly, the Thy1Tg(112) mouse had statistically similar staining to wildtype mice in lumbricals and significantly higher staining in all other tissues. Thy1Tg(115) mice, however, had significantly lower staining intensity than wildtype mice in all muscles, with the exception of the sternomastoid. Additionally, these mice had a much larger IQR than the other genotypes with MOG3. Using sternomastoid muscle as an example, wildtype mice had a median staining intensity of 167 AU, with an IQR of 131 AU. Thy1Tg(115) mice showed a much more wide spread of data with a median of 130.0 AU and an IQR of 245.5 AU. Upon examination of the images, this large IQR appeared to be due to

inconsistencies between NMJ staining in the same muscle, with only some NMJs having positive staining. In contrast, wildtype, NFLTg and Thy1Tg(112) had much more consistent staining between NMJs in the same muscle.

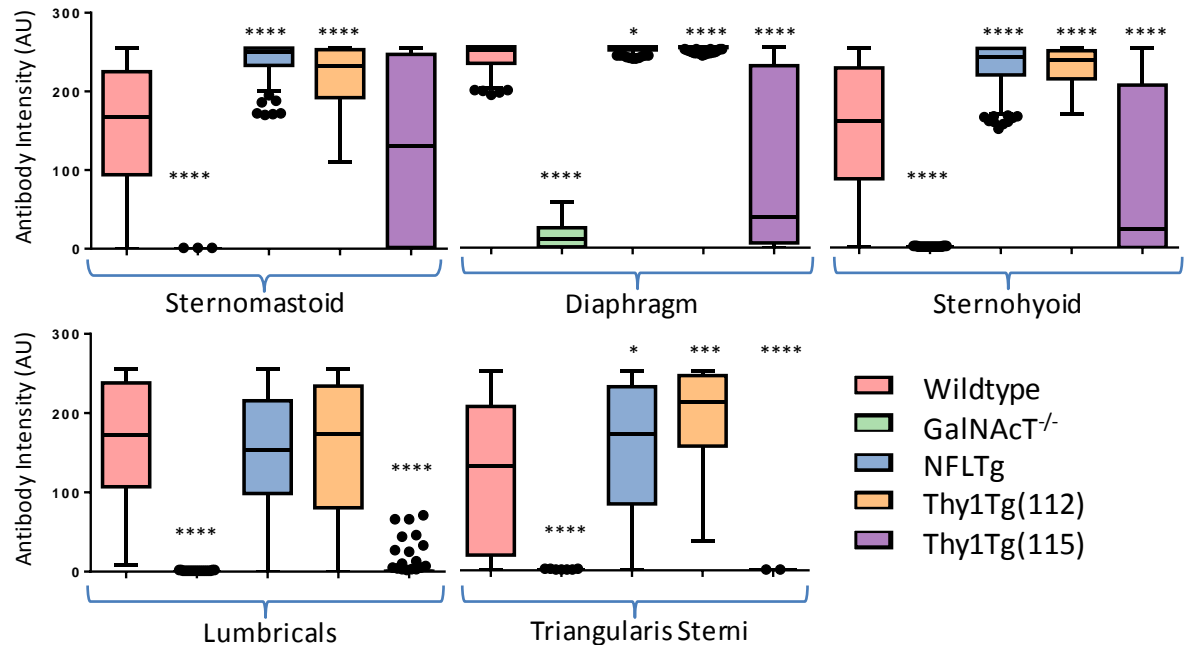


**Figure 3.1: Anti-GD1b staining at the nerve terminal in various muscles in wildtype, GalNAcT<sup>-/-</sup>, NFLTg and Thy1Tg (line 112 and 115) mice (n=3 per group).** Sections of muscle were stained with MOG3, a monoclonal anti-GD1b antibody followed by anti-mouse IgG3-TRITC secondary antibody. NMJs were identified with the addition of BTx-488. Staining was quantified by the intensity of antibody overlying BTx staining. Staining was observed in wildtype mice and abolished in GalNAcT<sup>-/-</sup> mice. NFLTg and Thy1Tg(112) showed either comparable staining to wildtype or higher staining than wildtype mice. Staining in Thy1Tg(115) was consistently lower than wildtype mice except in sternomastoid. Kruskal-Wallis with Dunn's multiple comparisons test vs wildtype mice. \*= $p < 0.05$ , \*\*= $p < 0.001$ , \*\*\*\*= $p < 0.0001$ . Non-parametric data displayed as Tukey box plot (see section 2.20).

### 3.2.2 DG2 staining

In mice tested against anti-GM1 antibody DG2, all rescue strains showed some degree of staining in sternomastoid and diaphragm (Figure 3.2). In sternomastoid muscle, this staining was consistently lower than wildtype mice but in diaphragm NFLTg mice show significantly higher staining intensity than wildtype mice, whereas both Thy1Tg strains were statistically similar to wildtype. In sternohyoid muscle NFLTg and Thy1Tg(112) again showed a restoration of staining intensity but not to levels akin to wildtype mice. In contrast, staining in Thy1Tg(115) mice was not restored. In the lumbricals and TS muscle, staining was also very low or

negative in all rescue strains, indicating a much lower restoration of GM1 in these tissues.

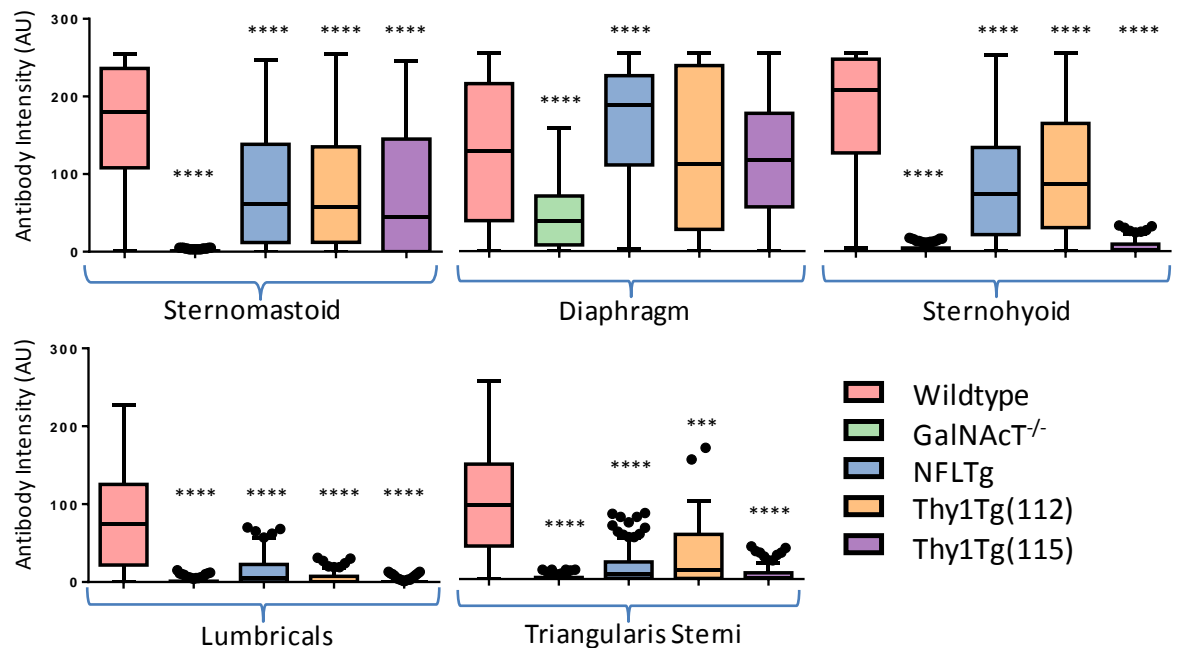


**Figure 3.2: DG2 staining at the nerve terminal in various muscles in wildtype, GalNAcT<sup>-/-</sup>, NFLTg and Thy1Tg (line 112 and 115) mice (n=3 per group).** Sections of muscle were stained with DG2, a monoclonal anti-GM1 antibody, followed by anti-mouse IgG3-TRITC secondary antibody. NMJs were identified with the addition of BTx-488. Staining was quantified by the intensity of antibody overlying BTx staining. Staining was observed in wildtype mice and abolished in GalNAcT<sup>-/-</sup> mice. NFLTg, Thy1Tg(112) and Thy1Tg(115) showed a degree of restored antibody staining but this was consistently lower to wildtype except NFL Tg diaphragm. Kruskal-Wallis with Dunn's multiple comparisons test vs. wildtype mice. \*\*\*=p<0.001, \*\*\*\*=p<0.0001. Non-parametric data displayed as Tukey box plot (see section 2.20)

### 3.2.3 DG1 staining

DG1 is an antibody which binds to GM1 in ELISA but not in live wildtype mice tissue. This has been shown to be due to the inhibition of its binding to GM1 by nearby GD1a (Greenshields et al., 2009). This antibody was included in this panel screening to test whether the rescue of GalNAcT expression in neurons resulted in similar ganglioside distribution on the membrane. If the restored gangliosides were similarly distributed to wildtype mice, it would be expected that the DG1 would not bind.

As was the case in wildtype mice, DG1 showed very little/no staining in most tissues (Figure 3.3). Diaphragm appears to have high staining in all rescue strains but this was due to high background fluorescence in this tissue, though all rescue strains were higher than wildtype mice. However diaphragm was the only muscle where this was the case as all other muscles showed either statistically similar or lower staining than in wildtype mice.

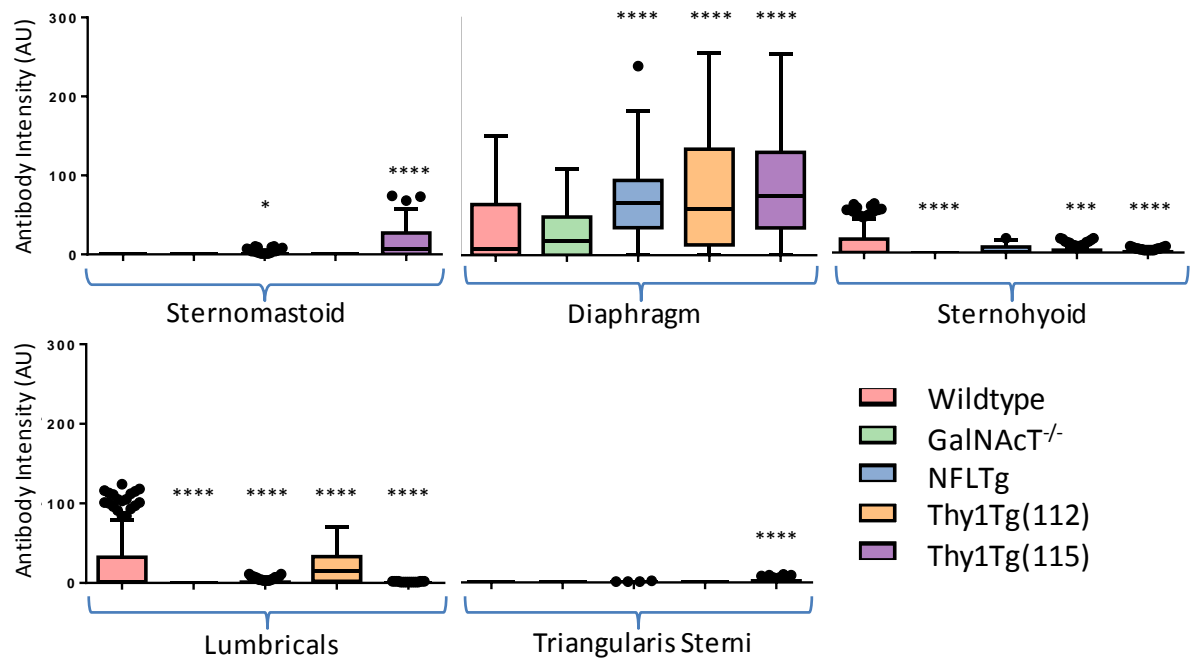


**Figure 3.3: DG1 staining at the nerve terminal in various muscles in wildtype, GalNAcT<sup>-/-</sup>, NFLTg and Thy1Tg (line 112 and 115) mice (n=3 per group).** Sections of muscle were stained with DG1, a monoclonal anti-GM1 antibody which has previously been shown not to bind live wildtype tissue, followed by anti-mouse IgG2b-TRITC secondary antibody. NMJs were identified with the addition of BTx-488. Staining was quantified by the intensity of antibody overlying BTx staining. Staining was not observed in wildtype mice and NFLTg, Thy1Tg(112) and Thy1Tg(115) showed staining similar or lower than wildtype mice in all muscles except diaphragm, where they had significantly higher staining. Kruskal-Wallis with Dunn's multiple comparisons test vs wildtype mice. \*= $p < 0.05$ , \*\*= $p < 0.001$ , \*\*\*\*= $p < 0.0001$ . Non-parametric data displayed as Tukey box plot (see section 2.20)

### 3.2.4 MOG35 staining

This anti-GD1a antibody has also been shown to bind poorly in wildtype mouse tissue, instead optimal binding being shown previously in GD3s<sup>-/-</sup> which over-express GD1a (Goodfellow et al., 2005).

As expected, MOG35 showed poor staining in all wildtype muscle (Figure 3.4). This poor staining was reflected in rescue lines with each muscle being negative for MOG35 presence at the nerve terminal.

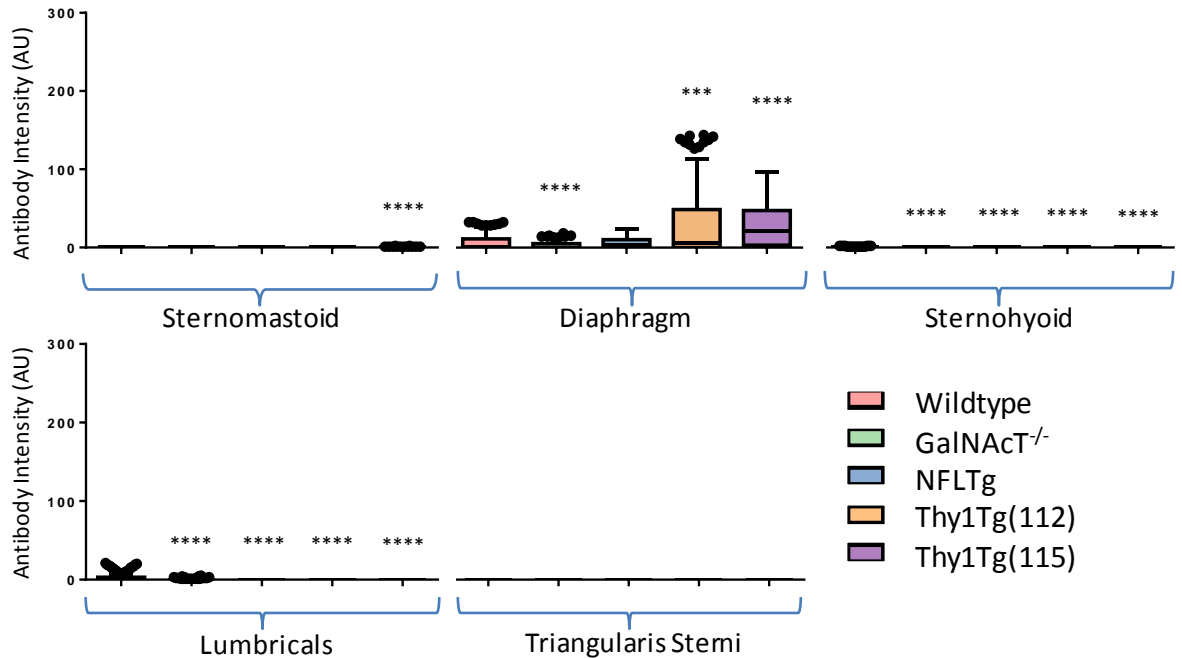


**Figure 3.4: MOG35 staining at nerve terminals in various muscles in wildtype, GalNAcT<sup>-/-</sup>, NFLTg and Thy1Tg (line 112 and 115) mice (n=3 per group).** Sections of muscle were stained with MOG35, a monoclonal anti-GD1a antibody which has previously been shown not to bind well in wildtype tissue, followed by anti-mouse IgG2b-TRITC secondary antibody. NMJs were identified with the addition of BTx-488. Staining was quantified by the intensity of antibody overlying BTx staining. Staining was not observed in either wildtype mice or any of the rescue strains Kruskal-Wallis with Dunn's multiple comparisons test vs. wildtype mice. \*= $p < 0.05$ , \*\*\*= $p < 0.001$ , \*\*\*\*= $p < 0.0001$ . Non-parametric data displayed as Tukey box plot (see section 2.20)

### 3.2.5 Summary

As Thy1Tg(115) appeared to show inconsistent expression of GalNAcT-driven GD1b, this line was immediately ruled out to be carried forward for future experiments. Differences between Thy1Tg(112) and NFLTg were minor and often when staining was statistically different to wildtype mice, there was no statistical difference between the two neuronal rescue strains. For this reason, and due to the ongoing characterisation of this mouse by other members of the lab, the NFLTg was used as data generated by both myself and other lab members could be mutually beneficial.

### 3.3 Illustrative binding profiles of GalNAcT<sup>-/-</sup>-*Tg(neuronal)* and GalNAcT<sup>-/-</sup>-*Tg(glial)* mice

Having selected mice with NFL-driven GalNAcT expression, these mice will now be known throughout this thesis as GalNAcT<sup>-/-</sup>-*Tg(neuronal)* mice. As quantitative staining intensity data does not fully show the nuances of antibody binding, whole mount illustrative images were taken of those antibodies which had produced the best binding in the various muscle sections. Additionally, another GD1b antibody which also binds to GT1b, MOG16, was used. In addition to the previously investigated GalNAcT<sup>-/-</sup>-*Tg(neuronal)* mouse, GalNAcT<sup>-/-</sup>-*Tg(glial)* mice were incorporated to investigate binding differences between mice with neuronal and glial directed expression of GalNAcT and thus complex gangliosides. For this study live TS muscle was used.

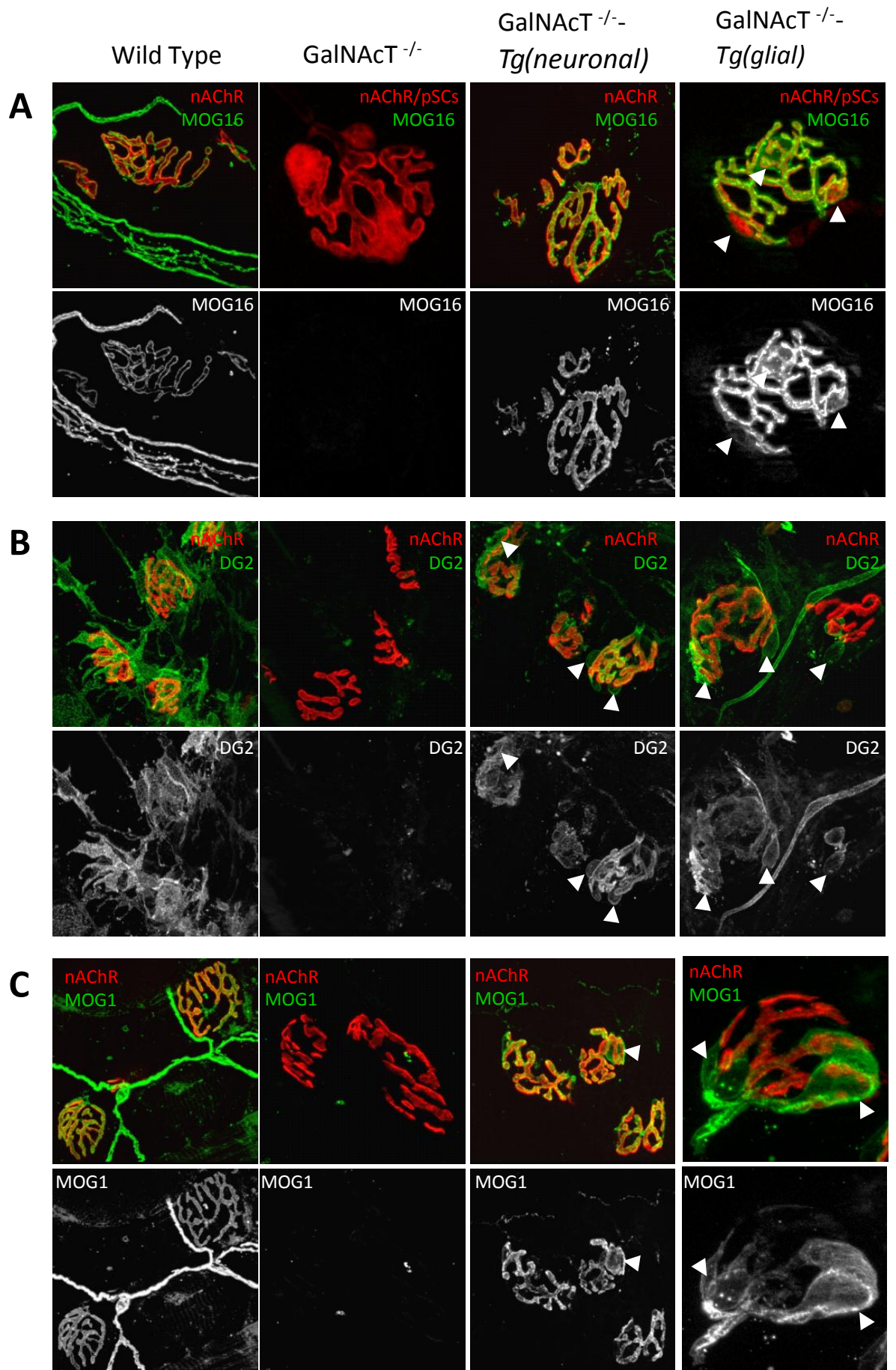


(Figure on previous page)

**Figure 3.5: Binding pattern in TS muscles of mouse monoclonal antibodies in four mouse strains.** Staining with antibodies against complex gangliosides is absent in GalNAcT<sup>-/-</sup> mice but restored in neuronal and glial structures in GalNAcT<sup>-/-</sup>-*Tg(neuronal)* and GalNAcT<sup>-/-</sup>-*Tg(glial)* mice respectively. MOG16 (A) binds clearly to neuronal structures in wildtype and GalNAcT<sup>-/-</sup>-*Tg(neuronal)* mice. In GalNAcT<sup>-/-</sup>-*Tg(glial)* mice, pSC body staining is seen weakly, as well as more strongly to processes overlying the NMJ. This is also the case for DG2 (B) and MOG1 (C), though some additional glial staining is seen in GalNAcT<sup>-/-</sup>-*Tg(neuronal)* mice (indicated by arrows). DG2 also binds kranocytes in wildtype mice which partially obscure the neuronal staining seen at the NMJ.

As was the case for sectioned muscle, all antibodies bound well in wildtype mice and were absent in GalNAcT<sup>-/-</sup> mice. Once again, staining was reinstated in both rescue strains. However, slight differences were seen in the specific NMJ structures being bound in the different rescue mice strains. MOG16 staining shows a neuronal binding pattern in wildtype mice, with no apparent pSC staining (Figure 3.5A). This neuronal pattern of staining is rescued in GalNAcT<sup>-/-</sup>-*Tg(neuronal)* mice, where gangliosides should be available on the axonal membrane. In GalNAcT<sup>-/-</sup>-*Tg(glial)* mice, staining is also present but is on glial, rather than neuronal structures (pSC body indicated by white arrowhead). A similar staining pattern is found with MOG1 (Figure 3.5B), with neuronal binding seen in wildtype and GalNAcT<sup>-/-</sup>-*Tg(neuronal)* mouse. Interestingly however, pSCs also appear to be bound by MOG1 in GalNAcT<sup>-/-</sup>-*Tg(neuronal)* mice, though this does not occur in wildtype mice. In the GalNAcT<sup>-/-</sup>-*Tg(glial)* mouse, MOG1 staining is seemingly only on the pSC cell bodies and the processes it extends over the NMJ. In wildtype mice, DG2 binds to GM1-positive kranocytes which can be seen capping the NMJ (Figure 3.5C), when no kranocyte staining was present, clear nerve terminal binding could be seen. Neuronal and again also glial structures show positive DG2 staining in GalNAcT<sup>-/-</sup>-*Tg(neuronal)* mice, whereas in the GalNAcT<sup>-/-</sup>-*Tg(glial)* mouse, binding appears to be present only on glial structures, though not on processes over every NMJ (example image shows one NMJ with DG2 staining over processes and one without). However, it is important to note that in both rescue strains, no kranocyte staining is present with DG2, confirming the KO of GalNAcT in other cell types.

### 3.4 Comparison of gait parameters between wildtype, GalNAcT<sup>-/-</sup> and rescue mouse strains

Observationally, GalNAcT<sup>-/-</sup>-*Tg(neuronal)* mice lack the age-dependant phenotype seen with GalNAcT<sup>-/-</sup> mice. Contrastingly, the phenotype of GalNAcT<sup>-/-</sup>-*Tg(glial)* appears equal to, or worse than, GalNAcT<sup>-/-</sup> mice, with an apparent exaggeration of the Parkinson-like tremor. It has already been demonstrated that this degenerative phenotype is accompanied by alterations in gait parameters in GalNAcT<sup>-/-</sup> mice when compared to wildtype mice (Chiavegatto et al., 2000). Specifically, GalNAcT<sup>-/-</sup> mice were shown to have a reduced stride length, stride width and hind-paw print length. Therefore, to see if the observational differences in phenotype of the rescue mice could be quantified, mice were trained on a Digigait™ treadmill and gait parameters were measured. As some animals do not run well on the treadmill, even following training, the groups were as follows: wildtype n=4, GalNAcT<sup>-/-</sup> n=4, GalNAcT<sup>-/-</sup>-*Tg(neuronal)* n=7, GalNAcT<sup>-/-</sup>-*Tg(glial)* n=3.

Of the parameters measured by the Digigait™ software, 6 are shown (Figure 3.6). These include the equivalent measurements which were previously shown to be altered in GalNAcT<sup>-/-</sup> mice, with stance width substituting for stride width and paw area for paw print length. No significant differences were observed in stance width, stride length and paw area between wildtype mice and GalNAcT<sup>-/-</sup>, GalNAcT<sup>-/-</sup>-*Tg(neuronal)* or GalNAcT<sup>-/-</sup>-*Tg(glial)* (Figure 3.6 A, C, E). Hind limbs have an increased stance width variability in GalNAcT<sup>-/-</sup> (p<0.05) and GalNAcT<sup>-/-</sup>-*Tg(glial)* mice compared to wildtype, though this does not reach significance in the GalNAcT<sup>-/-</sup>-*Tg(glial)* mice (Figure 3.6B). Similarly, stride length variability is significantly higher in both left and right forelimbs in GalNAcT<sup>-/-</sup> (p<0.05) and GalNAcT<sup>-/-</sup>-*Tg(glial)* (p<0.001 for left forelimb, p<0.05 for right forelimb) mice compared with the normal fluctuations in stride length (about 1cm in wildtype mice). The GalNAcT<sup>-/-</sup>-*Tg(neuronal)* mice do not show any differences from wildtype mice. Finally, paw area variability is increased in GalNAcT<sup>-/-</sup>-*Tg(glial)* hind limbs (p<0.001) and left forelimb (p<0.001). GalNAcT<sup>-/-</sup> mice show similar paw area variability to wildtype in hind limbs but a slight increase in both forelimbs, reaching significance in the left forelimb (p<0.05).

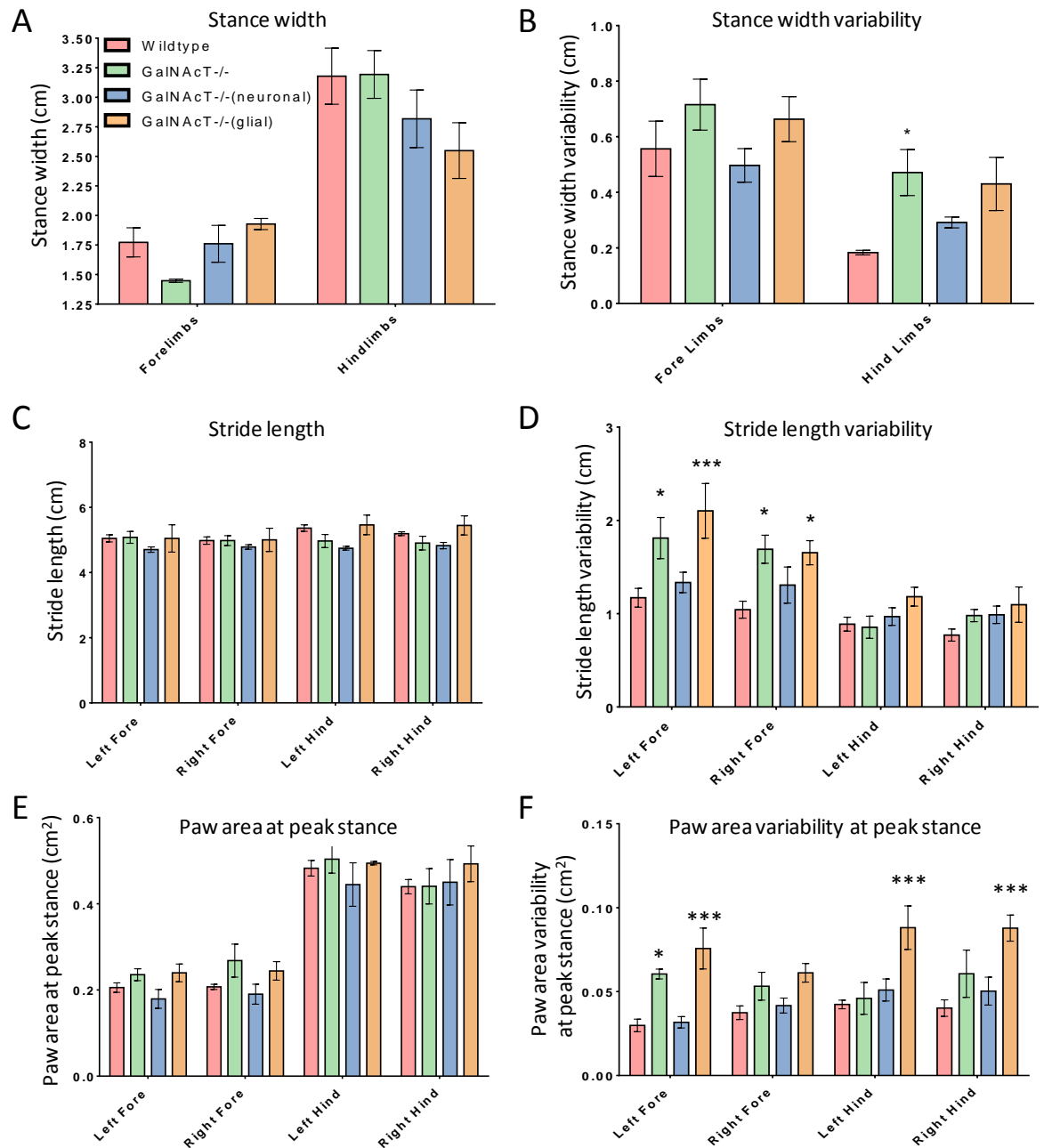


**Figure 3.6: Comparison of gait parameters between 4 mouse strains.** No changes were observed in stance width (A), stride length (C) or paw area at peak stance (E). Increases in stance width variability (B) were observed between the hind limbs of GalNAcT<sup>-/-</sup> and wildtype mice. Similarly, increased stride length variability (D) was seen between forelimbs of GalNAcT<sup>-/-</sup> and GalNAcT<sup>-/-</sup>-*Tg(glia)* mice vs. wildtype mice. Paw area variability (F) was increased in GalNAcT<sup>-/-</sup>-*Tg(glia)* mice hind limbs but not GalNAcT<sup>-/-</sup> forelimbs. Two way ANOVA with Dunnett's multiple comparisons test vs. wildtype mice. \*= $p < 0.05$ , \*\*\*= $p < 0.001$ , \*\*\*\*= $p < 0.0001$ .

### 3.5 Comparison of axon regeneration in wildtype, GalNAcT<sup>-/-</sup> and GalNAcT<sup>-/-</sup>-Tg(*neuronal*) mice

GalNAcT<sup>-/-</sup> mice have previously been shown to have delayed nerve regeneration following hypoglossal nerve transection compared with wildtype mice (Kittaka et al., 2008). To determine whether the neuronal rescue of complex ganglioside expression, which is sufficient to rescue the degenerative phenotype seen in these GalNAcT<sup>-/-</sup> mice, can also restore the delay in regeneration in GalNAcT<sup>-/-</sup> mice, mice underwent a sciatic nerve crush followed by 8 weeks of regeneration. This period of regeneration was chosen based on previous studies in wildtype mice which took 10 weeks to have fully mono-innervated lumbrical NMJs.

#### 3.5.1 Lumbrical re-innervation

Lumbricals were scored manually as being either vacant, polyinnervated or mono-innervated. One hundred NMJs were scored per mouse. Chi-squared analysis was performed on the contingency table to determine whether there were differences in the NMJ innervations state of the three genotypes after 8 weeks. No significant difference was observed in the state of NMJ innervation among the groups (Figure 3.7).

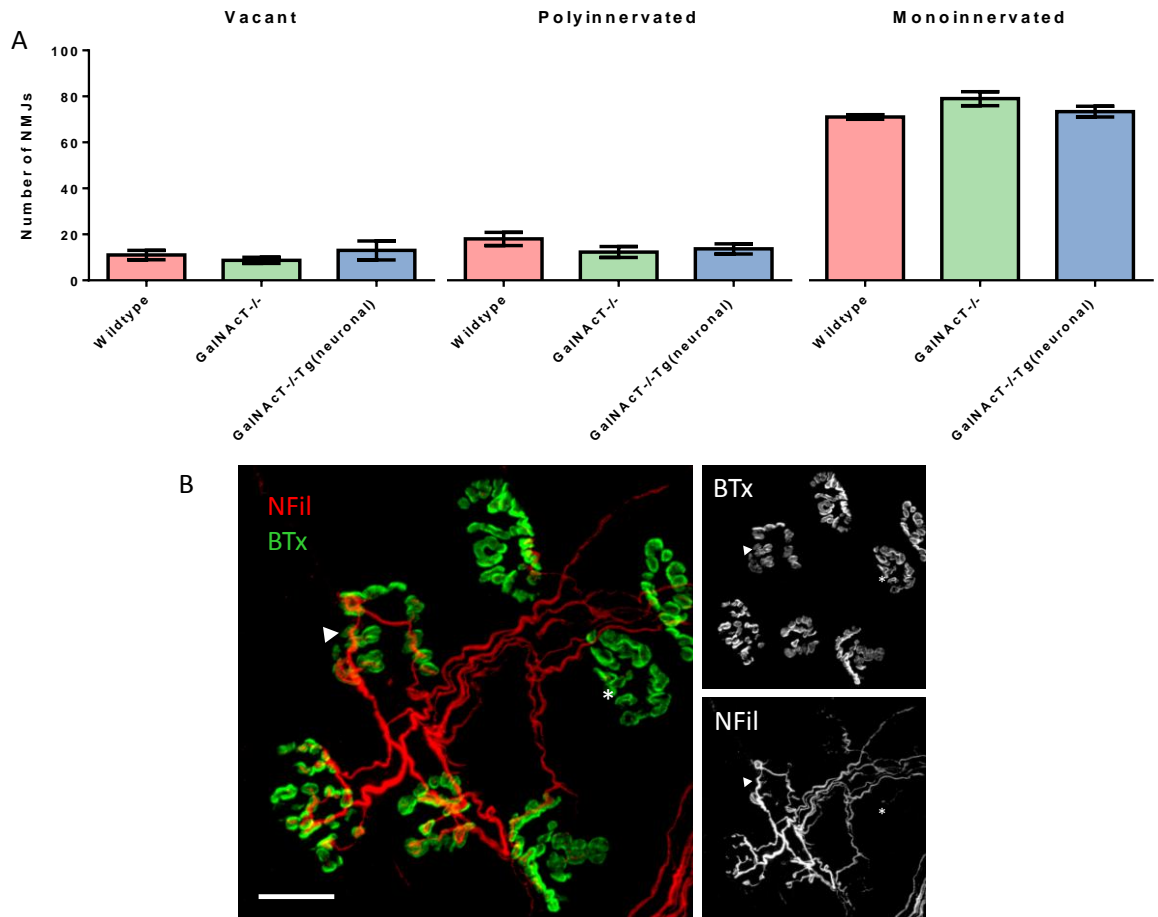


**Figure 3.7: Comparison of axon regeneration in wildtype, GalNAcT<sup>-/-</sup> and GalNAcT<sup>-/-</sup>Tg(*neuronal*) mice (n=3 per group). Innervation of lumbrical muscles 8 weeks following sciatic nerve crush. **A.** Counts of NMJs which were vacant, polyinnervated or monoinnervated. No significant differences existed between these groups (p=0.1086, Chi squared test). **B.** Example image from wildtype mouse showing a vacant NMJ (asterisk), a polyinnervated NMJ (arrowhead) and monoinnervated NMJs.**

### 3.5.2 Sciatic and tibial nerve light morphometry

Transverse sections of sciatic and tibial nerves taken 1 and 2 cm distal from the crush site respectively, were analysed by light microscopy for myelinated fibres (Figure 3.8). As with the lumbrical innervation, there was no significant difference between the presences of myelinated fibres in sciatic or tibial nerve among any of the genotypes. Compared with control nerves from the contralateral leg, the myelinated fibres of crushed sciatic and tibial nerves were smaller in caliber, consistent with regenerating fibres.

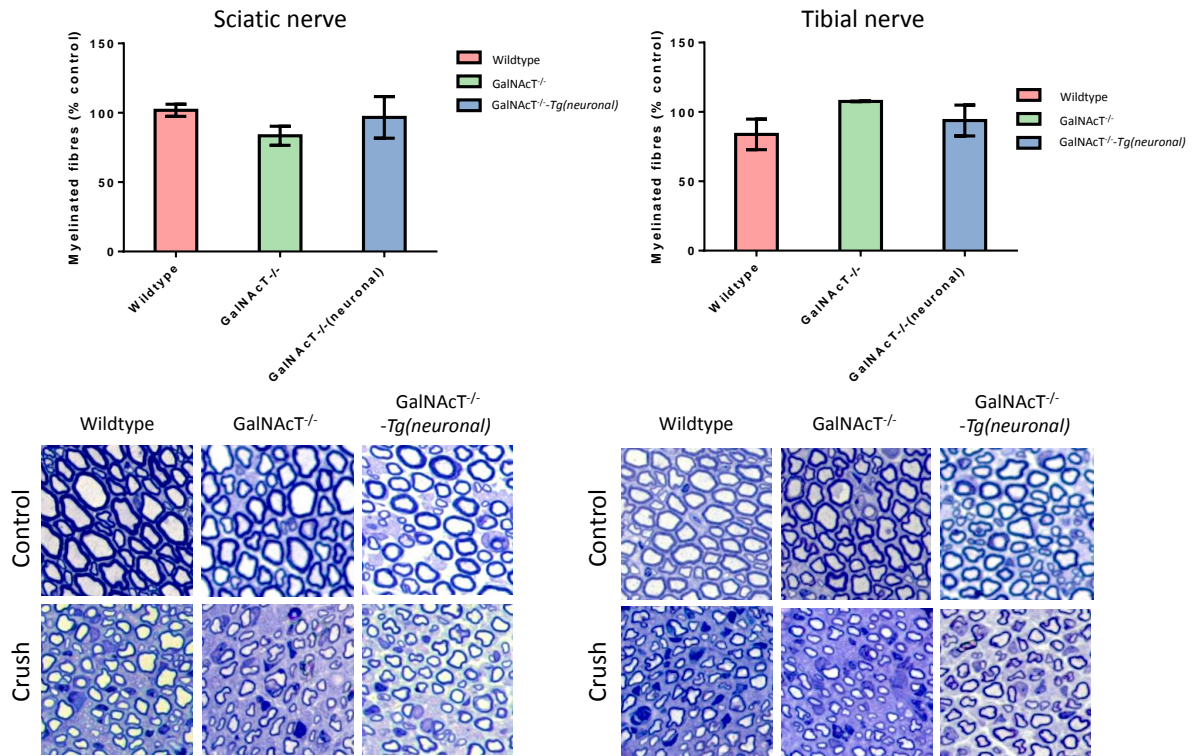


**Figure 3.8: Comparison of myelinated fibre presence among wildtype, GalNAcT<sup>-/-</sup> and GalNAcT<sup>-/-</sup>Tg(neuronal) mice 8 weeks following sciatic nerve crush.** Sciatic and tibial nerves from each genotype (n=3) were examined by light morphometry for the presence of myelinated fibres. Graphs displayed as percentage of control nerve from contralateral leg of each animal. No significant differences exist in the number of myelinated fibres present among any of the genotypes. One way ANOVA with Tukey's multiple comparison test.

### 3.6 Discussion

To confirm that complex gangliosides were not only re-instated but comparable to wildtype by immuno-fluorescence, various tissues were screened against a panel of antibodies whose binding patterns were known in wildtype tissue. The results of this analysis confirmed the expected wildtype binding pattern, with strong anti-GD1b antibody staining in all tissues, strong anti-GM1 staining with DG2 in all tissues, no anti-GM1 staining with DG1 and no GD1a staining with MOG35. Neuronal rescue of GalNAcT and therefore complex ganglioside expression, resulted in restored antibody staining in most cases, though to varying degrees. NFLTg, and Thy1(112) mice, appeared to have similar or increased GD1b expression, as evidenced by the significantly higher binding presence of MOG35 staining in most tissues. However, the Thy1(115) mouse

appeared to have an uneven GalNAcT expression, with some junctions showing positive staining and some showing very little within the same piece of tissue. DG2 staining appeared to show lower intensity staining in both neuronal rescue lines, indicating that GM1 expression in these mice is lower at the terminal than wildtype mice. This is unsurprising considering the lower GalNAcT enzyme expression levels in these mice as compared to wildtype mice (Yao et al., 2014). However, staining was still present, indicating GM1 was still at the terminal. The lack of DG1 antibody binding in these rescue mice provides some degree of support that GM1 and GD1a, are presented in the membrane in a similar manner to wildtype mice, where GD1a inhibits DG1 binding to GM1 (Greenshields et al., 2009). The lack of binding of MOG35 in rescue lines also confirmed this hypothesis, as, although it has been shown to bind well when GD1a is overexpressed (Goodfellow et al., 2005), wildtype binding has never been easy to show. Glycoarray analysis of MOG35 (data not shown) showed that this antibody is inhibited by GT1b, which is absent in  $GD3s^{-/-}$  mice, presumably leading to the increased binding in these mice. Therefore with the relative similarity in ganglioside expression and membrane placement, it was clear that both NFLTg and Thy1(112) mice could be used in future experiments to compare to wildtype mice. NFLTg mice were used in all experiments from this point onwards and are referred to as  $GalNAcT^{-/-}$ -*Tg(neuronal)* mice.

Despite having confirmed that anti-ganglioside antibody binding is roughly similar in intensity between wildtype and  $GalNAcT^{-/-}$ -*Tg(neuronal)* mice, the nuances of binding are not able to be distinguished in tissue sections, therefore whole mount TS was used. The  $GalNAcT^{-/-}$ -*Tg(glial)* mouse was included, which allowed the visualisation of staining in mice which should have complex gangliosides only on glial cells. As expected for the two different rescue strains, each showed staining on the structures where GalNAcT had been re-expressed. Staining was seen for all antibodies on the neuronal structures in  $GalNAcT^{-/-}$ -*Tg(neuronal)* mice and on the glial structures in  $GalNAcT^{-/-}$ -*Tg(glial)* mice. However, in  $GalNAcT^{-/-}$ -*Tg(neuronal)* mice, the pSCs also appeared to be stained in some cases. The NFL promoter used to drive GalNAcT expression can be found to be active in pSCs. Work in this lab has confirmed that SCs from  $GalNAcT^{-/-}$ -*Tg(neuronal)* mice co-cultured along with DRG neurons from  $GalNAcT^{-/-}$  mice show activation of NFL promoter by NFL mRNA expression, despite no protein

expression (G. Meehan, unpublished data). However, when cultured alone, no mRNA expression was present. This is not the first time that neurofilament promoter activity has been detected in SCs (Sotelo-Silveira et al., 2000), but previously the expression has been shown to be transient and only in response to axonal injury or demyelination (Fabrizi et al., 1997). Despite this potential for additional pSC expression, neuronal reintroduction is clear and previous evidence of glial expression of NFL mRNA has been shown to only be in immature SCs or SCs which are responding to injury (Haynes et al., 1999;Fabrizi et al., 1997), therefore the use of this mouse strain is still justified.

As well as the restored ganglioside synthesis,  $\text{GalNAcT}^{-/-}\text{-Tg}(\text{neuronal})$  mice also appear phenotypically like wildtype mice, lacking the Parkinson-like tremor associated with aged  $\text{GalNAcT}^{-/-}$  mice (Chiavegatto et al., 2000). A series of behavioural tests confirmed that even aged  $\text{GalNAcT}^{-/-}\text{-Tg}(\text{neuronal})$  mice performed as well as wildtype mice in grip strength, Rotarod and grid walking in a recent publication (Yao et al., 2014). Conversely, restoration of complex gangliosides in the glia does not prevent the degenerative phenotype seen in  $\text{GalNAcT}^{-/-}$  mice. As previous deficits in gait were also seen in  $\text{GalNAcT}^{-/-}$  mice (Chiavegatto et al., 2000), Digigait™ was used to analyse differences in gait parameters between the four genotypes. In this study, mice were between 12 and 18 months of age; equal to or greater than the age where gait deficits had been seen in  $\text{GalNAcT}^{-/-}$  mice previously (Chiavegatto et al., 2000).  $\text{GalNAcT}^{-/-}$  mice in this previous study were shown to have a reduced stride length, stance width and hind paw print length but using the Digigait™, there were no significant differences in the equivalent parameters in our mice. However, larger variability was seen in each of these parameters between  $\text{GalNAcT}^{-/-}$  and wildtype mice. This means that although the mean values were not different, the normal fluctuations seen with these measurements are increased, implying movement control is impaired. Interestingly, increases in gait variability were seen most often in  $\text{GalNAcT}^{-/-}\text{-Tg}(\text{glial})$  mice when compared to wildtype, indicating a more severe phenotype than  $\text{GalNAcT}^{-/-}$  mice. This correlates with other behavioural data on these mice where they scored equal to or worse than  $\text{GalNAcT}^{-/-}$  mice (Yao et al., 2014). Morphological characterisation has shown that these mice have similar numbers of degenerative axons to  $\text{GalNAcT}^{-/-}$  mice in both peripheral and central nervous system sites, and that these mice have a

more pronounced lengthening of Nav1.6 clusters in PNS nodes of Ranvier (Yao et al., 2014).

Due to the apparent rescue of the behavioural phenotype in  $\text{GalNAcT}^{-/-}$ - $\text{Tg}(\text{neuronal})$  mice, it was proposed that the inhibition in nerve regeneration observed previously in  $\text{GalNAcT}^{-/-}$  mice (Kittaka et al., 2008) may also be rescued in  $\text{GalNAcT}^{-/-}$ - $\text{Tg}(\text{neuronal})$  mice. Previous, unpublished data in this lab has shown that 6 weeks following a nerve crush in wildtype mice, approximately 50% of lumbrical NMJs are mono-innervated and by 10 weeks, 100% are mono-innervated (K. Greenshields, unpublished data). Therefore, to observe differences between wildtype,  $\text{GalNAcT}^{-/-}$  and  $\text{GalNAcT}^{-/-}$ - $\text{Tg}(\text{neuronal})$  strains, an intermediate 8 week timepoint was chosen. However, by lumbrical analysis alone, there was no difference in the stage of regeneration between strains. This indicated there was no initial difference between wildtype and  $\text{GalNAcT}^{-/-}$  mice at this time point and therefore nothing to be “rescued” in  $\text{GalNAcT}^{-/-}$ - $\text{Tg}(\text{neuronal})$  mice. The initial study showing impaired regeneration in  $\text{GalNAcT}^{-/-}$  mice had shown inhibited regeneration in the hypoglossal nerve. Regeneration was scored by the number of HRP positive neurons following injection of HRP in the tongue (Kittaka et al., 2008). There is a possibility that by simply scoring the lumbricals as “mono-innervated”, we have not taken into consideration earlier branching of the axon, therefore one motor axon may for instance be innervating more than one NMJ, until appropriate pruning takes place, meaning retrograde HRP transport may be directed to a smaller number of neurons. Therefore had we analysed it in the same fashion as Kittaka et al, there may have been more of an indication of inhibited regeneration. However, the animals appeared to have regained function of their legs by this timepoint indicating that if there was any impaired regeneration in  $\text{GalNAcT}^{-/-}$  mice, it was subtle. In addition, the similar numbers of myelinated fibres in the sciatic and tibial nerves provide further evidence that no major regeneration differences exist among these genotypes. The results of this study do appear to correlate with a previous study in this laboratory whereby  $\text{GalNAcT}^{-/-}$  mice also regenerated at the same rate as wildtype mice following a very site-specific distal injury of the motor nerve terminal (Rupp et al., 2013). Gangliosides have been proposed to have a role in regeneration due to the enhanced nerve regeneration seen following exogenous ganglioside injection (Itoh et al., 1999; Kittaka et al., 2008). In

GalNAcT<sup>-/-</sup> mice, the over-expression of simple gangliosides GM3, GD3 and GT3 may compensate for the lack of complex gangliosides, meaning the overall effect on regeneration is not large enough to be seen in the paradigm described here.

This chapter has delivered some information on the binding profiles of GalNAcT<sup>-/-</sup>-*Tg(neuronal)* and GalNAcT<sup>-/-</sup>-*Tg(glial)* mice in comparison to GalNAcT<sup>-/-</sup> and wildtype mice using various antibodies, as well as providing some basic characterisation of gait and regeneration in these newly developed mice.

## 4 Development of an active immunisation model of GBS

### 4.1 Introduction

Inherent self-tolerance to gangliosides prevents wildtype mice from mounting an antibody response when immunised with gangliosides. Therefore, in order to model the effects of anti-ganglioside antibodies *in vivo*, wildtype mice containing the target ganglioside on their peripheral nerve membranes must be injected with monoclonal antibodies produced from GalNAcT<sup>-/-</sup> or GD3s<sup>-/-</sup> mice which lack the intended target antigen. This has proven to be a successful way of modelling the anti-ganglioside antibody mediated injury of peripheral nerves *in vivo* (Halstead et al., 2004; Halstead et al., 2008). However, this does not mimic the induction of disease in patients, where antibodies are produced by individuals who lack tolerance to gangliosides and therefore produce an antibody reaction. The GalNAcT<sup>-/-</sup>-Tg(*neuronal*) and GalNAcT<sup>-/-</sup>-Tg(*glial*) mouse strains were created as a means to overcome tolerance in wildtype mice while still retaining target on disease-relevant sites. Indeed, in an earlier pilot study in this laboratory, GalNAcT<sup>-/-</sup>-Tg(*neuronal*) mice were shown to produce an immune response when immunised with GT1b-containing liposomes (S. Rinaldi, unpublished data). When these mice were injected with NHS to induce an injury, there was no difference in motor control or co-ordination by behavioural testing methods. Plethysmography data did show a reduction in tidal volume at later timepoints, indicating diaphragm injury. Weak presence of complement pathway components overlying the diaphragm NMJs was also seen. In this chapter, GalNAcT<sup>-/-</sup> mice serve as a negative control for all behavioural and immunohistological tests as their lack of GD1b target ganglioside means no antibody binding and injury should occur.

### 4.2 Passive immunisation of mice with anti-GD1b antibody

Based on the high binding of anti-GD1b antibodies MOG3 and MOG1 in wildtype mice and both strains of rescue mice (Chapter 3), GD1b was the antigen of choice for trialling an active immunisation in the transgenic mouse lines. A preliminary passive immunisation model was used to demonstrate the ability of antibodies targeting GD1b to injure the membrane *in vivo*, as measured by behavioural testing and plethysmography, and *ex vivo*, by immunofluorescent

analysis of the diaphragm. The injection of antibody was accompanied 16 hours later by the injection of NHS to induce complement-mediated injury. This protocol has been used previously to demonstrate anti-GQ1b antibody's ability to cause damage to motor nerve terminals *in vivo* (Halstead et al., 2004; Halstead et al., 2008). The diaphragm is used as a site of interest as it has rich motor innervation from the phrenic nerve and is a muscle which lies in close proximity to the injection sites of antibody and NHS. It is therefore a muscle which is likely to be measurably injured. The antibody used to passively immunise the mice was MOG1. Three animals (4-6 weeks old) were used per genotype, however due to an unsuccessful NHS injection (subcutaneous injection rather than i.p.) in one GalNAcT<sup>-/-</sup>-*Tg(neuronal)* mouse, this mouse was excluded from all injury analysis, but was included when assessing antibody deposition at the diaphragm NMJs.

#### **4.2.1 Behaviour and plethysmography**

Mice did not appear to be affected by antibody injection alone, with the exception of one wildtype mouse which seemed to be less active than its two counterparts. Following injection of NHS, all wildtype mice appeared very ill, with pinched abdomens (example best displayed in image of GalNAcT<sup>-/-</sup>-*Tg(neuronal)* mouse, Figure 4.1A), and laboured breathing. They also had difficulty moving (wildtype mouse seen in Figure 4.1A shown with splayed hind-limbs) but this may have been as a consequence of their breathing difficulties rather than direct muscle impairment. Rotarod testing performed 2 hours post NHS injection indicated a very sharp, significant decrease in their latency to fall (one-way ANOVA,  $p < 0.01$  vs baseline), as mice were unable to maintain their normal running speed or grip onto the Rotarod (Figure 4.1B). In contrast, GalNAcT<sup>-/-</sup> mice appeared normal following NHS injection with no change in Rotarod testing score (Figure 4.1B). GalNAcT<sup>-/-</sup>-*Tg(neuronal)* mice also appeared ill, though not as severely as wildtype mice. Performance on Rotarod was significantly decreased versus baseline (one-way ANOVA,  $p < 0.01$  vs baseline) (Figure 4.1B). Although GalNAcT<sup>-/-</sup>-*Tg(glial)* mice appeared more lethargic than GalNAcT<sup>-/-</sup> mice, they did not appear to have any breathing difficulties and lacked the pinched waist seen in wildtype and GalNAcT<sup>-/-</sup>-*Tg(neuronal)* mice. Despite this, Rotarod performance was significantly decreased in GalNAcT<sup>-/-</sup>-

*Tg(glial)* mice post-NHS compared to baseline (one-way ANOVA,  $p < 0.05$  vs baseline).

Whole body plethysmography was performed to indicate deficits in diaphragm function, as measured by tidal volume. Wildtype mice showed a decrease in tidal volume, reaching significance compared to baseline from 90 minutes post-NHS injection (two-way ANOVA,  $p < 0.05$ ), and continuing to decrease at 120 minutes (two-way ANOVA,  $p < 0.01$ ). Similarly, *GalNAcT<sup>-/-</sup>-Tg(neuronal)* mice showed a decrease in tidal volume, reaching significance at 120 minutes (two-way ANOVA,  $p < 0.05$ ). No significant decrease was seen in either *GalNAcT<sup>-/-</sup>* or *GalNAcT<sup>-/-</sup>-Tg(glial)* mice, though *GalNAcT<sup>-/-</sup>-Tg(glial)* mice did trend towards a decrease in tidal volume over time (Figure 4.1C). Respiratory rate did not appear to be affected by NHS injection as no significant changes from baseline were observed in any mouse strain following NHS (Figure 4.1D).

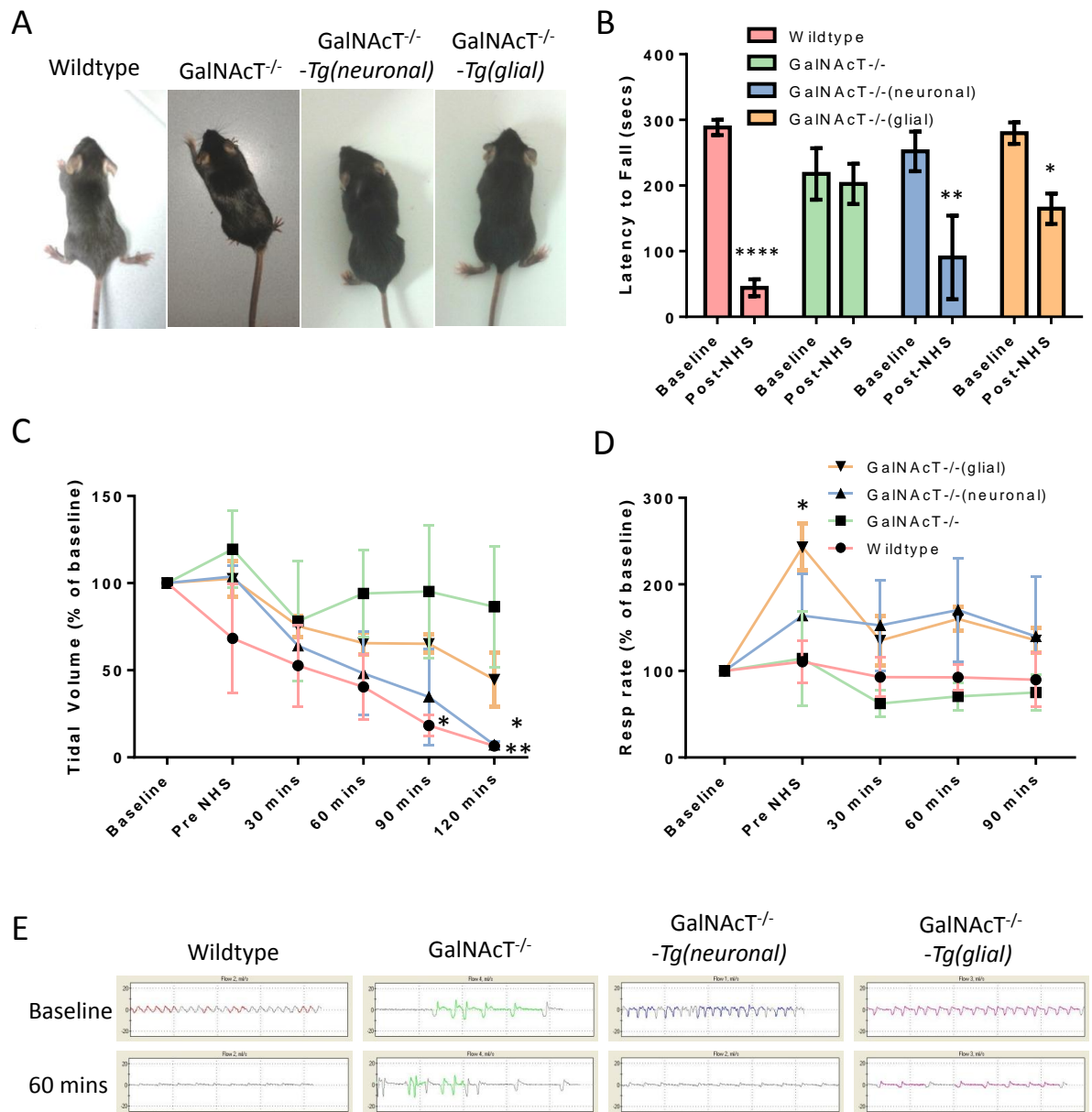


**Figure 4.1: *In vivo* analysis of injury in wildtype, GalNAct<sup>-/-</sup>, GalNAct<sup>-/-</sup>-Tg(neuronal) and GalNAct<sup>-/-</sup>-Tg(glial) mice following MOG1 + NHS mediated injury. A:** Wildtype mice (n=3) appeared very sick, were unable to support weight and had pinched waists whereas GalNAct<sup>-/-</sup> mice (n=3) appeared normal. GalNAct<sup>-/-</sup>-Tg(neuronal) mice (n=2 for this analysis) also had pinched waists. GalNAct<sup>-/-</sup>-Tg(glial) mice (n=3) appeared lethargic but were otherwise normal. **B:** Rotarod analysis showed a vast decrease in latency to fall in wildtype mice post-NHS vs pre NHS. GalNAct<sup>-/-</sup>-Tg(neuronal) and GalNAct<sup>-/-</sup>-Tg(glial) also showed significantly lower scores post-NHS. GalNAct<sup>-/-</sup> mice scored no differently. \*= $p < 0.05$ , \*\*= $p < 0.01$ , \*\*\*\*= $p < 0.0001$ , two-way ANOVA with Sidak's multiple comparison's test. **C:** Tidal volume was significantly lower than baseline from 90 minutes onwards in wildtype mice. The same occurred in GalNAct<sup>-/-</sup>-Tg(neuronal) mice after 120 minutes. No significant differences were observed in GalNAct<sup>-/-</sup> or GalNAct<sup>-/-</sup>-Tg(glial) mice. **D:** No difference was seen in respiratory rate with the exception of an increase between baseline and pre-NHS in GalNAct<sup>-/-</sup>-Tg(glial) mice. \*= $p < 0.05$ , \*\*= $p < 0.01$ , two-way ANOVA with Dunnett's multiple comparison's test. **E:** Example breath traces from the four mouse strains at baseline and 60 minutes post-NHS.

#### 4.2.2 Tissue analysis

Diaphragms taken from the mice at sacrifice 3-4 hours post NHS were sectioned at 8  $\mu\text{m}$  and analysed for presence of IgG3, C3, MAC and NFil as described in section 2.16. Both wildtype and  $\text{GalNacT}^{-/-}\text{-Tg}(\text{neuronal})$  mice showed deposition of IgG3 at the NMJ, indicating MOG1 antibody had bound there following injection (Figure 4.2A).  $\text{GalNacT}^{-/-}$  mice were negative for IgG3. Although some antibody was present in  $\text{GalNacT}^{-/-}\text{-Tg}(\text{glial})$  mice, it was often not found directly over the BTx signal, instead appearing to be on pSC cell bodies, but not on the processes covering the NMJ. Corresponding to the deposition of IgG3, wildtype and  $\text{GalNacT}^{-/-}\text{-Tg}(\text{neuronal})$  mice also showed C3 deposition whereas  $\text{GalNacT}^{-/-}$  mice were negative for C3 staining. The  $\text{GalNacT}^{-/-}\text{-Tg}(\text{glial})$  mice which had showed little IgG3 deposition directly overlying the BTx signal, showed strong C3 deposition, both overlying BTx and again on pSC cell bodies. Deposition of MAC was also present in wildtype,  $\text{GalNacT}^{-/-}\text{-Tg}(\text{neuronal})$  and  $\text{GalNacT}^{-/-}\text{-Tg}(\text{glial})$  mice and absent in  $\text{GalNacT}^{-/-}$  mice, indicating culmination of the complement cascade following C3 deposition. The presence of NFil was significantly reduced in wildtype,  $\text{GalNacT}^{-/-}\text{-Tg}(\text{neuronal})$  and  $\text{GalNacT}^{-/-}\text{-Tg}(\text{glial})$  mice compared to  $\text{GalNacT}^{-/-}$ . The  $\text{GalNacT}^{-/-}$  mice also did appear to have a lower than expected NFil presence, however this was similar to PBS control (PBS control data not shown).

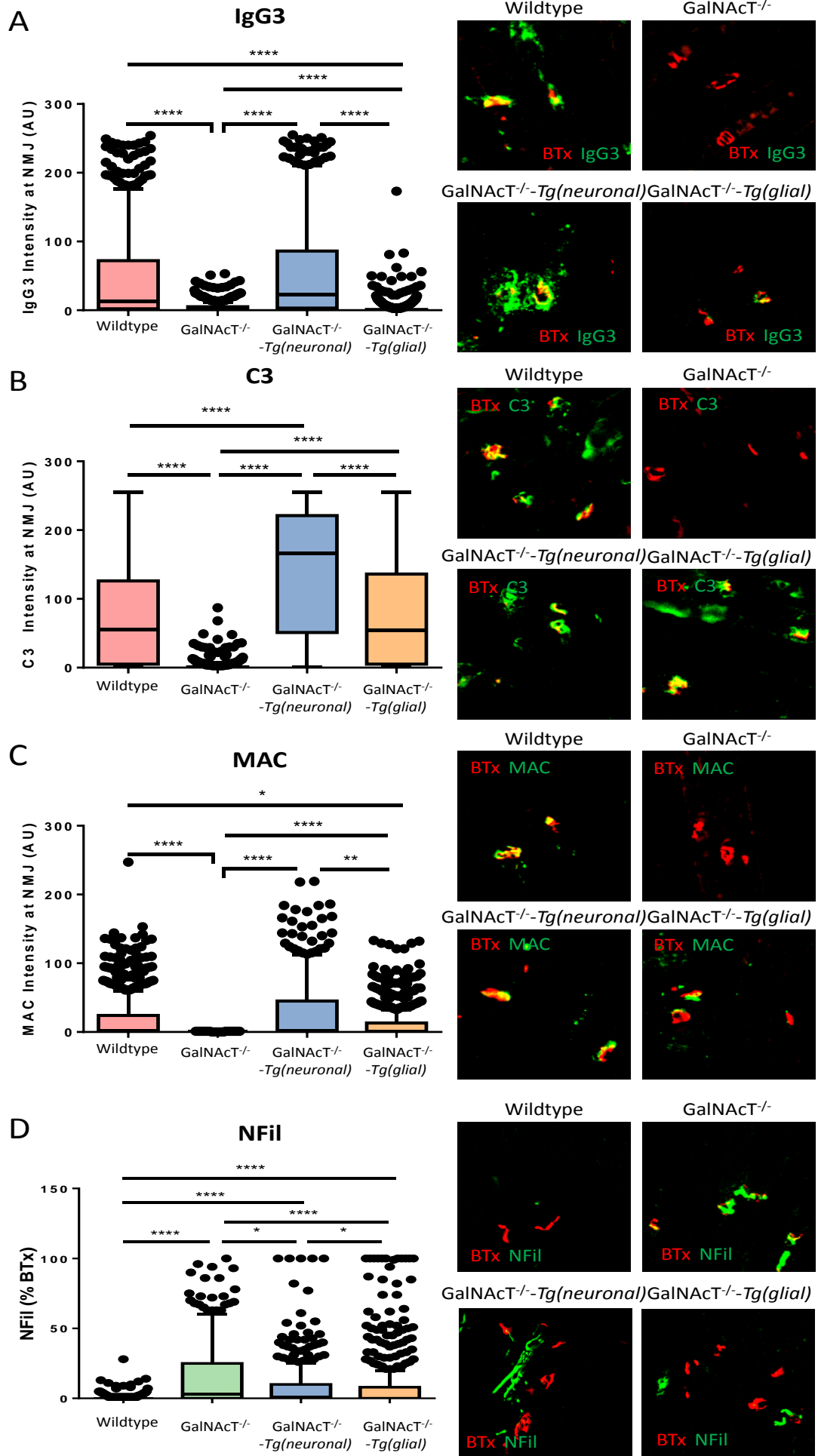


(Figure on previous page)

**Figure 4.2: Ex vivo analysis of diaphragm injury in wildtype, GalNAcT<sup>-/-</sup>, GalNAcT<sup>-/-</sup>-Tg(*neuronal*) and GalNAcT<sup>-/-</sup>-Tg(*glial*) mice following MOG1 + NHS mediated injury.** **A:** IgG3 was deposited over nerve terminals of wildtype and GalNAcT<sup>-/-</sup>-Tg(*neuronal*) endplates. Little was present directly over the BTx signal of GalNAcT<sup>-/-</sup>-Tg(*glial*) mice endplates, though staining was seen on what appeared to be pSC cell bodies. Negligible amounts were present on the nerve terminals of GalNAcT<sup>-/-</sup> mice. **B:** C3 was deposited over the nerve terminals of wildtype, GalNAcT<sup>-/-</sup>-Tg(*neuronal*) and GalNAcT<sup>-/-</sup>-Tg(*glial*) mice with GalNAcT<sup>-/-</sup>-Tg(*neuronal*) mice showing significantly higher deposition than wildtype and GalNAcT<sup>-/-</sup>-Tg(*glial*). Negligible amounts of C3 were present on GalNAcT<sup>-/-</sup> mice endplates. **C:** MAC deposits were also seen in wildtype, GalNAcT<sup>-/-</sup>-Tg(*neuronal*) and GalNAcT<sup>-/-</sup>-Tg(*glial*) mice and were absent in GalNAcT<sup>-/-</sup> mice. **D:** Nfil overlying the BTx signal was reduced in wildtype, GalNAcT<sup>-/-</sup>-Tg(*neuronal*) and GalNAcT<sup>-/-</sup>-Tg(*glial*) mice compared with GalNAcT<sup>-/-</sup>, with wildtype mice showing the lowest Nfil presence. \*= $p < 0.05$ , \*\*= $p < 0.01$ , \*\*\*\*= $p < 0.0001$ , Kruskal-Wallis with Dunn's multiple comparison test. A minimum of 228 NMJs were analysed per group. Non-parametric data displayed as Tukey box plot (see section 2.20).

### 4.3 Active immunisation of mice with GD1b-containing liposomes

Initial immunisations were performed as per a previously used immunisation protocol in GalNAcT<sup>-/-</sup> and wildtype mice (Bowes et al., 2002). These immunisations (protocol A) resulted in a successful immune response in all mice but no injury was detectable by behavioural tests, plethysmography or tissue analysis (data not shown). To attempt to gain a larger immune response in a shorter period of time, immunisations were performed using a slightly modified protocol which combined the hapten-carrier-like effect of ova-containing liposomes used in protocol A, with the adjuvant effect of monophosphoryl lipid A (MPLA) into a short series of immunisations spaced closer together (protocol B). Lipid A is a derivative of endotoxin lipopolysaccharide (LPS) found on the coats of gram negative bacteria such as *C. jejuni*. It is often used as an adjuvant due to its ability to bind to TLR4 on antigen presenting cells, enhancing the antigen-specific antibody response (Alving et al., 2012).

#### 4.3.1 Immune response

Blood samples were taken on day 0, 19 and 22 with terminal samples taken on day 25-27 (mice were culled in batches of 4 over these days). Serum was tested by ELISA against GD1b and analysed by two-way ANOVA with Tukey's multiple comparison's test.

#### 4.3.1.1 IgM response

All groups showed a rise in serum OD values over the immunisation period, with wildtype mice being consistently lower than all other groups (Figure 4.3), though only significantly lower than GalNACT<sup>-/-</sup> mice sera values at the day 22 timepoint ( $p < 0.05$ ). Serum analysis by glycoarray was performed at day 22 to indicate the pattern of immune response to liposome components plus two structurally similar gangliosides, GM1 and GT1b. Despite some small cross reactivity with GT1b and its complexes in some mice (regardless of genotype, examples shown in Figure 4.3B) the immune response seemed to be specific to GD1b and its complexes. Sphingomyelin and GM1 appeared to consistently inhibit binding to GD1b. Reflecting the day 22 ELISA data, GalNACT<sup>-/-</sup> mice sera showed the strongest glycoarray binding signals against GD1b, wildtype the weakest and rescue mice lay somewhere in the middle. Some mice, regardless of genotype, also showed responses to DCP alone and all mice showed responses to cholesterol alone, though cholesterol reactivity is commonly found in naïve mice also (G. Meehan, unpublished data).

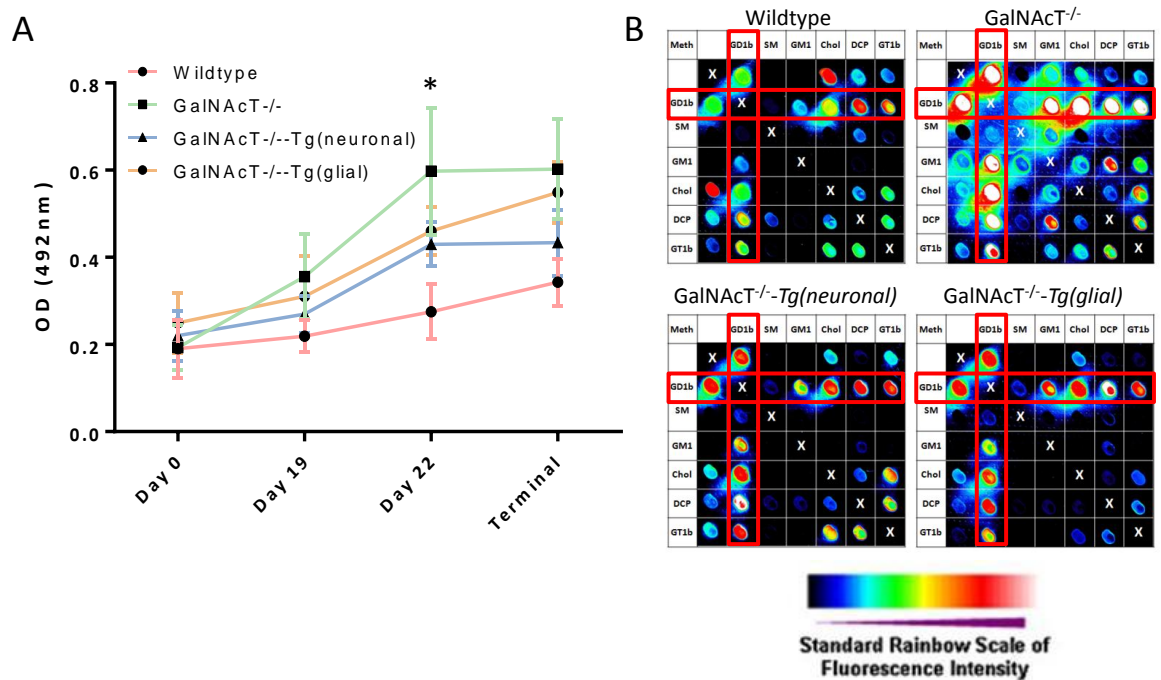


**Figure 4.3: IgM reactivity in GD1b-immunised mice. A:** Serum IgM response to GD1b by ELISA. All groups had a baseline IgM response which rose over time. Wildtype mice showed lower OD values than other groups at day 19, 22 and terminal, though was only significantly lower than GalNAcT<sup>-/-</sup> at day 22. **B:** Glycoarray analysis showing illustrative IgM responses at day 22 to GD1b and other liposome components both alone and in complex. A weak signal against GD1b is present in the wildtype mouse, whereas the GalNAcT<sup>-/-</sup> mouse shows strong reactivity to GD1b. GalNAcT<sup>-/-</sup>-Tg(neuronal) and GalNAcT<sup>-/-</sup>-Tg(glial) mice show very similar GD1b signals. All mice do also show reactivity to some other liposome components. Arrays are read by reading along both axes to find the resulting combination of lipids, with a line of symmetry marked by white crosses. The GD1b columns are highlighted by a red box. \*=p<0.05 vs wildtype, two-way ANOVA with Tukey's multiple comparison test.

#### 4.3.1.2 IgG response

No IgG response was detectable by ELISA until the day 22 timepoint, following the 3 i.v. booster injections (Figure 4.4). At this timepoint, wildtype mice sera showed significantly lower IgG reactivity than GalNAcT<sup>-/-</sup> sera and GalNAcT<sup>-/-</sup>-Tg(glial) sera (p<0.0001 vs. GalNAcT<sup>-/-</sup> and p<0.01 vs. GalNAcT<sup>-/-</sup>-Tg(glial)). Optical density values of GalNAcT<sup>-/-</sup>-Tg(neuronal) mice sera were not significantly different from wildtype sera at day 22 and were significantly lower than GalNAcT<sup>-/-</sup> mice sera at this timepoint (p<0.01). GalNAcT<sup>-/-</sup> mice sera show a further increase in OD at the terminal timepoint, with OD values remaining significantly higher than wildtype and GalNAcT<sup>-/-</sup>-Tg(neuronal) mice sera and

being also now significantly higher than  $\text{GalNAcT}^{-/-}\text{-Tg}(glial)$  mice sera ( $p < 0.0001$  vs wildtype,  $p < 0.01$  vs.  $\text{GalNAcT}^{-/-}\text{-Tg}(neuronal)$  and  $\text{GalNAcT}^{-/-}\text{-Tg}(glial)$ ). Both  $\text{GalNAcT}^{-/-}\text{-Tg}(neuronal)$  and  $\text{GalNAcT}^{-/-}\text{-Tg}(glial)$  mice sera showed significantly higher OD values than wildtype mice at the terminal timepoint (Figure 4.4A). Glycoarrays of IgG responses showed similar patterns to IgM responses with GD1b and its complexes showing up in the sera from all genotypes. GD1b signal again showed similar patterns to that seen by ELISA at day 22 with  $\text{GalNAcT}^{-/-}$  sera showing the strongest signal, followed by  $\text{GalNAcT}^{-/-}\text{-Tg}(glial)$ ,  $\text{GalNAcT}^{-/-}\text{-Tg}(neuronal)$  then wildtype mice sera. Sphingomyelin again appeared to inhibit the signal of GD1b alone and whereas only some mice showed reactivity to other liposome components, all mice sera showed cholesterol reactivity.

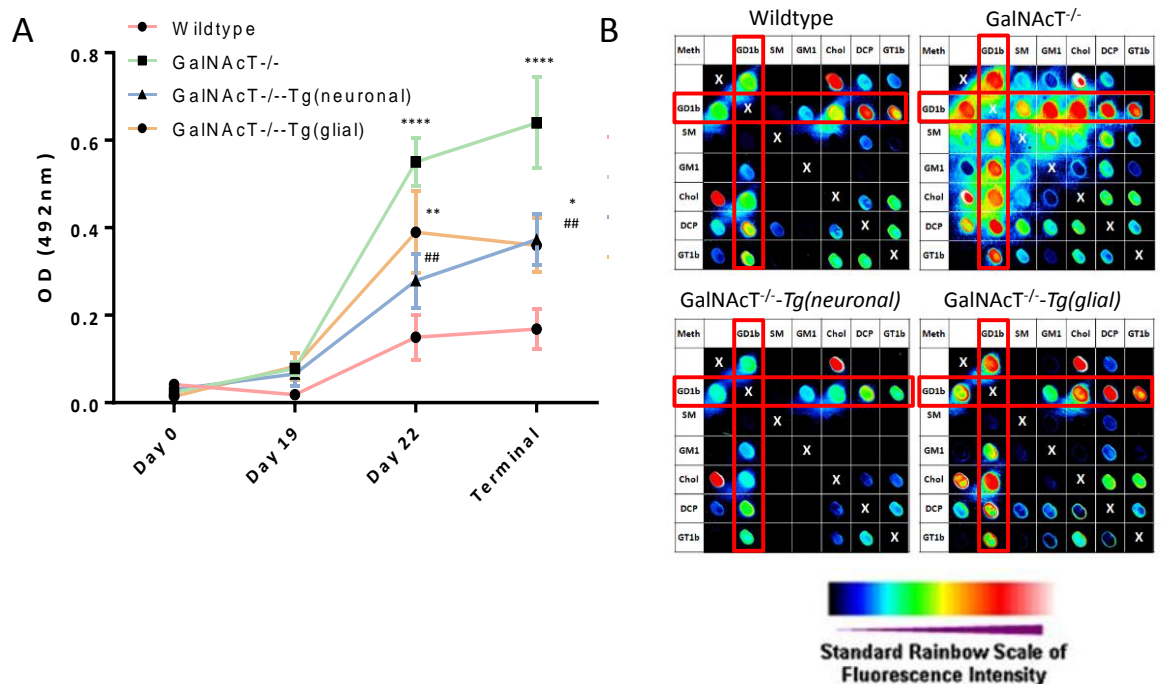


**Figure 4.4: IgG reactivity in GD1b-immunised mice.** **A:** Serum IgG response to GD1b by ELISA. No significant difference was present among groups until day 22 when wildtype mice showed significantly lower OD values than  $\text{GalNAcT}^{-/-}$  and  $\text{GalNAcT}^{-/-}\text{-Tg}(glial)$  mice. By the terminal timepoint wildtype mice had significantly lower OD values than all other groups. **B:** Glycoarray analysis showing illustrative IgG responses at day 22 to GD1b and other liposome components both alone and in complex. A weak GD1b signal is present in the wildtype and  $\text{GalNAcT}^{-/-}\text{-Tg}(neuronal)$  mouse whereas the  $\text{GalNAcT}^{-/-}$  and  $\text{GalNAcT}^{-/-}\text{-Tg}(glial)$  mouse show stronger reactivity to GD1b. As with IgM, all mice also show reactivity to other some other liposome components. \* denotes significance vs. wildtype, # denotes significance vs.  $\text{GalNAcT}^{-/-}$ , two-way ANOVA with Tukey's multiple comparison test. The GD1b column is highlighted by a red box.

### **4.3.2 Behavioural testing and plethysmography**

Following injection of NHS, no significant changes were seen in Rotarod performance in any of the groups (Figure 4.5). Tidal volume did not show major differences among groups over time (Figure 4.5A). The only differences were seen between wildtype and  $\text{GalNAcT}^{-/-}\text{-Tg}(glial)$  60 minutes post NHS ( $p < 0.05$ ). Similarly, though most groups showed a decline in respiratory rate from pre-NHS, no significant differences were observed among groups, indicating that these changes were not due to anti-GD1b related immune injury and may instead be due to the higher volume of NHS injected (Figure 4.5B). Some additional behavioural tests were employed to try and detect injury in the active immunisation paradigm (Figure 4.5E). No significant differences were observed in the mouse's latency to walk from an open balance beam to an enclosed platform, nor in either forelimb or total grip strength.

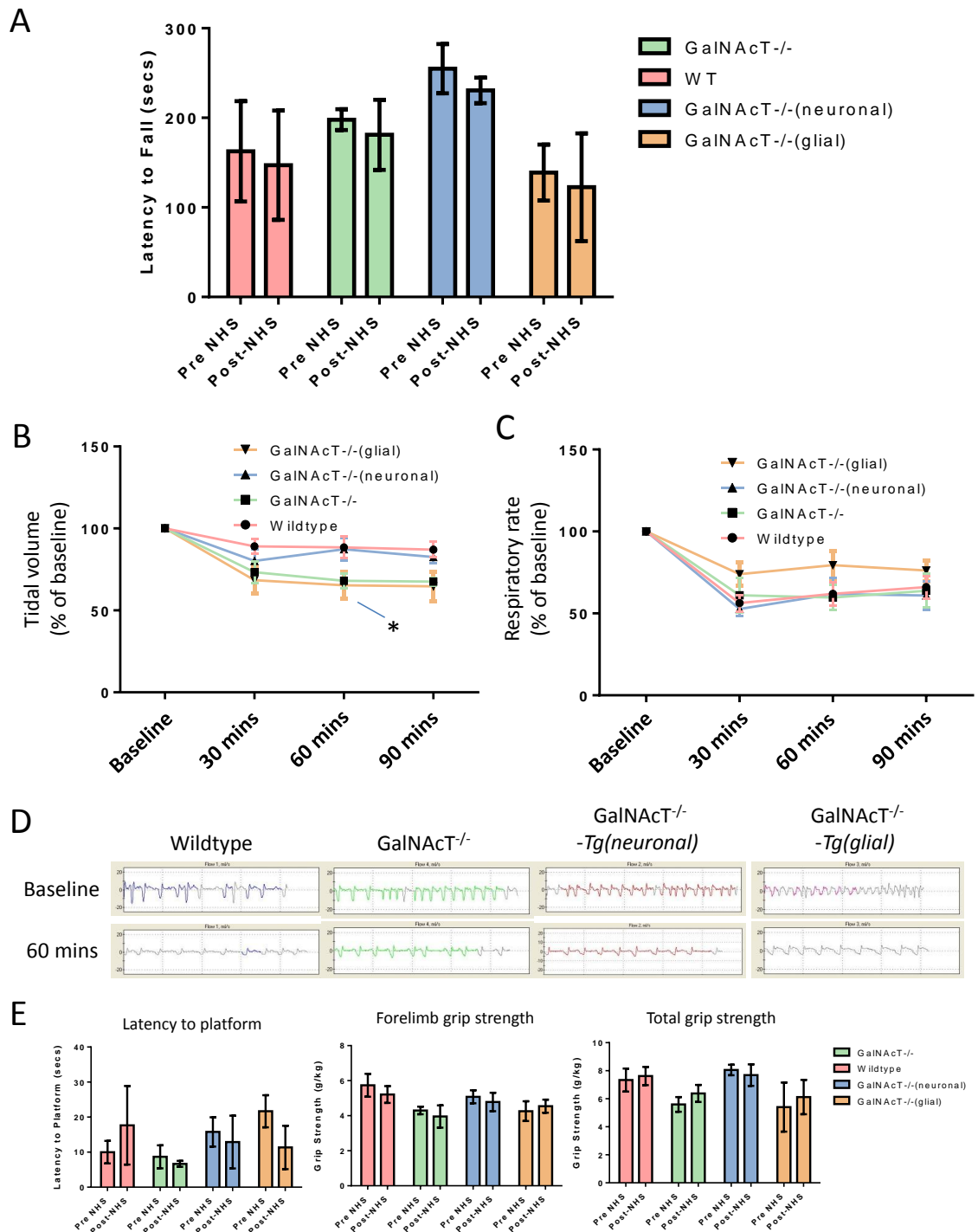


**Figure 4.5: Rotarod and plethysmography data from immunised mice both before and after NHS injection. A:** Rotarod data ( $n=3$  per group) no significant difference was observed following NHS injection in any group (two-way ANOVA with Sidak's multiple comparison's test). **B:** Tidal volume shown as a percentage of baseline values (before NHS was given). Following NHS injection little change was seen. The only significant difference among groups was between wildtype and  $\text{GaINAcT}^{-/-}\text{-Tg}(glial)$  at 60 minutes ( $p<0.05$ ). **C:** Respiratory rate shown as a percentage of baseline values. All groups showed a slight reduction in respiratory rate however no significant change was observable among groups at any timepoint. **D:** Example breath traces from genotypes both pre-NHS and 90 minutes post-NHS. **E:** Additional behavioural tests showing no significant difference between pre and post NHS.  $*=p<0.05$ , two-way ANOVA with Dunnett's multiple comparison's test.

### 4.3.3 Tissue analysis

Diaphragms taken from mice 3-4 hours post-NHS injection were sectioned at 8  $\mu\text{m}$  and analysed for presence of IgG, IgM C3, MAC and NFil as described in section 2.16 (Figure 4.6, IgG data not shown). Neither IgM (Figure 4.6A) nor IgG (data not shown) was present on the nerve terminals of any mouse strain at detectable levels (median of 0.00 for all groups) even though circulating antibodies were found in the serum. In spite of this, some C3 activation appeared to have occurred. Despite some high background, C3 activation was lower in  $\text{GalNAcT}^{-/-}$  mice in comparison to wildtype,  $\text{GalNAcT}^{-/-}\text{-Tg}(\text{neuronal})$  and  $\text{GalNAcT}^{-/-}\text{-Tg}(\text{glial})$  mice (median of 12.00 AU vs. 39.00, 71.00 and 94.00 respectively). Despite the deposition of C3, no MAC deposition was seen in any mouse group and as a result, no injury was seen to the NFil. In fact wildtype and  $\text{GalNAcT}^{-/-}\text{-Tg}(\text{neuronal})$  mice had a higher percentage of NFil presence at the endplate than  $\text{GalNAcT}^{-/-}$  mice.

Tissue was also analysed for presence of immune cells using CD11b as a pan-immune cell marker, though all diaphragms were found to be negative (sciatic nerve taken 7 days post crush was used as positive control). This work was carried out by Su Yan, as part of her project for the degree of Master of Research.



(Figure on previous page)

**Figure 4.6: Analysis of diaphragm from actively immunised mice following NHS injection.** **A:** IgM was not detectable at the nerve terminals of mice from any group (n=3 per group). **B:** C3 was deposited over the nerve terminals of wildtype, GalNACT<sup>-/-</sup>-*Tg(neuronal)* and GalNACT<sup>-/-</sup>-*Tg(glial)* mice with little to none present in GalNACT<sup>-/-</sup> mice. **C:** MAC was not deposited over the nerve terminals of mice in any group despite C3 activation. **D:** NFil was present overlying the BTx signal but was lower in GalNACT<sup>-/-</sup> and GalNACT<sup>-/-</sup>-*Tg(glial)* mice compared with wildtype and GalNACT<sup>-/-</sup>-*Tg(neuronal)*. \*=p<0.05, \*\*=p<0.001, \*\*\*\*=p<0.0001, Kruskal-Wallis with Dunn's multiple comparison test. A minimum of 246 NMJs were analysed per group. Non-parametric data displayed as Tukey box plot (see section 2.20).

#### 4.3.4 Topical complement assay

To assess whether the serum from the actively immunised mice was able to exert pathogenic effects *ex vivo*, a topical complement assay was performed with serum taken from these mice (n=3 per genotype). Serum was applied to fresh frozen sections of naïve wildtype diaphragm, followed by incubation with 4% NHS to induce complement activation. Sera from all genotypes failed to induce MAC deposition (Figure 4.7.A). Diaphragm incubated with 10 µg/ml MOG1 antibody served as a positive control.

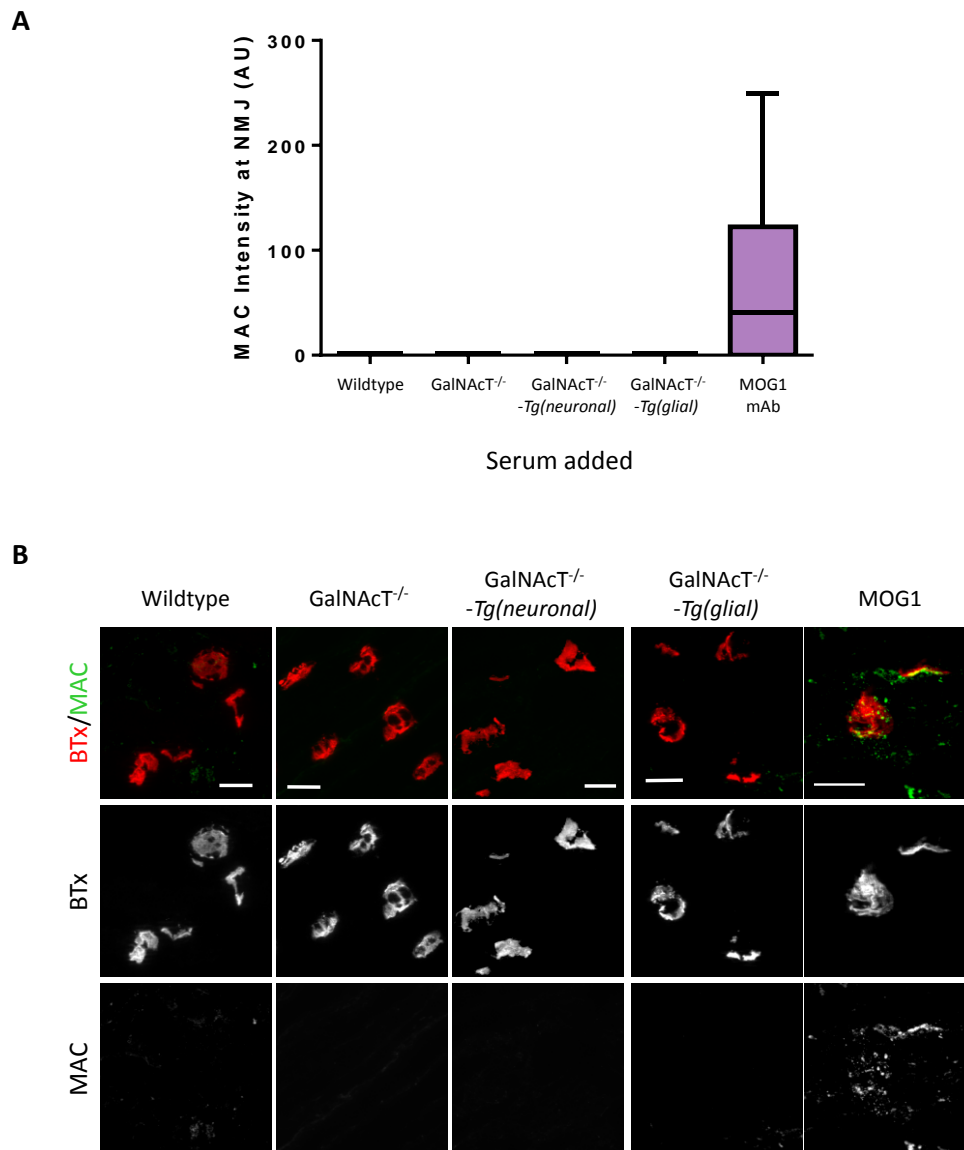


**Figure 4.7: Serum from actively immunised mice does not result in MAC deposition in wildtype diaphragm. A:** Serum from GD1b-immunised wildtype, GalNAcT<sup>-/-</sup>, GalNAcT<sup>-/-</sup>-Tg(neuronal) and GalNAcT<sup>-/-</sup>-Tg(glia) failed to produce MAC following incubation with NHS in wildtype diaphragm sections. Incubation with MOG1 monoclonal antibody as a positive control did. **B:** Illustrative images showing absence of MAC deposition overlying BTx signal following treatment with actively immunised mouse serum followed by NHS. MOG1 incubation followed by NHS results in MAC presence at the endplate. A minimum of 261 NMJs were analysed per group. Non-parametric data displayed as Tukey box plot (see section 2.20).

#### 4.3.5 ELISpots

To confirm that the differences in immune responses to GD1b seen in the serum of actively immunised mice was due to differential activation of B cells, ELISpots were performed using splenocytes taken from actively immunised mice upon sacrifice (Figure 4.8, n=3 per group). IgM reactive spot numbers were higher

than IgG. Though no significant difference existed among any of the genotypes, spots were most numerous from splenocytes from GalNAcT<sup>-/-</sup> mice probed for both IgM and IgG (4.28±1.14 spots/10<sup>6</sup> cells and 1.67±1.20 spots/10<sup>6</sup> cells, respectively). As a secondary measure of GD1b-specific B-cell activity, splenocytes were kept alive in RPMI with 20% FCS for 7 days and supernatant collected on day 7, concentrated 5x and tested by ELISA. Again no significant difference existed among the genotypes but GalNAcT<sup>-/-</sup> mice showed the highest OD value in the IgG ELISA (0.65±0.45 OD). Due to the high background in the negative wells of the IgM plate, values appeared low all around, with wildtype mice showing the highest OD values (0.20±0.12 OD).

This result implied that the anti-GD1b response between wildtype and GalNAcT<sup>-/-</sup> was similar, despite a significant difference being observed in serum antibody levels by ELISA. The immunisation was repeated using only wildtype and GalNAcT<sup>-/-</sup> mice to confirm this result. In this instance cells were plated at 3x10<sup>5</sup> cells/well. Once again no significant difference was observed between the wildtype and GalNAcT<sup>-/-</sup> anti-GD1b specific immune response for either IgM (6.75±3.65 vs. 5.33±1.054 spots/3x10<sup>5</sup> cells respectively) or IgG (0.25±0.16 vs. 1.167±0.726 spots/3x10<sup>5</sup> cells respectively). Once again IgM values were higher than IgG (Figure 4.9).

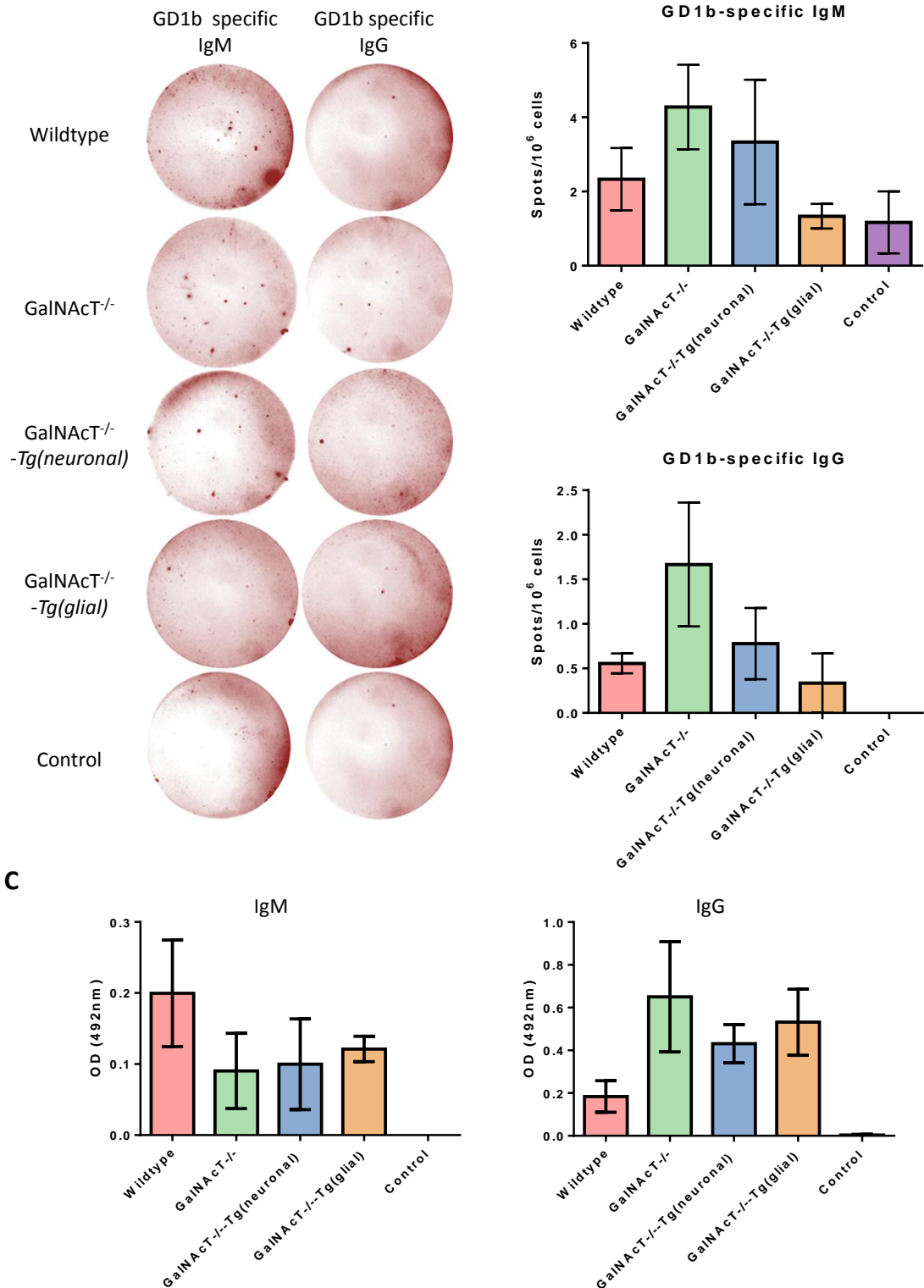


**Figure 4.8: Immune reactivity of various mouse strains to GD1b liposomes.**

Splenocytes from immunised mice were cultured from spleens taken upon sacrifice and maintained in T25 flasks for 7 days. On day 2 ELISpot analyses was performed by applying 10<sup>6</sup> cells/well to a GD1b coated plate. **A:** Representative ELISpot wells probed for IgG or IgM. **B:** GD1b-specific IgM and IgG spot production from immunised mice and control naïve mice. No significant differences existed among groups (one-way ANOVA with Tukey's multiple comparison test) **C:** Supernatant from splenocytes was removed after 7 days and analysed for GD1b-specific IgM and IgG production. No significant differences existed among groups (one-way ANOVA with Tukey's multiple comparison test).

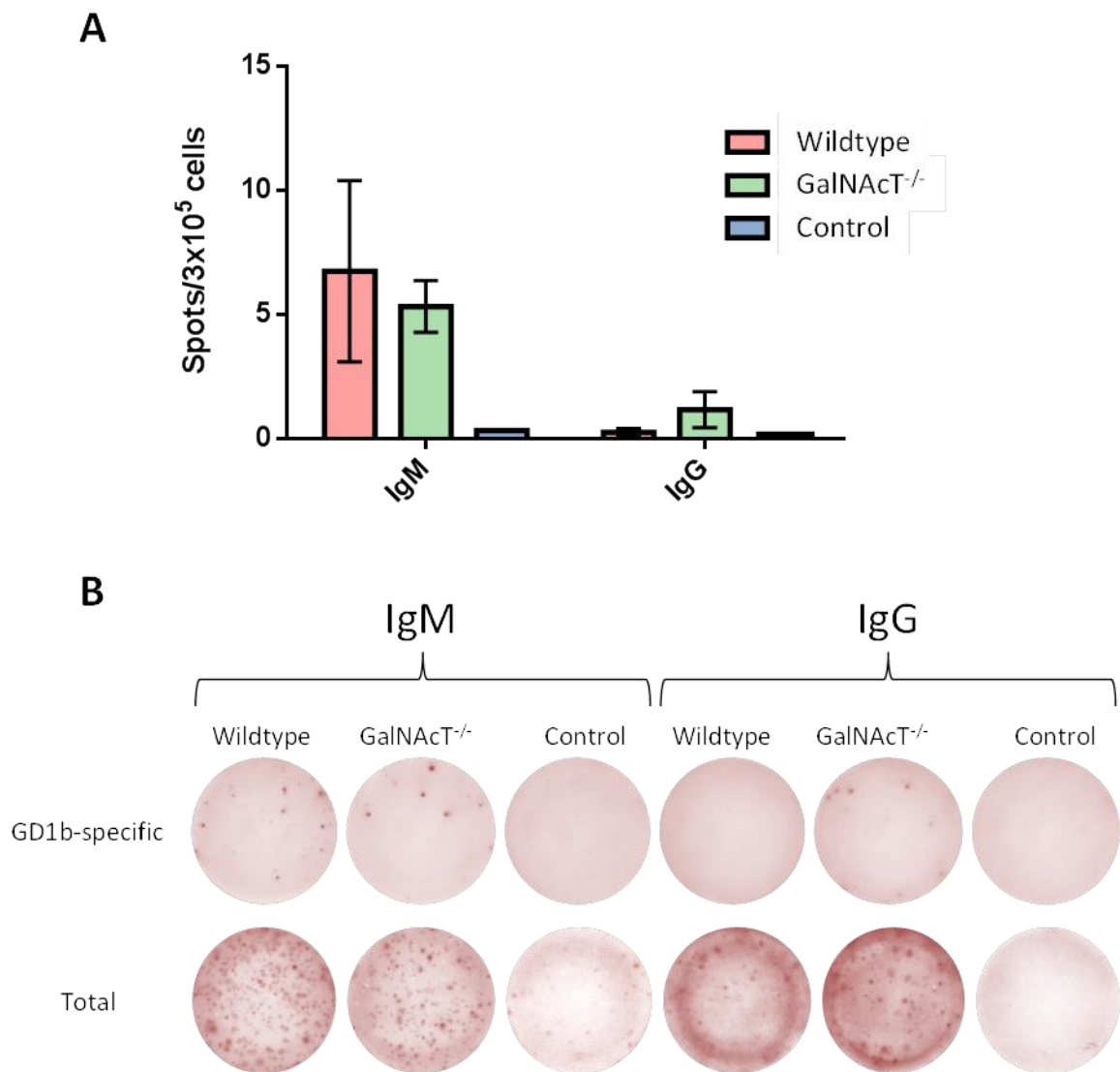


**Figure 4.9: ELISpot analysis of spleen B cell reactivity to GD1b liposome.** Splenocytes from GD1b-immunised wildtype and GalNAcT<sup>-/-</sup> mice (n=4 per group) mice were applied to a GD1b-coated plate at 3x10<sup>5</sup> cells/well. **A:** No significant difference was observed between the spot number of wildtype and GalNAcT<sup>-/-</sup> mice (one-way ANOVA). Control mouse was unimmunised (n=1) and showed no GD1b-specific response. **B:** Representative ELISpot wells probed for GD1b-specific or total IgG or IgM.

#### 4.4 Discussion

The passive immunisation protocol used in this study has been used before to demonstrate anti-ganglioside antibody mediated injury to wildtype diaphragm in a MFS mouse model (Halstead et al., 2004; Halstead et al., 2005a; Halstead et al., 2008). Passive immunisation of wildtype, GalNAcT<sup>-/-</sup>-*Tg(neuronal)* and GalNAcT<sup>-/-</sup>-*Tg(glial)* mice did result in a detectable injury *in vivo*, with wildtype and GalNAcT<sup>-/-</sup>-*Tg(neuronal)* mice showing reduced tidal volumes indicating

diaphragm injury. These mice, and the  $\text{GalNAcT}^{-/-}\text{-Tg}(glial)$  mice also showed reduced ability to stay on the Rotarod. This is most likely due to diaphragm injury resulting in breathing difficulties rather than functional deficits in the limb muscles, as the NHS is unlikely to be systemically distributed at this timepoint (Halstead et al., 2008).  $\text{GalNAcT}^{-/-}\text{-Tg}(glial)$  mice were less severely ill and diaphragms showed lower IgG3 deposits over the endplate, but there was some loss of neurofilament. In *ex vivo* TS preparations,  $\text{GalNAcT}^{-/-}\text{-Tg}(glial)$  mice show MOG1 binding on pSC cell bodies and the processes they extend over the nerve terminal. IgG3 deposits in the diaphragms of passively immunised mice appeared to show strongest staining on the cell bodies and not the processes. Therefore, it is unclear whether the loss of NFil seen in these mice is due to direct complement activation on the processes (antibody may be present but much lower than staining on cell bodies), resulting in a secondary loss of NFil from lack of pSC support, or if the nerve terminal itself is subjected to bystander injury due to its close proximity to the pSCs. A previous study using *ex vivo* hemidiaphragms has shown that pSC injury without nerve terminal damage is possible, therefore the former assumption is the most likely in this instance (Halstead et al., 2005b). This also may explain why the  $\text{GalNAcT}^{-/-}\text{-Tg}(glial)$  mice did not appear to be as severely affected as wildtype and  $\text{GalNAcT}^{-/-}\text{-Tg}(neuronal)$  mice at the earlier stages of behavioural testing, but  $\text{GalNAcT}^{-/-}\text{-Tg}(glial)$  mice did trend towards lower tidal volume by the 120 minute timepoint and showed a reduced Rotarod performance which again was 2-3 hours post NHS treatment.

As the passive immunisation with MOG1 showed a quantifiable injury in wildtype and both rescue strains, an attempt was made to actively immunise these mice then to use NHS to induce an injury. This followed on from a previous unpublished study by Dr S. Rinaldi, where  $\text{GalNAcT}^{-/-}\text{-Tg}(neuronal)$  mice were successfully immunised with GT1b-containing liposomes to produce anti-GT1b antibodies. Using GD1b-containing liposomes, this study has shown that these mice and additionally the  $\text{GalNAcT}^{-/-}\text{-Tg}(glial)$  mice can be successfully immunised with GD1b-containing liposomes, producing both IgM and IgG antibodies against GD1b at intermediate levels compared to  $\text{GalNAcT}^{-/-}$  and wildtype mice, which produce higher and lower responses respectively. The low serum presence of antibodies in wildtype mice compared with  $\text{GalNAcT}^{-/-}$  mice

corresponded with previous immunisation studies using these mice in active immunisation studies (Bowes et al., 2002; Lunn et al., 2000). Since  $\text{GalNAcT}^{-/-}$ -*Tg(neuronal)* and  $\text{GalNAcT}^{-/-}$ -*Tg(glial)* mice are able to produce antibodies against a target ganglioside, they clearly do not possess the same level of tolerance as wildtype mice. It is unknown precisely why these mice lack tolerance to a self-lipid. It may be that the lower levels of enzyme expression result in levels of target antigen production which are below the critical threshold for induction of tolerance. B cells which are autoreactive can avoid deletion if antigen levels are low enough. These cells are termed to be clonally ignorant (Thomas, 2001). Alternatively, the global KO of the *B4galnt1* gene in these mice may result in the developing B cells being unexposed to the presence of GD1b which is only re-introduced in neurons and glia of  $\text{GalNAcT}^{-/-}$ -*Tg(neuronal)* and  $\text{GalNAcT}^{-/-}$ -*Tg(glial)* mice, respectively. In the thymus, T cells are presented with tissue-specific antigens by means of the autoimmune regulator gene *Aire*, which promotes expression of genes which are only present in specialised peripheral tissues. This process allows any self-reactive T-cells to be deleted (Liston et al., 2003). The bone marrow, on the other hand, does not have an equivalent regulatory mechanism for tissue-specific antigen presentation. B cells may therefore not be presented with GD1b in  $\text{GalNAcT}^{-/-}$ -*Tg(neuronal)* and  $\text{GalNAcT}^{-/-}$ -*Tg(glial)* mice, allowing them to react with target upon immunisation.

Based on the wildtype mice's apparent tolerance to GD1b resulting in the low presence of antibody in the serum, it was unsurprising that no injury was detectable by *in vivo* testing or *ex vivo* diaphragm analysis. Similarly, with  $\text{GalNAcT}^{-/-}$  mice, injury to NMJs would not be expected as these mice do not contain the target antigen. Despite a detectable level of both IgG and IgM antibody in the serum of  $\text{GalNAcT}^{-/-}$ -*Tg(neuronal)* and  $\text{GalNAcT}^{-/-}$ -*Tg(glial)* mice and the known expression of the target antigen, these mice also did not show any behavioural or functional changes and negligible immunoglobulin was detectable at the endplate. C3 was however present at the nerve terminals of all mice groups which express GD1b (wildtype,  $\text{GalNAcT}^{-/-}$ -*Tg(neuronal)* and  $\text{GalNAcT}^{-/-}$ -*Tg(glial)*). Despite this, no MAC deposition occurred and subsequently, differences in NFil at the endplate are not likely due to antibody and complement-mediated injury. Unexpectedly, NFil presence was lower in

GalNAcT<sup>-/-</sup> and GalNAcT<sup>-/-</sup>-*Tg(glial)* mice. Although these mice are approximately 3 months old at time of sacrifice, they may already be showing some of the degenerative phenotype associated with aged GalNAcT<sup>-/-</sup> and GalNAcT<sup>-/-</sup>-*Tg(glial)* mice (Yao et al., 2014).

As it has proven difficult to show any injury at mouse endplates using anti-ganglioside antibody alone, NHS is administered to induce injury. This is thought to overcome the endogenous mouse complement regulators which prevent cascade activation as these regulators do not affect human complement. It is possible that levels of antibody were so low that only low levels of human C3 were activated. This may allow endogenous soluble complement regulating factors present in the administered NHS to prevent the activation of the terminal pathway. S protein is one soluble factor which acts on the C5b-9 complex, preventing it from inserting into the membrane (Podack et al., 1978). If this was present in sufficient amount in the NHS injected into the mice, it may have inhibited MAC deposition thereby preventing injury to the NFil at the nerve terminal. This effect may only be apparent when antibody levels are relatively low. Alternatively, the antibodies seen in the serum of these mice may not be pathogenic antibodies. Instead these antibodies may be *cis*-inhibited by surrounding glycolipids, preventing binding to GD1b when it is in complex with other gangliosides or lipids. This effect has been demonstrated before with many ganglioside-binding ligands (Greenshields et al., 2009; Rinaldi et al., 2009; Rinaldi et al., 2013). Glycoarray analysis of serum at day 22 showed inhibition by GM1 fairly consistently in all mouse strains which could result in decreased binding at the nerve terminal, where GM1 is known to be expressed (Hansson et al., 1977; Ganser et al., 1983). Results from the topical application of the sera from the actively immunised mice followed by 4% NHS were consistent with results from the *in vivo* work with no MAC deposition occurring.

As GalNAcT<sup>-/-</sup>-*Tg(neuronal)* and GalNAcT<sup>-/-</sup>-*Tg(glial)* mice showed intermediate serum levels of antibody compared with the low values seen in wildtype and the higher values seen in GalNAcT<sup>-/-</sup> mice, ELISpots were performed to measure differences in the immune response more directly than serum analysis. No significant difference was observed in the GD1b-specific IgG and IgM production among the mice groups, indicating that the levels of antibody seen in the serum

were not reflective of the antibody being produced at a plasma cell level. However, the trend was towards a higher production in GalNAcT<sup>-/-</sup> mice.

The successful immunisation of these mice but inability for the antibodies produced to cause injury could have been caused by a number of factors. Firstly, the antibodies may not have been produced at high enough concentrations; spot numbers were low in ELISpots. Secondly, the antibodies may not have been pathogenic. Antibodies can be prevented from binding their target epitope by surrounding structures, rendering them non-pathogenic (Greenshields et al., 2009). However the activation of C3 at the endplates, suggest that at least some of the antibodies produced have the ability to bind. In reality it is likely that a combination of these factors is preventing sufficient complement activation and MAC deposition to result in a measurable injury, with only a portion of the already low-level of antibodies produced being pathogenic. Further improvements to the immunisation protocol may result in an increased antibody production and thus increase the likelihood of producing a measurable injury. The necessity of NHS administration is in some ways beneficial, as it means we can control when injury is introduced in these mice. However, one single NHS injection may not be the optimal way of inducing injury in a long-term immunisation model, where mice have constant, low levels of circulating antibodies. Indeed, it was unsurprising that no infiltration of immune cells were seen at the diaphragm so soon after a single NHS injection. A protocol involving regular, small injections of NHS, may be more likely to produce a successful active immunisation model which more keenly reflects the clinical situation.

The most intriguing factor of these results was that despite no significant differences in antibody production at a plasma cell level, there were significant differences in the serum of the four different mouse groups. In particular it appeared that wildtype mice, despite having a very low serum presence of anti-GD1b antibodies, showed almost equal IgM production to GalNAcT<sup>-/-</sup> *Tg(neuronal)* mice by ELISpot and splenocyte supernatant ELISA, and only slightly lower production of IgG by the same methods. It was hypothesised that the difference between the serum levels and the actual antibody production may be caused by the previously demonstrated ability of cells, particularly the motor nerve terminal, to internalise antibody (Fewou et al., 2012; Iglesias-Bartolome et

al., 2006; Iglesias-Bartolome et al., 2009). This possibility was therefore addressed in the remainder of this thesis.

## 5 Ability of the NMJ to clear anti-GD1b antibody

### 5.1 Introduction

As described in the previous chapter, circulating anti-GD1b antibody was present in the sera of GalNAcT<sup>-/-</sup>-*Tg(neuronal)* and GalNAcT<sup>-/-</sup>-*Tg(glial)* mice after active immunisation with GD1b liposomes. These levels were somewhat intermediate compared to levels in wildtype mice and GalNAcT<sup>-/-</sup> mice, which showed lower and higher OD values by ELISA respectively. These intermediate levels of circulating antibody were not able to induce any functional deficits in these mice when NHS was given i.p., though they did induce some minor evidence of complement activation at the NMJ itself. Despite the differences seen in serum levels of antibody, ELISpots performed on splenocytes from immunised mice showed that no statistically significant difference in antibody production existed between the responses of any of the genotypes. Taking into account these findings, along with the knowledge that antibodies against gangliosides can be taken up at wildtype and GD3s<sup>-/-</sup> mouse motor nerve terminals (Fewou et al., 2012), it was hypothesised that antibodies are produced to a similar degree in all genotypes, but levels of antibody in the serum may be being affected by this internalisation.

The aim of this chapter is to investigate the phenomenon of anti-ganglioside antibody internalisation, especially at the NMJ, utilising GalNAcT<sup>-/-</sup>-*Tg(neuronal)* and GalNAcT<sup>-/-</sup>-*Tg(glial)* mice to look at membrane-specific uptake, and to determine whether the internalisation here is enough to affect the circulating levels of anti-ganglioside antibody *in vivo*. As this chapter followed on from investigations performed in mice which were immunised with GD1b, the anti-GD1b antibody MOG1 was used in all studies in this chapter.

### 5.2 *Ex vivo* uptake of anti-GD1b antibody

Whole mount TS preparations were used to investigate the internalisation of MOG1 *ex vivo*. This has been done before previously in wildtype mice, but the present study has included GalNAcT<sup>-/-</sup>-*Tg(neuronal)*, GalNAcT<sup>-/-</sup>-*Tg(glial)* mice and GalNAcT<sup>-/-</sup> mice. Where possible, the same endplate was imaged pre and post-permeabilisation. For full methods please refer to Chapter 2 section 2.10.3.

Wildtype mice showed strong neuronal presence of antibody immediately after incubation with MOG1 (0 minutes timepoint, median 85.00 AU), with no apparent staining of pSCs (Figure 5.1A, B). Following incubation at 37°C for 30 minutes, a reduction in the levels of antibody intensity at the nerve terminal was seen (Figure 5.1A), leaving reduced staining (median 57.00 AU), however this reduction was not significant. After 60 minutes at 37°C, there were similar levels of staining intensity overlying the NMJ (median 61.00 AU, Figure 5.1B). These decreases were not statistically significant compared with 0 minutes, however some NMJs completely lacked in antibody staining at the 60 minutes timepoint (Figure 5.1A). Tissue was then permeabilised and reprobbed with secondary antibody, revealing presence of anti-GD1b antibody in junctions which previously were antibody negative or had very weak staining (Figure 5.1A). Despite this clear visual difference, following permeabilisation, the 30 and 60 minute timepoints were statistically lower than 0 minutes with medians of 173.00 AU and 155.00 AU respectively compared with 223.00 AU (Figure 5.1C). The staining following permeabilisation was punctate and appeared to be within the nerve terminal, with no discernible presence in pSCs. Although not directly comparable due to the further addition of secondary antibody and the potential internalisation which may have occurred even during the 4°C antibody incubation step, the 0 minutes timepoint was also compared directly with 60 minutes before and after Triton. Still no significant difference is observed vs. 60 minutes before permeabilisation; however an increase is seen in staining at 60 minutes + Triton when compared to 0 minutes - Triton.

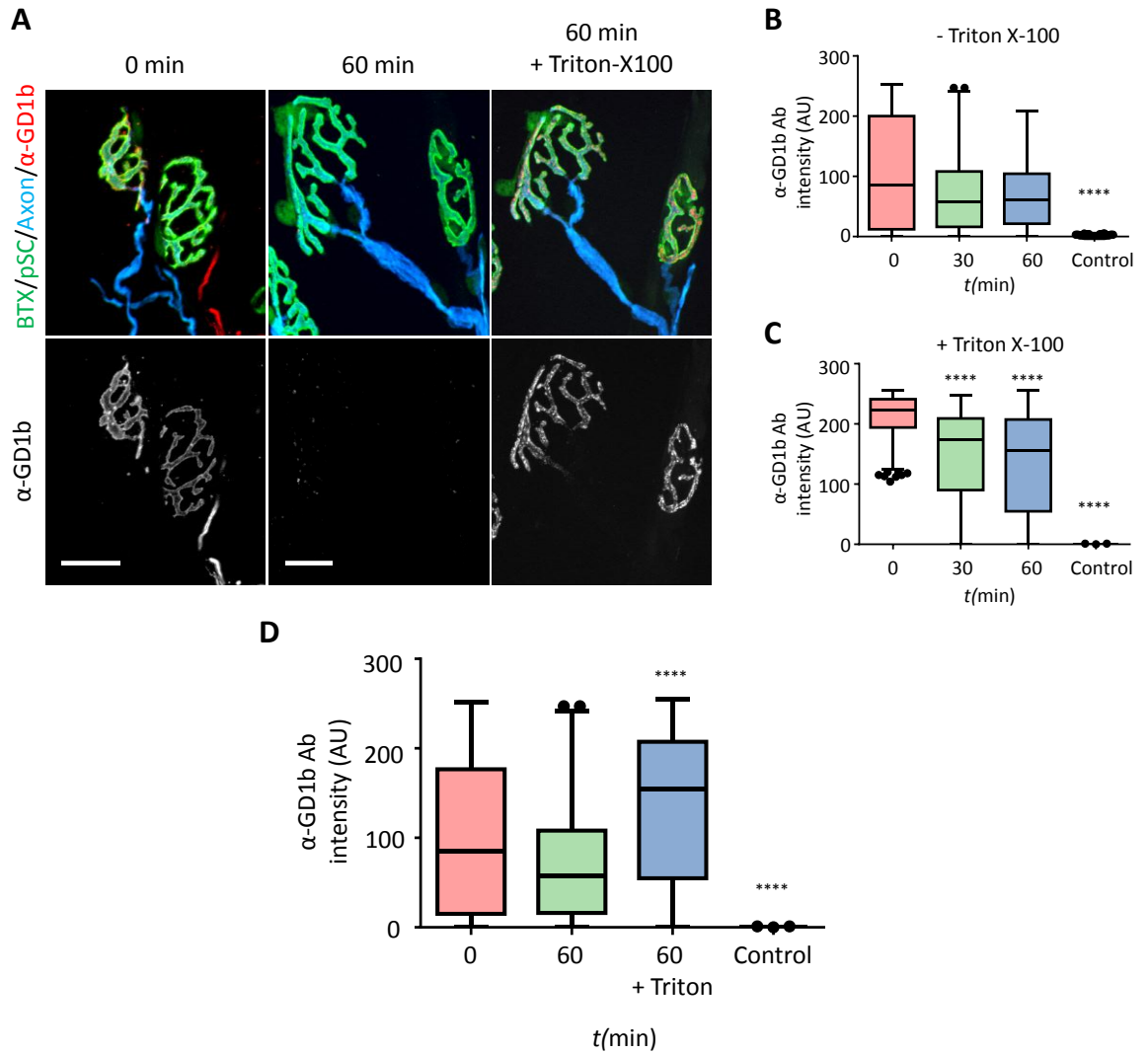


**Figure 5.1: Internalisation of anti-GD1b antibody occurs at the nerve terminal after 30 minutes at 37°C in wildtype mice.** Wildtype mice (n=3) TS muscle was labelled with anti-GD1b antibody for 30 minutes at 4°C then rinsed and either fixed immediately (0 minutes) or moved to 37°C for 30 minutes or 60 minutes. Junctions were analysed for presence of antibody. The preparations were then permeabilised, reprobed with secondary antibody and re-analysed. **A:** Illustrative images show the wildtype motor endplates were labelled at 0 minutes with anti-GD1b antibody, but upon incubation at 37°C for 60 minutes, labelling is reduced. Permeabilisation of the membrane with Triton X-100 reveals presence of antibody within the motor nerve terminal. **B:** Quantification of antibody binding shows that after 30 and 60 minutes at 37°C there was a decrease in presence of anti-GD1b antibody compared with 0 minutes though not significant. **C:** Following permeabilisation, a difference still existed between 30 and 60 minute timepoints and 0 minutes. **D:** When 0 minutes is compared with 60 minutes  $\pm$  Triton, still no significant difference is observed when compared with - Triton and a significant increase is seen compared with + Triton. Scale Bar = 20  $\mu$ m. \*\*\*\* =  $p < 0.0001$  vs. 0 minutes, Kruskal-Wallis with Dunn's multiple comparisons test. Controls are secondary antibody only. A minimum of 107 NMJs were analysed per group. Non-parametric data displayed as Tukey box plot (see section 2.20).

In  $\text{GalNAcT}^{-/-}\text{-Tg}(\text{neuronal})$  tissue, a similar, but more clear cut phenomenon is observed. Immediately after incubation at  $4^{\circ}\text{C}$ , anti-GD1b antibody presence is apparent at the NMJ, including staining of pSCs (Figure 5.2A). This staining was reduced following 30 or 60 minutes at  $37^{\circ}\text{C}$  (median 68.50 and 75.00 AU respectively vs. 0 minutes median of 240.00 AU). Neuromuscular junctions which had previously shown little or no staining after 30 or 60 minutes at  $37^{\circ}\text{C}$  did show presence of antibody following permeabilisation and re-probing with secondary antibody. Compared with the 0 minute timepoint there appeared to be little difference between medians of 30 and 60 minute timepoint (median of 255.00 AU vs. 233.00 and 244.00 AU respectively), though this difference was significant in both cases ( $p < 0.0001$ ).

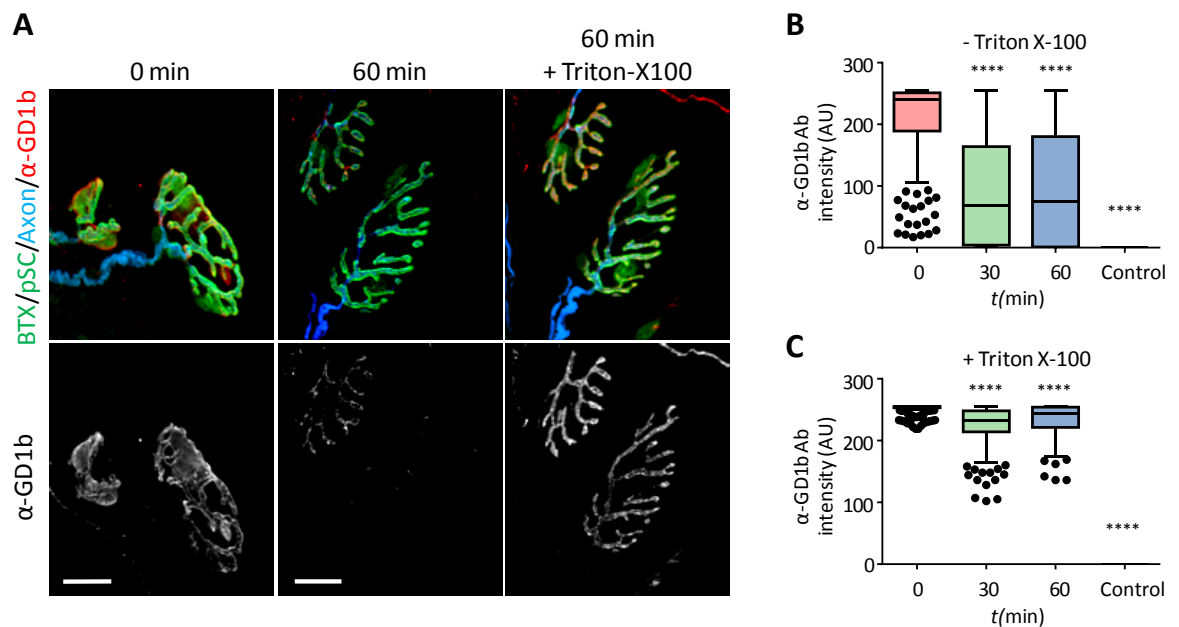


**Figure 5.2: Internalisation of anti-GD1b antibody occurs at the nerve terminal after 30 minutes at  $37^{\circ}\text{C}$  in  $\text{GalNAcT}^{-/-}\text{-Tg}(\text{neuronal})$  mice.**  $\text{GalNAcT}^{-/-}\text{-Tg}(\text{neuronal})$  mice ( $n=3$ ) TS muscle was labelled with anti-GD1b antibody for 30 minutes at  $4^{\circ}\text{C}$  then rinsed and either fixed immediately (0 minutes) or moved to  $37^{\circ}\text{C}$  for 30 minutes or 60 minutes. Junctions were analysed for presence of antibody. The preparations were then permeabilised, re-probed with secondary antibody and re-analysed. **A:** Illustrative images show the NMJs were labelled at 0 minutes with anti-GD1b antibody, but upon incubation at  $37^{\circ}\text{C}$ , labelling is no longer present. Permeabilisation of the membrane with Triton X-100 reveals presence of antibody within the motor nerve terminal. **B:** Quantification of antibody binding shows that after 30 and 60 minutes at  $37^{\circ}\text{C}$  there was a significant decrease in presence of anti-GD1b antibody compared with 0 minutes. **C:** Following permeabilisation, a significant difference still existed between 30 and 60 minute timepoints and 0 minutes, however there was a large reduction in the differences. Scale Bar =  $20\ \mu\text{m}$ . \*\*\*\* =  $p < 0.0001$  vs. 0 minutes, Kruskal-Wallis with Dunn's multiple comparisons test. Controls are secondary antibody only. A minimum of 197 NMJs were analysed per group. Non-parametric data displayed as Tukey box plot (see section 2.20).

As shown in Chapter 3, anti-GD1b antibody binds to pSCs at the NMJ in GalNAcT<sup>-/-</sup>-*Tg(glial)* mice. Mice expressing GFP in their glial cells (with highest expression in the pSCs) were used for this experiment to enable quantification, which normally uses BTx alone as a marker of the nerve terminal. Following 30 and 60 minutes at physiological temperatures the glial antibody staining disappears (Figure 5.3A). The intensity of antibody at the junction is decreased significantly from a median of 226.5 AU at 0 minutes to 11.0 AU at 30 minutes and further to 0.0 by 60 minutes ( $p < 0.0001$  in both cases, Figure 5.3B). After permeabilisation at the 30 minutes timepoint an increase is seen in antibody intensity compared to unpermeabilised tissue, though this figure is still significantly lower than 0 minutes ( $p < 0.0001$ , median 237 AU vs. 107 AU). Unlike wildtype and GalNAcT<sup>-/-</sup>-*Tg(neuronal)* mice however, staining does not reappear at the 60 minutes timepoint following permeabilisation, either in the pSC body or in the nerve terminal. Levels of antibody intensity remain lower than the 0 minutes timepoint ( $p < 0.0001$ , median 237.00 AU vs. 10.00 AU, Figure 5.3C).

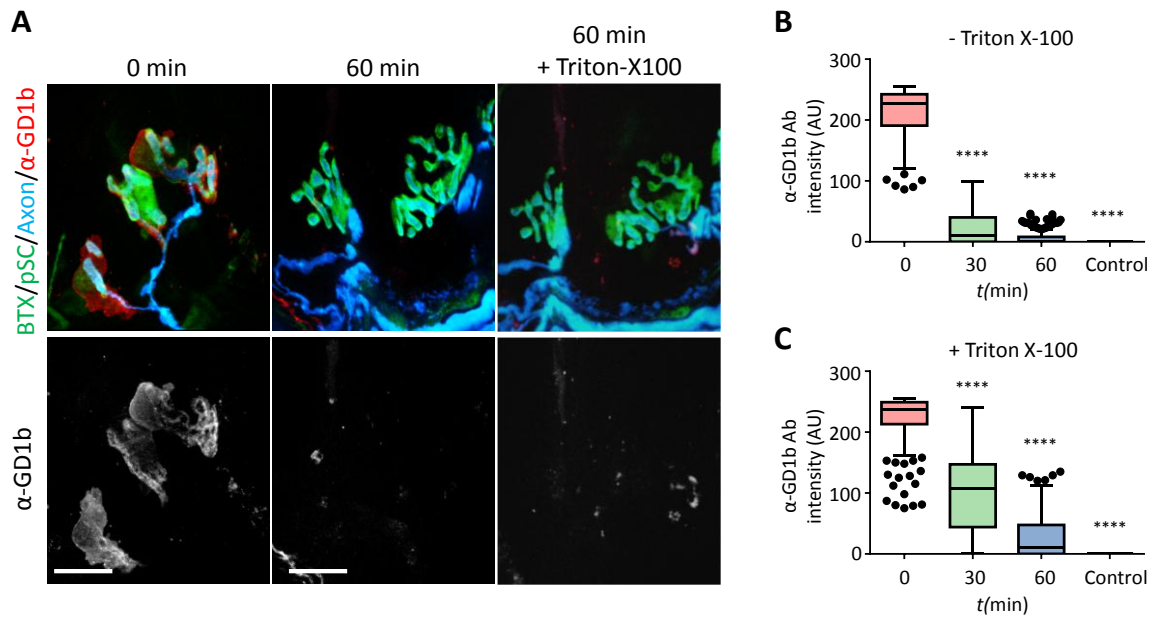


**Figure 5.3: Internalisation of anti-GD1b antibody occurs at the nerve terminal after 30 minutes at 37°C in GalNAcT<sup>-/-</sup>-Tg(*glial*) mice.** GalNAcT<sup>-/-</sup>-Tg(*glial*) mice (n=3) TS muscle was labelled with anti-GD1b antibody for 30 minutes at 4°C then rinsed and either fixed immediately (0 minutes) or moved to 37°C for 30 minutes or 60 minutes. Junctions were analysed for presence of antibody. The preparations were then permeabilised, re-probed with secondary antibody and re-analysed. **A:** Illustrative images show the NMJs were labelled at 0 minutes with anti-GD1b antibody, but upon incubation at 37°C, labelling is no longer present. Permeabilisation of the membrane with Triton X-100 reveals presence of antibody within the motor nerve terminal. **B:** Quantification of antibody binding shows that after 30 and 60 minutes at 37°C there was a significant decrease in presence of anti-GD1b antibody compared with 0 minutes. **C:** Following permeabilisation, a significant difference still existed between 30 and 60 minute timepoints and 0 minutes. Scale Bar = 20  $\mu$ m. \*\*\*\* =  $p < 0.0001$  vs. 0 minutes, Kruskal-Wallis with Dunn's multiple comparisons test. Controls are secondary antibody only. A minimum of 122 NMJs were analysed per group. Non-parametric data displayed as Tukey box plot (see section 2.20).

As expected, no binding was seen at the 0 minutes timepoint in GalNAcT<sup>-/-</sup> mice which lack GD1b target (median 0 AU). Therefore following 30 and 60 minutes at 37°C, the NMJs were still negative for anti-GD1b (medians of 0 AU also). Critically, when tissue is permeabilised, NMJs remain vacant of anti-GD1b antibody, indicating that uptake into nerve terminal was reliant on the presence of GD1b on the plasma membrane.

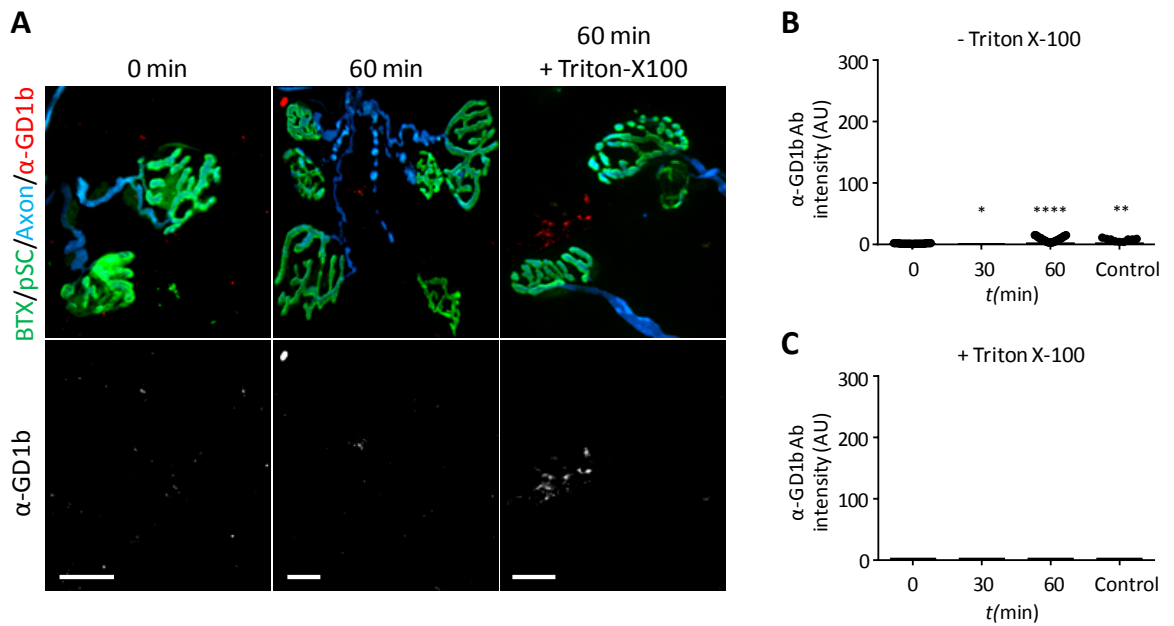


**Figure 5.4: Internalisation of anti-GD1b antibody does not occur at nerve terminals lacking GD1b ganglioside.** GalNACT<sup>-/-</sup> mice (n=3) TS muscle was labelled with anti-GD1b antibody for 30 minutes at 4°C then rinsed and either fixed immediately (0 minutes) or moved to 37°C for 30 minutes or 60 minutes. Junctions were analysed for presence of antibody. The preparations were then permeabilised, re-probed with secondary antibody and re-analysed. **A:** Illustrative images show the GalNACT<sup>-/-</sup> NMJs showed no binding at 0 minutes with anti-GD1b antibody, and also no binding was seen following incubation at 37°C. Permeabilisation of the membrane with Triton X-100 shows no antibody presence in the nerve terminal. **B:** Quantification of antibody binding, shows that after 30 and 60 minutes at 37°C there were slight but significant differences in presence of antibody over the NMJ, however the level of binding is almost non-existent at all timepoints. **C:** Following permeabilisation, a similar slight but significant difference still existed but binding was still non-existent at all timepoints. Scale Bar = 20  $\mu$ m. \*= $p$ <0.05, \*\*= $p$ <0.01, \*\*\* =  $p$ <0.0001 vs. 0 minutes, Kruskal-Wallis with Dunn's multiple comparisons test. Controls are secondary antibody only. A minimum of 55 NMJs were analysed per group. Non-parametric data displayed as Tukey box plot (see section 2.20).

### 5.2.1 Fate of antibody at the nerve terminal

As antibody presence in the nerve terminal after 30 and 60 minutes appeared punctate in wildtype, GalNACT<sup>-/-</sup>-*Tg(neuronal)* and, where present, in GalNACT<sup>-/-</sup>-*Tg(glial)* mice, it was thought likely that the antibody would co-localise with some part of the vesicle trafficking system. A preliminary attempt was made to find where the antibody localises to in the nerve terminal. This required a labelled monoclonal antibody; however attempts to label MOG1 and MOG16 failed or resulted in antibody not binding successfully as tested by glycoarray (data not shown).

### 5.2.2 Autophagy inhibition in *GalNAcT<sup>-/-</sup>-Tg(glia)* mice

As the *GalNAcT<sup>-/-</sup>-Tg(glia)* mice showed no restoration of antibody intensity at the 60 minute timepoint following permeabilisation and had low values even at 30 minutes, it was thought that the antibody may have been degraded in these preparations. To inhibit lysosomal breakdown of antibody by preventing vesicle acidification, Ringer's was modified to contain  $\text{NH}_4\text{Cl}$  (see Chapter 2.1.4.1) during the incubation period at 37°C.

However, the prevention of vesicle acidification did not result in a significant difference in antibody presence following permeabilisation when compared with tissue incubated in normal Ringer's (Figure 5.5).

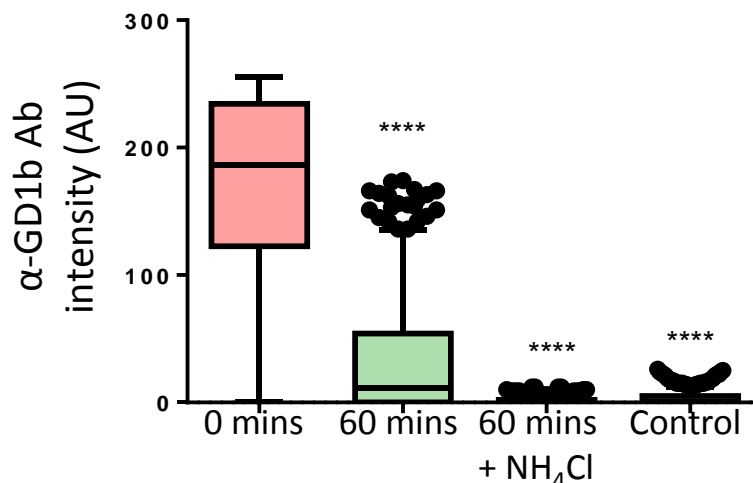


**Figure 5.5: Inhibition of vesicle acidification does not increase presence of MOG1 in *GalNAcT<sup>-/-</sup>-Tg(glia)* mouse perisynaptic Schwann cells following incubation at physiological temperatures.** *GalNAcT<sup>-/-</sup>-Tg(glia)* mouse (n=3) TS muscle was labelled with anti-GM1 antibody for 30 minutes at 4°C then rinsed and either fixed immediately (0 minutes at 37°C) or moved to 37°C for 60 minutes. Junctions were analysed for presence of antibody. The preparations were then permeabilised, re-probed with secondary antibody and re-analysed. Tissue where antibody had been incubated at 37°C in normal Ringer's or Ringer's containing  $\text{NH}_4\text{Cl}$  were both statistically lower than at 0 minutes, with even lower values seen with  $\text{NH}_4\text{Cl}$  tissue. \*\*\*\* =  $p < 0.0001$  vs. 0 minutes, Kruskal-Wallis with Dunn's multiple comparisons test. A minimum of 244 junctions were analysed. Control was secondary antibody only. A minimum of 244 NMJs were analysed per group. Non-parametric data displayed as Tukey box plot (see section 2.20).

### 5.3 *In vivo* uptake of anti-GD1b antibody

To see whether the clearance of these antibodies at nerve terminals is sufficient to affect levels of antibody in the circulation, MOG1 antibody was injected into wildtype, GalNAcT<sup>-/-</sup> and GalNAcT<sup>-/-</sup>-*Tg(neuronal)* mice i.p. and circulating levels of antibody monitored over a seven day time period. As the half-life of IgG3 in mice serum is seven days, no timepoints after this were monitored. Sera from mice were run on plates alongside monoclonal antibody control and the results expressed as a percentage of the control OD at 5 µg /ml.

#### 5.3.1 Serum levels of anti-GD1b antibody

At baseline, all mice showed no GD1b reactivity by ELISA. Serum antibody levels peaked for all genotypes at day 1 following the injection (Figure 5.6) but wildtype mice showed significantly lower values than both the GalNAcT<sup>-/-</sup> and the GalNAcT<sup>-/-</sup>-*Tg(neuronal)* mice even at this early timepoint ( $p < 0.001$  and  $p < 0.05$ , mean 11.67% of control). From this time point onwards, wildtype levels continued to decrease culminating in values 4.00% of that of the control at day 7. These mice therefore appear to clear the antibody from their circulation rapidly. Conversely, serum levels of MOG1 in GalNAcT<sup>-/-</sup> mice remained significantly higher than wildtype at all timepoints, peaking at day 1 (mean 31.12% of control) then maintaining a high level of circulating antibody throughout the experiment (mean 24.47% of control on day 7). Comparing this with wildtype results, this indicates that the lack of target in these mice prevents their clearing the antibody from the bloodstream. Levels of antibody in GalNAcT<sup>-/-</sup>-*Tg(neuronal)* mice sera lay somewhere in between levels of wildtype and GalNAcT<sup>-/-</sup> mice. Values in these mice were significantly higher than wildtype, but not GalNAcT<sup>-/-</sup> mice on day 1 (mean 24.41% of control) but on day 2 values had decreased so as to be neither significantly different from wildtype or GalNAcT<sup>-/-</sup> mice. From day 6 levels of antibody in GalNAcT<sup>-/-</sup>-*Tg(neuronal)* mice had reached levels significantly lower than GalNAcT<sup>-/-</sup> mice ( $p < 0.01$ ) (mean 9.03% of control). Therefore, like the wildtype mice, these mice also appear to be able to clear the circulating antibody however at a much slower rate than their counterparts.

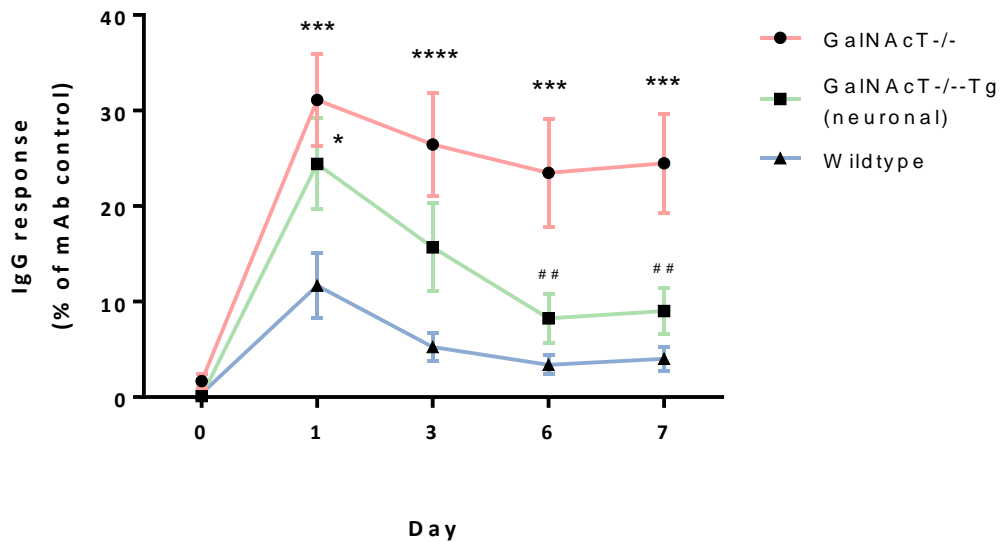


**Figure 5.6: MOG1 serum presence by ELISA over 7 days.** Data normalised to MOG1 antibody as a positive control. Wildtype mice (n=9) clear antibody quickly from their circulation, most being cleared even at the day 1 timepoint. GalNAcT<sup>-/-</sup> mice (n=8) do not clear the antibody and show high levels even at day 7. GalNAcT<sup>-/-</sup>-Tg(*neuronal*) mice (n=8) show a peak at day 1 and a decline over the remaining days, indicating a slow clearance of antibody. \*= $p < 0.05$ , \*\*\*= $p < 0.001$ , \*\*\*\*= $p < 0.0001$  vs. wildtype. ##= $p < 0.01$  vs. GalNAcT<sup>-/-</sup>, two-way ANOVA with Tukey's multiple comparison test.

### 5.3.2 Tissue analysis

Mice which had been injected with antibody and sacrificed after 7 days showed no presence of antibody at the diaphragm, regardless of mouse strain (data not shown). Spinal cord was taken at C3-C5, where the phrenic nucleus is located (Qiu et al., 2010), and stained for antibody. Wildtype and GalNAcT<sup>-/-</sup> mice were negative for any antibody but in GalNAcT<sup>-/-</sup>-Tg(*neuronal*) mice, a weak pattern of staining was present which was not seen in the other mouse strains (Figure 5.7). When co-stained with NeuN, the neuron cell bodies appeared negative for this staining (not shown) and as such, antibody presence was quantified by analysing the average TRITC intensity in the field of view (FOV), with at least 3 images taken per animal. There was no significant difference in the intensity when measured in this manner.

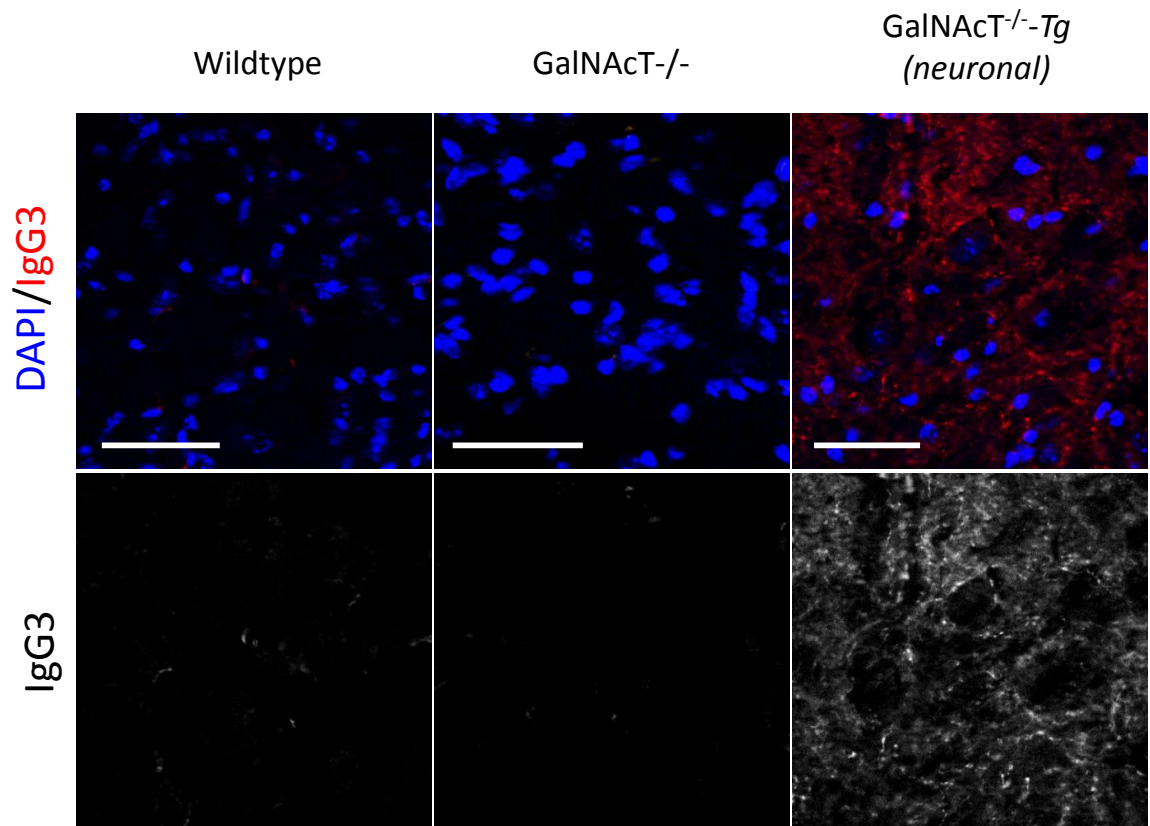


**Figure 5.7: Presence of IgG3 antibody in the cervical cord 7 days after injection.** Only GalNAcT<sup>-/-</sup>Tg(*neuronal*) mice showed any IgG3 in their cord 7 days after i.p. injection of 250 µg of MOG1 antibody. The antibody showed a distinct staining pattern which was not present in large neurons.

Attempts were made to identify where the antibody was localised to in the spinal cord after 7 days. Co-staining for MAP2 for dendrites and synaptophysin for synapses showed no co-localisation, indicating the antibody localisation was probably non-specifically distributed in the neuropil (Figure 5.8).

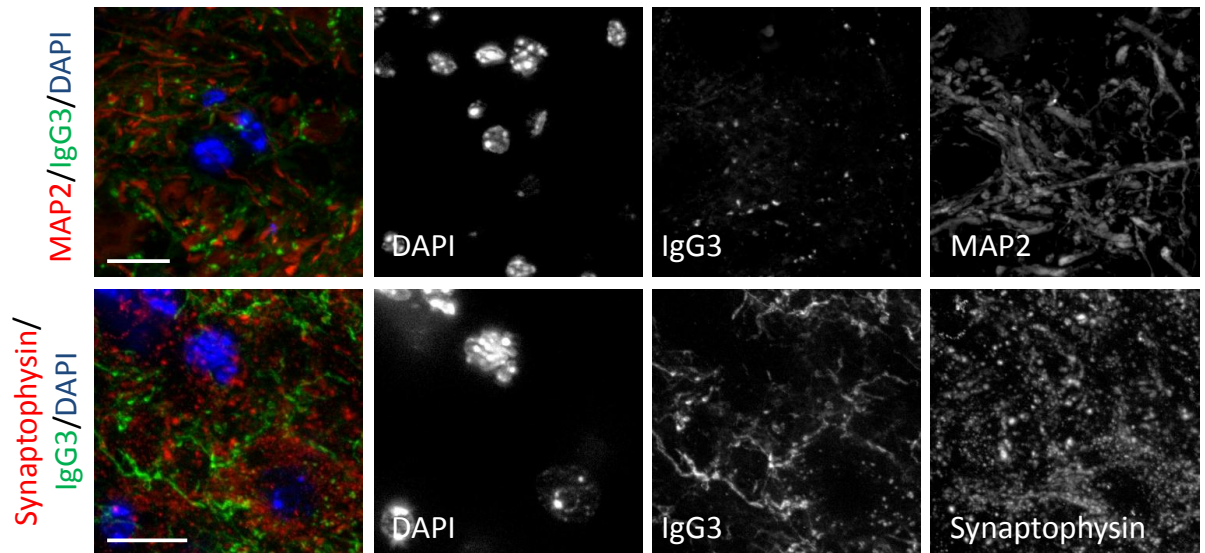


**Figure 5.8: Antibody found in the ventral horn of  $\text{GalNAcT}^{-/-}\text{-Tg}(\text{neuronal})$  mice does not co-localise with MAP2 or synaptophysin.** Spinal cords taken from  $\text{GalNAcT}^{-/-}\text{-Tg}(\text{neuronal})$  mice 7 days after MOG1 injection show antibody in the ventral horn but the antibody does not appear to be in neuronal cell bodies or processes. Co-stain with MAP2 shows the antibody is not present in dendrites and with synaptophysin shows that antibody is not in synapses. Scale bar = 20  $\mu\text{m}$

As antibody had been trafficked to the spinal cord, it was thought likely that it had come there by retrograde transport, however by the 7 day timepoint this antibody may have been further trafficked out of the cell body, in a similar manner to tetanus toxin. Therefore, MOG1 presence in the cord was probed for after 1 day using the spinal cords of mice which had been given 1 mg of MOG1 injected i.p. for passive immunisation (see section 4.2). In this case, antibody was found in the ventral horn neurons of  $\text{GalNAcT}^{-/-}\text{-Tg}(\text{neuronal})$  mice, but not in  $\text{GalNAcT}^{-/-}$  mice. Antibody was only very occasionally seen in wildtype mice but, when present, was always weaker than in  $\text{GalNAcT}^{-/-}\text{-Tg}(\text{neuronal})$  mice. Spinal cords of  $\text{GalNAcT}^{-/-}\text{-Tg}(\text{glial})$  mice were also analysed and were negative for antibody in the cord. Antibody presence was quantified by both positive/negative cell counts and fluorescent intensity of antibody overlying the NeuN-positive signal of the neuron. When analysed by positive/negative cell counts, a chi squared test showed significant differences between positive and negative cells among groups. Multiple Fisher's exact tests showed  $\text{GalNAcT}^{-/-}\text{-Tg}(\text{neuronal})$  mice had a significantly higher number of positive cells than wildtype,  $\text{GalNAcT}^{-/-}$  and  $\text{GalNAcT}^{-/-}\text{-Tg}(\text{glial})$  mice by Fisher's exact test (Figure

5.9, data displayed as percentage positive cells/total cells counted). A similar result was seen when the antibody intensity was measured in NeuN positive cells, with GalNAcT<sup>-/-</sup>-*Tg(neuronal)* mice having higher intensity antibody staining than wildtype, GalNAcT<sup>-/-</sup> and GalNAcT<sup>-/-</sup>-*Tg(glial)* mice (median of 10 AU vs. median of 0 for all other mouse strains, Kruskal-Wallis,  $p < 0.0001$  against wildtype and GalNAcT<sup>-/-</sup>,  $p < 0.001$  vs GalNAcT<sup>-/-</sup>-*Tg(glial)*).

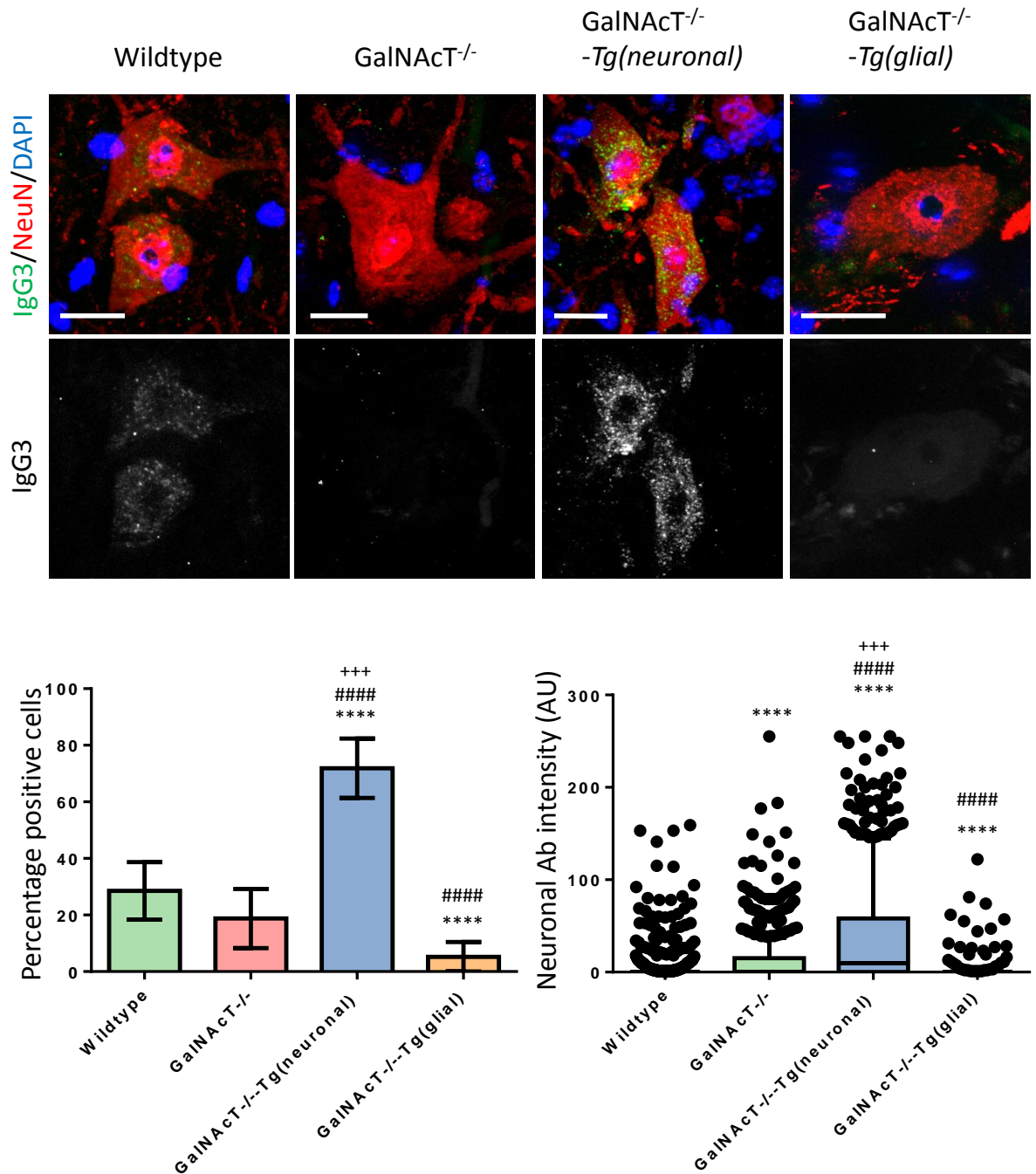


**Figure 5.9: Presence of IgG3 in cervical cord 1 day following injection of 1 mg of MOG1.** No antibody was present in GalNAcT<sup>-/-</sup> or GalNAcT<sup>-/-</sup>-Tg(glia) mice and some weak staining was occasionally present in wildtype mice. GalNAcT<sup>-/-</sup>-Tg(neuronal) mice showed clear presence of antibody in ventral horn neurons. This was quantified in 2 ways: **B:** Percentage of positive cells per FOV were significantly higher in GalNAcT<sup>-/-</sup>-Tg(neuronal) mice compared with wildtype, GalNAcT<sup>-/-</sup> and GalNAcT<sup>-/-</sup>-Tg(glia) mice (chi squared test followed by multiple Fisher's exact tests). **C:** Antibody staining intensity in NeuN positive cells was significantly higher in GalNAcT<sup>-/-</sup>-Tg(neuronal) mice compared with wildtype, GalNAcT<sup>-/-</sup> and GalNAcT<sup>-/-</sup>-Tg(glia) mice (Kruskal-Wallis with Dunn's multiple comparison test). \*\*\*\*= $p < 0.0001$  vs. wildtype, ####= $p < 0.0001$  vs. GalNAcT<sup>-/-</sup>, +++= $p < 0.001$  vs. GalNAcT<sup>-/-</sup>-Tg(glia). Non-parametric data displayed as Tukey box plot (see section 2.20).

To attempt to address whether the antibody was localised to a specific subcellular compartment the antibody in the neurons, spinal cords from *GalNAcT<sup>-/-</sup>-Tg(neuronal)* mice were re-stained with anti-Lamp-2 antibody to look for co-localisation with lysosomes, as the staining appeared vesicular. Lamp-2 staining often overlapped with IgG3, but many “vesicles” of IgG3 were not Lamp-2 positive. Pearson’s correlation coefficient was calculated using co-localisation module of AxioVision software. When the cells were selected within a ROI, Pearson’s coefficient was zero, indicating the co-localisation was random (Figure 5.10).

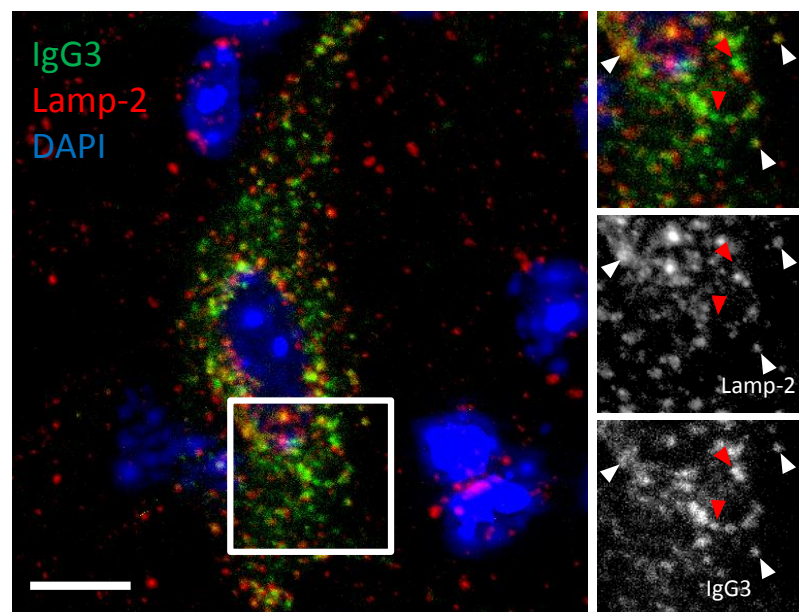


**Figure 5.10: Antibody was only occasionally co-localised with Lamp-2 in ventral horn neurons.** Neurons from *GalNAcT<sup>-/-</sup>-Tg(neuronal)* mice which were shown to contain presence of IgG3 were co-stained with an anti-Lamp2 antibody to indicate presence of lysosomes. Although antibody did occasionally co-localise with lysosomes (white arrowheads), it was also seen in vesicular structures which were not Lamp positive (red arrowheads). When cells were selected as ROI, Pearson’s coefficients were 0.00.

## 5.4 Discussion

Previously published data have shown that following incubation at physiological temperatures, anti-GD1b antibody is cleared rapidly from the NMJ in wildtype mice in *ex vivo* muscle preparations. This antibody is then found in the nerve terminal following permeabilisation of the tissue (Fewou et al., 2012). In the present study, there was not quite a significant decrease at 30 and 60 minutes,

though this may have been due to low staining at 0 minutes in one wildtype mouse. Following permeabilisation, staining intensity following 30 or 60 minutes at 37°C did not quite reach levels equivalent to 0 minutes. However, as observed visually and as shown in the illustrative images, many NMJs which showed no staining at 60 minutes before permeabilisation, showed intracellular antibody following permeabilisation and reprobing with secondary. Additionally, this work has been done before showing a clear internalisation in these mice (Fewou et al., 2012). Expanding on previous work, this study also showed that *GalNAcT<sup>-/-</sup>-Tg(neuronal)* mice, which express complex gangliosides on neuronal membranes, also take up antibody, confirming the nerve terminal's ability to endocytose bound antibody. These mice did on occasion show staining in pSCs at 0 minutes (unlike wildtype which do not have GD1b on pSCs), but this did not seem to hinder the uptake into the nerve terminal. Conversely, in *GalNAcT<sup>-/-</sup>-Tg(glial)* mice, pSCs were the only cells which displayed presence of antibody at 0 minutes. Following permeabilisation, tissue displayed some sparse, punctate staining in pSCs at the 30 minutes timepoint. However, by 60 minutes there was no clear antibody presence in either the pSCs or the nerve terminal. This may be explained either by the antibody being recycled to the pSC surface and released from the cell, or that the antibody is taken up by these cells and degraded within 60 minutes at 37°C. The sparse, punctate staining at 30 minutes supported the latter theory. Perisynaptic Schwann cells have previously been shown to have lysosomal activity in the context of nervous system development and injury (Holtzman and Novikoff, 1965; Jung et al., 2011; Song et al., 2008), but it has never been shown at healthy NMJs. An attempt to inhibit lysosomal activity using NH<sub>4</sub>Cl did not result in the presence of more antibody at the NMJ following permeabilisation, indicating this is perhaps not the mechanism by which antibody is cleared in these mice following incubation at 37°C. However other mechanisms of lysosome inhibition may be employed to confirm that lysosomes do not contribute to antibody degradation, for example Bafilomycin, a V-ATPase inhibitor, which also prevents acidification of lysosomes (Yoshimori et al., 1991). The fate of anti-GD1b antibody taken up by pSCs requires further investigation but it is clear that at earlier timepoints during incubation at physiological temperature the antibody is present in the pSC cell body.

To investigate if this uptake phenomenon could affect levels of circulating antibody *in vivo*, wildtype, GalNAcT<sup>-/-</sup> and GalNAcT<sup>-/-</sup>-Tg(*neuronal*) mice were injected with MOG1 and serum levels were monitored over time. It was shown that wildtype mice clear the antibody very quickly, with very low levels even 1 day after injection. GalNAcT<sup>-/-</sup> mice however, do not show any ability to clear the antibody and GalNAcT<sup>-/-</sup>-Tg(*neuronal*) mice clear the antibody much slower than wildtype mice. Wildtype mice, which had cleared a lot of the antibody even by the one day timepoint, have a high global expression of target GD1b as, though enriched in the nervous system, gangliosides are ubiquitously expressed on plasma membranes. GD1b has been shown to be expressed in tissues such as the liver and kidney (Holthofer et al., 1994;Rodrigo et al., 1987). Therefore it is likely that this ubiquitous distribution of target, has resulted in widespread antibody binding and internalisation along with their target ganglioside by clathrin-independent endocytosis (Crespo et al., 2008;Fewou et al., 2012), thereby rapidly clearing MOG1 from the circulation. It may be argued that this difference in clearance rate may be due to the higher GalNAcT enzyme activity in wildtype mice (100%) compared with GalNAcT<sup>-/-</sup>-Tg(*neuronal*) mice (5.3%) (Yao et al., 2014). However, as discussed in Yao et al, the reduction in enzyme expression may be due to a dilution factor as tests were performed on whole brain, thus wildtype enzyme expression levels would include all non-neuronal complex ganglioside expression (Yao et al., 2014). Further, the staining intensity is similar at wildtype mouse NMJs to that of GalNAcT<sup>-/-</sup>-Tg(*neuronal*) mice as demonstrated in Chapter 3, indicating that ultimately ganglioside presence is similar in these mice at the relevant sites. In addition, preliminary staining work in other peripheral tissues (spleen, kidney, heart and liver) from GalNAcT<sup>-/-</sup>-Tg(*neuronal*) mice showed an absence of antiganglioside antibody reactivity, implying that other non-neuronal tissues are free of complex gangliosides (unpublished observations). GalNAcT<sup>-/-</sup> mice, which lack GD1b target, showed prolonged presence of MOG1 antibody. Considering the rapid clearance in wildtype mice, this indicates that the lack of clearance is related to the absence of target ganglioside. This again coincides with *ex vivo* results where no non-specific uptake of antibody was seen in GalNAcT<sup>-/-</sup> mice. Like the wildtype mice, the GalNAcT<sup>-/-</sup>-Tg(*neuronal*) mice also express GD1b target but in this instance only in neuronal membranes. Expression is therefore restricted compared with wildtype mice and uptake is less widespread. This results in a more prolonged

exposure to circulating antibody. In wildtype mice the *in vivo* uptake was widespread due to the large availability of GD1b. However, in GalNAcT<sup>-/-</sup>-*Tg(neuronal)* mice, the uptake can almost solely be attributed to motor nerve terminal clearance, as node of Ranvier lack the same ability to internalise antibody (Fewou et al., 2012). The consequences of internalisation at the motor nerve terminal were not known using *ex vivo* preparations alone (Fewou et al., 2012), however using *in vivo* techniques it appears that the antibody is retrogradely transported to the spinal cord. In wildtype mice, comparatively little antibody will likely be taken up at the nerve terminals due to the wide availability and access to GD1b elsewhere. It was therefore unsurprising to see very little antibody in wildtype ventral horn neurons. However, in GalNAcT<sup>-/-</sup>-*Tg(neuronal)* mice, visible amounts of GD1b have been trafficked from the periphery to the motor neurons. Only the anti-GD1b antibody trafficked from the diaphragm was looked for, by imaging the C3-5 portion of the cord. However, antibody would likely be present throughout the cord as an i.p. injection was given, therefore any skeletal muscle which was exposed to circulating antibody could have taken it up. Intraperitoneal injection allowed much higher amounts of antibody to be injected, due to the limitations in intramuscular injection volume in mice. Previous studies looking at retrograde antibody trafficking have been done in rats which have a larger muscle volume than mice and therefore can be injected with larger volumes of antibody i.m. The retrograde transport of antibodies against synaptic membrane components has been shown before (Fabian and Ritchie, 1986; Fabian and Petroff, 1987; Fabian, 1988; Fabian, 1991; Ritchie et al., 1985; Ritchie et al., 1986; Wenthold et al., 1984) therefore it was an unsurprising, yet novel finding that anti-ganglioside antibodies are also transported to the spinal cord. Following the serum clearance study, which extended out 7 days since the initial injection, antibody appeared to be in the phrenic nucleus neuropil. The same result was seen previously with monoclonal antibodies targeting synaptosome components (Ritchie et al., 1986), where the authors could not further localise the antibody but surmised that it either be in fine dendrites or to have been further transferred out of motor neurons following retrograde transport. The latter option seems the most likely considering that antibody presence did not coincide with MAP2 staining, indicating no presence in dendrites. Further, at the 1 day timepoint antibody was visible in the neuron cell bodies in GalNAcT<sup>-/-</sup>-*Tg(neuronal)* mice and,

though some antibody was present in lysosomes, some antibody appeared to be localised in other punctate structures in the cell. It is surmised that this other antibody was localised to recycling endosomes, which would carry the antibody to the cell surface, explaining its presence in the neuropil at the 7 day timepoint. The recycling of anti-ganglioside antibody has been shown previously in CHO-K1 cells (Iglesias-Bartolome et al., 2006; Iglesias-Bartolome et al., 2009). The consequences of antibody being transported to the spinal cord are as yet unknown. Hyper-reflexia, a symptom seen occasionally in the recovery phase in cases of AMAN (Baheti et al., 2010; McKhann et al., 1991; Yuki et al., 2012), has been shown by electrophysiological tests to be associated in some cases with increased motor neuron excitability. This has been suggested to be caused by disruption of the inhibitory interneurons, which mediate the activity of spinal cord motor neurons (Kuwabara et al., 1999; Yuki et al., 2012). If anti-ganglioside antibody is trafficked to the spinal cord in GBS patients, and then trans-synaptically transported outwith the neuron, it is conceivable that it may bind to the membrane of inhibitory interneurons, as is the pathway of tetanus toxin. Withal, patients who suffer from BBE, a condition which shares diagnostic features with MFS, present with drowsiness and coma in addition to ataxia and ophthalmoplegia. These features are thought to be due a transient, inflammatory brainstem injury (Shahrizaila and Yuki, 2013). Both BBE and MFS are associated with anti-GQ1b antibodies, suggesting a common immune-mediated mechanism in both diseases. Anti-GQ1b antibodies are thought to bind to the oculomotor nerve paranodes and NMJs to cause ophthalmoplegia and ptosis which occurs with both of these conditions. The current hypothesis of inflammatory brainstem injury in BBE is the entrance of anti-GQ1b antibody into the CNS via the circulation, but the uptake of anti-GQ1b antibodies by the motor nerve terminals may result in retrograde trafficking to the brainstem, where it may be trans-synaptically spread to bind to surrounding nuclei. The oculomotor nerve (the third cranial nerve) is thought to be the main nerve affected in MFS, and has a high GQ1b content (Chiba et al., 1993). This nerve projects to the periphery from the oculomotor nucleus which in the human brainstem is located close by to the midbrain reticular formation, the dorsal raphe nucleus and the mesencephalic trigeminal nucleus (Allen Institute for Brain Science, 2014). These are all components of the reticular activating system (RAS), a circuit of several connected nuclei originating in the brainstem and connecting to the cortex. It is

involved in the control of arousal and wakefulness (Yeo et al., 2013). If trans-synaptic spread of anti-GQ1b antibody is occurring in BBE patients, the antibody may be binding to these RAS components, causing inflammatory injury. Damage to these regions has been shown to be associated with coma (Garcia-Rill, 1997). Further study of the retrograde and potentially trans-synaptic transport of antibody is warranted to discover the effects of intraneuronal anti-ganglioside antibody. As preliminary studies were proof of antibody clearance, no behavioural or functional tests were employed in these mice to test whether intra-neuronal IgG had a detrimental effect.

To our knowledge, this is the first time that pathogenic anti-ganglioside antibodies such as MOG1, which bind and injure tissue in the presence of a source of complement, have been shown to be regulated by the ability of cell membranes to internalise these antibodies. The implication of this is that the availability of the target antigen may regulate how long the antibody is present in the circulation. In patients this may mean that antibodies which target epitopes which are widely expressed (the equivalent of wildtype mice) are cleared quickly and are less available to cause extensive injury. However antibodies which target epitopes which are expressed at a lower level (the equivalent of *GalNAcT<sup>-/-</sup>-Tg(neuronal)* mice), will circulate longer. This prolonged exposure may not affect the NMJs as they are able to endocytose antibody, but the NoR, which have less capacity for antibody uptake (Fewou et al., 2012) may be more vulnerable to antibody attack. This may provide evidence as to why the node of Ranvier is thought to be a site of damage in axonal GBS, (Griffin et al., 1996;Hafer-Macko et al., 1996a;Kuwabara et al., 1998) but evidence of damage to motor nerve terminals has been conflicting (Ho et al., 1997;Kuwabara et al., 2007;Kuwabara et al., 2011;Spaans et al., 2003). Antibody binding does not reduce the number of gangliosides available, suggesting that gangliosides are recycled to the cell surface following internalisation (Fewou et al., 2012). Antibodies may therefore still be able to bind and injure the nerve terminal at high serum concentrations, when endocytic machinery is likely to be saturated. The effect this uptake phenomenon may have in patients would therefore depend on antibody specificity (the epitope to which it binds), and availability (the serum

concentration of this antibody), as well as the relative availability of the target epitope, and the endocytic capacity of the target membrane.

## 6 Ability of the NMJ to clear anti-GM1 antibody

### 6.1 Introduction

The previous chapter demonstrated that the ability of MOG1, an anti-GD1b antibody, to be internalised by GD1b-expressing membranes, especially the motor nerve terminals, can affect the amount of circulating MOG1 available *in vivo*. It therefore seemed prudent to demonstrate this ability with other antibodies. GM1 is commonly a target for autoantibodies in AMAN (Ho et al., 1995; Kuwabara et al., 1998; Ogawara et al., 2000). Therefore DG2, an anti-GM1 antibody which is known to bind well to wildtype mouse tissue (Greenshields et al., 2009) and was shown in Chapter 3 to successfully bind to GalNACT<sup>-/-</sup>-*Tg(neuronal)* and GalNACT<sup>-/-</sup>-*Tg(glial)* mouse tissue, was used to determine whether antibodies against GM1 behaved in a similar fashion to anti-GD1b antibody. Previous work using other anti-GM1 antibodies has suggested they are internalised when bound to GM1 in a variety of cell types, but are subsequently recycled back to the cell surface (Iglesias-Bartolome et al., 2009). The first paper demonstrating the ability of anti-ganglioside antibodies to be internalised at motor nerve terminals demonstrated the presence of DG2 in motor nerve terminals of GD3s<sup>-/-</sup> mice following internalisation (Fewou et al., 2012), but has not demonstrated the internalisation dynamics of DG2 in wildtype or GalNACT<sup>-/-</sup>-*Tg(neuronal)* mice.

### 6.2 Ex vivo uptake of anti-GM1 antibody

As the principle of antibody uptake had already been demonstrated with MOG1, where the most thorough uptake in *ex vivo* preparations had occurred following 60 minutes at 37°C, the 30 minute timepoint was left out of this experiment.

As shown in Chapter 3, DG2 antibody often bound to NMJ-capping kranocytes in wildtype mice. These cells were identified by their shape and are known to have GM1 due to the binding of cholera toxin (Court et al., 2008). The staining of these cells with DG2 often obscured true nerve terminal binding, though kranocytes were not present over all NMJs. In these kranocyte-lacking NMJs, it was clear that at 0 minutes there was antibody present on the motor nerve terminal, node of Ranvier and on the terminal myelinating SC (Figure 6.1A,

white arrowhead). Staining of these structures was not present at every NMJ however. Quantitatively, the DG2 was significantly reduced at the wildtype nerve terminal following 60 minutes at physiological temperatures ( $p < 0.0001$ , median of 25.75 AU vs. 3.00 AU respectively, Figure 6.1B). Visually, the staining on kranocytes, nodes of Ranvier and terminal Schwann cell remained (Figure 6.1A,B). When the membrane was permeabilised with Triton X-100 and reprobbed with secondary antibody, NMJs which had appeared negative for antibody before permeabilisation, still appeared negative (Figure 6.1A). When this was quantified, a discrepancy still remained between antibody intensity at the endplate at 0 minute and 60 minute timepoints, with higher intensity staining at the 0 minutes timepoint ( $p < 0.0001$ , median of 11.00 AU vs. 0.00 AU, Figure 6.1C).

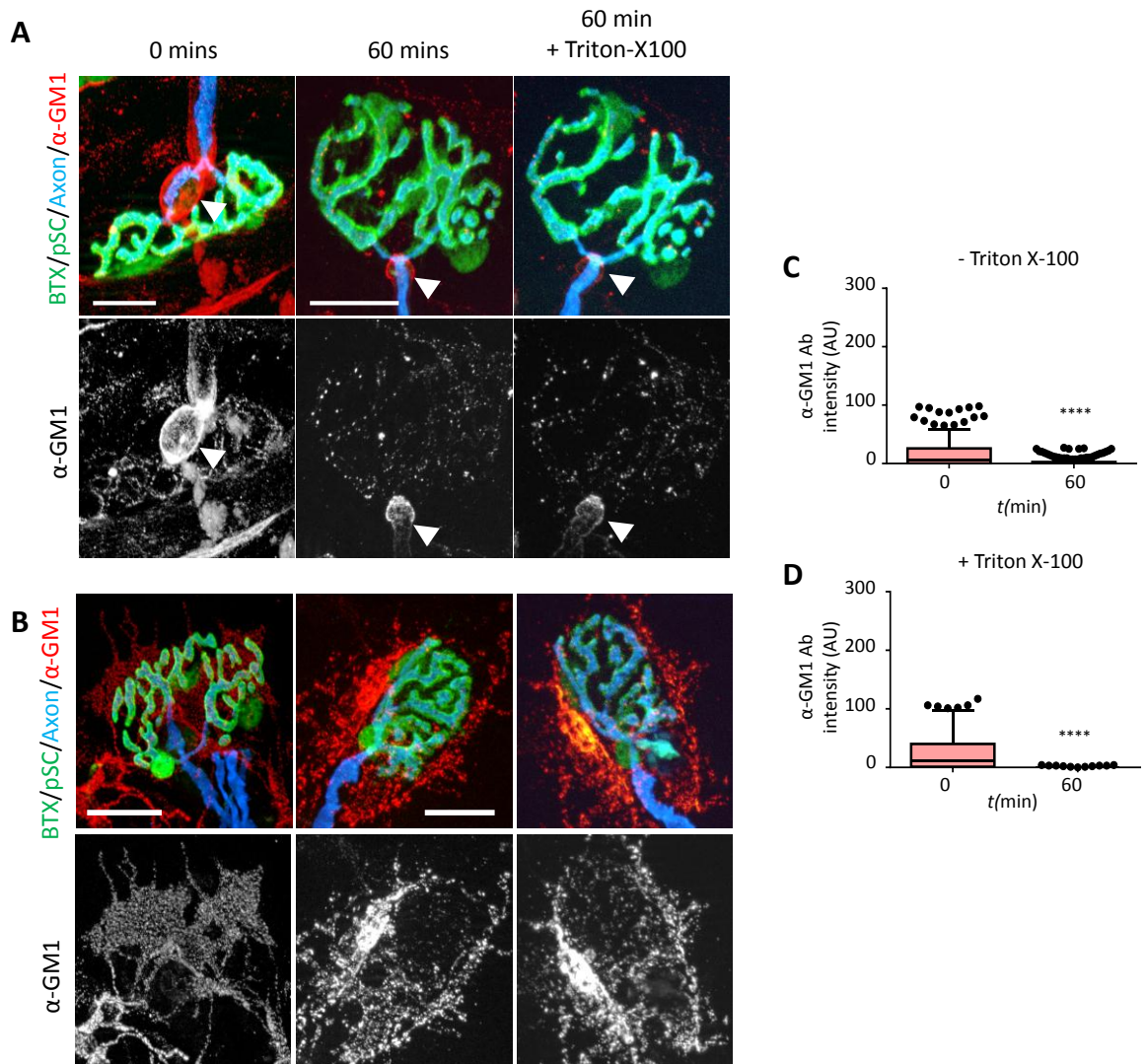


**Figure 6.1: Anti-GM1 antibody is cleared from the nerve terminal after 60 minutes at 37°C in wildtype mice.** Wildtype mice (n=3) TS muscle was labelled with anti-GM1 antibody for 30 minutes at 4°C then rinsed and either fixed immediately (0 minutes at 37°C) or moved to 37°C for 60 minutes. Endplates were analysed for presence of antibody. The preparations were then permeabilised, re-probed with secondary antibody and re-analysed. **A:** Examples of NMJs which were not obscured by cranocyte staining. NMJs were labelled weakly at 0 minutes with anti-GM1 antibody, but upon incubation at 37°C, labelling is no longer present at the nerve terminal but is still present on the terminal myelinating SC (white arrowhead). Permeabilisation of the membrane with Triton X-100 reveals no reappearance of antibody in the nerve terminal. **B:** Examples of cranocyte staining at NMJs. Cranocytes are labelled at 0 minutes but fail to internalise antibody by 60 minutes at 37°C. Staining appears very similar post-permeabilisation. **C:** Quantification shows that after 60 minutes at 37°C there was a significant decrease in presence of anti-GM1 antibody overlying the BTx signal, compared with 0 minutes. **D:** Following permeabilisation, a significant difference still existed between the 60 minute timepoint and 0 minutes. Scale Bar = 20  $\mu$ m. \*\*\*\* =  $p < 0.0001$  vs. 0 minutes, Mann-Whitney test. A minimum of 192 NMJs were analysed per group. Non-parametric data displayed as Tukey box plot (see section 2.20).

In  $\text{GalNAcT}^{-/-}\text{-Tg}(\text{neuronal})$  mice, no antibody was seen on kranocytes but was detectable at the nerve terminal as well as occasionally on the same terminal myelinating SCs seen in the wildtype mice (Figure 6.2A). After 60 minutes at  $37^{\circ}\text{C}$ , staining overlying the BTx signal is significantly reduced compared to 0 minutes ( $p < 0.0001$ , median of 33 AU vs. 0.0 AU respectively, Figure 6.2B). Once again however, the staining does not reappear following permeabilisation and reprobing with secondary antibody, and a significant difference still exists between 0 and 60 minutes ( $p < 0.0001$ , median of 127.0 AU vs. 9.0 AU, Figure 6.2C).

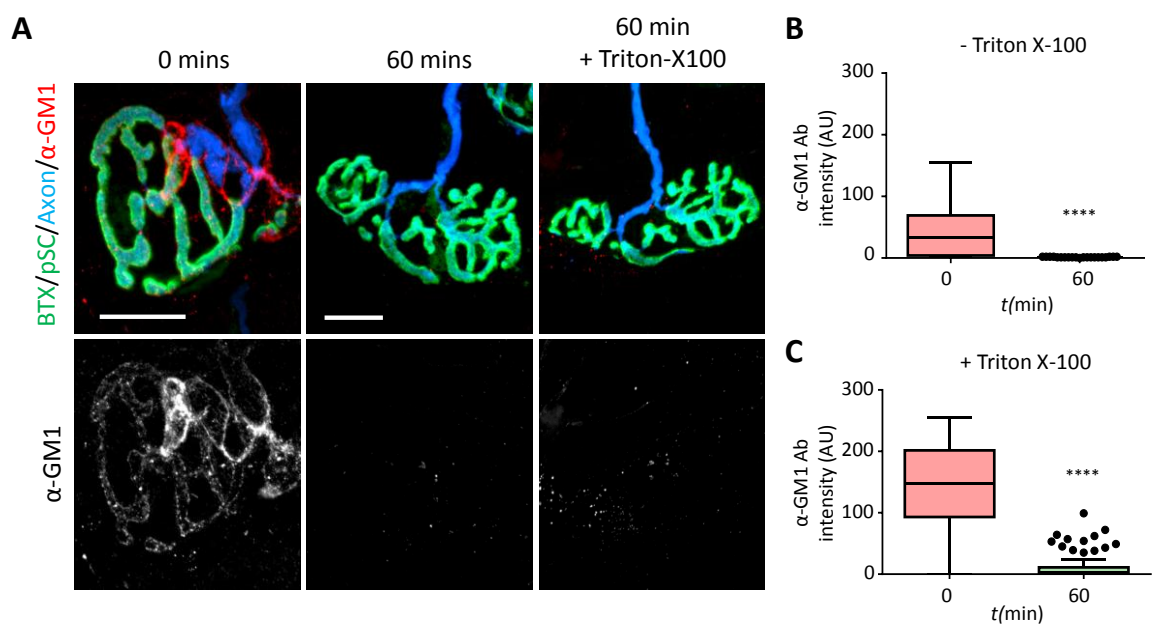


**Figure 6.2: Anti-GM1 antibody is cleared from the nerve terminal after 60 minutes at  $37^{\circ}\text{C}$  in  $\text{GalNAcT}^{-/-}\text{-Tg}(\text{neuronal})$  mice.**  $\text{GalNAcT}^{-/-}\text{-Tg}(\text{neuronal})$  mice ( $n=3$ ) TS muscle was labelled with anti-GM1 antibody for 30 minutes at  $4^{\circ}\text{C}$  then rinsed and either fixed immediately (0 minutes at  $37^{\circ}\text{C}$ ) or moved to  $37^{\circ}\text{C}$  for 60 minutes. Endplates were analysed for presence of antibody. The preparations were then permeabilised, reprobbed with secondary antibody and re-analysed. **A:** Nerve terminals and terminal Schwann cells were labelled at 0 minutes with anti-GM1 antibody, but upon incubation at  $37^{\circ}\text{C}$ , labelling is no longer present at the nerve terminal. Permeabilisation of the membrane with Triton X-100 reveals no reappearance of antibody in the nerve terminal. **B:** Quantification shows that after 60 minutes at  $37^{\circ}\text{C}$  there was a significant decrease in presence of anti-GM1 antibody compared with 0 minutes. **C:** Following permeabilisation, a significant difference still existed between the 60 minute timepoint and the 0 minutes timepoint. Scale Bar =  $20\ \mu\text{m}$ . \*\*\*\* =  $p < 0.0001$  vs. 0 minutes, Mann-Whitney test. A minimum of 191 NMJs were analysed per group. Non-parametric data displayed as Tukey box plot (see section 2.20).

As shown in chapter 3,  $\text{GalNAcT}^{-/-}\text{-Tg}(glial)$  mice, show only occasional, weak staining over the pSCs following incubation with DG2. Quantification of antibody signal overlying the BTx was therefore not performed in  $\text{GalNAcT}^{-/-}\text{-Tg}(glial)$  mice. Instead, most staining is seen over the internodal and paranodal myelin. The terminal myelinating Schwann cell labelled in wildtype and  $\text{GalNAcT}^{-/-}\text{-Tg}(neuronal)$  mice is also DG2 positive (Figure 6.3). As seen with wildtype and  $\text{GalNAcT}^{-/-}\text{-Tg}(neuronal)$  mice, this nodal and SC staining is still present at 60 minutes and therefore does not appear to have been internalised.

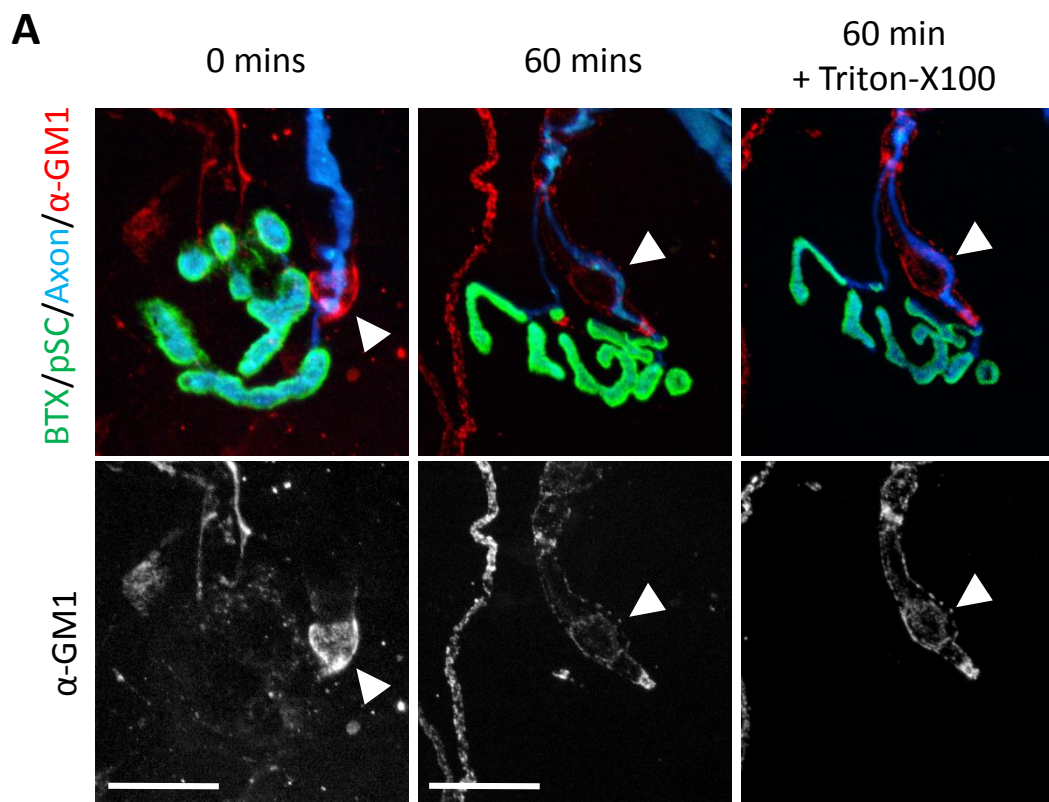


**Figure 6.3:** Anti-GM1 antibody does not bind at the NMJ in  $\text{GalNAcT}^{-/-}\text{-Tg}(glial)$  mice, but binds the myelin sheath and terminal myelinating SC.  $\text{GalNAcT}^{-/-}\text{-Tg}(glial)$  mouse TS muscle was labelled with anti-GM1 antibody for 30 minutes at  $4^{\circ}\text{C}$  then rinsed and either fixed immediately (0 minutes at  $37^{\circ}\text{C}$ ) or moved to  $37^{\circ}\text{C}$  for 60 minutes. Junctions were analysed for presence of antibody. The preparations were then permeabilised, re-probed with secondary antibody and re-analysed. **A:** No antibody labelling was present overlying the BTx signal immediately following anti-GM1 antibody incubation. Instead only the myelin sheath and the terminal myelinating SC are labelled. Upon incubation at  $37^{\circ}\text{C}$ , labelling is still present on the terminal myelinating SC (white arrowhead) and NoR. Permeabilisation of the membrane with Triton X-100 therefore made no difference to the surface-bound antibody signal at 60 minutes. Scale bar =  $20\ \mu\text{m}$ .

In GalNAcT<sup>-/-</sup> mice, no anti-GM1 antibody binding is seen at the NMJ at 0 minutes. After tissue was washed and placed at 37°C for 60 minutes, there was still no binding of antibody over the junction. This was reflected in the quantitation which showed median values of 0.00 AU for both 0 and 60 minutes and no significant difference between these timepoints. As was the case with GD1b, when the tissue was permeabilised no antibody was seen within the nerve terminal in GalNAcT<sup>-/-</sup> mice at either 0 minutes or 60 minutes timepoint (Figure 6.4A). This indicated that once again initial binding to the target ganglioside is needed before internalisation at the nerve terminal can occur. Quantitatively, a significant increase was seen in the 0 minute timepoint, but binding was still visually negative (median of 0.00 AU for both).

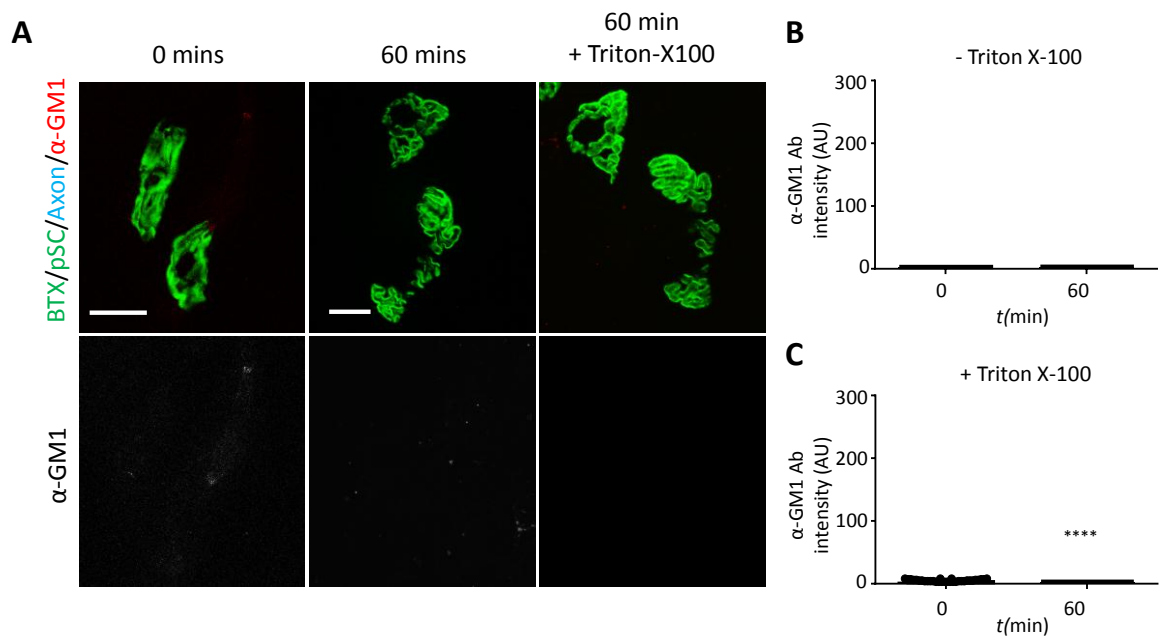


**Figure 6.4: Internalisation of anti-GM1 antibody does not occur at nerve terminals lacking GM1 ganglioside.** GalNAcT<sup>-/-</sup> mice (n=3) TS muscle was labelled with anti-GM1 antibody for 30 minutes at 4°C then rinsed and either fixed immediately (0 minutes) or moved to 37°C for 30 minutes or 60 minutes. Junctions were analysed for presence of antibody. The preparations were then permeabilised, reprobbed with secondary antibody and re-analysed. **A:** Illustrative images show the GalNAcT<sup>-/-</sup> NMJs showed no binding at 0 minutes with anti-GM1 antibody, and also no binding was seen following incubation at 37°C. Permeabilisation of the membrane with Triton X-100 shows no antibody presence in the nerve terminal. **B:** Quantification of antibody binding shows that before Triton, there was no antibody present over the NMJ. **C:** Following permeabilisation, a slight rise in intensity at the 0 minutes timepoint meant a slight but significant difference arose between 0 and 60 minutes, however binding was still virtually non-existent at both timepoints. Scale Bar = 50  $\mu$ m. \*\*\*\* =  $p < 0.0001$  vs 0 minutes, Mann-Whitney test. A minimum of 200 NMJs were analysed per group. Non-parametric data displayed as Tukey box plot (see section 2.20).

### 6.2.1 Autophagy inhibition in *GalNACT<sup>-/-</sup>-Tg(neuronal)* mice

The apparent disappearance of DG2 from the nerve terminal may be due to recycling of the antibody back to the cell surface, or by degradation within the nerve terminal or nearby structure. To examine the latter possibility, a pilot attempt (n=1) was made to inhibit potential breakdown of DG2 by preventing vesicle acidification using  $\text{NH}_4\text{Cl}$ . This was done in the *GalNACT<sup>-/-</sup>-Tg(neuronal)* mouse to ensure that staining on the nerve terminal was not obscured by kranocyte staining. This initial study appeared to show some restoration of antibody intensity when  $\text{NH}_4\text{Cl}$  is added to Ringer's solution for the 60 minute incubation at  $37^\circ\text{C}$  suggesting that DG2 may be at least partially degraded by the nerve terminal. The presence of DG2 in tissue incubated with  $\text{NH}_4\text{Cl}$ + Ringer's was punctate. Only images and quantification of permeabilised tissue are shown (Figure 6.5).

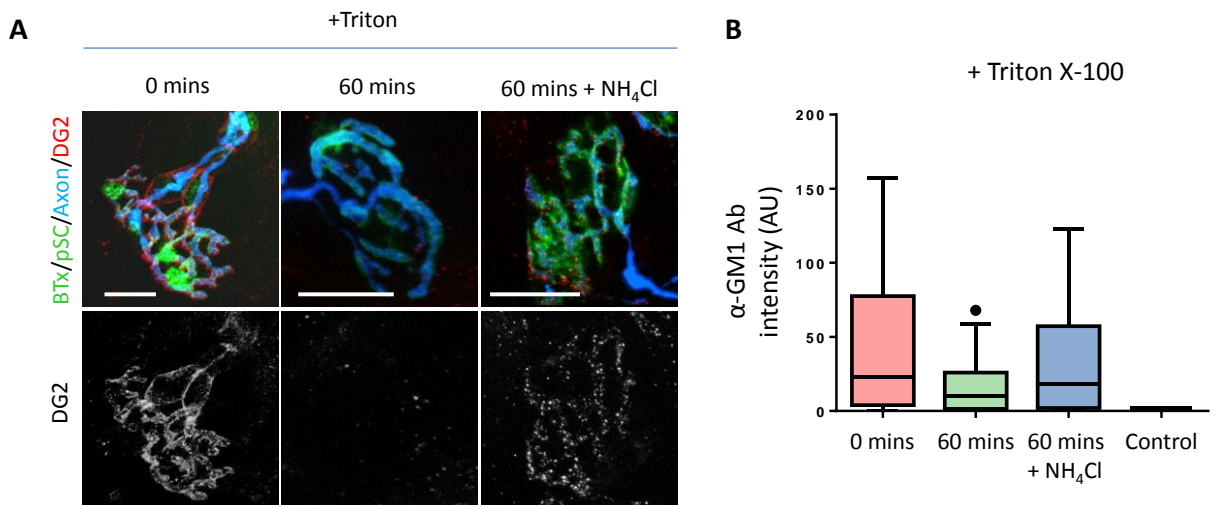


**Figure 6.5: Pilot study indicates inhibition of vesicle acidification increases DG2 presence following incubation at physiological temperatures.** *GalNACT<sup>-/-</sup>-Tg(neuronal)* mouse (n=1) TS muscle was labelled with anti-GM1 antibody for 30 minutes at  $4^\circ\text{C}$  then rinsed and either fixed immediately (0 minutes at  $37^\circ\text{C}$ ) or moved to  $37^\circ\text{C}$  for 60 minutes. Junctions were analysed for presence of antibody. The preparations were then permeabilised, re-probed with secondary antibody and re-analysed. Only images and quantification from permeabilised tissue is shown. **A:** Surface DG2 is present at the nerve terminal and on terminal SCs at the 0 minutes timepoint. Very little antibody was present within the nerve terminal at the 60 minutes timepoint following permeabilisation. In tissue where antibody had been incubated at  $37^\circ\text{C}$  in Ringer's containing  $\text{NH}_4\text{Cl}$ , more antibody appeared to be present in the nerve terminal at 60 minutes. **B:** Quantification of DG2 intensity implied a slight increase in antibody presence in  $\text{NH}_4\text{Cl}$  treated group. Control was secondary only. Non-parametric data displayed as Tukey box plot (see section 2.20).

### 6.2.2 Fate of antibody following disappearance at the NMJ

Attempts were made to track DG2's movement over time at the NMJ and pinpoint where it is cleared to. Firstly DG2 was labelled with Alexa Fluor 488 fluorescent dye which was tested by array and tissue preps to confirm its binding to GM1 (Figure 6.6)

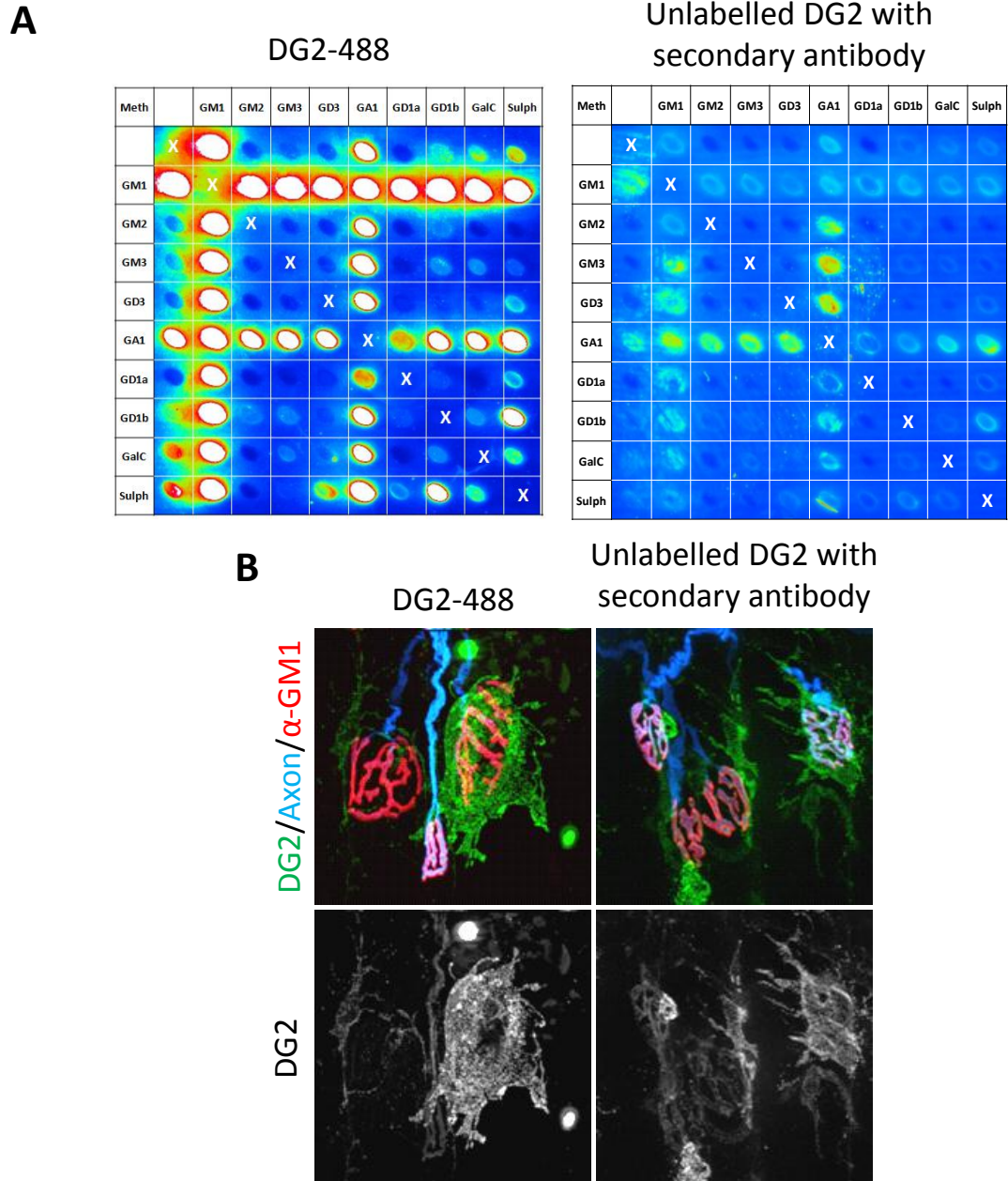


**Figure 6.6: Testing of labelled DG2 antibody on glycoarray and in whole mount TS tissue.** **A:** Glycoarray analysis was performed using the standard protocol but for DG2-488 the secondary antibody step was missed out. Binding patterns were similar for both antibodies, though intensity levels were higher using labelled antibody (array shown is saturated for DG2-488 but weak for unlabelled DG2). **B:** TS was probed with primary antibody (either labelled or unlabelled DG2). For labelled DG2 the secondary antibody step was removed. Comparable binding is seen between DG2-488 and unlabelled DG2 followed by secondary antibody.

Firstly an attempt was made to look at the DG2 binding in tissue at 0, 30 and 60 minutes to distinguish whether there was a movement of antibody from apparent surface binding to internalisation, using both wildtype and *GalNAcT<sup>-/-</sup>*-*Tg(neuronal)* mice (n=3). In wildtype mice, most NMJs were obscured by kranocyte staining, which appeared to vary in intensity from junction to junction (Fig 6.4). As shown in section 6.2, this staining remained present even at the 60 minute timepoint (images not shown). Where nerve terminal binding is not obscured by kranocytes, the binding appeared punctate at 30 minutes and had completely disappeared by 60 minutes (Figure 6.7).

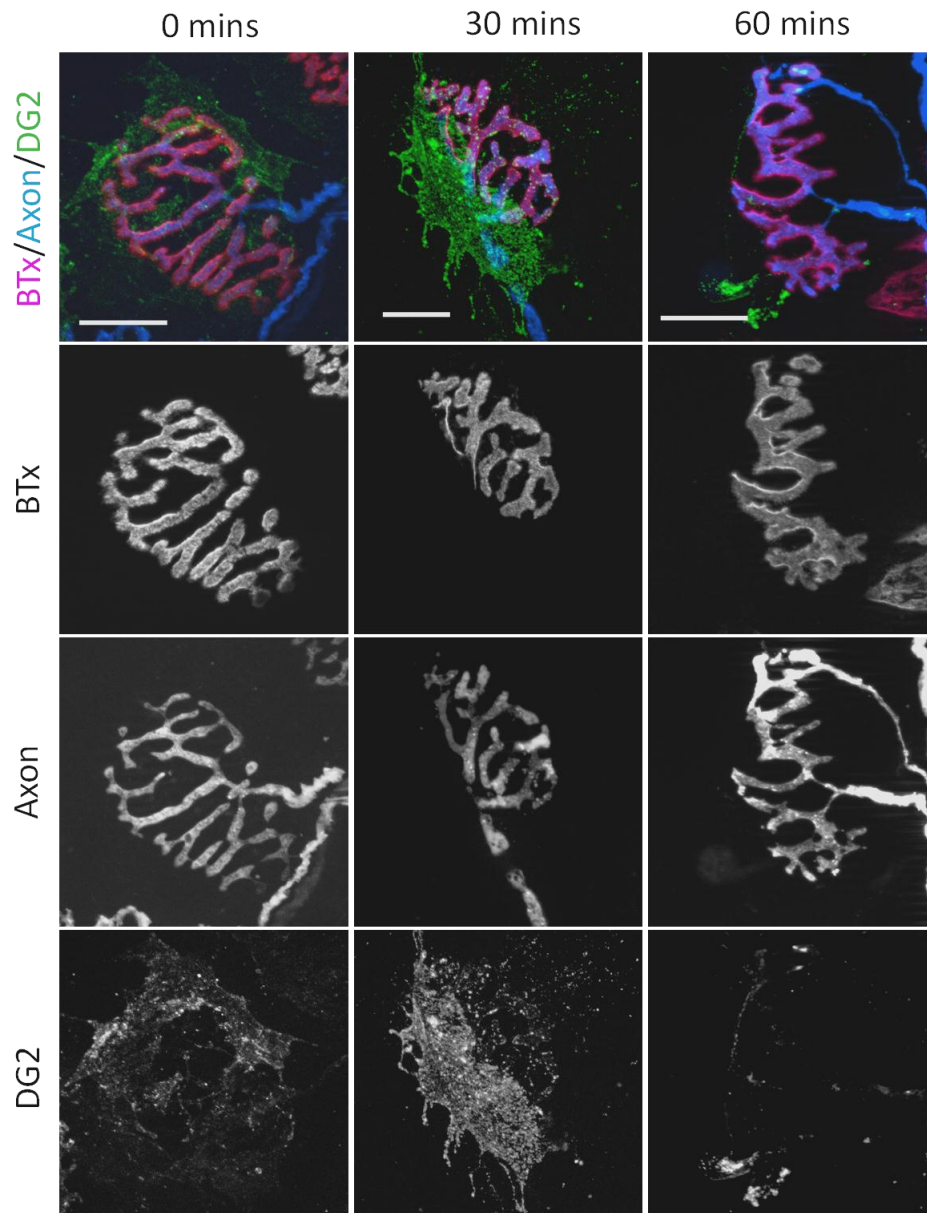


**Figure 6.7: Binding of DG2-488 in wildtype TS muscle following 0, 30 and 60 minutes at physiological temperatures.** TS tissue was labelled with DG2-488 at 4°C then either fixed immediately or incubated at 37°C for 30 or 60 minutes. At 0 minutes kranocyte staining is seen over some NMJs and weakly over the nerve terminal. At 30 minutes kranocytes are still stained and nerve terminal staining looks punctate. At 60 minutes nerve terminal staining had disappeared completely (junction shown did not have a kranocyte present, however kranocyte staining was seen over other NMJs).

In  $\text{GalNAcT}^{-/-}\text{-Tg}(\text{neuronal})$  mice (Figure 6.8), staining was initially present over the nerve terminal, though again this varied in intensity between junctions with some NMJs showing very weak staining even at the 0 minutes timepoint, perhaps due to the lower enzyme activity in these mice (Yao et al., 2014). After 30 minutes, the antibody appeared punctate and in some junctions, presumably

those which would have shown weaker staining at 0 minutes, had completely disappeared. By 60 minutes all antibody had disappeared in these mice.

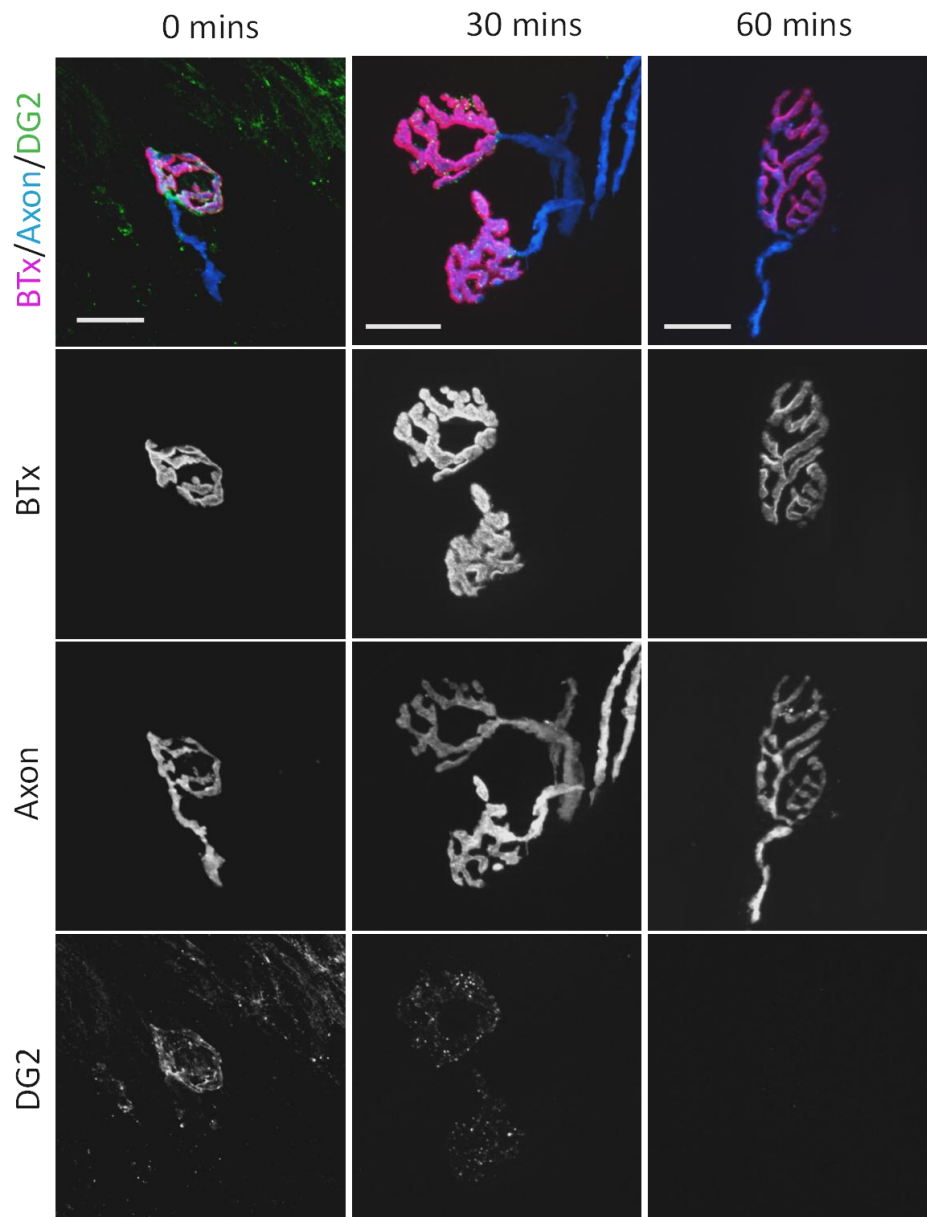


**Figure 6.8: Binding of DG2-488 in *GalNACT<sup>-/-</sup>-Tg(neuronal)* TS muscle following 0, 30 and 60 minutes at physiological temperatures.** TS tissue was labelled with DG2-488 at 4°C then either fixed immediately or incubated at 37°C for 30 or 60 minutes. At 0 minutes weak nerve terminal and occasionally pSC staining is seen at the NMJs. At 30 minutes nerve terminal staining looks weaker and more punctate. At 60 minutes nerve terminal staining has disappeared completely.

## 6.3 In vivo uptake of anti-GM1 antibody

### 6.3.1 Serum levels of anti-GM1 antibody

As it was successfully demonstrated that MOG1 was cleared from the circulation in mice which had high amounts of target, the same paradigm was explored with DG2. The *ex vivo* results dictated that the DG2 antibody was cleared from the NMJ as seen with MOG1, but not trafficked to inside the nerve terminal in the same way. Even though the antibodies were trafficked differently from the nerve terminal, it was thought likely that a change in serum presence would still be detectable.

The opportunity to explore differences between tissue-binding and non-tissue binding anti-GM1 was afforded by using DG1 in addition to DG2 in the experiment. As shown in chapter 3, DG2 binds the nerve terminals of wildtype and GalNacT<sup>-/-</sup>-*Tg(neuronal)* mice, but not those of GalNacT<sup>-/-</sup> mice. GalNacT<sup>-/-</sup>-*Tg(glial)* mice show only very occasional and very weak pSC binding and therefore were excluded from this experiment. DG1 on the other hand does not bind in any of the genotypes due to its inhibition of GM1 binding by surrounding GD1a ganglioside (Greenshields et al., 2009) (see Chapter 3 and Figure 6.9). The convenient fact that these two anti-GM1 antibodies are of different IgG subtypes meant that both antibodies could be injected simultaneously into the mice, and the serum presence of each of them monitored using the same experimental paradigm as used in Chapter 5. Serum was tested in ELISA and subtype-specific HRP-conjugated secondary antibodies were used to detect antibody presence. This would allow us to confirm the importance of pathogenicity in an antibody's ability to be cleared.

The experiment was initially conducted in wildtype mice alone (n=3). As different secondary antibodies were used, statistics were performed vs. baseline levels for each antibody as levels between antibodies are not directly comparable. Results showed that levels of DG2, the pathogenic, tissue-binding antibody, were not significantly higher than baseline at the day 1 timepoint (mean 0.007 OD vs. 0.001 OD) and remained so over the course of the experiment. This appeared to be similar to the levels of MOG1 in the serum at day 1 in wildtype mice. Conversely, levels of DG1 were significantly higher than

baseline values at day 1 (1.26 OD vs. 0.02 OD) and remained so over the rest of the experiment.

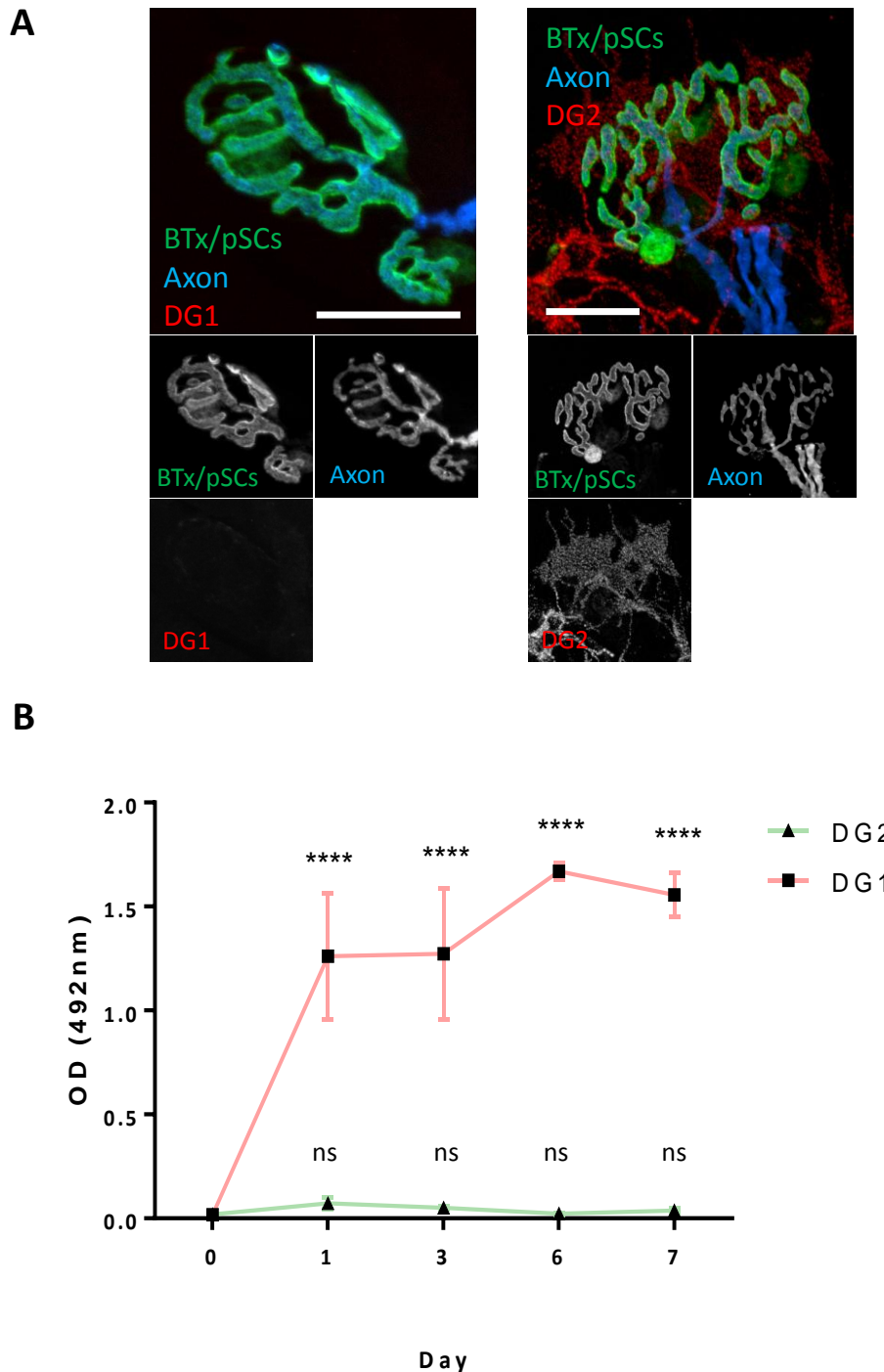


**Figure 6.9: Difference in tissue-binding ability of DG1 and DG2 affects their clearance from serum in wildtype mice.** **A:** DG1 does not bind the NMJ in live wildtype TS whereas DG2 does. **B:** Although not directly comparable as they were detected with different secondary antibodies, there is a large difference between presence of DG1 and DG2 in wildtype mice even as soon as 1 day post-injection. Statistics shown for each antibody are compared with day 0, preinjection, by two-way ANOVA with Dunnett's multiple comparison test. DG1 presence in the serum remained statistically higher than preinjection values over the 7 day time course, whereas DG2 is rapidly cleared, never differing from baseline values. DG1: \*\*\*\*= $p < 0.0001$  vs. day 0. DG2: ns= $p > 0.05$  vs. day 0.

The experiment was then repeated, this time including GalNAcT<sup>-/-</sup> and GalNAcT<sup>-/-</sup>-Tg(*neuronal*) along with wildtype mice (n=3 per group). The use of these mice allowed confirmation that DG2 was making its way into the circulation in wildtype mice before being cleared by comparing binding in mice with less/no target antigen (Figure 6.10). Values of DG1 OD were high 1 day following injection and remained high throughout the experiment in the sera of all three mouse strains. No significant difference existed among the sera OD values of any mouse strains at any timepoint with the exception of GalNAcT<sup>-/-</sup> vs. wildtype at the day 3 timepoint (two way ANOVA, p<0.05). DG2 showed much the same pattern of clearance as MOG1; Wildtype mice clear the antibody very quickly, with very low OD values seen in the sera even at the one day timepoint. GalNAcT<sup>-/-</sup> mice have a high peak in OD at day 1, which remains high throughout the remainder of the experiment (the slight decrease seen over the 7 days is likely due to the normal half-life of IgG in mice). GalNAcT<sup>-/-</sup>-Tg(*neuronal*) mice cleared DG2 from their serum at a much slower rate than wildtype mice. GalNAcT<sup>-/-</sup>-Tg(*neuronal*) mice sera show a significantly higher OD value on day one than wildtype mice (p<0.001, Two-way ANOVA), which then dips by day 3 to be statistically similar to wildtype mice sera, and continues to decrease over the remainder of the experiment. Values of OD in GalNAcT<sup>-/-</sup>-Tg(*neuronal*) sera were consistently lower than GalNAcT<sup>-/-</sup> mice.

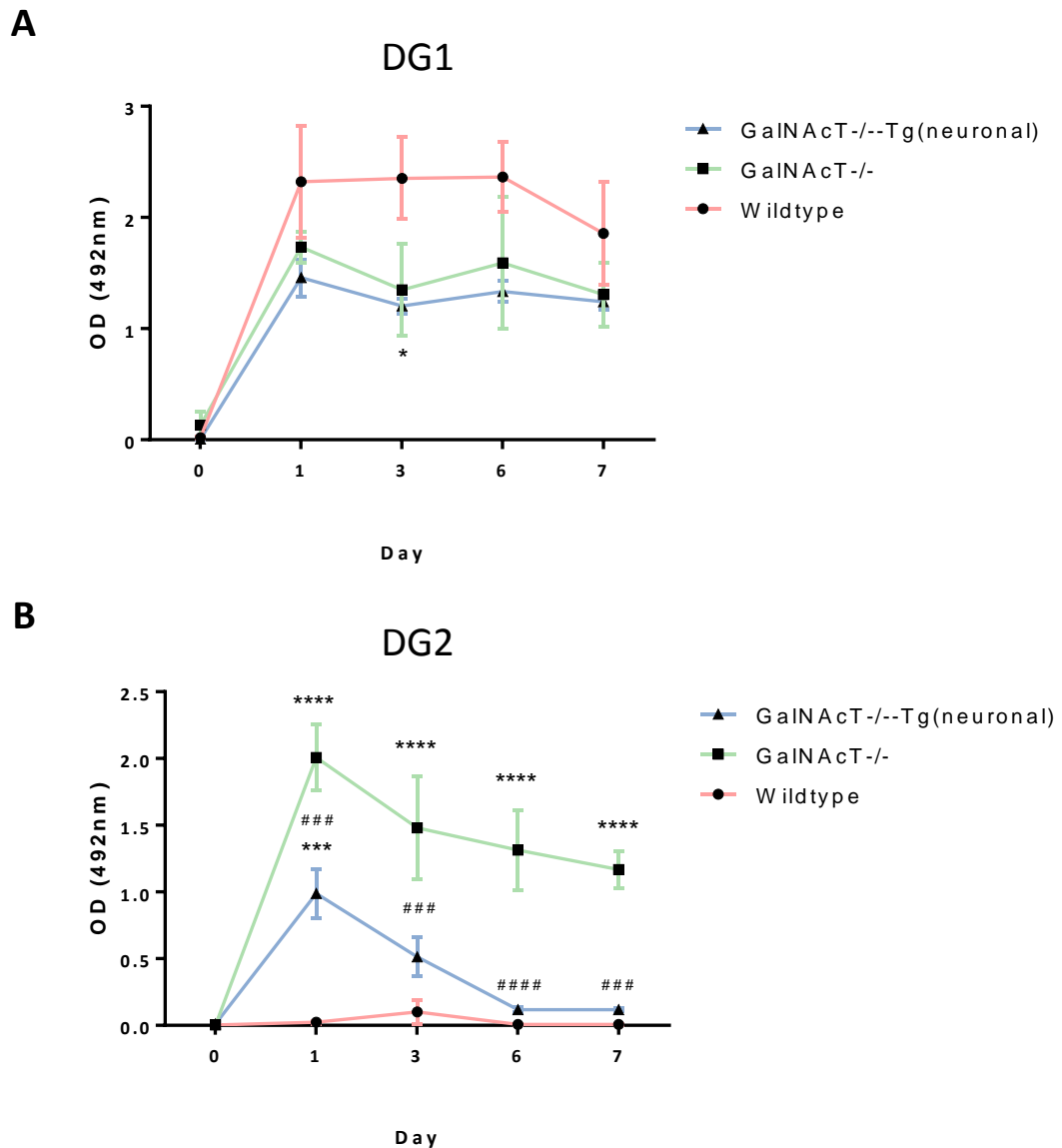


**Figure 6.10: DG1 and DG2 serum presence by ELISA over 7 days in wildtype, GalNAcT<sup>-/-</sup> and GalNAcT<sup>-/-</sup>Tg(*neuronal*) mice.** Mice (n=3 per group) were injected i.p. with both antibodies (250  $\mu$ g each) on day 0, following baseline blood sample. DG1 remained in the circulation of all mice over the 7 days. Contrastingly, DG2 was quickly cleared in wildtype mice and more slowly in GalNAcT<sup>-/-</sup>Tg(*neuronal*) mice. DG2 levels in GalNAcT<sup>-/-</sup> mice sera remained high over the 7 days, two-way ANOVA with Dunnett's multiple comparison test.

### 6.3.2 Tissue analysis

As with MOG1 in Chapter 5, an attempt was made to look for DG2 in the spinal cord of mice following i.p. injection. This was done in a separate experiment as part of a project carried out by A. Cunningham as part of an undergraduate honours project. Only GalNAcT<sup>-/-</sup>Tg(*neuronal*) mice were used to increase the

chances of finding intraneuronal antibody.  $\text{GalNAcT}^{-/-}\text{-Tg}(\text{neuronal})$  mice were injected with 2 mg of DG2 and antibody was searched for after 1 day and after 7 days ( $n=3$  per group) at both the diaphragm and in the spinal cord. Diaphragm was positive for antibody after 1 day but negative for antibody after 7 days. Spinal cord gave very negligible results with no distinctly obvious DG2 presence at either timepoint (data not shown). This was not unexpected due to the absence of internalised antibody at the nerve terminal in whole mount TS preparations.

## 6.4 Discussion

The concept that anti-ganglioside antibodies are internalised has already been established both in cell culture, and *ex vivo* at the motor nerve terminals of wildtype mice (Fewou et al., 2012; Iglesias-Bartolome et al., 2006; Iglesias-Bartolome et al., 2009). Chapter 5 demonstrated that antibodies against GD1b can be rapidly taken up by motor nerve terminals when GD1b is present on the presynaptic membrane (i.e. in wildtype and  $\text{GalNAcT}^{-/-}\text{-Tg}(\text{neuronal})$  mice). MOG1 can also be cleared by pSCs (as shown in  $\text{GalNAcT}^{-/-}\text{-Tg}(\text{glial})$  mice), though the fate of the antibody following clearance in these mice is less certain. It was also shown that this clearance by the nerve terminal, and by other GD1b-presenting membranes, can have a significant effect on levels of circulating antibody *in vivo*. Due to the significance of anti-GM1 antibodies in relation to disease, the same paradigms were investigated using DG2, an anti-GM1 antibody. Previously, anti-GM1 antibodies have been shown to be internalised by a variety of cell lines, only to be recycled back to the plasma membrane (Iglesias-Bartolome et al., 2009). Contrastingly, previous work in this laboratory using DG2 has shown that this anti-GM1 antibody is taken up by PC12 cells, and co-localises with lysosomes, indicating its fate is degradation rather than recycling (Fewou et al., 2012). Nerve terminal studies in  $\text{GD3s}^{-/-}$  mice using DG2 indicated that the antibody was taken up by the nerve terminal following incubation at physiological temperature, and is found there following permeabilisation (Fewou et al., 2012). However, chapter 6 has demonstrated that in wildtype mice anti-GM1 antibody DG2, is cleared from the nerve terminal within 60 minutes at physiological temperature, but is not present following permeabilisation of the nerve terminal membrane. In light of previous work in cell culture, this may

have meant that the antibody is either being recycled to the cell surface, or is being degraded somehow within the nerve terminal. A pilot study indicated that lysosomal inhibition by  $\text{NH}_4\text{Cl}$  resulted in increased antibody presence in the nerve terminal following permeabilisation of tissue incubated at physiological temperature for 60 minutes. It is difficult to draw conclusions from only one experiment however the results warrant further investigation into the potential degradation of DG2 at the nerve terminal. Lysosomes have been shown to be present in peripheral axons and in nerve terminals, and increase in response to peripheral nerve injury (Jung et al., 2011; Jung et al., 2014; Song et al., 2008; Xu et al., 2002). Additionally, if DG2 antibody was instead being recycled back out of the nerve terminal, it would be expected that *in vivo*, the presence of DG2 in the serum would have been prolonged, especially in  $\text{GalNAcT}^{-/-}\text{-Tg}(\text{neuronal})$  mice. This was not the case as when DG2 was injected i.p. into mice, it was cleared from the serum in a much similar fashion to anti-GD1b antibody MOG1; Wildtype mice cleared DG2 within 1 day and  $\text{GalNAcT}^{-/-}\text{-Tg}(\text{neuronal})$  mice, in which serum clearance can be mostly attributed to the nerve terminal, cleared the serum within 6 days of injection. It therefore seems more likely that DG2 is being degraded or further trafficked from within the terminal. It is possible that DG2 and MOG1 share a trafficking pathway but that DG2 is trafficked much faster; MOG1 may perform a similar vanishing act if incubated for a longer period of time. On the other hand, gangliosides have been shown to be differentially trafficked following binding and internalisation (Crespo et al., 2008), therefore the two antibodies may be destined for different fates upon their arrival in the nerve terminal. This would certainly explain the lack of DG2 detected in the spinal cord following i.p. injection, despite MOG1 being detectable in a similar experimental paradigm.

Importantly, as demonstrated previously (Fewou et al., 2012), anti-GM1 antibody binding at the node of Ranvier was not internalised, and still remained present at the 60 minute timepoint. As well as nerve terminal and node of Ranvier staining, DG2 was also seen on a terminal myelinating SC, present immediately proximal to the nerve terminal and appearing to be located between the last two nodes of Ranvier (ensheathing the final internode). This cell is S100 positive, as demonstrated by presence of cytoplasmic GFP in fluorescent mice, and sulphatide-positive, as demonstrated by anti-sulphatide antibodies (G. Meehan,

unpublished data). DG2 binds sulphatide in addition to GM1, both in ELISA (D. Nicholls, unpublished data) and glycoarray. It was thought that this cell was therefore showing sulphatide staining, however the presence of high cholesterol can inhibit DG2-sulphatide binding and in  $CST^{-/-}$  mice, this cell is still labelled with DG2. Additionally, in  $CST^{-/-}$  x  $GalNAcT^{-/-}$  mice, no staining is present. It was concluded that the staining was in fact of DG2 binding GM1, and therefore it appears GM1 is not internalised at this site.

This chapter demonstrated the importance of antibody pathogenicity by utilising two antibodies which bind GM1 in ELISA, but only one of which binds in live tissue (Greenshields et al., 2009). DG2, a tissue-binding antibody, is cleared from wildtype and  $GalNAcT^{-/-}$ -*Tg(neuronal)* mice serum in much the same way as MOG1, indicating a similar dependence on target availability. Likewise,  $GalNAcT^{-/-}$  mice, which could not clear MOG1 from their serum, also fail to clear DG2 as they lack the target GM1. DG1 does not bind live tissue due to *cis* inhibition by nearby GD1a (Greenshields et al., 2009). Consequently, following injection of DG1, wildtype,  $GalNAcT^{-/-}$  and  $GalNAcT^{-/-}$ -*Tg(neuronal)* mice all failed to clear this antibody from their sera over 7 days. This experiment highlights the potential discrepancy between the antibodies found in the serum and the antibodies which cause disease (summarised in Figure 6.11).

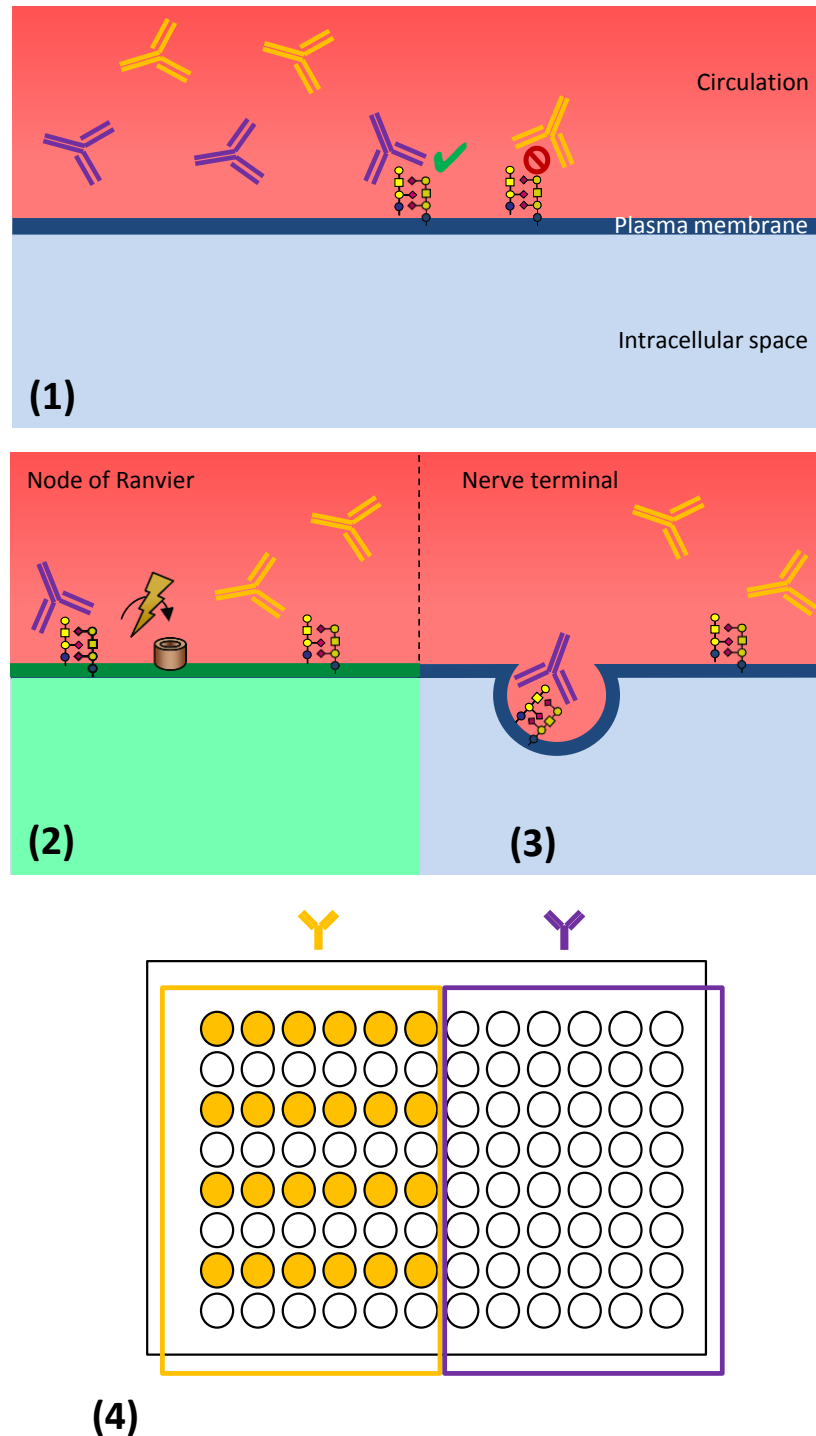


**Figure 6.11: Anti-ganglioside antibodies detectable in patient sera by ELISA do not necessarily represent the disease-causing antibodies. (1)** Polyclonal antibodies mounted in response to *C. jejuni* infection. One antibody type can bind to its target antigen, termed cis independent (purple). Another antibody type is blocked from its target binding site by surrounding lipids, termed cis inhibition (yellow). **(2)** If it is on a membrane which does not allow for internalisation, such as the NoR, this antibody can activate complement and cause MAC pore formation, leading to injury. If it is on a membrane which is endocytically active, the antibody is taken into the cell. **(3)** In either case, the non-binding antibody has nowhere to go and continues to circulate in the blood. **(4)** When serum is screened, the tissue-binding antibody has been removed from the circulation, resulting in a negative or weak ELISA result, whereas the non-binding antibody shows up strongly positive.

It is now widely accepted that anti-ganglioside antibodies have a pathogenic role in GBS and in chronic variations such as MMN, but it has often proven difficult to show direct pathogenicity of patient sera in mouse models of autoimmune neuropathy without overexpression of target antigen (Goodfellow et al., 2005; Jacobs et al., 2002; Zitman et al., 2011b). Similarly, when monoclonal antibodies are cloned from patient peripheral blood mononuclear cells, they provide a spectrum of different binding patterns in the rodent nervous system (O'Hanlon et al., 1996), with some antibodies binding well to neuronal structures, and some not binding at all. Although differences exist between the neuronal membrane composition of rodent and human nerves, the clearance of pathogenic antibodies by internalisation may explain this failure to induce injury in mouse models. Studies which have successfully found anti-GM1, GD1a or GM1/GD1a complex positive patient sera to be pathogenic, have done so in GD3s<sup>-/-</sup> mice, which overexpress a-series gangliosides. In this instance the membrane organisation is altered, and the target which is normally masked from the remaining serum antibodies, may be presented in a fashion which allows antibody binding.

It is an important finding that the antibodies found in the serum are not necessarily pathogenic, though it is likely that they bind to either the same ganglioside target, or a structurally similar ganglioside.

## 7 Uptake of anti-GD1b antibody is activity dependent

### 7.1 Introduction

The motor nerve terminal has a high ability to take up anti-GD1b ganglioside, as demonstrated in chapter 5, though the mechanisms behind this are unclear. In various cell culture experiments, ganglioside recycling and the resulting anti-ganglioside antibody uptake, has been shown to occur by clathrin independent, caveolin-mediated endocytosis. In *in vivo* anti-ganglioside uptake experiments (Chapter 5 and 6) wildtype mice were able to clear antibody at a much faster rate than GalNAcT<sup>-/-</sup>-*Tg(neuronal)* mice, indicating that non-neuronal cells are taking up antibody. On the evidence of cell culture experiments, this non-neuronal uptake is presumed to be caveolae-dependent. As *ex vivo* preparations have shown, the motor nerve terminal rapidly endocytoses anti-ganglioside antibody, but the node of Ranvier does not, (Fewou et al., 2012) and Chapter 6), indicating that most of the clearance seen in GalNAcT<sup>-/-</sup>-*Tg(neuronal)* *in vivo* experiments (Chapter 5 and 6) was due to clearance by the nerve terminal. As the motor nerve terminal is a highly active membrane which lacks caveolae, it was hypothesised that the uptake of this antibody may be enhanced, or dependent on, nerve terminal activity. This would also further explain the previous observation that the NoRs, which are relatively stable structures with a slow membrane turnover to maintain their specialised function of action potential propagation (Zhang et al., 2012), may not have the ability to internalise antibody at the same rate (Fewou et al., 2012). Previously, entry of botulinum neurotoxin, which binds to surface GT1b and GD1b gangliosides, was shown to be activity dependent at motor nerve terminals in both nerve stimulation and KCl-induced membrane activity paradigms (Dong et al., 2003; Rummel et al., 2009). This chapter therefore aimed to demonstrate whether the internalisation of anti-ganglioside antibody at the nerve terminal is enhanced by nerve terminal activity. As this is a proof of concept study, experiments thus far have only been carried out on wildtype mice.

### 7.2 Stimulation of nerve terminals with KCl

Initially, to study the effect of activity dependent uptake, the internalisation of MOG1 antibody was compared in unstimulated tissue and tissue stimulated with

the addition of KCl into the Ringer's medium. A high extracellular concentration of  $K^+$  causes depolarisation of the nerve terminal and initiates calcium-induced release of acetylcholine-containing vesicles, followed by their subsequent recycling by endocytosis. Following labelling with MOG1, wildtype TS tissue was incubated in a Ringer's solution with an increased  $K^+$  concentration (56 mM vs 4.5 mM in standard Ringer's solution) to induce membrane activity for 10 minutes (n=3). Compared with unstimulated tissue, tissues exposed to high  $K^+$  showed significantly lower MOG1 staining at the nerve terminal ( $p < 0.0001$ , medians of 35.00 AU vs. 6.00 AU respectively). Instead, high KCl-treated tissue showed equivalent staining to unstimulated tissue which had been incubated in Ringer's for a further 20 minutes at room temperature (median of 12.00 AU,  $p > 0.05$ ), where, based on previous observations, endocytosis would have been expected to occur in a temperature dependent manner (Figure 7.1).

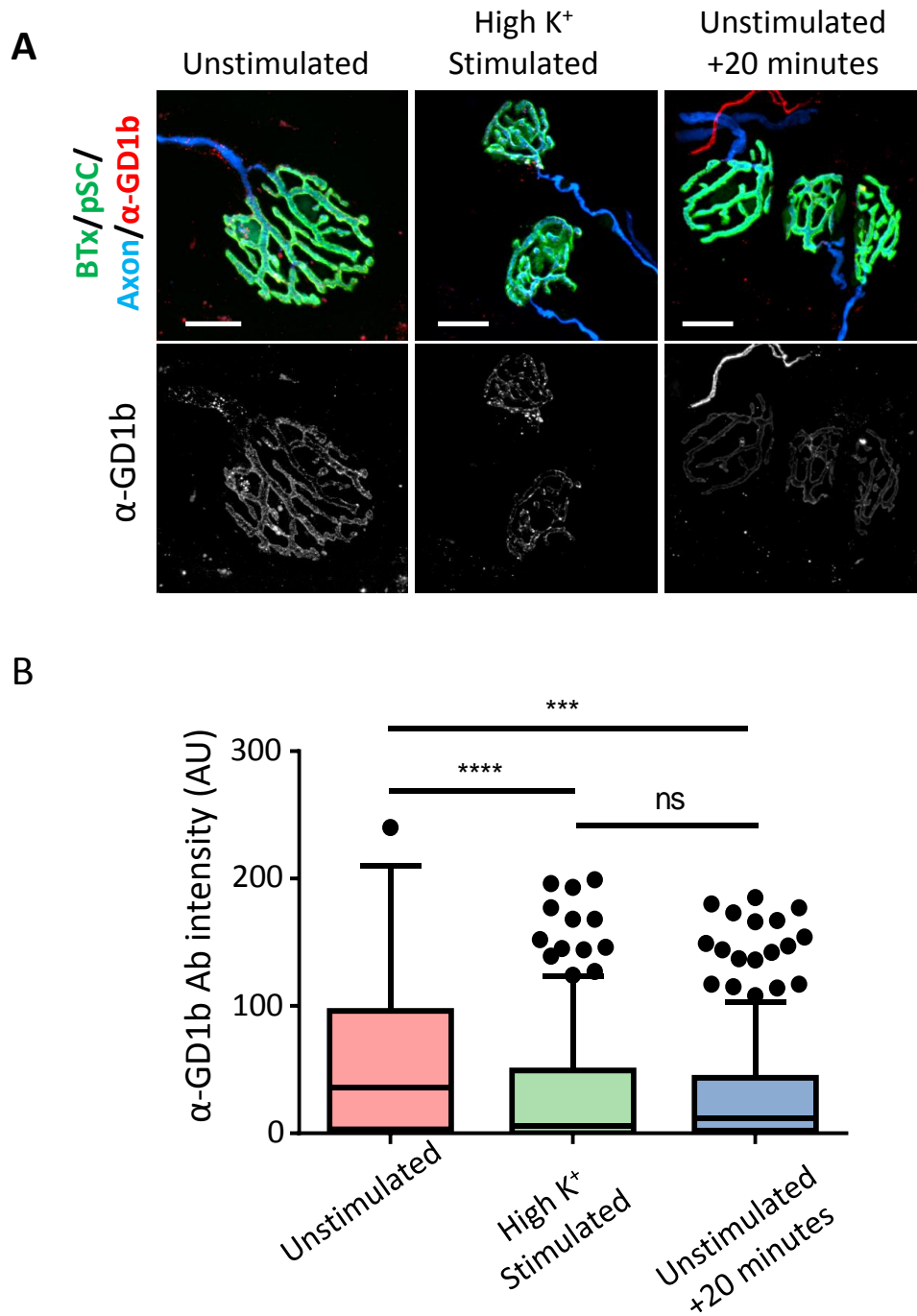


**Figure 7.1: Internalisation of anti-GD1b antibody is accelerated by K<sup>+</sup> induced nerve terminal stimulation.** Wildtype (n=3) TS muscle was labelled with anti-GD1b antibody MOG1, then washed and either incubated at room temperature for 10 minutes with normal Ringer's (unstimulated) or high K<sup>+</sup> Ringers (high K<sup>+</sup> stimulated) or with normal Ringer's for 30 minutes at room temperature (Unstimulated +20 minutes). **A:** Illustrative pictures show the MOG1 signal, which overlies the endplate in unstimulated tissue, is reduced in stimulated tissue and tissue which had a further 20 minute incubation at room temperature. **B:** Quantitatively, high K<sup>+</sup> stimulated tissue shows significantly reduced staining compared with unstimulated tissue, and shows equivalent levels to unstimulated tissue which has been incubated for an extra 20 minutes at room temperature. Scale bar = 20  $\mu$ m. \*\*\*=p<0.001, \*\*\*\*=p<0.0001, Kruskal-Wallis with Dunn's multiple comparison test. A minimum of 226 NMJs were analysed per group. Non-parametric data displayed as Tukey box plot (see section 2.20).

To investigate whether this high  $K^+$  induced acceleration was enough to reduce the amount of damage caused by complement activation, stimulated and unstimulated tissue were subsequently washed and incubated with 40% NHS for 30 minutes at  $37^{\circ}\text{C}$  ( $n=3$ ). Neuromuscular junctions were then analysed for deposition of MAC (Figure 7.2). There was no significant difference between MAC deposition in unstimulated tissue and tissue which had been stimulated with a high  $K^+$  concentration (medians of 86.00 AU vs 68.00 respectively,  $p>0.05$ ). Both of these tissues had statistically higher staining than unstimulated tissue which had been incubated at room temperature for a further 50 minutes ( $p<0.0001$ , median of 2.00 AU). The deposition of MAC in both cases was accompanied by a loss of CFP in the motor nerve terminal, indicating the disruption of the nerve terminal integrity.

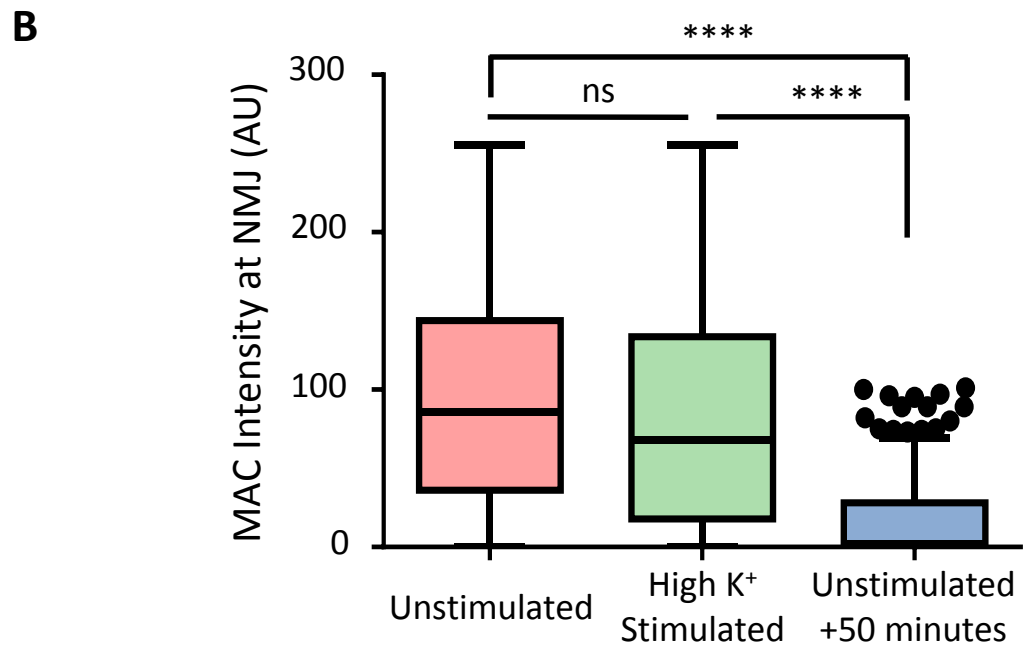
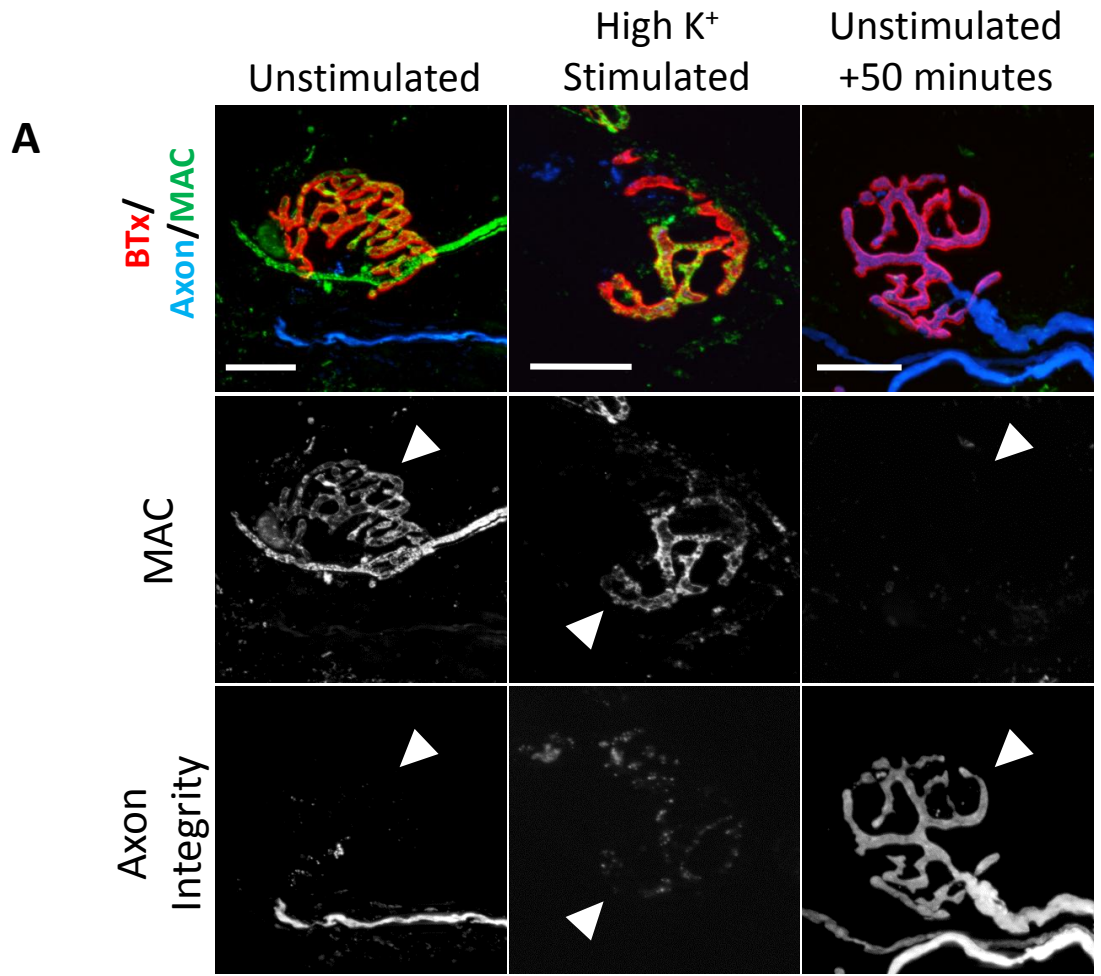


(Figure on previous page)

**Figure 7.2: Accelerated internalisation of anti-GD1b antibody by K<sup>+</sup> induced nerve terminal stimulation does not reduce MAC deposition at motor nerve terminals.** Wildtype (n=3) TS muscle was labelled with anti-GD1b antibody MOG1, washed and incubated at room temperature for 10 minutes with normal Ringer's (unstimulated) or high K<sup>+</sup> Ringers (high K<sup>+</sup> stimulated) or with normal Ringer's for 60 minutes at room temperature (Unstimulated +50 minutes). Tissue was then incubated with 40% NHS for 30 minutes at 37°C. **A:** Illustrative pictures show MAC deposition over the endplates of unstimulated and stimulated tissue, which is accompanied by loss of axonal CFP. White arrow head indicates expected CFP presence indicated by BTx signal. MAC deposition is lower in tissue which was incubated for a further 50 minutes at room temperature. **B:** Quantitatively, unstimulated and high K<sup>+</sup> stimulated tissue show equivalent levels of MAC intensity overlying the BTx signal. Unstimulated tissue incubated for an extra 50 minutes at room temperature, showed significantly reduced MAC intensity compared to both other tissues. Scale bar = 20 µm. \*\*\*\*=p<0.0001, Kruskal-Wallis with Dunn's multiple comparison test. A minimum of 363 NMJs were analysed per group. Non-parametric data displayed as Tukey box plot (see section 2.20).

### 7.3 Electrical stimulation of intercostal nerves

To further study the effect of stimulation-induced uptake of anti-GD1b antibody, wildtype TS muscle was incubated with MOG1 antibody, washed with Ringer's then the intercostal nerves, which supply the TS, were electrically stimulated to induce membrane activity. Electrical stimulation was confirmed by muscle twitching in response to nerve stimulation only, (rather than direct muscle stimulation). If stimulation in this manner could not be confirmed tissue was not included in the experiment. Nerve terminals from stimulated tissues (n=3) showed weaker anti-GD1b antibody staining than those from unstimulated tissue (n=3)(Figure 7.3A). Nodes of Ranvier (example shown by white arrowhead in Figure 7.3A) appeared to still show staining following stimulation. Quantitatively (Figure 7.3B), the antibody intensity at unstimulated nerve terminals was significantly higher than TS muscle which had been electrically stimulated (p<0.0001, median of 53 AU vs. 5 AU respectively).

To demonstrate that the clearance of antibody was indeed due to uptake into the nerve terminal, membrane was permeabilised with Triton X-100 and reprobed with secondary. When reanalysed, previously weakly or negatively stained NMJs were shown to be highly positive for antibody and this staining appeared to be within the nerve terminal, indicating the antibody had been taken into the nerve terminal following stimulation. Quantitatively, there was no

difference between antibody intensity between stimulated and unstimulated tissue following permeabilisation (median of 97 AU vs. 81 AU respectively).

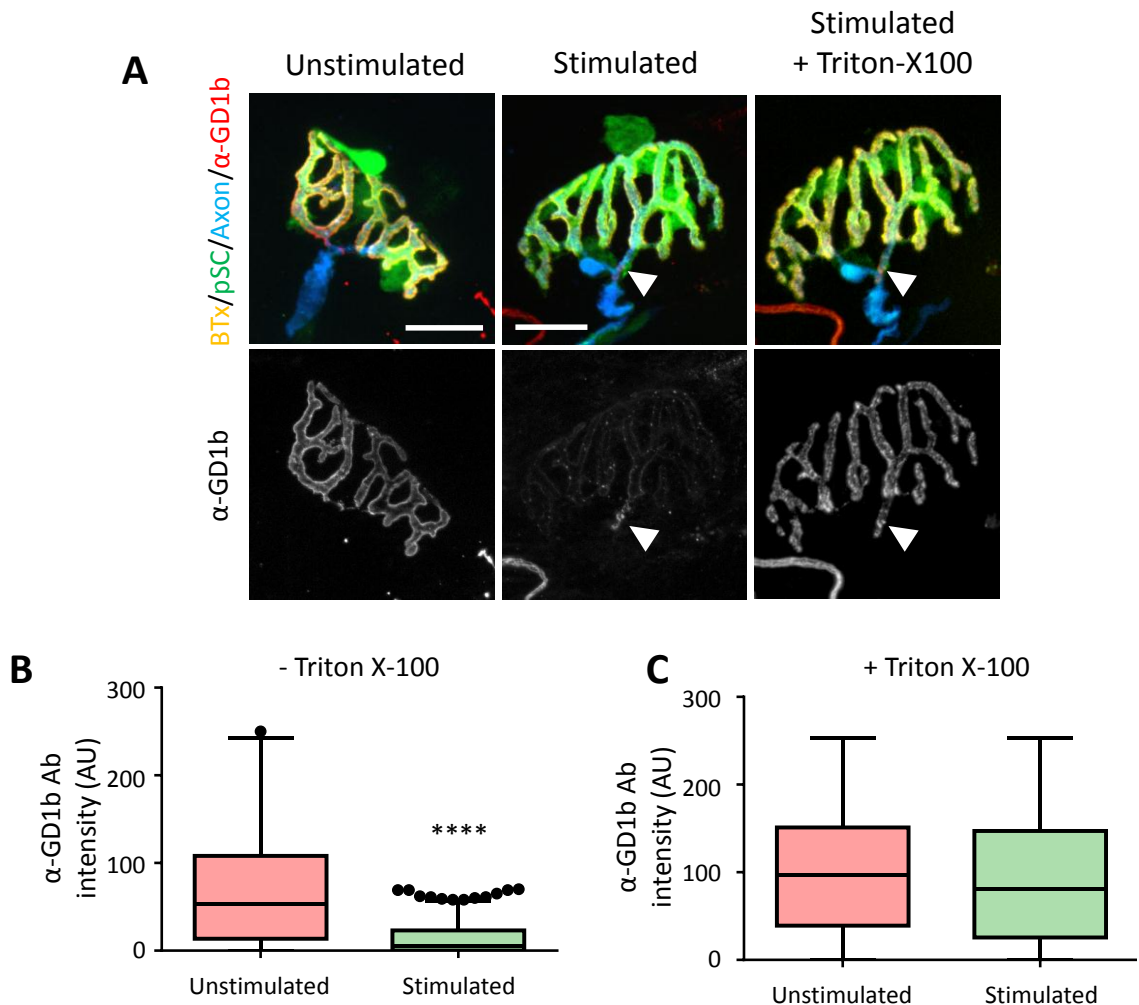


**Figure 7.3: Electrical stimulation of intercostal nerves increases the uptake of anti-GD1b antibody at wildtype TS motor nerve terminals.** Wildtype ( $n=3$ ) TS muscle was labelled with anti-GD1b antibody MOG1, then washed and the intercostal nerves of one TS per mouse was stimulated, while the other remained unstimulated. Once analysed, tissue was permeabilised, reprobbed with secondary antibody and reanalysed for antibody presence. **A:** Unstimulated NMJ showing anti-GD1b antibody deposition at the nerve terminal and stimulated NMJ showing much fainter anti-GD1b presence at the nerve terminal and brighter antibody staining at the terminal node of Ranvier (white arrowhead). When permeabilised and restained with secondary antibody, the same stimulated nerve terminal showed strong antibody presence **B:** Quantitatively, the nerve terminals of stimulated TS tissue showed significantly reduced anti-GD1b antibody staining. **C.** When tissue was permeabilised, levels of antibody were no different in stimulated tissue compared to unstimulated tissue. Scale bar = 20  $\mu$ m. \*\*\*\*= $p < 0.0001$  vs unstimulated, Mann-Whitney test. A minimum of 230 NMJs were analysed per group. Non-parametric data displayed as Tukey box plot (see section 2.20).

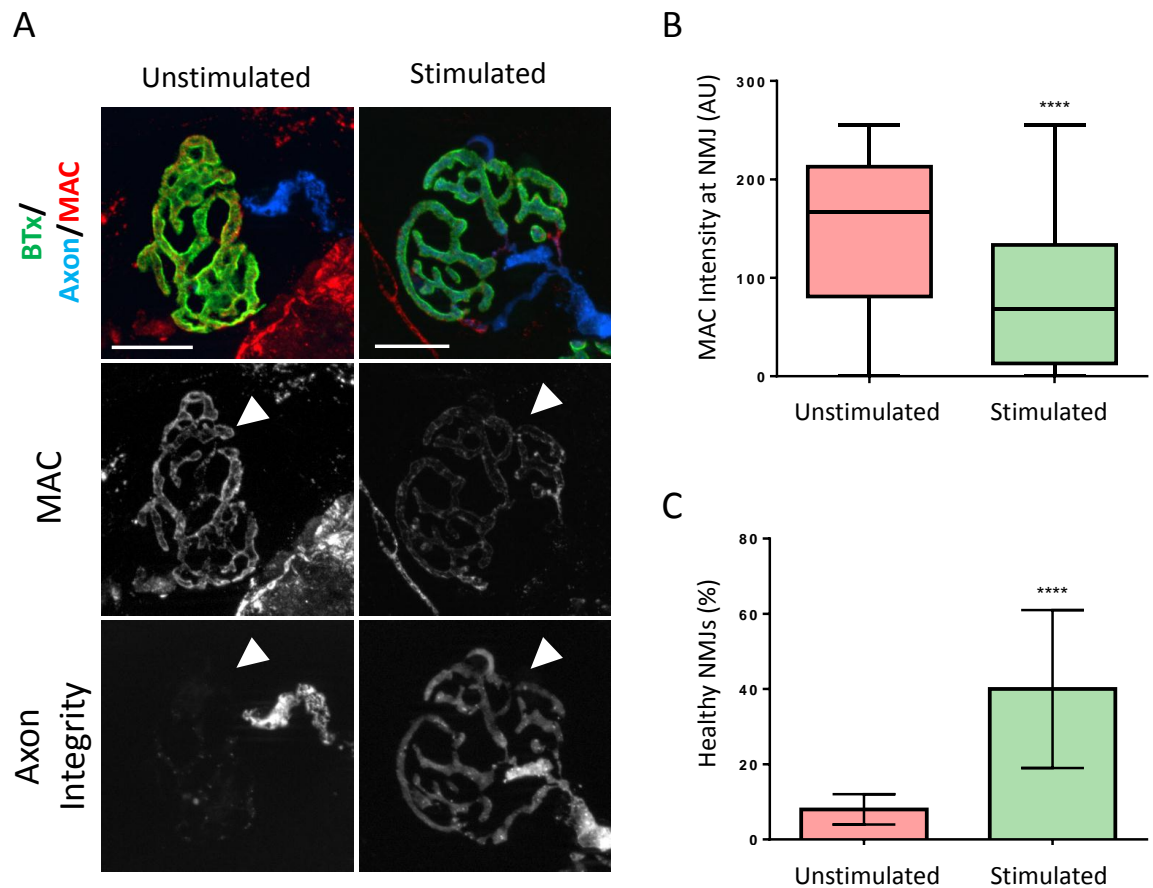


**Figure 7.4: Accelerated internalisation of anti-GD1b antibody by intercostal nerve stimulation results in reduced MAC deposition at motor nerve terminals and increased presence of healthy NMJs.** Wildtype (n=3) TS muscle was labelled with anti-GD1b antibody MOG1, then washed and the intercostal nerves of one TS per mouse was stimulated, while the other remained unstimulated. **A:** Illustrative pictures show strong MAC deposition at unstimulated nerve terminals, whereas MAC deposition is weak over the endplates of stimulated muscle. This is accompanied by retention of CFP in the nerve terminal. White arrow head indicates where CFP should be as indicated by BTx signal. **B:** Quantitatively, stimulated tissue shows statistically reduced MAC staining at the NMJ when compared with unstimulated tissue (\*\*\*\*=p<0.0001 vs. unstimulated, Mann-Whitney test). A minimum of 182 NMJs were analysed per group. Non-parametric data displayed as Tukey box plot (see section 2.20). **C:** Fisher's exact test indicated that stimulated TS had more healthy NMJs than unstimulated as indicated by the presence of CFP (displayed as mean % of total junctions analysed). Scale bar = 20  $\mu$ m. \*\*\*\*=p<0.0001 vs. unstimulated.

To determine whether the reduced anti-GD1b antibody intensity evoked by intercostal nerve stimulation resulted in protection of the nerve terminal from complement-mediated injury, unstimulated and stimulated tissue was this time washed then treated with 40 % NHS for 30 minutes at 37°C and stained for MAC deposition to indicate terminal complement pathway activation. The intensity of MAC deposition was analysed and the number of healthy NMJs were also counted by the presence or absence of CFP (n=3). Stimulated TS muscle showed significantly lower MAC deposition (Figure 7.4B) than unstimulated tissue

(median of 68 AU vs. 167 AU respectively,  $p < 0.0001$ ). This reduction in MAC deposition was accompanied by a reduction in the number of nerve terminals which were negative for CFP. Total CFP positive and CFP negative nerve terminals were compared by Fisher's exact test, which showed a significantly higher presence of CFP-positive NMJs in stimulated tissue compared with unstimulated ( $p < 0.0001$ ). Data is displayed as the mean percentage of healthy NMJs (Figure 7.4C).

## 7.4 Discussion

Previously, it has been shown that at physiological temperatures anti-ganglioside antibody can be taken up at the nerve terminal by a previously undefined mechanism. Contrastingly, these antibodies remains surface-bound on other structures such as the NoR, a stable membrane with slow turnover of its components, to maintain its specialised function (Fewou et al., 2012; Zhang et al., 2012). This has subsequently been confirmed in chapter 5 and 6 of this thesis. When considering these differences in anti-ganglioside antibody internalisation, it was considered that the specialised nature of the nerve terminal for vesicle release and recycling, may account for its enhanced uptake ability. Many studies have looked at the uptake of toxins which bind gangliosides at the motor nerve terminal. Botulinum toxin, a GD1b-binding toxin (Schiavo et al., 2000), is taken into the nerve terminal in a temperature and activity-dependent manner (Black and Dolly, 1986), with internalisation being prevented at temperatures of 4°C. So far, work on anti-ganglioside antibody uptake at the nerve terminal has been investigated using physiological temperatures, but this chapter has demonstrated that internalisation of antibody is also increased by nerve terminal activity. The increase in uptake by temperature and activity may both be neurotransmitter release-associated as spontaneous vesicle release has been shown to increase at higher temperatures (Gansel et al., 1987; Greenshields et al., 2009; Nishimura, 1986). As the motor nerve terminal is a specialised membrane with no caveolae and high vesicular cycling, it is unsurprising that the antibody internalisation mechanisms at this site differs from the caveolin-mediated endocytosis which has been demonstrated in cell work (Fewou et al., 2012; Sharma et al., 2003; Singh et al., 2003). This does not exclude the possibility that antibody uptake at other membranes *in vivo* is not

mediated by caveolae; as discussed in chapter 5, despite the difference in whole brain enzyme expression levels between wildtype and *GalNAcT<sup>-/-</sup>-Tg(neuronal)* mice, levels of ganglioside expression at the membrane appear consistent as demonstrated by similar staining intensities of anti-ganglioside antibodies (see chapter 3). Therefore the rapid clearance of MOG1 and DG2 by wildtype mice in chapter 5 and 6 when compared with *GalNAcT<sup>-/-</sup>-Tg(neuronal)* mice indicates a contribution of clearance by non-neuronal cells. These non-neuronal cells may be clearing the antibody via caveolae. Vascular endothelial cells are known to express gangliosides (Cho et al., 2012) and often blood vessels are detected in muscle-nerve preparations using in-house anti-ganglioside antibodies (Willison lab, unpublished observations). These cells are also sites of high caveolae presence (Frank et al., 2003); therefore, it is possible that the endothelial cells are responsible for a large portion of non-neuronal antibody clearance.

Increased nerve terminal uptake of botulinum toxin by nerve stimulation results in increased paralytic halftime as it is within the nerve terminal that the toxin exerts its pathologic effects (Rummel et al., 2009). In contrast, removal of anti-ganglioside antibody from the plasma membrane surface will prevent its interaction with complement, thus alleviating the extent of nerve terminal injury. The use of KCl to depolarise the nerve terminal membrane has previously been shown to be sufficient to increase botulinum toxin entry into PC12 cells and mouse motor nerve terminals (Dong et al., 2003), and was therefore used to initially demonstrate whether anti-ganglioside antibody underwent the same activity-dependent uptake. In this chapter, high  $K^+$  concentration did indeed result in a significantly decreased presence of anti-GD1b antibody on the nerve terminal surface, indicating an increased uptake of antibody at this site. However, when tissue stimulated with a high  $K^+$  concentration was then exposed to NHS, this increased uptake was not sufficient to result in decreased MAC deposition on the endplate. More physiologically relevant however, is the stimulation of the nerves supplying the TS. This resulted in a more obvious decrease in surface antibody presence, which was shown to be present within the nerve terminal following tissue permeabilisation and reincubation with secondary antibody. In an NHS-mediated injury paradigm, this reduction in surface antibody was enough to result in significantly reduced terminal complement pathway activation, as indicated by a reduction in MAC deposition.

The resulting decrease in MAC deposition was accompanied by the presence of more CFP-positive NMJs. While at early timepoints, the absence of CFP does not always coincide with the destruction of axonal NFil following a MAC-mediated injury (Rupp et al., 2012); it can be equated with a breach of axonal membrane integrity. Therefore, if a NMJ still retains CFP in its motor nerve terminal, it is safe to assume that the axon has been spared from membrane damage. Therefore, it appears that increased nerve terminal activity results in its self-preservation from antibody and complement mediated attack.

Thus far this effect has only been demonstrated *ex vivo* and in wildtype mice due to time constraints; however, a robust animal model is still needed to determine the impact of this effect *in vivo*. Stimulation has been shown to increase botulinum toxin uptake at its target site, reducing the spread of toxin to nearby muscles (Horisberger et al., 2013; Hughes and Whaler, 1962). By the same principle, it is possible that voluntary muscle contraction or even peripheral nerve stimulation may be able to enhance anti-ganglioside antibody uptake and thus reduce the available pathogenic anti-ganglioside antibody. It is hypothesised that animals which are more active (i.e. by using a forced exercise treadmill paradigm) may be able to clear antibody from their serum faster than less active (unexercised) animals. A similar study has been performed in rats using the established P2-peptide induced EAN model of GBS. In the group of exercised animals, the clinical score, CMAP amplitudes and motor conduction velocities were significantly improved compared to the non-exercised group (Calik et al., 2012). The authors hypothesise that exercise-induced changes in immune cell activation, quantity, cytokine secretion or trafficking are responsible for the improvements. Conceivably, a reduction in anti-P2 antibody could account for the subsequent immune cell changes. It is difficult to draw too much from this model as it is so different from our proposed model (the use of rats instead of mice, P2 peptide instead of ganglioside, myelin injury instead of axonal injury, and the training of only the exercised rat group before injury induction) but provides some background data supporting the effect of exercise on immune-mediated neuropathies. If a forced-exercise model can demonstrate an effect on circulating antibodies, and antibody and complement-mediated injury, the effect of nerve terminal activity on antibody clearance may have important clinical consequences.

For an acute condition such as AMAN, the effect of activity-dependent internalisation of antibody would presumably be dependent on how much damage has already been caused. In this proof-of-principle, *ex vivo* study, NHS was administered after the antibody incubation and stimulation so it is unclear whether this would have any major effects in patients where acute antibody attack had already occurred. Presumably, if exercise or nerve stimulation was able to reduce circulating antibody levels, the incidence of ongoing injury in GBS would be reduced, thus allowing a faster recovery time. This may theoretically be especially useful in patients who have chronic autoimmune neuropathies, such as MMN, who have prolonged motor weakness due to circulating anti-GM1 IgM antibodies (Pestronk et al., 1988). However, evidence of the effects of exercise in autoimmune neuropathy patients has been conflicting. Most GBS studies have been conducted in patients who are in the recovery phase, where antibodies are still present but at a much lower titre than immediately after GBS onset (Odaka et al., 2003). Some studies have shown that exercise in the recovery phase of GBS results in improved prognosis, though this may be due to an improvement of physical fitness. Withal, some studies have found an improvement in physical fitness, but no improvement in the patients' perceived fatigue (Bussmann et al., 2007; Fisher and Stevens, 2008; Mobbs et al., 2007). Following intense exercise, both MMN and GBS patients can experience prolonged weakness and potential muscle damage, resulting from the overwork of the few muscle fibres which are still receiving stimulation (Bassile, 1996). Additionally, studies have shown that in MMN, nerve stimulation can cause activity-dependent conduction block due to hyperpolarisation of the axonal membrane (Nodera et al., 2006).

Before effects in patients are considered, it is clearly important to first establish whether forced exercise can affect *in vivo* models of disease and whether the activity dependency is common to antibodies targeting other gangliosides.

## 8 Discussion

Infection with *C.jejuni* can, in rare cases, lead to the generation of antibodies which cross-react with peripheral nerves. In the case of motor axonal and sensory forms of GBS, as well as chronic variants CIDP and MMN, circulating antibodies have been shown to be directed towards gangliosides, while the target antigen in AIDP remains elusive. Currently there is no mouse model which mimics GBS, though rabbits which have been immunised with gangliosides GM1 and GD1b go on to develop peripheral motor and sensory neuropathy respectively (Yuki et al., 2001; Yuki et al., 2004; Kusunoki et al., 1996). This lab has created GalNAcT<sup>-/-</sup>-*Tg(neuronal)* and GalNAcT<sup>-/-</sup>-*Tg(glial)* mice which have the synthesis of complex ganglioside restricted to their neurons or glia respectively. These mice were developed with the original aim of being used as part of active immunisation models of GBS. This restriction of GalNAcT enzyme expression, and thus the expression of complex gangliosides, was hoped to overcome the tolerance to ganglioside immunisation which has been shown previously in wildtype mice (Bowes et al., 2002; Lunn et al., 2000), with the view to demonstrate the differences between neuronal and glial-directed antibody attack. These mice can also be used in determining the role and significance of neuronal or glial complex ganglioside expression at specialised nervous system membrane domains (Yao et al., 2014). In GalNAcT<sup>-/-</sup> mice, the global loss of complex gangliosides results in an age-dependent degenerative phenotype accompanied by neurodegeneration, demyelination and nodal disruption (Chiavegatto et al., 2000; Sheikh et al., 1999; Susuki et al., 2007a). The restoration of neuronal complex ganglioside expression is enough to save this phenotype (Yao et al., 2014). These mice have many potential roles in the investigation of anti-ganglioside antibody mediated binding and injury at specific membrane sites. In patients, anti-ganglioside mediated injury occurs only on peripheral nerve membranes (neuronal and potentially also glial), despite the fact that gangliosides are present ubiquitously. Therefore, the use of these mice can mimic the site-specific antibody targeting that is seen in human disease.

The aims of this thesis were to use these mice as tools to create an active immunisation model of GBS, and subsequently to investigate the injury caused by an endogenous antibody response to ganglioside liposome immunisation. In

addition, the membrane-specificity of complex ganglioside expression also allowed an investigation into the effect of antibody internalisation at specific sites. In particular, interest lay in the internalisation of anti-ganglioside antibody at the nerve terminal, which was previously demonstrated to occur *ex vivo* in wildtype and GD3s<sup>-/-</sup> mice (Fewou et al., 2012). This latter aim was met with the novel finding that circulating anti-ganglioside antibody levels can be affected by their internalisation by ganglioside-expressing membranes and that the circulating antibodies which remain are not necessarily pathogenic.

## 8.1 Main findings

The work detailed in the first part of this thesis aimed to demonstrate that GalNAcT<sup>-/-</sup>-*Tg(neuronal)* and GalNAcT<sup>-/-</sup>-*Tg(glial)* mice, could be actively immunised and show a neuronal or glial injury upon the introduction of NHS. This was done with the hope of creating a model of disease where anti-ganglioside antibody and complement mediated injury could be achieved *in vivo* with endogenously produced antibodies. Previously, to mimic disease *in vivo* in mice, a passive transfer protocol was used, where a high affinity monoclonal antibody is injected directly into the mice, followed by NHS 16 hours later (Halstead et al., 2005a; Halstead et al., 2008). While this approach is effective in demonstrating the effect of anti-ganglioside antibody and complement on the peripheral nervous system of mice, it does not faithfully mimic the clinical situation. In patients, an antecedent infection or vaccination initiates an immune response which results in an endogenous antibody and complement mediated attack of gangliosides on peripheral nerves. An active immunisation model of disease would more accurately imitate this situation. This would allow us to more authentically study disease pathogenesis, with the ultimate goal of developing and testing new therapeutics. A similar study was attempted by a previous lab member who demonstrated an immune response to GT1b following immunisation with GT1b-containing liposomes. However, a robust injury was not detected following NHS injection, with only a slight reduction in tidal volume and negligible complement deposition (S. Rinaldi, unpublished data). GT1b was chosen as a target in this previous study as thin layer chromatography had demonstrated a comparable restoration of GT1b presence in GalNAcT<sup>-/-</sup>-*Tg(neuronal)* mice to wildtype mice. A passive transfer model confirmed that an

injury could be demonstrated following injection of the in-house monoclonal antibody MOG16, which targets both GT1b and GD1b. After demonstrating in chapter 3 that GD1b was highly present at the nerve terminal of *GalNAcT<sup>-/-</sup>-Tg(neuronal)* and *GalNAcT<sup>-/-</sup>-Tg(glial)* mice using anti-GD1b antibody MOG1, it was considered that GD1b may be a better target, and that perhaps the injury previously demonstrated using MOG16 may be due to its target of GD1b rather than GT1b. Thus, it was had hoped that immunising the mice with this antigen, rather than GT1b, would result in a more robust injury. This was supported by the evidence that injury can be induced by passive transfer of anti-GD1b antibody MOG1 and NHS in Chapter 4. As in the previous study with GT1b, it was demonstrated that, unlike wildtype mice, *GalNAcT<sup>-/-</sup>-Tg(neuronal)* and *GalNAcT<sup>-/-</sup>-Tg(glial)* mice responded well to immunisation with GD1b-containing liposomes, though neither strain responded as well as the GD1b-lacking *GalNAcT<sup>-/-</sup>* mice. However, even with modification of the immunisation procedure to include the adjuvant MPLA, once again a robust injury was not detectable in these mice in response to the circulating antibodies, even when NHS was injected as a source of complement. ELISpot data from two different GD1b liposome immunisation experiments implied that at the B-cell level, no significant difference existed between wildtype and *GalNAcT<sup>-/-</sup>* response to immunisations. This led to the belief that another factor was affecting the amount of detectable antibody in the serum of these different mouse strains. A previous study had already demonstrated that anti-ganglioside antibodies can be internalised at the nerve terminals of wildtype or *GD3s<sup>-/-</sup>* mice in *ex vivo* TS preparations (Fewou et al., 2012). It was therefore felt that an investigation was warranted into whether this phenomenon may be reducing circulating antibody levels, and subsequently the likelihood of an effective injury. The aims of these investigations were to expand on the knowledge already gained from wildtype and *GD3s<sup>-/-</sup>* mice, using the *GalNAcT<sup>-/-</sup>-Tg(neuronal)* and occasionally *GalNAcT<sup>-/-</sup>-Tg(glial)* mice to demonstrate the effects of site-specific uptake. Here I will summarise what I consider to be the main novel findings of this thesis and their implications in the wider field of GBS research.

### **8.1.1 Receptor-dependent internalisation can affect circulating levels of anti-ganglioside antibody**

To date, the primary mechanisms by which antibody levels have been shown to be cleared from the circulation is by non-specific pinocytotic uptake, followed by lysosomal degradation (Mould and Sweeney, 2007). The FcRn has been shown to prolong IgG half-life in the serum, by salvaging IgG scavenged in this way and recycling it back to the circulation (Lobo et al., 2004). This thesis has emphasized the importance of receptor-mediated endocytosis as another major mechanism of antibody regulation. Specifically, this thesis has looked at the uptake of anti-ganglioside antibodies, which are elevated in the sera of patients with GBS (Ilyas et al., 1988b; Ilyas et al., 1988a; Ho et al., 1995; Kuwabara et al., 1998; Ogawara et al., 2000). Using a passive immunisation protocol whereby monoclonal anti-ganglioside antibody was injected i.p., it was shown that antibody against ganglioside may be cleared from the circulation in wildtype and GalNAcT<sup>-/-</sup>-Tg(*neuronal*) mice, but not in GalNAcT<sup>-/-</sup> mice. This lack of clearance in GalNAcT<sup>-/-</sup> mice demonstrates that the binding of the antibody to target is required for the effect (Figure 5.5). This is a crucial piece of insight into antibody handling, especially in the context of our animal models, where, even in passive immunisation experiments, antibody levels may be being rapidly reduced within 1 day of injection, as in the wildtype mice. This may not be of major importance when injecting large quantities of antibody. For example, when 1 mg of MOG1 was passively injected to demonstrate injury in Chapter 4, injury and (although not shown) serum antibody levels in wildtype mice and GalNAcT<sup>-/-</sup>-Tg(*neuronal*) mice were similar. In this case, it is assumed that levels of antibody were so high (1 mg) as to saturate the internalisation machinery. When considering the active immunisation model attempted in this thesis, a chronic but presumably lower level of antibody is produced, therefore not saturating the process of internalisation. It was proposed that the effect of antibody internalisation is responsible for the low levels of antibody seen in actively immunised wildtype mice. Similarly, in GalNAcT<sup>-/-</sup>-Tg(*neuronal*) mice, which showed an intermediate level of antibody production against GD1b, internalisation prevents a sufficient level of pathogenic antibody presence in the serum to result in a robust, detectable injury either by *in vivo* testing methods, or at the immunohistological level. Further optimisation of the immunisation

procedure may be required to gain such a level of antibody. The concept that receptor-dependent uptake may affect serum levels of antibodies is supported by, and may help explain, the fact that polyreactive monoclonal antibodies have a shorter half-life than monoreactive monoclonal antibodies; Polyreactive antibodies may bind and be internalised at more sites than monoreactive antibodies, thus monoreactive antibodies remain for longer in the serum (Sigounas et al., 1994).

The idea that wildtype mice may not be immunologically tolerant to glycolipid immunisation is also a novel concept. It has been demonstrated that, when immunised with gangliosides, wildtype mice respond much more poorly than mice which have disrupted target ganglioside synthesis (Bowes et al., 2002; Lunn et al., 2000). It has been presumed that these mice are simply tolerant to glycolipid immunisation with a self-antigen. Tolerance exists to prevent an immune reaction against host cells, thus preventing autoimmune conditions such as GBS from developing. Although in wildtype mice gangliosides are more enriched in nervous system tissues, their expression is ubiquitous. It is therefore likely that any auto-reactive T and B cells have been removed in these mice. In  $\text{GalNAcT}^{-/-}$  mice however, no complex gangliosides are expressed, therefore their naïve T and B cells will recognise them as “foreign” antigens upon exogenous delivery of ganglioside-expressing liposomes. The resulting immune response in these mice will therefore be unhindered by tolerance. In this thesis, the difference in the serum antibody level in wildtype and  $\text{GalNAcT}^{-/-}$  mice was shown once again, with the additional observation that responses in  $\text{GalNAcT}^{-/-}$ -*Tg(neuronal)* and  $\text{GalNAcT}^{-/-}$ -*Tg(glial)* mice, which have restricted  $\text{GalNAcT}$  expression, are intermediate. It was considered that these mice may have intermediate levels of tolerance either because antigen levels were below some critical threshold (Thomas, 2001) or because their B cells were not being exposed to the “self” antigen as it was restricted to tissue-specific sites, a problem overcome by T cells through the autoimmune regulator gene *Aire* (Liston et al., 2003). However, GD1b-specific ELISpots indicated that the anti-GD1b IgG and IgM immune responses were statistically similar in all mouse strains. As this seemed to contradict what was thought about tolerance in wildtype mice, the experiment was repeated again using freshly immunised wildtype mice and  $\text{GalNAcT}^{-/-}$  mice. Once again no significant difference existed

between the anti-GD1b IgG or IgM producing cells, though less IgG was being produced in both strains (unsurprising at such an early timepoint following immunisation). While a role for tolerance on the levels of antibody seen in the serum cannot be completely ruled out, the new knowledge that antibodies can be cleared at a rate which is dependent on the expression levels of their target receptor, suggests the possibility that any antibodies produced by wildtype and GalNAcT<sup>-/-</sup>-*Tg(neuronal)* mice may be cleared in the same manner. The low levels of antibody seen in wildtype mouse serum would therefore be due to faster rates of clearance rather than higher tolerance. This could mean that antibody clearance by receptor-mediated internalisation could confer another means of tolerance by removing the antibody produced by autoreactive B cells.

### ***8.1.2 Motor nerve terminal is a major site of activity dependent antibody clearance***

Although the concept that circulating pathogenic antibody can be regulated by receptor-dependent internalisation is interesting in itself, the use of GalNAcT<sup>-/-</sup>-*Tg(neuronal)* mice in the clearance studies allowed us to account for the clearance by neuronal cells only. GalNAcT<sup>-/-</sup>-*Tg(neuronal)* mice cleared the antibody from the circulation at a slower rate than wildtype mice. Enzyme expression has been shown to be lower in GalNAcT<sup>-/-</sup>-*Tg(neuronal)* mice when compared to wildtype mice. However, as discussed in Chapter 5, these levels were measured in whole brain, therefore including non-neuronal cells in the assay. These non-neuronal cells will have normal ganglioside expression in wildtype mice but intentionally lack the GalNAcT enzyme in GalNAcT<sup>-/-</sup>-*Tg(neuronal)* mice. Further, staining profiles in Chapter 3 showed similar levels of anti-ganglioside antibody intensity between wildtype and GalNAcT<sup>-/-</sup>-*Tg(neuronal)* mice, indicating that levels of ganglioside are similar on the neuronal membranes of these mice. It is therefore more likely that the faster rate of clearance in wildtype mice is due to non-neuronal uptake. Subtracting the differences to account for non-neuronal cells, uptake by neuronal cells still accounted for a great proportion of clearance, and alone managed to clear the antibody from the circulation within 6 days. The node of Ranvier has previously demonstrated an inability to clear antibody (Fewou et al., 2012). Even the distal nodes in TS preparations, which have only weak BNB protection (McGonigal et

al., 2010) were shown in Chapter 6 to be unable to internalise bound anti-GM1 antibody (see Figure 6.1 and 6.3 for examples) as well as in Chapter 7 for anti-GD1b antibody (Figure 7.3). Antibody may also be binding at the nerve roots in *GalNAcT<sup>-/-</sup>-Tg(neuronal)* mice, a region of the PNS which lacks BNB protection (Weerasuriya and Mizisin, 2011) and has been shown to be affected in rabbit models of AMAN (Susuki et al., 2003). However, it is more likely that the nerve roots would act in a similar manner to the node of Ranvier as these sites lack the same active membrane of the nerve terminal. Therefore, it is likely that the clearance seen in *GalNAcT<sup>-/-</sup>-Tg(neuronal)* mice is almost solely attributable to clearance by the motor nerve terminal, making it a major scavenger of pathogenic antibody. This concept has been discussed previously with the *ex vivo* observations of anti-ganglioside antibody uptake at wildtype and *GD3s<sup>-/-</sup>* mouse motor nerve terminals (Fewou et al., 2012; Fewou et al., 2014), however the use of *GalNAcT<sup>-/-</sup>-Tg(neuronal)* mice alongside wildtype and *GalNAcT<sup>-/-</sup>* mice *in vivo* clearly demonstrates how major the effect neuronal uptake truly has on antibody levels. This lends more credence to the hypothesis that this motor nerve terminal internalisation is the key factor differentiating why nodal injury is more apparent in patients than motor nerve terminal injury (Ho et al., 1997; Kuwabara et al., 2011; Spaans et al., 2003; Griffin et al., 1996; Hafer-Macko et al., 1996a; Kuwabara et al., 1998), despite the nerve terminal's ability to be injured by anti-ganglioside antibodies and complement in *ex vivo* muscle-nerve preparations (Goodfellow et al., 2005; Goodyear et al., 1999; Halstead et al., 2004; Halstead et al., 2005b). In wildtype mice, although GD1b is enriched on neurons, it is also present in many other tissues, hence the rapid uptake seen in these mice. Gangliosides, and their associated antibody ligands, have been shown previously in cell work to be mostly internalised via clathrin independent, mainly caveolin-mediated, endocytosis (Crespo et al., 2008; Singh et al., 2003; Fewou et al., 2012). It is hypothesised that the non-neuronal uptake of antibodies in wildtype mice, which accounts for their rapid ability to clear antibody, is mostly due to caveolin-mediated uptake. It is likely that much of this uptake may occur in vascular endothelial cells, where gangliosides are widely expressed (Cho et al., 2012) and where caveolae are most abundant (Frank et al., 2003). This widespread non-neuronal uptake may offer an explanation as to why, in patients, antibodies directed against ubiquitously-expressed gangliosides do not result in injury to tissues other than peripheral

nerves. Contrastingly, uptake at the nerve terminal was shown to be activity dependent, implying that the uptake at this site is reliant rather on the vesicle recycling pathways which occur following neurotransmitter release.

The question may be asked: why are patient anti-ganglioside antibodies not cleared rapidly if they, like wildtype mice, have ubiquitous ganglioside expression? Although the situation in patients is clearly more complex and not as fully understood as in the simplified mouse model, two explanations are brought to mind. Firstly, the levels of pathogenic antibody in patients may simply be too high for clearance to occur effectively, thereby allowing binding of sites which cannot effectively internalise antibody, such as the NoR. Secondly, the antibody MOG1 has been shown to bind GD1b in a *cis*-independent manner (Rinaldi et al., 2009), presumably allowing the widespread GD1b binding and subsequent internalisation observed in wildtype mice. In patients, antibodies with the same *cis*-independent binding may also be quickly cleared from the circulation. However, patients will also likely produce antibodies which are *cis*-inhibited by surrounding glycolipids, or bind neoepitopes formed by gangliosides in complex with other lipids. The clearance of these antibodies will therefore be restricted to precise sites where the local microenvironment permits binding. In this case, the effect of uptake is likely to be similar to that of *GalNAcT<sup>-/-</sup>-Tg(neuronal)* mice, where the target is restricted to the neurons. This restricted uptake would therefore lead to prolonged presence of circulating antibody. While this prolonged exposure may not affect the nerve terminal which can clear the antibody before injury can take place, the node of Ranvier remains vulnerable to circulating antibody.

### **8.1.3 Uptake may result in spinal cord trafficking**

Following injection of 1 mg of MOG1, presence of this antibody was detectable in the ventral motor neurons after 1 day. This is the first time this has been demonstrated with antibodies which target gangliosides. Although shown only with one anti-ganglioside antibody in this thesis, the supporting evidence of anti-synaptosome monoclonal antibodies and antisera uptake from previous studies serves to highlight the possibility that anti-ganglioside antibodies may be retrogradely transported to the spinal cord following uptake at the motor nerve

terminal (see chapter 5) (Fabian and Ritchie, 1986; Fabian and Petroff, 1987; Fabian, 1988; Fabian, 1991; Ritchie et al., 1985; Ritchie et al., 1986; Wenthold et al., 1984). The consequences of this are as of yet unknown. However, the demonstration that 7 days following antibody injection in GalNAcT<sup>-/-</sup>-*Tg(neuronal)* mice, antibody was seen in the cord neuropil outwith the motor neuron, implies that these antibodies are not fully degraded following their uptake. Instead some may be released from the motor neuron to bind to nearby neurons and potentially have pathogenic effects within the CNS. Inhibitory interneuron damage has been implicated in the hyper-reflexia seen in some AMAN cases (Kuwabara et al., 1999; Yuki et al., 2012). Similarly, damage to the brainstem has been implicated in the alteration of consciousness seen in BBE patients (Shahrizaila and Yuki, 2013). The retrograde transport of anti-ganglioside antibody to the spinal cord, followed by the potential trans-synaptic spread to surrounding spinal cord or brainstem nuclei may result in antibody-mediated damage to these areas. It would be interesting to further investigate whether trans-synaptic spread of retrogradely transported antibody could be responsible for the damage seen in these subsets of disease.

#### ***8.1.4 Antibodies in patient serum may not be pathogenic***

One of the most significant findings of this thesis is that pathogenic, tissue binding antibodies are quickly cleared from the circulation at points where antibodies may bind and be endocytosed. In contrast, antibodies which react with gangliosides in ELISA but do not bind in tissue cannot be internalised in the same receptor-dependent manner as pathogenic antibodies. These antibodies thereby remain in the circulation for longer periods of time (Figure 6.9). The two antibodies used to demonstrate this, DG1 and DG2, were first shown to have differing abilities to bind GM1 in the living membrane by Greenshields et al. The authors showed that, despite both antibodies having been raised against GM1 in mice, only DG2 could bind to its target uninhibited, while DG1 binding was hindered by the presence of nearby GD1a (Greenshields et al., 2009). This inhibitory GD1a effect was also demonstrated with human anti-GM1 IgM monoclonal antibodies isolated from MMN patients. The authors concluded that the binding of antibodies seen in ELISA or glycoarray does not mimic their pathogenic potential in living tissue. The demonstration that only the tissue-

binding DG2 antibody can be cleared from the circulation serves to establish the effects of this finding *in vivo*. The clinical consequence of this finding is that the patient antibodies detected by solid-phase diagnostic assays do not represent the same cohort of antibodies which can cause neuropathology. This may explain why the detection of anti-ganglioside antibodies in the serum does not always correspond with the progression of disease (for example Press et al showed peak antibody during the recovery phase of GBS) (Odaka et al., 2003; Press et al., 2001), a fact which had led to some debate as to whether anti-ganglioside antibodies are the disease-causing agent in GBS. It also presents a justification as to why serum from GBS patients, while highly positive for anti-ganglioside antibodies by ELISA, has rarely been found to cause damage when used in mouse studies even with significant modulation of the membrane, either by using mice which overexpress target ganglioside, and/or neuraminidase treatment to unmask hidden epitopes (Goodfellow et al., 2005; Jacobs et al., 2002; Zitman et al., 2011b). Following the study by Greenshields et al, patient sera would be expected to contain both pathogenic and non-pathogenic antibody and therefore should still have pathogenic potential when exogenously added to tissue. However, in light of the ability of pathogenic antibody to be cleared from the circulation, it is more likely that patient sera contain a considerably lower proportion of pathogenic antibody in comparison to non-pathogenic. This principle may also be used as a possible explanation as to why antibody binding was hard to show in the active immunisation studies shown in chapter 4, despite anti-GD1b antibody presence being confirmed by ELISA and glycoarray.

## **8.2 Additional insight and future work**

### ***8.2.1 Parallel studies supporting the concept of antibody internalisation***

Originally intended as part of this thesis, it soon became clear that time constraints would prevent me from undertaking some experiments which would expand the scope of investigation of anti-ganglioside antibody clearance. For instance, when it was shown that levels of MOG1 (an IgG) could be rapidly depleted in wildtype and GalNAcT<sup>-/-</sup>-Tg(*neuronal*) mice, it became of interest to show that this concept is also true of pentameric IgM molecules. It was assumed

that this would be the case based on a pilot study carried out by myself in the early stages of investigation, but also by a previous study showing monoclonal IgM antibody targeting thy1.1 (which is highly enriched at the neuronal plasma membrane), can be retrogradely transported to the spinal cord, implying its uptake at the nerve terminal (Fabian, 1990). Using the same protocol set out in this thesis, MOM8 (an anti-GD1b IgM monoclonal antibody) was injected into wildtype,  $\text{GalNAcT}^{-/-}$  and  $\text{GalNAcT}^{-/-}\text{-Tg}(\text{neuronal})$  mice. This IgM antibody was also rapidly cleared in wildtype mice, with intermediate rate of clearance in  $\text{GalNAcT}^{-/-}\text{-Tg}(\text{neuronal})$  mice and in  $\text{GalNAcT}^{-/-}$  mice (Figure 8.1). Antibody is significantly higher than wildtype mice in  $\text{GalNAcT}^{-/-}$  and  $\text{GalNAcT}^{-/-}\text{-Tg}(\text{neuronal})$  mice at day 1, but decreases to similar levels from day 3 onwards. This was unsurprising since the half-life of IgMs in mouse circulation is around 3 days (Vieira and Rajewsky, 1988; Zuckier et al., 1989). This work was performed by C. Paton as fulfilment of her degree of Master of Science.

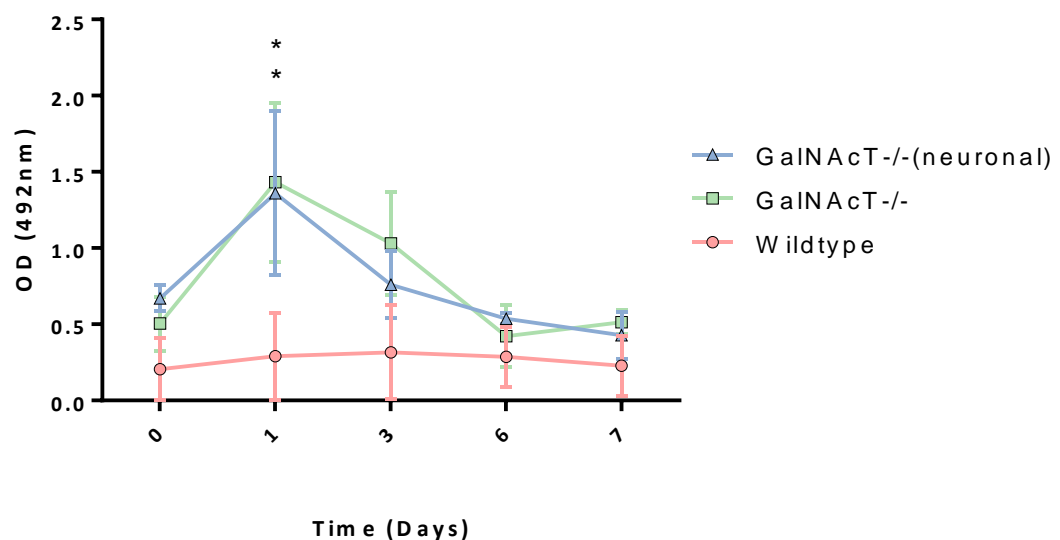


**Figure 8.1: MOM8 serum presence by ELISA over 7 days.** Wildtype mice (n=3) clear antibody quickly from their circulation, most being cleared even at the day 1 timepoint.  $\text{GalNAcT}^{-/-}$  (n=2) and  $\text{GalNAcT}^{-/-}\text{-Tg}(\text{neuronal})$  mice (n=3) show a peak at day 1 and a decline over the remaining days, indicating a slow clearance of antibody. IgM half-life in mice is around 3 days explaining the low levels at day 6 and 7.  $*=p<0.05$  vs. wildtype. Two-way ANOVA with Tukey's multiple comparison test.

To link this work back to patient studies it is important that this phenomenon can be demonstrated using patient-derived antibodies. If, as shown with the mouse monoclonal antibody DG1, non-pathogenic antibodies are left to circulate

in the serum, then the serum antibodies detected by ELISA in patients, which are likely not pathogenic, would therefore be unlikely to bind in mouse tissue. In contrast, monoclonal antibodies derived from patient PBMCs in theory represent an entire repertoire of antibodies produced by the patient, including both pathogenic and non-pathogenic. Using an anti-GM1, IgM monoclonal antibody derived from an MMN patient which was previously shown to bind mouse NMJs (G. Meehan, unpublished data), plus serum taken from the same patient, we were able to show *ex vivo* that the patient serum neglected to bind to GD3s<sup>-/-</sup>TS (even with neuraminidase treatment to strip nearby sialic acid-bearing gangliosides), whereas the monoclonal antibody bound to the NMJ (R. McGonigal, unpublished data). However, the monoclonal antibody still required a GD3s<sup>-/-</sup> mouse which overexpress GM1, plus neuraminidase treatment in order to bind. Thus, although the serum did not show any ability to bind tissue, the monoclonal would not bind without membrane manipulation. Additionally, although patient serum is polyclonal, the concentration of the multiple antibodies is unknown and likely to be lower than the monoclonal antibody. To address this, another human monoclonal antibody will be used which can bind wildtype mouse membrane without membrane manipulation. This antibody is from a patient with Chronic Ataxic Neuropathy, Ophthalmoplegia, Monoclonal IgM protein, cold Agglutinins and Disialosyl antibodies (CANOMAD) and targets b-series gangliosides (Willison et al., 1996). The ability of these two antibodies to be cleared from the mouse circulation will be compared. This experiment is ongoing.

## **8.2.2 Future work**

### **8.2.2.1 Active immunisation model of GBS**

The results of this thesis offer a new outlook on antibody processing in autoimmune neuropathies. However, one of the initial goals I had aimed to achieve was to develop an active immunisation model of GBS using GalNAcT<sup>-/-</sup>-*Tg(neuronal)* and GalNAcT<sup>-/-</sup>-*Tg(glial)* mice. This was only partially completed as, though the immunised animals developed an antibody response, no injury was detectable upon transfer of exogenous complement. As part of the investigation into why this may have been the case, the phenomenon of antibody internalisation was explored. It is thought that the removal of pathogenic

antibody from the circulation by receptor-dependent uptake may have resulted in too low a level to cause injury. In order to develop a model whereby injury can be detectable following an immune response, further modifications to the immunisation protocol may be needed to a) induce a higher immune response and b) increase the likelihood of complement activation by injecting NHS at more than one timepoint. The knowledge that the motor nerve terminal is such a scavenger of anti-ganglioside antibody warrants that immunohistological evidence of antibody and complement deposition is likely to be difficult to find here and therefore looking for said evidence at nodes may prove more prudent.

#### **8.2.2.2 Investigation of antibody uptake at places other than the motor nerve terminal**

Wildtype mice clear anti-ganglioside antibody from their circulation more rapidly than  $\text{GalNAcT}^{-/-}\text{-Tg}(\text{neuronal})$  mice. The difference between the abilities of wildtype and  $\text{GalNAcT}^{-/-}\text{-Tg}(\text{neuronal})$  mice to clear anti-ganglioside antibody is therefore likely due to the expression of ganglioside on non-neuronal cells contributing to the receptor-dependant uptake of said antibody. The use of fluorescent ganglioside analogues, ganglioside-binding toxins and antibodies targeting gangliosides have all been used to study the internalisation of gangliosides in cells (Crespo et al., 2008; Singh et al., 2003; Fewou et al., 2012). These studies have suggested that the gangliosides are internalised by clathrin-independent endocytosis, mainly by caveolae. It is therefore hypothesised that the clearance of antibodies in wildtype mice is mostly due to caveolae-mediated endocytosis at non-neuronal sites. To investigate this hypothesis we will employ the use of caveolin 1<sup>-/-</sup> mice which lack any caveolae (Razani et al., 2001). In collaboration with the lab of Dr Ben Nichols, these mice will be used as part of a clearance study using the same protocol as detailed in this thesis. Previously, the internalisation of gangliosides has been shown to be impaired in cells which lack caveolin 1 (Iglesias-Bartolome et al., 2009). Therefore, it is expected that, if antibodies are indeed being cleared mainly by caveolae in non-neuronal cells, the rate of clearance will not be as rapid in caveolin 1<sup>-/-</sup> mice as in wildtype mice.

### 8.2.2.3 Retrograde transport and trans-synaptic spread of antibody

The potential that antibody can be retrogradely transported and spread trans-synaptically to nearby neurons is one of the most interesting possibilities to explore in the future. In this thesis, the weak presence of anti-GD1b antibody MOG1 was shown outwith the neuron in  $\text{GalNAcT}^{-/-}\text{-Tg}(\text{neuronal})$  mice 7 days after an i.p. injection of 250  $\mu\text{g}$ . At the earlier timepoint of 1 day (following a larger, 1 mg dose of antibody), antibody was shown within the motor neuron. The anti-GM1 antibody DG2 was, however, not found distinctly in the neurons either at 1 day or 7 days post injection of 2 mg antibody. Due to issues with tissue staining at the time, it would be of importance to repeat this study, this time using the same protocol as with MOG1, to absolutely rule out DG2 being trafficked to the spinal cord. On a similar note, repeating the inhibition of DG2 breakdown using  $\text{NH}_4\text{Cl}$  (assuming similar results are obtained) would justify the absence of DG2 in the cord. It would also be of interest to use the more precise method of intramuscular injections for both MOG1 and DG2. This will result in a larger amount of antibody being taken up by one particular muscle, thus increasing the likelihood of finding a substantial amount in a particular spinal nucleus. Future investigations would require further evidence showing the location of antibody presence at different timepoints following the initial arrival in the spinal cord. Behavioural tests could also be employed to determine whether the antibody presence is having any central nervous system effects such as is seen in some cases of AMAN and BBE. As an immune-mediated attack on the brainstem has been implicated in BBE (Shahrizaila and Yuki, 2013), staining for complement activation and infiltration of immune cells would also be useful, to see if the antibodies are having similar pathogenic effects in the CNS as in the PNS.

### 8.2.2.4 Can exercise increase the clearance of antibody from the circulation?

With the new finding that motor nerve terminal activity can increase the speed of antibody uptake in wildtype *ex vivo* muscle nerve preparations, it would be of interest to determine the effect of stimulation in  $\text{GalNAcT}^{-/-}$ ,  $\text{GalNAcT}^{-/-}\text{-Tg}(\text{neuronal})$  and  $\text{GalNAcT}^{-/-}\text{-Tg}(\text{glial})$  mice. It would be expected that, like in wildtype mice, stimulation of the nerve terminal in  $\text{GalNAcT}^{-/-}\text{-Tg}(\text{neuronal})$  mice would also result in activity-dependent uptake. This is because the target

ganglioside is only expressed in the neurons of these mice and it is the specialised vesicular cycling in the nerve terminal which results in the effect. However, as  $\text{GalNAcT}^{-/-}$  and  $\text{GalNAcT}^{-/-}\text{-Tg}(glial)$  mice do not bind antibody on their neuronal membranes, there would be no effect expected. Nevertheless, the  $\text{GalNAcT}^{-/-}\text{-Tg}(glial)$  mice may show some increase in uptake in response to stimulation due to the pSC's ability to sense nerve terminal activity and their own ability to release neurotransmitter (Jahromi et al., 1992; Robitaille et al., 1997; Rochon et al., 2001).

Forced exercise paradigms, such as treadmill running, are widely used to study the benefits of exercise. Therefore, to determine whether the activity-dependent uptake of antibody is relevant *in vivo*, this type of experiment would be ideal for measuring the clearance over time in exercise and non-exercised animal groups. For this type of study it would be more prudent to use  $\text{GalNAcT}^{-/-}\text{-Tg}(neuronal)$  mice (if, as mentioned, *ex vivo* studies show the same effect as in wildtype mice) for two reasons: firstly, wildtype mice clear the antibody so quickly anyway that no difference would be able to be seen at the current dose of antibody. Secondly, using  $\text{GalNAcT}^{-/-}\text{-Tg}(neuronal)$  mice we will be able to ensure that the clearance seen is almost solely due to the nerve terminal uptake.

### 8.3 Concluding remarks

In the end, this thesis has investigated the regulation of anti-ganglioside antibodies by receptor-dependent internalisation, and how this can affect the circulating antibodies in the serum of mice. Expanding on work which previously demonstrated anti-ganglioside antibody's ability to bind and be internalised in both cell culture experiments and at the mouse motor nerve terminal (Fewou et al., 2012), this thesis has demonstrated *ex vivo* that both neuronal and glial membranes have the ability to clear the antibody, though the fate of antibody following uptake into the pSCs is still unclear. The effect of this internalisation has also now been demonstrated *in vivo*, with a clear, rapid internalisation which is dependent on the presence of target, and can result in the retrograde transport of antibody to the spinal cord. Additionally, it has been shown that while pathogenic anti-ganglioside antibodies can be cleared from the circulation

by this receptor-dependent mechanism, non-pathogenic anti-ganglioside antibodies are left to circulate for longer. A summary of this hypothesised regulation of anti-ganglioside antibody by endocytosis is displayed in Figure 8.2 on the following page. These are novel observations in the context of GBS, the true effects of which are yet to be fully explored.

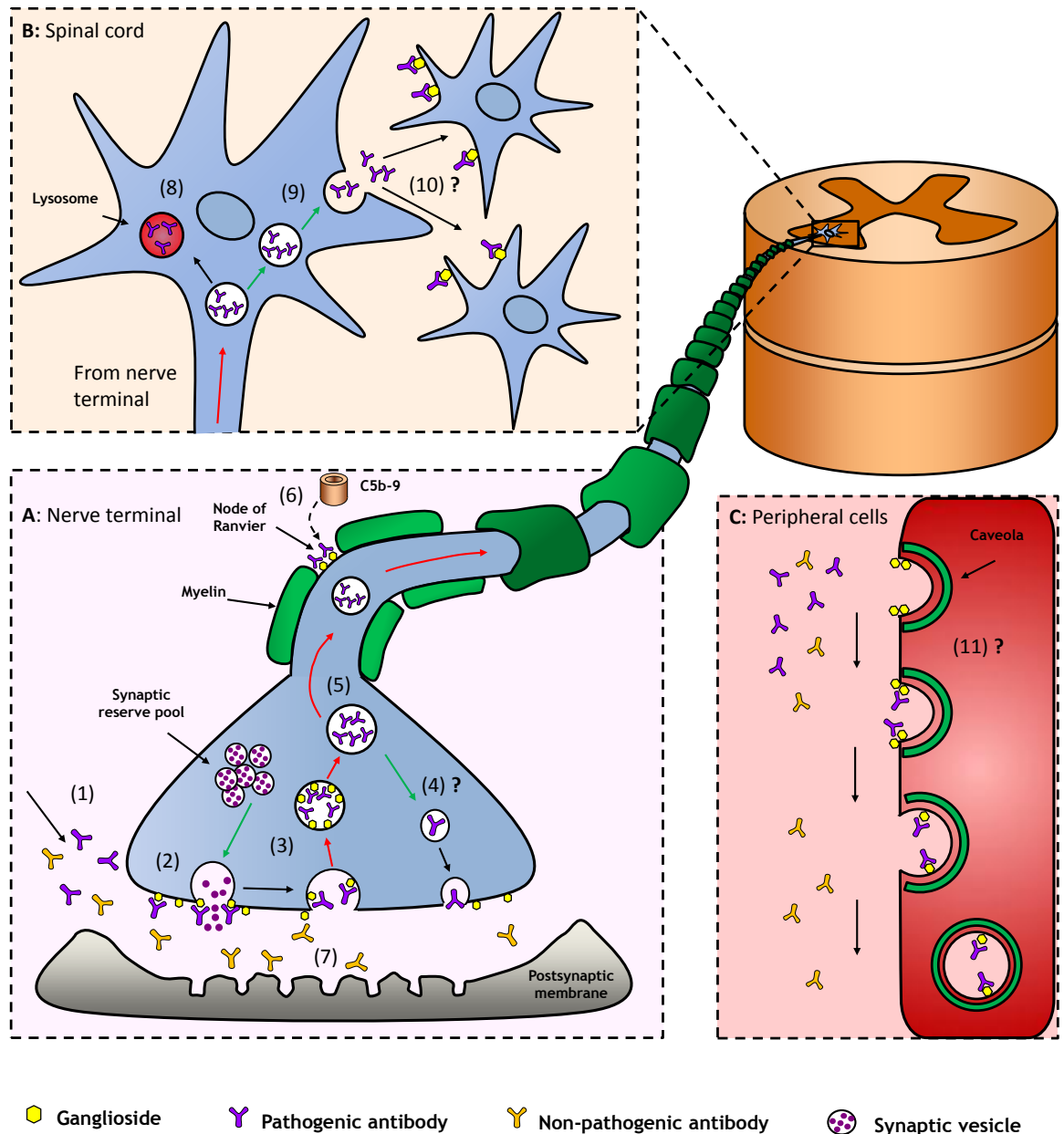


**Figure 8.2: Schematic representation of the hypothesis of anti-ganglioside antibody internalisation.** **A:** Pathogenic and non-pathogenic antibodies arrive at the nerve terminal from the circulation (1). Vesicles containing ACh fuse with the membrane (2), where pathogenic antibody has bound to gangliosides. During vesicle retrieval, gangliosides and their attached antibodies are taken into the cell (3). Antibodies may be returned to the surface at this point (4), or can undergo retrograde transport up the axon to the motor neuron in the spinal cord (5). Pathogenic anti-ganglioside antibody which binds at the node of Ranvier cannot be internalised here and instead activates complement resulting in C5b-9 (MAC) deposition (6). Meanwhile, non-pathogenic antibody cannot bind ganglioside at the nerve terminal and therefore is not internalised (7). **B:** Retrogradely transported antibody now present in ventral horn motor neurons may be degraded in lysosomes (8), or recycled to the neuron surface (9) where it may be free to bind to adjacent neurons and cause pathogenic effects (10). **C:** Elsewhere in the body, circulating pathogenic antibody may bind to its target ganglioside in the membrane of non-neuronal cells, particularly vascular endothelial cells which are rich in caveolae. Once bound, antibodies may be endocytosed via the caveolae and thus cleared from the circulation (11). Exocytic pathways are shown by green arrows while endocytic pathways are shown by red arrows.

## List of Publications

### Papers

Yao D, McGonigal R, Barrie JA, Cappell J, Cunningham ME, Meehan GR, Fewou SN, Edgar JM, Rowan E, Ohmi Y, Furukawa K, Furukawa K, Brophy PJ, Willison HJ (2014) Neuronal Expression of GalNAc Transferase Is Sufficient to Prevent the Age-Related Neurodegenerative Phenotype of Complex Ganglioside-Deficient Mice. *J Neurosci* 34:880-891.

### Abstracts

Madeleine E. Cunningham, Rhona McGonigal, Claire Paton, Gavin R. Meehan, Jennifer Barrie, Hugh J. Willison (2014). *Clearance of anti-ganglioside antibodies by endocytosis is a major attenuator of their pathological effects*. Updates in neuroscience: Peripheral Nervous System (PNS) in development and disease. July 1-4 2014,

Madeleine E. Cunningham, Gavin R. Meehan, Paul Edmondson, Jennifer Barrie, Rhona McGonigal, Hugh Willison (2013). *Neuronal uptake of circulating antiganglioside antibodies from motor nerve terminals*. PNS Biennial meeting, Saint Malo, June 29-July 3, 2013. *J.PNS* 18:S1-S131.

Madeleine E. Cunningham, Angie Rupp, Denggao Yao, Hugh J. Willison (2012). *The role of gangliosides in motor nerve terminal regeneration: a fluorescence imaging study in mice*. PNS/INC congress, Rotterdam, June 24-27, 2012,

## References

- Albers JW, Donofrio PD, McGonagle TK (1985) Sequential electrodiagnostic abnormalities in acute inflammatory demyelinating polyradiculoneuropathy. *Muscle Nerve* 8:528-539.
- Allen Institute for Brain Science (2014) BrainSpan reference atlas. [online] Available from atlas.brainmap.org [Accessed Jan'15]
- Allen JA, Halverson-Tamboli RA, Rasenick MM (2007) Lipid raft microdomains and neurotransmitter signalling. *Nat Rev Neurosci* 8:128-140.
- Alving CR, Rao M, Steers NJ, Matyas GR, Mayorov AV (2012) Liposomes containing lipid A: an effective, safe, generic adjuvant system for synthetic vaccines. *Expert Rev Vaccines* 11:733-744.
- Ambache N (1948) Peripheral action of botulinum toxin. *Nature* 161:482.
- Ambache N, Morgan RS, Wright GP (1948) The action of tetanus toxin on the acetylcholine and cholinesterase contents of the rabbit's iris. *Br J Exp Pathol* 29:408-418.
- Ang CW, Jacobs BC, Laman JD (2004) The Guillain-Barre syndrome: a true case of molecular mimicry. *Trends Immunol* 25:61-66.
- Angelucci A, Clasca F, Sur M (1996) Anterograde axonal tracing with the subunit B of cholera toxin: a highly sensitive immunohistochemical protocol for revealing fine axonal morphology in adult and neonatal brains. *J Neurosci Methods* 65:101-112.
- Asbury AK (1978) Criteria for diagnosis of Guillain-Barre syndrome. *Ann Neurol* 3:565-566.
- Asbury AK, Cornblath DR (1990) Assessment of current diagnostic criteria for Guillain-Barre syndrome. *Ann Neurol* 27 Suppl:S21-S24.
- Asbury AK, McKhann GM (1997) Changing views of Guillain-Barre syndrome. *Ann Neurol* 41:287-288.
- Aspinall GO, Fujimoto S, McDonald AG, Pang H, Kurjanczyk LA, Penner JL (1994) Lipopolysaccharides from *Campylobacter jejuni* associated with Guillain-Barre syndrome patients mimic human gangliosides in structure. *Infect Immun* 62:2122-2125.
- Astrow SH, Son YJ, Thompson WJ (1994a) Differential neural regulation of a neuromuscular junction-associated antigen in muscle fibers and Schwann cells. *J Neurobiol* 25:937-952.

Astrow SH, Son YJ, Thompson WJ (1994b) Differential neural regulation of a neuromuscular junction-associated antigen in muscle fibers and Schwann cells. *J Neurobiol* 25:937-952.

Auld DS, Robitaille R (2003) Perisynaptic Schwann cells at the neuromuscular junction: nerve- and activity-dependent contributions to synaptic efficacy, plasticity, and reinnervation. *Neuroscientist* 9:144-157.

Austin JH (1958) Recurrent polyneuropathies and their corticosteroid treatment; with five-year observations of a placebo-controlled case treated with corticotrophin, cortisone, and prednisone. *Brain* 81:157-192.

Baalasubramanian S, Harris CL, Donev RM, Mizuno M, Omidvar N, Song WC, Morgan BP (2004) CD59a is the primary regulator of membrane attack complex assembly in the mouse. *J Immunol* 173:3684-3692.

Baheti NN, Manuel D, Shinde PD, Radhakrishnan A, Nair M (2010) Hyperreflexic Guillain-Barre syndrome. *Ann Indian Acad Neurol* 13:305-307.

Bassile CC (1996) Guillain-Barre Syndrome and Exercise Guidelines. *Journal of Neurologic Physical Therapy* 20.

Bastiani M, Liu L, Hill MM, Jedrychowski MP, Nixon SJ, Lo HP, Abankwa D, Luetterforst R, Fernandez-Rojo M, Breen MR, Gygi SP, Vinten J, Walser PJ, North KN, Hancock JF, Pilch PF, Parton RG (2009) MURC/Cavin-4 and cavin family members form tissue-specific caveolar complexes. *J Cell Biol* 185:1259-1273.

Bauder AR, Ferguson TA (2012) Reproducible mouse sciatic nerve crush and subsequent assessment of regeneration by whole mount muscle analysis. *J Vis Exp*.

Bax M, Kuijff ML, Heikema AP, Van RW, Bruijns SC, Garcia-Vallejo JJ, Crocker PR, Jacobs BC, van Vliet SJ, van KY (2011) *Campylobacter jejuni* lipooligosaccharides modulate dendritic cell-mediated T cell polarization in a sialic acid linkage-dependent manner. *Infect Immun* 79:2681-2689.

Berryman ER, Harris RL, Moalli M, Bagi CM (2009) Digigait quantitation of gait dynamics in rat rheumatoid arthritis model. *J Musculoskelet Neuronal Interact* 9:89-98.

Bersano A, Carpo M, Allaria S, Franciotta D, Citterio A, Nobile-Orazio E (2006) Long term disability and social status change after Guillain-Barre syndrome. *J Neurol* 253:214-218.

Black JD, Dolly JO (1986) Interaction of 125I-labeled botulinum neurotoxins with nerve terminals. II. Autoradiographic evidence for its uptake into motor nerves by acceptor-mediated endocytosis. *J Cell Biol* 103:535-544.

Bordet J (1898) Sur l'agglutination et la dissolution des globules rouge par le sérum d'animaux injecties de sang defibiné. *Annales de l'Institut Pasteur* 12:688.

Bowes T, Wagner ER, Boffey J, Nicholl D, Cochrane L, Benboubetra M, Conner J, Furukawa K, Furukawa K, Willison HJ (2002) Tolerance to self gangliosides is the major factor restricting the antibody response to lipopolysaccharide core

oligosaccharides in *Campylobacter jejuni* strains associated with Guillain-Barre syndrome. *Infect Immun* 70:5008-5018.

Brosnan JV, Craggs RI, King RH, Thomas PK (1987) Reduced susceptibility of T cell-deficient rats to induction of experimental allergic neuritis. *J Neuroimmunol* 14:267-282.

Bu J, Bruckner SR, Sengoku T, Geddes JW, Estus S (2003) Glutamate regulates caveolin expression in rat hippocampal neurons. *J Neurosci Res* 72:185-190.

Buchner H (1889) Über die nahere Natur der bakterientodtenden Substanz in Blutserum. *Zentralblatt Fur Bakteriologie* 6:561.

Bussmann JB, Garssen MP, van Doorn PA, Stam HJ (2007) Analysing the favourable effects of physical exercise: relationships between physical fitness, fatigue and functioning in Guillain-Barre syndrome and chronic inflammatory demyelinating polyneuropathy. *J Rehabil Med* 39:121-125.

Calik MW, Shankarappa SA, Stubbs EB, Jr. (2012) Forced-exercise attenuates experimental autoimmune neuritis. *Neurochem Int* 61:141-145.

Chiavegatto S, Sun J, Nelson RJ, Schnaar RL (2000) A functional role for complex gangliosides: motor deficits in GM2/GD2 synthase knockout mice. *Exp Neurol* 166:227-234.

Chiba A, Kusunoki S, Obata H, Machinami R, Kanazawa I (1993) Serum anti-GQ1b IgG antibody is associated with ophthalmoplegia in Miller Fisher syndrome and Guillain-Barre syndrome: clinical and immunohistochemical studies. *Neurology* 43:1911-1917.

Chiba A, Kusunoki S, Obata H, Machinami R, Kanazawa I (1997) Ganglioside composition of the human cranial nerves, with special reference to pathophysiology of Miller Fisher syndrome. *Brain Res* 745:32-36.

Chiba A, Kusunoki S, Shimizu T, Kanazawa I (1992) Serum IgG antibody to ganglioside GQ1b is a possible marker of Miller Fisher syndrome. *Ann Neurol* 31:677-679.

Chigorno V, Riva C, Valsecchi M, Nicolini M, Brocca P, Sonnino S (1997) Metabolic processing of gangliosides by human fibroblasts in culture--formation and recycling of separate pools of sphingosine. *Eur J Biochem* 250:661-669.

Cho JH, Kim JS, Lim MU, Min HK, Kwak DH, Ryu JS, Lee JT, Kim SU, Kim CH, Kim CH, Koo DB, Chang KT, Choo YK (2012) Human leukocytes regulate ganglioside expression in cultured micro-pig aortic endothelial cells. *Lab Anim Res* 28:255-263.

Christiansen D, Vaughan HA, Milland J, Dodge N, Mouhtouris E, Smyth MJ, Godfrey DI, Sandrin MS (2011) Antibody responses to glycolipid-borne carbohydrates require CD4+ T cells but not CD1 or NKT cells. *Immunol Cell Biol* 89:502-510.

Cobb BA, Wang Q, Tzianabos AO, Kasper DL (2004) Polysaccharide processing and presentation by the MHCII pathway. *Cell* 117:677-687.

- Connor EA, McMahan UJ (1987) Cell accumulation in the junctional region of denervated muscle. *J Cell Biol* 104:109-120.
- Court F, Gillingwater TH, Melrose S, Sherman DL, Greenshields KN, Morton AJ, Harris JB, Willison HJ, Ribchester RR (2008) Identity, developmental restriction and reactivity of extralaminar cells capping mammalian neuromuscular junctions. *J Cell Sci* 121:3901-3911.
- Crespo PM, von MN, Iglesias-Bartolome R, Daniotti JL (2008) Complex gangliosides are apically sorted in polarized MDCK cells and internalized by clathrin-independent endocytosis. *FEBS J* 275:6043-6056.
- Dale HH, Feldberg W, Vogt M (1936) Release of acetylcholine at voluntary motor nerve endings. *J Physiol* 86:353-380.
- Daniotti JL, Iglesias-Bartolome R (2011) Metabolic pathways and intracellular trafficking of gangliosides. *IUBMB Life* 63:513-520.
- Deinhardt K, Berninghausen O, Willison HJ, Hopkins CR, Schiavo G (2006) Tetanus toxin is internalized by a sequential clathrin-dependent mechanism initiated within lipid microdomains and independent of epsin1. *J Cell Biol* 174:459-471.
- Dong M, Richards DA, Goodnough MC, Tepp WH, Johnson EA, Chapman ER (2003) Synaptotagmins I and II mediate entry of botulinum neurotoxin B into cells. *J Cell Biol* 162:1293-1303.
- Eldar AH, Chapman J (2014) Guillain Barre syndrome and other immune mediated neuropathies: diagnosis and classification. *Autoimmun Rev* 13:525-530.
- Fabian RH (1988) Uptake of plasma IgG by CNS motoneurons: comparison of antineuronal and normal IgG. *Neurology* 38:1775-1780.
- Fabian RH (1990) Uptake of antineuronal IgM by CNS neurons: comparison with antineuronal IgG. *Neurology* 40:419-422.
- Fabian RH (1991) Retrograde axonal transport and transcytosis of immunoglobulins: implications for the pathogenesis of autoimmune motor neuron disease. *Adv Neurol* 56:433-444.
- Fabian RH, Petroff G (1987) Intraneuronal IgG in the central nervous system: uptake by retrograde axonal transport. *Neurology* 37:1780-1784.
- Fabian RH, Ritchie TC (1986) Intraneuronal IgG in the central nervous system. *J Neurol Sci* 73:257-267.
- Fabrizi C, Kelly BM, Gillespie CS, Schlaepfer WW, Scherer SS, Brophy PJ (1997) Transient expression of the neurofilament proteins NF-L and NF-M by Schwann cells is regulated by axonal contact. *J Neurosci Res* 50:291-299.
- Fagerlund MJ, Eriksson LI (2009) Current concepts in neuromuscular transmission. *Br J Anaesth* 103:108-114.

- Feng G, Mellor RH, Bernstein M, Keller-Peck C, Nguyen QT, Wallace M, Nerbonne JM, Lichtman JW, Sanes JR (2000) Imaging neuronal subsets in transgenic mice expressing multiple spectral variants of GFP. *Neuron* 28:41-51.
- Ferreira VP, Pangburn MK, Cortes C (2010) Complement control protein factor H: the good, the bad, and the inadequate. *Mol Immunol* 47:2187-2197.
- Fewou SN, Plomp JJ, Willison HJ (2014) The pre-synaptic motor nerve terminal as a site for antibody-mediated neurotoxicity in autoimmune neuropathies and synaptopathies. *J Anat* 224:36-44.
- Fewou SN, Rupp A, Nickolay LE, Carrick K, Greenshields KN, Pediani J, Plomp JJ, Willison HJ (2012) Anti-ganglioside antibody internalization attenuates motor nerve terminal injury in a mouse model of acute motor axonal neuropathy. *J Clin Invest* 122:1037-1051.
- Fisher M (1956) An unusual variant of acute idiopathic polyneuritis (syndrome of ophthalmoplegia, ataxia and areflexia). *N Engl J Med* 255:57-65.
- Fisher TB, Stevens JE (2008) Rehabilitation of a marathon runner with Guillain-Barre syndrome. *J Neurol Phys Ther* 32:203-209.
- Frank PG, Woodman SE, Park DS, Lisanti MP (2003) Caveolin, caveolae, and endothelial cell function. *Arterioscler Thromb Vasc Biol* 23:1161-1168.
- Fujimoto S, Yuki N, Itoh T, Amako K (1992) Specific serotype of *Campylobacter jejuni* associated with Guillain-Barre syndrome. *J Infect Dis* 165:183.
- Galban-Horcajo F, Fitzpatrick AM, Hutton AJ, Dunn SM, Kalna G, Brennan KM, Rinaldi S, Yu RK, Goodyear CS, Willison HJ (2012) Antibodies to heteromeric glycolipid complexes in multifocal motor neuropathy. *Eur J Neurol*.
- Galli G, Nuti S, Tavarini S, Galli-Stampino L, De LC, Casorati G, Dellabona P, Abrignani S (2003) CD1d-restricted help to B cells by human invariant natural killer T lymphocytes. *J Exp Med* 197:1051-1057.
- Gansel M, Penner R, Dreyer F (1987) Distinct sites of action of clostridial neurotoxins revealed by double-poisoning of mouse motor nerve terminals. *Pflugers Arch* 409:533-539.
- Ganser AL, Kirschner DA, Willinger M (1983) Ganglioside localization on myelinated nerve fibres by cholera toxin binding. *J Neurocytol* 12:921-938.
- Garcia-Rill E (1997) Disorders of the reticular activating system. *Med Hypotheses* 49:379-387.
- Gatchalian CL, Schachner M, Sanes JR (1989) Fibroblasts that proliferate near denervated synaptic sites in skeletal muscle synthesize the adhesive molecules tenascin(J1), N-CAM, fibronectin, and a heparan sulfate proteoglycan. *J Cell Biol* 108:1873-1890.
- Geleijns K, Jacobs BC, Van RW, Tio-Gillen AP, Laman JD, van Doorn PA (2004) Functional polymorphisms in LPS receptors CD14 and TLR4 are not associated

with disease susceptibility or *Campylobacter jejuni* infection in Guillain-Barre patients. *J Neuroimmunol* 150:132-138.

Gong Y, Tagawa Y, Lunn MP, Laroy W, Heffer-Lauc M, Li CY, Griffin JW, Schnaar RL, Sheikh KA (2002) Localization of major gangliosides in the PNS: implications for immune neuropathies. *Brain* 125:2491-2506.

Goodfellow JA, Bowes T, Sheikh K, Odaka M, Halstead SK, Humphreys PD, Wagner ER, Yuki N, Furukawa K, Furukawa K, Plomp JJ, Willison HJ (2005) Overexpression of GD1a ganglioside sensitizes motor nerve terminals to anti-GD1a antibody-mediated injury in a model of acute motor axonal neuropathy. *J Neurosci* 25:1620-1628.

Goodyear CS, O'Hanlon GM, Plomp JJ, Wagner ER, Morrison I, Veitch J, Cochrane L, Bullens RW, Molenaar PC, Conner J, Willison HJ (1999) Monoclonal antibodies raised against Guillain-Barre syndrome-associated *Campylobacter jejuni* lipopolysaccharides react with neuronal gangliosides and paralyze muscle-nerve preparations. *J Clin Invest* 104:697-708.

Granseth B, Odermatt B, Royle SJ, Lagnado L (2007) Clathrin-mediated endocytosis: the physiological mechanism of vesicle retrieval at hippocampal synapses. *J Physiol* 585:681-686.

Greenshields KN, Halstead SK, Zitman FM, Rinaldi S, Brennan KM, O'Leary C, Chamberlain LH, Easton A, Roxburgh J, Padiani J, Furukawa K, Furukawa K, Goodyear CS, Plomp JJ, Willison HJ (2009) The neuropathic potential of anti-GM1 autoantibodies is regulated by the local glycolipid environment in mice. *J Clin Invest* 119:595-610.

Greer JJ, Allan DW, Martin-Caraballo M, Lemke RP (1999) An overview of phrenic nerve and diaphragm muscle development in the perinatal rat. *J Appl Physiol* (1985 ) 86:779-786.

Gregson NA, Johnson AR, Wheeler DF, Voaden MJ (1989) Immunolocalization of the gangliosides GM1 and GD3 in cultured explants and sections of the rat retina. *Biochem Soc Trans* 17:222-223.

Griffin JW, Li CY, Macko C, Ho TW, Hsieh ST, Xue P, Wang FA, Cornblath DR, McKhann GM, Asbury AK (1996) Early nodal changes in the acute motor axonal neuropathy pattern of the Guillain-Barre syndrome. *J Neurocytol* 25:33-51.

Guillain G, Barre JA, Strohl A (1916) Sur un syndrome de radiculonévrite avec hyperalbuminose du liquide cephalorachidien sans réaction cellulaire. Remarques sur les caracteres cliniques et graphiques des reflexes tendineux. *Bull Soc Med Hop Paris* 40:1462-1470.

Gustavsson J, Parpal S, Karlsson M, Ramsing C, Thorn H, Borg M, Lindroth M, Peterson KH, Magnusson KE, Stralfors P (1999) Localization of the insulin receptor in caveolae of adipocyte plasma membrane. *FASEB J* 13:1961-1971.

Hadden RD, Cornblath DR, Hughes RA, Zielasek J, Hartung HP, Toyka KV, Swan AV (1998) Electrophysiological classification of Guillain-Barre syndrome: clinical

associations and outcome. Plasma Exchange/Sandoglobulin Guillain-Barre Syndrome Trial Group. *Ann Neurol* 44:780-788.

Hafer-Macko C, Hsieh ST, Li CY, Ho TW, Sheikh K, Cornblath DR, McKhann GM, Asbury AK, Griffin JW (1996a) Acute motor axonal neuropathy: an antibody-mediated attack on axolemma. *Ann Neurol* 40:635-644.

Hafer-Macko CE, Sheikh KA, Li CY, Ho TW, Cornblath DR, McKhann GM, Asbury AK, Griffin JW (1996b) Immune attack on the Schwann cell surface in acute inflammatory demyelinating polyneuropathy. *Ann Neurol* 39:625-635.

Halstead SK, Humphreys PD, Goodfellow JA, Wagner ER, Smith RA, Willison HJ (2005a) Complement inhibition abrogates nerve terminal injury in Miller Fisher syndrome. *Ann Neurol* 58:203-210.

Halstead SK, Morrison I, O'Hanlon GM, Humphreys PD, Goodfellow JA, Plomp JJ, Willison HJ (2005b) Anti-disialosyl antibodies mediate selective neuronal or Schwann cell injury at mouse neuromuscular junctions. *Glia* 52:177-189.

Halstead SK, O'Hanlon GM, Humphreys PD, Morrison DB, Morgan BP, Todd AJ, Plomp JJ, Willison HJ (2004) Anti-disialoside antibodies kill perisynaptic Schwann cells and damage motor nerve terminals via membrane attack complex in a murine model of neuropathy. *Brain* 127:2109-2123.

Halstead SK, Zitman FM, Humphreys PD, Greenshields K, Verschuuren JJ, Jacobs BC, Rother RP, Plomp JJ, Willison HJ (2008) Eculizumab prevents anti-ganglioside antibody-mediated neuropathy in a murine model. *Brain* 131:1197-1208.

Hansson HA, Holmgren J, Svennerholm L (1977) Ultrastructural localization of cell membrane GM1 ganglioside by cholera toxin. *Proc Natl Acad Sci U S A* 74:3782-3786.

Hausman SZ, Burns DL (1993) Binding of pertussis toxin to lipid vesicles containing glycolipids. *Infect Immun* 61:335-337.

Hayer A, Stoeber M, Ritz D, Engel S, Meyer HH, Helenius A (2010) Caveolin-1 is ubiquitinated and targeted to intraluminal vesicles in endolysosomes for degradation. *J Cell Biol* 191:615-629.

Haynes LW, Schmitz S, Clegg JC, Fooks AR (1999) Expression of neurofilament L-promoter green-fluorescent protein constructs in immortalized Schwann cell-neuron coculture. *Neurosci Lett* 271:155-158.

Hill MM, Bastiani M, Luetterforst R, Kirkham M, Kirkham A, Nixon SJ, Walser P, Abankwa D, Oorschot VM, Martin S, Hancock JF, Parton RG (2008) PTRF-Cavin, a conserved cytoplasmic protein required for caveola formation and function. *Cell* 132:113-124.

Hiraga A, Mori M, Ogawara K, Kojima S, Kanesaka T, Misawa S, Hattori T, Kuwabara S (2005) Recovery patterns and long term prognosis for axonal Guillain-Barre syndrome. *J Neurol Neurosurg Psychiatry* 76:719-722.

Ho TW, Hsieh ST, Nachamkin I, Willison HJ, Sheikh K, Kiehlbauch J, Flanigan K, McArthur JC, Cornblath DR, McKhann GM, Griffin JW (1997) Motor nerve terminal degeneration provides a potential mechanism for rapid recovery in acute motor axonal neuropathy after *Campylobacter* infection. *Neurology* 48:717-724.

Ho TW, Mishu B, Li CY, Gao CY, Cornblath DR, Griffin JW, Asbury AK, Blaser MJ, McKhann GM (1995) Guillain-Barre syndrome in northern China. Relationship to *Campylobacter jejuni* infection and anti-glycolipid antibodies. *Brain* 118 ( Pt 3):597-605.

Ho TW, Willison HJ, Nachamkin I, Li CY, Veitch J, Ung H, Wang GR, Liu RC, Cornblath DR, Asbury AK, Griffin JW, McKhann GM (1999) Anti-GD1a antibody is associated with axonal but not demyelinating forms of Guillain-Barre syndrome. *Ann Neurol* 45:168-173.

Holmgren J, Lonroth I, Mansson J, Svennerholm L (1975) Interaction of cholera toxin and membrane GM1 ganglioside of small intestine. *Proc Natl Acad Sci U S A* 72:2520-2524.

Holthofer H, Reivinen J, Miettinen A (1994) Nephron segment and cell-type specific expression of gangliosides in the developing and adult kidney. *Kidney Int* 45:123-130.

Holtzman E, Novikoff AB (1965) Lysosomes in the rat sciatic nerve following crush. *J Cell Biol* 27:651-669.

Horisberger M, Fortuna R, Valderrabano V, Herzog W (2013) Long-term repetitive mechanical loading of the knee joint by in vivo muscle stimulation accelerates cartilage degeneration and increases chondrocyte death in a rabbit model. *Clin Biomech (Bristol , Avon)* 28:536-543.

Hughes R, Whaler BC (1962) Influence of nerve-ending activity and of drugs on the rate of paralysis of rat diaphragm preparations by *Cl. botulinum* type A toxin. *J Physiol* 160:221-233.

Hughes RA (1990) Guillain-Barré syndrome. Springer-Verlag, Heidelberg (1990).

Hughes RA, Kadlubowski M, Gray IA, Leibowitz S (1981) Immune responses in experimental allergic neuritis. *J Neurol Neurosurg Psychiatry* 44:565-569.

Huizinga R, Van RW, Bajramovic JJ, Kuijf ML, Laman JD, Samsom JN, Jacobs BC (2013) Sialylation of *Campylobacter jejuni* endotoxin promotes dendritic cell-mediated B cell responses through CD14-dependent production of IFN-beta and TNF-alpha. *J Immunol* 191:5636-5645.

Ichikawa H, Kamiya Y, Susuki K, Suzuki M, Yuki N, Kawamura M (2002) Unilateral oculomotor nerve palsy associated with anti-GQ1b IgG antibody. *Neurology* 59:957-958.

Iglesias-Bartolome R, Crespo PM, Gomez GA, Daniotti JL (2006) The antibody to GD3 ganglioside, R24, is rapidly endocytosed and recycled to the plasma membrane via the endocytic recycling compartment. Inhibitory effect of brefeldin A and monensin. *FEBS J* 273:1744-1758.

- Iglesias-Bartolome R, Trenchi A, Comin R, Moyano AL, Nores GA, Daniotti JL (2009) Differential endocytic trafficking of neuropathy-associated antibodies to GM1 ganglioside and cholera toxin in epithelial and neural cells. *Biochim Biophys Acta* 1788:2526-2540.
- Ilyas AA, Li SC, Chou DK, Li YT, Jungalwala FB, Dalakas MC, Quarles RH (1988a) Gangliosides GM2, IV4GalNAcGM1b, and IV4GalNAcGC1a as antigens for monoclonal immunoglobulin M in neuropathy associated with gammopathy. *J Biol Chem* 263:4369-4373.
- Ilyas AA, Willison HJ, Dalakas MC, Whitaker JN, Quarles RH (1988b) Identification and characterization of gangliosides reacting with IgM paraproteins in three patients with neuropathy associated with biconal gammopathy. *J Neurochem* 51:851-858.
- Ilyas AA, Willison HJ, Quarles RH, Jungalwala FB, Cornblath DR, Trapp BD, Griffin DE, Griffin JW, McKhann GM (1988c) Serum antibodies to gangliosides in Guillain-Barre syndrome. *Ann Neurol* 23:440-447.
- Inoue K, Nelson RA, Jr. (1965) The isolation and characterization of a new component of hemolytic complement, C'3e. *J Immunol* 95:355-367.
- Islam Z, Jacobs BC, van BA, Mohammad QD, Islam MB, Herbrink P, Diorditsa S, Luby SP, Talukder KA, Endtz HP (2010) Axonal variant of Guillain-Barre syndrome associated with *Campylobacter* infection in Bangladesh. *Neurology* 74:581-587.
- Itoh M, Fukumoto S, Baba N, Kuga Y, Mizuno A, Furukawa K (1999) Prevention of the death of the rat axotomized hypoglossal nerve and promotion of its regeneration by bovine brain gangliosides. *Glycobiology* 9:1247-1252.
- IUPAC-IUB Commission on Biochemical Nomenclature (1977) The nomenclature of lipids. *Eur J Biochem* 79.
- Jacobs BC, Bullens RW, O'Hanlon GM, Ang CW, Willison HJ, Plomp JJ (2002) Detection and prevalence of alpha-latrotoxin-like effects of serum from patients with Guillain-Barre syndrome. *Muscle Nerve* 25:549-558.
- Jahromi BS, Robitaille R, Charlton MP (1992) Transmitter release increases intracellular calcium in perisynaptic Schwann cells in situ. *Neuron* 8:1069-1077.
- Ji YH, Fujita T, Hatsuse H, Takahashi A, Matsushita M, Kawakami M (1993) Activation of the C4 and C2 components of complement by a proteinase in serum bactericidal factor, Ra reactive factor. *J Immunol* 150:571-578.
- Jung J, Cai W, Jang SY, Shin YK, Suh DJ, Kim JK, Park HT (2011) Transient lysosomal activation is essential for p75 nerve growth factor receptor expression in myelinated Schwann cells during Wallerian degeneration. *Anat Cell Biol* 44:41-49.
- Jung J, Jo HW, Kwon H, Jeong NY (2014) ATP release through lysosomal exocytosis from peripheral nerves: the effect of lysosomal exocytosis on peripheral nerve degeneration and regeneration after nerve injury. *Biomed Res Int* 2014:936891.

- Kaida K, Kusunoki S, Kamakura K, Motoyoshi K, Kanazawa I (2000) Guillain-Barre syndrome with antibody to a ganglioside, N-acetylgalactosaminyl GD1a. *Brain* 123 ( Pt 1):116-124.
- Kaida K, Morita D, Kanzaki M, Kamakura K, Motoyoshi K, Hirakawa M, Kusunoki S (2004) Ganglioside complexes as new target antigens in Guillain-Barre syndrome. *Ann Neurol* 56:567-571.
- Kaida K, Morita D, Kanzaki M, Kamakura K, Motoyoshi K, Hirakawa M, Kusunoki S (2007) Anti-ganglioside complex antibodies associated with severe disability in GBS. *J Neuroimmunol* 182:212-218.
- Kannagi R, Stroup R, Cochran NA, Urdal DL, Young WW, Hakomori Si (1983) Factors Affecting Expression of Glycolipid Tumor Antigens: Influence of Ceramide Composition and Coexisting Glycolipid on the Antigenicity of Ganglioside in Murine Lymphoma Cells. *Cancer Research* 43:4997-5005.
- Karnovsky MJ, Kleinfeld AM, Hoover RL, Klausner RD (1982) The concept of lipid domains in membranes. *J Cell Biol* 94:1-6.
- Kawai H, Allende ML, Wada R, Kono M, Sango K, Deng C, Miyakawa T, Crawley JN, Werth N, Bierfreund U, Sandhoff K, Proia RL (2001) Mice expressing only monosialoganglioside GM3 exhibit lethal audiogenic seizures. *J Biol Chem* 276:6885-6888.
- Kerschensteiner M, Reuter MS, Lichtman JW, Misgeld T (2008) Ex vivo imaging of motor axon dynamics in murine triangularis sterni explants. *Nat Protoc* 3:1645-1653.
- Kittaka D, Itoh M, Ohmi Y, Kondo Y, Fukumoto S, Urano T, Tajima O, Furukawa K, Furukawa K (2008) Impaired hypoglossal nerve regeneration in mutant mice lacking complex gangliosides: down-regulation of neurotrophic factors and receptors as possible mechanisms. *Glycobiology* 18:509-516.
- Klenk E (1935) Über die Natur der Phosphatide und anderer Lipide des Gehirns und der Leber bei der Niemann-Pick'schen Krankheit. *Zeitschrift für Physiologische Chemie* 235:24-25.
- Koirala S, Qiang H, Ko CP (2000) Reciprocal interactions between perisynaptic Schwann cells and regenerating nerve terminals at the frog neuromuscular junction. *J Neurobiol* 44:343-360.
- Koski CL, Sanders ME, Swoveland PT, Lawley TJ, Shin ML, Frank MM, Joiner KA (1987) Activation of terminal components of complement in patients with Guillain-Barre syndrome and other demyelinating neuropathies. *J Clin Invest* 80:1492-1497.
- Kuroki S, Saida T, Nukina M, Haruta T, Yoshioka M, Kobayashi Y, Nakanishi H (1993) *Campylobacter jejuni* strains from patients with Guillain-Barre syndrome belong mostly to Penner serogroup 19 and contain beta-N-acetylglucosamine residues. *Ann Neurol* 33:243-247.

- Kurzchalia TV, Dupree P, Parton RG, Kellner R, Virta H, Lehnert M, Simons K (1992) VIP21, a 21-kD membrane protein is an integral component of trans-Golgi-network-derived transport vesicles. *J Cell Biol* 118:1003-1014.
- Kusunoki S, Mashiko H, Mochizuki N, Chiba A, Arita M, Hitoshi S, Kanazawa I (1997) Binding of antibodies against GM1 and GD1b in human peripheral nerve. *Muscle Nerve* 20:840-845.
- Kusunoki S, Shimizu J, Chiba A, Ugawa Y, Hitoshi S, Kanazawa I (1996) Experimental sensory neuropathy induced by sensitization with ganglioside GD1b. *Ann Neurol* 39:424-431.
- Kuwabara S, Kokubun N, Misawa S, Kanai K, Iose S, Shibuya K, Noto Y, Mori M, Sekiguchi Y, Nasu S, Fujimaki Y, Hirata K, Yuki N (2011) Neuromuscular transmission is not impaired in axonal Guillain-Barre syndrome. *J Neurol Neurosurg Psychiatry* 82:1174-1177.
- Kuwabara S, Misawa S, Takahashi H, Sawai S, Kanai K, Nakata M, Mori M, Hattori T, Yuki N (2007) Anti-GQ1b antibody does not affect neuromuscular transmission in human limb muscle. *J Neuroimmunol* 189:158-162.
- Kuwabara S, Ogawara K, Koga M, Mori M, Hattori T, Yuki N (1999) Hyperreflexia in Guillain-Barre syndrome: relation with acute motor axonal neuropathy and anti-GM1 antibody. *J Neurol Neurosurg Psychiatry* 67:180-184.
- Kuwabara S, Yuki N, Koga M, Hattori T, Matsuura D, Miyake M, Noda M (1998) IgG anti-GM1 antibody is associated with reversible conduction failure and axonal degeneration in Guillain-Barre syndrome. *Ann Neurol* 44:202-208.
- Landry O (1859) Notesur la paralysie ascendante gigue. *Gazette Hebdomadaire* 6:472-474.
- Lehmann HC, Lopez PH, Zhang G, Ngyuen T, Zhang J, Kieseier BC, Mori S, Sheikh KA (2007) Passive immunization with anti-ganglioside antibodies directly inhibits axon regeneration in an animal model. *J Neurosci* 27:27-34.
- Leneman F (1966) The Guillain-Barre syndrome. Definition, etiology, and review of 1,100 cases. *Arch Intern Med* 118:139-144.
- Lewis RA, Sumner AJ, Brown MJ, Asbury AK (1982) Multifocal demyelinating neuropathy with persistent conduction block. *Neurology* 32:958-964.
- Lipardi C, Mora R, Colomer V, Paladino S, Nitsch L, Rodriguez-Boulan E, Zurzolo C (1998) Caveolin transfection results in caveolae formation but not apical sorting of glycosylphosphatidylinositol (GPI)-anchored proteins in epithelial cells. *J Cell Biol* 140:617-626.
- Liston A, Lesage S, Wilson J, Peltonen L, Goodnow CC (2003) Aire regulates negative selection of organ-specific T cells. *Nat Immunol* 4:350-354.
- Liu GF, Wu ZL, Wu HS, Wang QY, Zhao-Ri GT, Wang CY, Liang ZX, Cui SL, Zheng JD (2003) A case-control study on children with Guillain-Barre syndrome in North China. *Biomed Environ Sci* 16:105-111.

Liu S, Kandeve T, Tchervenkov J (2009) CD1d-mediated interaction between activated T cells and B cells is essential to B-cell proliferation and anti-alpha-Gal antibody production. *Transplant Proc* 41:398-402.

Lobo ED, Hansen RJ, Balthasar JP (2004) Antibody pharmacokinetics and pharmacodynamics. *J Pharm Sci* 93:2645-2668.

Lunn MP, Johnson LA, Fromholt SE, Itonori S, Huang J, Vyas AA, Hildreth JE, Griffin JW, Schnaar RL, Sheikh KA (2000) High-affinity anti-ganglioside IgG antibodies raised in complex ganglioside knockout mice: reexamination of GD1a immunolocalization. *J Neurochem* 75:404-412.

Magill CK, Tong A, Kawamura D, Hayashi A, Hunter DA, Parsadanian A, Mackinnon SE, Myckatyn TM (2007) Reinnervation of the tibialis anterior following sciatic nerve crush injury: a confocal microscopic study in transgenic mice. *Exp Neurol* 207:64-74.

McArdle JJ, Angaut-Petit D, Mallart A, Bournaud R, Faille L, Brigant JL (1981) Advantages of the triangularis sterni muscle of the mouse for investigations of synaptic phenomena. *J Neurosci Methods* 4:109-115.

McCarthy N, Giesecke J (2001) Incidence of Guillain-Barre syndrome following infection with *Campylobacter jejuni*. *Am J Epidemiol* 153:610-614.

McGonigal R, Rowan EG, Greenshields KN, Halstead SK, Humphreys PD, Rother RP, Furukawa K, Willison HJ (2010) Anti-GD1a antibodies activate complement and calpain to injure distal motor nodes of Ranvier in mice. *Brain* 133:1944-1960.

McGrogan A, Madle GC, Seaman HE, de Vries CS (2009) The epidemiology of Guillain-Barre syndrome worldwide. A systematic literature review. *Neuroepidemiology* 32:150-163.

McKhann GM, Cornblath DR, Griffin JW, Ho TW, Li CY, Jiang Z, Wu HS, Zhaori G, Liu Y, Jou LP, . (1993) Acute motor axonal neuropathy: a frequent cause of acute flaccid paralysis in China. *Ann Neurol* 33:333-342.

McKhann GM, Cornblath DR, Ho T, Li CY, Bai AY, Wu HS, Yei QF, Zhang WC, Zhaori Z, Jiang Z, . (1991) Clinical and electrophysiological aspects of acute paralytic disease of children and young adults in northern China. *Lancet* 338:593-597.

Miledi R, Slater CR (1970) On the degeneration of rat neuromuscular junctions after nerve section. *J Physiol* 207:507-528.

Mobbs RJ, Nair S, Blum P (2007) Peripheral nerve stimulation for the treatment of chronic pain. *J Clin Neurosci* 14:216-221.

Montesano R, Roth J, Robert A, Orci L (1982) Non-coated membrane invaginations are involved in binding and internalization of cholera and tetanus toxins. *Nature* 296:651-653.

- Montoyo HP, Vaccaro C, Hafner M, Ober RJ, Mueller W, Ward ES (2009) Conditional deletion of the MHC class I-related receptor FcRn reveals the sites of IgG homeostasis in mice. *Proc Natl Acad Sci U S A* 106:2788-2793.
- Mould DR, Sweeney KR (2007) The pharmacokinetics and pharmacodynamics of monoclonal antibodies--mechanistic modeling applied to drug development. *Curr Opin Drug Discov Devel* 10:84-96.
- Nachamkin I, et al. (2007) Patterns of Guillain-Barre syndrome in children: results from a Mexican population. *Neurology* 69:1665-1671.
- Ng JK, et al. (2012) Neurofascin as a target for autoantibodies in peripheral neuropathies. *Neurology* 79:2241-2248.
- Nicolson GL (1976) Transmembrane control of the receptors on normal and tumor cells. I. Cytoplasmic influence over surface components. *Biochim Biophys Acta* 457:57-108.
- Nishimura M (1986) Factors influencing an increase in spontaneous transmitter release by hypoxia at the mouse neuromuscular junction. *J Physiol* 372:303-313.
- Nodera H, Bostock H, Izumi Y, Nakamura K, Urushihara R, Sakamoto T, Murase N, Shimazu H, Kusunoki S, Kaji R (2006) Activity-dependent conduction block in multifocal motor neuropathy: magnetic fatigue test. *Neurology* 67:280-287.
- O'Hanlon GM, Humphreys PD, Goldman RS, Halstead SK, Bullens RW, Plomp JJ, Ushkaryov Y, Willison HJ (2003) Calpain inhibitors protect against axonal degeneration in a model of anti-ganglioside antibody-mediated motor nerve terminal injury. *Brain* 126:2497-2509.
- O'Hanlon GM, Paterson GJ, Wilson G, Doyle D, McHardie P, Willison HJ (1996) Anti-GM1 ganglioside antibodies cloned from autoimmune neuropathy patients show diverse binding patterns in the rodent nervous system. *J Neuropathol Exp Neurol* 55:184-195.
- Odaka M, Koga M, Yuki N, Susuki K, Hirata K (2003) Longitudinal changes of anti-ganglioside antibodies before and after Guillain-Barre syndrome onset subsequent to *Campylobacter jejuni* enteritis. *J Neurol Sci* 210:99-103.
- Ogawa-Goto K, Funamoto N, Abe T, Nagashima K (1990) Different ceramide compositions of gangliosides between human motor and sensory nerves. *J Neurochem* 55:1486-1493.
- Ogawara K, Kuwabara S, Mori M, Hattori T, Koga M, Yuki N (2000) Axonal Guillain-Barre syndrome: relation to anti-ganglioside antibodies and *Campylobacter jejuni* infection in Japan. *Ann Neurol* 48:624-631.
- Oh P, McIntosh DP, Schnitzer JE (1998) Dynamin at the neck of caveolae mediates their budding to form transport vesicles by GTP-driven fission from the plasma membrane of endothelium. *J Cell Biol* 141:101-114.
- Ohtsuka K, Nakamura Y, Hashimoto M, Tagawa Y, Takahashi M, Saito K, Yuki N (1998) Fisher syndrome associated with IgG anti-GQ1b antibody following

infection by a specific serotype of *Campylobacter jejuni*. *Ophthalmology* 105:1281-1285.

Okada M, Itoh MM, Haraguchi M, Okajima T, Inoue M, Oishi H, Matsuda Y, Iwamoto T, Kawano T, Fukumoto S, Miyazaki H, Furukawa K, Aizawa S, Furukawa K (2002) b-series Ganglioside deficiency exhibits no definite changes in the neurogenesis and the sensitivity to Fas-mediated apoptosis but impairs regeneration of the lesioned hypoglossal nerve. *J Biol Chem* 277:1633-1636.

Olive JM, Castillo C, Castro RG, de Quadros CA (1997) Epidemiologic study of Guillain-Barre syndrome in children <15 years of age in Latin America. *J Infect Dis* 175 Suppl 1:S160-S164.

Park DS, Woodman SE, Schubert W, Cohen AW, Frank PG, Chandra M, Shirani J, Razani B, Tang B, Jelicks LA, Factor SM, Weiss LM, Tanowitz HB, Lisanti MP (2002) Caveolin-1/3 double-knockout mice are viable, but lack both muscle and non-muscle caveolae, and develop a severe cardiomyopathic phenotype. *Am J Pathol* 160:2207-2217.

Pelkmans L, Kartenbeck J, Helenius A (2001) Caveolar endocytosis of simian virus 40 reveals a new two-step vesicular-transport pathway to the ER. *Nat Cell Biol* 3:473-483.

Peng L, Tepp WH, Johnson EA, Dong M (2011) Botulinum neurotoxin D uses synaptic vesicle protein SV2 and gangliosides as receptors. *PLoS Pathog* 7:e1002008.

Pestronk A, Choksi R, Blume G, Lopate G (1997) Multifocal motor neuropathy: serum IgM binding to a GM1 ganglioside-containing lipid mixture but not to GM1 alone. *Neurology* 48:1104-1106.

Pestronk A, Cornblath DR, Ilyas AA, Baba H, Quarles RH, Griffin JW, Alderson K, Adams RN (1988) A treatable multifocal motor neuropathy with antibodies to GM1 ganglioside. *Ann Neurol* 24:73-78.

Podack ER, Kolb WP, Muller-Eberhard HJ (1978) The C5b-6 complex: formation, isolation, and inhibition of its activity by lipoprotein and the S-protein of human serum. *J Immunol* 120:1841-1848.

Press R, Mata S, Lolli F, Zhu J, Andersson T, Link H (2001) Temporal profile of anti-ganglioside antibodies and their relation to clinical parameters and treatment in Guillain-Barre syndrome. *J Neurol Sci* 190:41-47.

Puga I, et al. (2012) B cell-helper neutrophils stimulate the diversification and production of immunoglobulin in the marginal zone of the spleen. *Nat Immunol* 13:170-180.

Qiu K, Lane MA, Lee KZ, Reier PJ, Fuller DD (2010) The phrenic motor nucleus in the adult mouse. *Exp Neurol* 226:254-258.

Razani B, Engelman JA, Wang XB, Schubert W, Zhang XL, Marks CB, Macaluso F, Russell RG, Li M, Pestell RG, Di VD, Hou H, Jr., Kneitz B, Lagaud G, Christ GJ, Edelmann W, Lisanti MP (2001) Caveolin-1 null mice are viable but show

evidence of hyperproliferative and vascular abnormalities. *J Biol Chem* 276:38121-38138.

Reynolds ML, Woolf CJ (1992) Terminal Schwann cells elaborate extensive processes following denervation of the motor endplate. *J Neurocytol* 21:50-66.

Riboni L, Bassi R, Conti M, Tettamanti G (1993) Metabolism of exogenous ganglioside GM1 in cultured cerebellar granule cells. The fatty acid and sphingosine moieties formed during degradation are re-used for lipid biosynthesis. *FEBS Lett* 322:257-260.

Richards DA, Guatimosim C, Rizzoli SO, Betz WJ (2003) Synaptic vesicle pools at the frog neuromuscular junction. *Neuron* 39:529-541.

Rinaldi S, Brennan KM, Goodyear CS, O'Leary C, Schiavo G, Crocker PR, Willison HJ (2009) Analysis of lectin binding to glycolipid complexes using combinatorial glycoarrays. *Glycobiology* 19:789-796.

Rinaldi S, Brennan KM, Kalna G, Walgaard C, van DP, Jacobs BC, Yu RK, Mansson JE, Goodyear CS, Willison HJ (2013) Antibodies to heteromeric glycolipid complexes in Guillain-Barre syndrome. *PLoS One* 8:e82337.

Rinaldi S, Brennan KM, Willison HJ (2010) Heteromeric glycolipid complexes as modulators of autoantibody and lectin binding. *Prog Lipid Res* 49:87-95.

Ritchie TC, Fabian RH, Choate JV, Coulter JD (1986) Axonal transport of monoclonal antibodies. *J Neurosci* 6:1177-1184.

Ritchie TC, Fabian RH, Coulter JD (1985) Axonal transport of antibodies to subcellular and protein fractions of rat brain. *Brain Res* 343:252-261.

Robitaille R (1998) Modulation of synaptic efficacy and synaptic depression by glial cells at the frog neuromuscular junction. *Neuron* 21:847-855.

Robitaille R, Jahromi BS, Charlton MP (1997) Muscarinic Ca<sup>2+</sup> responses resistant to muscarinic antagonists at perisynaptic Schwann cells of the frog neuromuscular junction. *J Physiol* 504 ( Pt 2):337-347.

Rochon D, Rouse I, Robitaille R (2001) Synapse-glia interactions at the mammalian neuromuscular junction. *J Neurosci* 21:3819-3829.

Rodrigo M, Hueso P, Cabezas JA (1987) Ganglioside composition of liver and kidney from rat after pentazocine treatment. *Comp Biochem Physiol B* 88:757-760.

Rothberg KG, Heuser JE, Donzell WC, Ying YS, Glenney JR, Anderson RG (1992) Caveolin, a protein component of caveolae membrane coats. *Cell* 68:673-682.

Rummel A, Hafner K, Mahrhold S, Darashchonak N, Holt M, Jahn R, Beermann S, Karnath T, Bigalke H, Binz T (2009) Botulinum neurotoxins C, E and F bind gangliosides via a conserved binding site prior to stimulation-dependent uptake with botulinum neurotoxin F utilising the three isoforms of SV2 as second receptor. *J Neurochem* 110:1942-1954.

- Rupp A, Cunningham ME, Yao D, Furukawa K, Willison HJ (2013) The effects of age and ganglioside composition on the rate of motor nerve terminal regeneration following antibody-mediated injury in mice. *Synapse*. 67(7):382-9
- Rupp A, Morrison I, Barrie JA, Halstead SK, Townson KH, Greenshields KN, Willison HJ (2012) Motor nerve terminal destruction and regeneration following anti-ganglioside antibody and complement-mediated injury: an in and ex vivo imaging study in the mouse. *Exp Neurol* 233:836-848.
- Salmon DA, Proschan M, Forshee R, Gargiullo P, Bleser W, Burwen DR, Cunningham F, Garman P, Greene SK, Lee GM, Vellozzi C, Yih WK, Gellin B, Lurie N (2013) Association between Guillain-Barre syndrome and influenza A (H1N1) 2009 monovalent inactivated vaccines in the USA: a meta-analysis. *Lancet* 381:1461-1468.
- Sawai S, Satoh M, Mori M, Misawa S, Sogawa K, Kazami T, Ishibashi M, Beppu M, Shibuya K, Ishige T, Sekiguchi Y, Noda K, Sato K, Matsushita K, Kodera Y, Nomura F, Kuwabara S (2014) Moesin is a possible target molecule for cytomegalovirus-related Guillain-Barre syndrome. *Neurology* 83:113-117.
- Schiavo G, Matteoli M, Montecucco C (2000) Neurotoxins affecting neuroexocytosis. *Physiol Rev* 80:717-766.
- Shahrizaila N, Yuki N (2013) Bickerstaff brainstem encephalitis and Fisher syndrome: anti-GQ1b antibody syndrome. *J Neurol Neurosurg Psychiatry* 84:576-583.
- Sharma DK, Choudhury A, Singh RD, Wheatley CL, Marks DL, Pagano RE (2003) Glycosphingolipids internalized via caveolar-related endocytosis rapidly merge with the clathrin pathway in early endosomes and form microdomains for recycling. *J Biol Chem* 278:7564-7572.
- Sheikh KA, Sun J, Liu Y, Kawai H, Crawford TO, Proia RL, Griffin JW, Schnaar RL (1999) Mice lacking complex gangliosides develop Wallerian degeneration and myelination defects. *Proc Natl Acad Sci U S A* 96:7532-7537.
- Siddiqui MR, Komarova YA, Vogel SM, Gao X, Bonini MG, Rajasingh J, Zhao YY, Brovkovich V, Malik AB (2011) Caveolin-1-eNOS signaling promotes p190RhoGAP-A nitration and endothelial permeability. *J Cell Biol* 193:841-850.
- Sigounas G, Harindranath N, Donadel G, Notkins AL (1994) Half-life of polyreactive antibodies. *J Clin Immunol* 14:134-140.
- Simons K, Gerl MJ (2010) Revitalizing membrane rafts: new tools and insights. *Nat Rev Mol Cell Biol* 11:688-699.
- Simons K, Ikonen E (1997) Functional rafts in cell membranes. *Nature* 387:569-572.
- Simons K, van Meer G (1988) Lipid sorting in epithelial cells. *Biochemistry* 27:6197-6202.
- Singer SJ, Nicolson GL (1972) The fluid mosaic model of the structure of cell membranes. *Science* 175:720-731.

- Singh RD, Puri V, Valiyaveetil JT, Marks DL, Bittman R, Pagano RE (2003) Selective caveolin-1-dependent endocytosis of glycosphingolipids. *Mol Biol Cell* 14:3254-3265.
- Sinha B, Koster D, Ruez R, Gonnord P, Bastiani M, Abankwa D, Stan RV, Butler-Browne G, Védie B, Johannes L, Morone N, Parton RG, Raposo G, Sens P, Lamaze C, Nassoy P (2011) Cells respond to mechanical stress by rapid disassembly of caveolae. *Cell* 144:402-413.
- Son YJ, Thompson WJ (1995a) Nerve sprouting in muscle is induced and guided by processes extended by Schwann cells. *Neuron* 14:133-141.
- Son YJ, Thompson WJ (1995b) Schwann cell processes guide regeneration of peripheral axons. *Neuron* 14:125-132.
- Son YJ, Trachtenberg JT, Thompson WJ (1996) Schwann cells induce and guide sprouting and reinnervation of neuromuscular junctions. *Trends Neurosci* 19:280-285.
- Song JW, Misgeld T, Kang H, Knecht S, Lu J, Cao Y, Cotman SL, Bishop DL, Lichtman JW (2008) Lysosomal activity associated with developmental axon pruning. *J Neurosci* 28:8993-9001.
- Sotelo-Silveira JR, Calliari A, Kun A, Benech JC, Sanguinetti C, Chalar C, Sotelo JR (2000) Neurofilament mRNAs are present and translated in the normal and severed sciatic nerve. *J Neurosci Res* 62:65-74.
- Soysal A, Aysal F, Caliskan B, Dogan AP, Mutluay B, Sakalli N, Baybas S, Arpacı B (2011) Clinico-electrophysiological findings and prognosis of Guillain-Barre syndrome - 10 years' experience. *Acta Neurol Scand* 123:181-186.
- Spaans F, Vredevelde JW, Morre HH, Jacobs BC, De Baets MH (2003) Dysfunction at the motor end-plate and axon membrane in Guillain-Barre syndrome: a single-fiber EMG study. *Muscle Nerve* 27:426-434.
- Stoeckel K, Schwab M, Thoenen H (1977) Role of gangliosides in the uptake and retrograde axonal transport of cholera and tetanus toxin as compared to nerve growth factor and wheat germ agglutinin. *Brain Res* 132:273-285.
- Sugiura Y, Furukawa K, Tajima O, Mii S, Honda T, Furukawa K (2005) Sensory nerve-dominant nerve degeneration and remodeling in the mutant mice lacking complex gangliosides. *Neuroscience* 135:1167-1178.
- Susuki K, Baba H, Tohyama K, Kanai K, Kuwabara S, Hirata K, Furukawa K, Furukawa K, Rasband MN, Yuki N (2007a) Gangliosides contribute to stability of paranodal junctions and ion channel clusters in myelinated nerve fibers. *Glia* 55:746-757.
- Susuki K, Nishimoto Y, Yamada M, Baba M, Ueda S, Hirata K, Yuki N (2003) Acute motor axonal neuropathy rabbit model: immune attack on nerve root axons. *Ann Neurol* 54:383-388.
- Susuki K, Rasband MN, Tohyama K, Koibuchi K, Okamoto S, Funakoshi K, Hirata K, Baba H, Yuki N (2007b) Anti-GM1 antibodies cause complement-mediated

disruption of sodium channel clusters in peripheral motor nerve fibers. *J Neurosci* 27:3956-3967.

Susuki K, Yuki N, Schafer DP, Hirata K, Zhang G, Funakoshi K, Rasband MN (2012) Dysfunction of nodes of Ranvier: a mechanism for anti-ganglioside antibody-mediated neuropathies. *Exp Neurol* 233:534-542.

Takamiya K, Yamamoto A, Furukawa K, Yamashiro S, Shin M, Okada M, Fukumoto S, Haraguchi M, Takeda N, Fujimura K, Sakae M, Kishikawa M, Shiku H, Furukawa K, Aizawa S (1996) Mice with disrupted GM2/GD2 synthase gene lack complex gangliosides but exhibit only subtle defects in their nervous system. *Proc Natl Acad Sci U S A* 93:10662-10667.

Takigawa T, Yasuda H, Kikkawa R, Shigeta Y, Saida T, Kitasato H (1995) Antibodies against GM1 ganglioside affect K<sup>+</sup> and Na<sup>+</sup> currents in isolated rat myelinated nerve fibers. *Ann Neurol* 37:436-442.

Tam CC, O'Brien SJ, Petersen I, Islam A, Hayward A, Rodrigues LC (2007) Guillain-Barre syndrome and preceding infection with campylobacter, influenza and Epstein-Barr virus in the general practice research database. *PLoS One* 2:e344.

Thomas JW (2001) Antigen-specific responses in autoimmunity and tolerance. *Immunol Res* 23:235-244.

Topp KS, Boyd BS (2006) Structure and biomechanics of peripheral nerves: nerve responses to physical stresses and implications for physical therapist practice. *Phys Ther* 86:92-109.

Townson K, Boffey J, Nicholl D, Veitch J, Bundle D, Zhang P, Samain E, Antoine T, Bernardi A, Arosio D, Sonnino S, Isaacs N, Willison HJ (2007) Solid phase immunoabsorption for therapeutic and analytical studies on neuropathy-associated anti-GM1 antibodies. *Glycobiology* 17:294-303.

Tran D, Carpentier JL, Sawano F, Gorden P, Orci L (1987) Ligands internalized through coated or noncoated invaginations follow a common intracellular pathway. *Proc Natl Acad Sci U S A* 84:7957-7961.

Trushina E, Du CJ, Parisi J, McMurray CT (2006) Neurological abnormalities in caveolin-1 knock out mice. *Behav Brain Res* 172:24-32.

Vedeler CA, Wik E, Nyland H (1997) The long-term prognosis of Guillain-Barre syndrome. Evaluation of prognostic factors including plasma exchange. *Acta Neurol Scand* 95:298-302.

Vieira P, Rajewsky K (1988) The half-lives of serum immunoglobulins in adult mice. *Eur J Immunol* 18:313-316.

Vosler PS, Brennan CS, Chen J (2008) Calpain-mediated signaling mechanisms in neuronal injury and neurodegeneration. *Mol Neurobiol* 38:78-100.

Vriesendorp FJ, Mishu B, Blaser MJ, Koski CL (1993) Serum antibodies to GM1, GD1b, peripheral nerve myelin, and *Campylobacter jejuni* in patients with

- Guillain-Barre syndrome and controls: correlation and prognosis. *Ann Neurol* 34:130-135.
- Waksman BH, Adams RD (1955) Allergic neuritis: an experimental disease of rabbits induced by the injection of peripheral nervous tissue and adjuvants. *J Exp Med* 102:213-236.
- Weerasuriya A, Mizisin AP (2011) The blood-nerve barrier: structure and functional significance. *Methods Mol Biol* 686:149-173.
- Weis J, Fine SM, David C, Savarirayan S, Sanes JR (1991) Integration site-dependent expression of a transgene reveals specialized features of cells associated with neuromuscular junctions. *J Cell Biol* 113:1385-1397.
- Wenthold RJ, Skaggs KK, Reale RR (1984) Retrograde axonal transport of antibodies to synaptic membrane components. *Brain Res* 304:162-165.
- Willison HJ (2012) The translation of the pathological findings described in humans to experimental models of acute motor axonal neuropathy. *J Peripher Nerv Syst* 17 Suppl 3:3-8.
- Willison HJ, Goodyear CS (2013) Glycolipid antigens and autoantibodies in autoimmune neuropathies. *Trends Immunol* 34:453-459.
- Willison HJ, Halstead SK, Beveridge E, Zitman FM, Greenshields KN, Morgan BP, Plomp JJ (2008) The role of complement and complement regulators in mediating motor nerve terminal injury in murine models of Guillain-Barre syndrome. *J Neuroimmunol* 201-202:172-182.
- Willison HJ, O'Hanlon GM, Paterson G, Veitch J, Wilson G, Roberts M, Tang T, Vincent A (1996) A somatically mutated human antiganglioside IgM antibody that induces experimental neuropathy in mice is encoded by the variable region heavy chain gene, V1-18. *J Clin Invest* 97:1155-1164.
- Willison HJ, Veitch J (1994) Immunoglobulin subclass distribution and binding characteristics of anti-GQ1b antibodies in Miller Fisher syndrome. *J Neuroimmunol* 50:159-165.
- Witebsky E, Rose NR, Terplan K, Paine JR, Egan RW (1957) Chronic thyroiditis and autoimmunization. *J Am Med Assoc* 164:1439-1447.
- Xu YF, Autio D, Rheuben MB, Atchison WD (2002) Impairment of synaptic vesicle exocytosis and recycling during neuromuscular weakness produced in mice by 2,4-dithiobiuret. *J Neurophysiol* 88:3243-3258.
- Yamashita T, Hashiramoto A, Haluzik M, Mizukami H, Beck S, Norton A, Kono M, Tsuji S, Daniotti JL, Werth N, Sandhoff R, Sandhoff K, Proia RL (2003) Enhanced insulin sensitivity in mice lacking ganglioside GM3. *Proc Natl Acad Sci U S A* 100:3445-3449.
- Yao D, McGonigal R, Barrie JA, Cappell J, Cunningham ME, Meehan GR, Fewou SN, Edgar JM, Rowan E, Ohmi Y, Furukawa K, Brophy PJ, Willison HJ (2014) Neuronal Expression of GalNAc Transferase Is Sufficient to Prevent the

Age-Related Neurodegenerative Phenotype of Complex Ganglioside-Deficient Mice. *J Neurosci* 34:880-891.

Yeo SS, Chang PH, Jang SH (2013) The ascending reticular activating system from pontine reticular formation to the thalamus in the human brain. *Front Hum Neurosci* 7:416.

Yoshimori T, Yamamoto A, Moriyama Y, Futai M, Tashiro Y (1991) Bafilomycin A1, a specific inhibitor of vacuolar-type H(+)-ATPase, inhibits acidification and protein degradation in lysosomes of cultured cells. *J Biol Chem* 266:17707-17712.

Yuki N, Koga M, Hirata K (1998) Isolated internal ophthalmoplegia associated with immunoglobulin G anti-GQ1b antibody. *Neurology* 51:1515-1516.

Yuki N, Kokubun N, Kuwabara S, Sekiguchi Y, Ito M, Odaka M, Hirata K, Notturmo F, Uncini A (2012) Guillain-Barre syndrome associated with normal or exaggerated tendon reflexes. *J Neurol* 259:1181-1190.

Yuki N, Kuwabara S, Koga M, Hirata K (1999) Acute motor axonal neuropathy and acute motor-sensory axonal neuropathy share a common immunological profile. *J Neurol Sci* 168:121-126.

Yuki N, Miyatake T, Ichihashi Y, Sato S, Katagiri T (1992a) IgM anti-(GalNAc beta 1-4 Gal[3-2 alpha NeuAc] beta 1-) antibody-mediated cytotoxicity in a patient with amyotrophic lateral sclerosis-like disorder. *Muscle Nerve* 15:1371-1373.

Yuki N, Sato S, Tsuji S, Hozumi I, Miyatake T (1993a) An immunologic abnormality common to Bickerstaff's brain stem encephalitis and Fisher's syndrome. *J Neurol Sci* 118:83-87.

Yuki N, Susuki K, Koga M, Nishimoto Y, Odaka M, Hirata K, Taguchi K, Miyatake T, Furukawa K, Kobata T, Yamada M (2004) Carbohydrate mimicry between human ganglioside GM1 and *Campylobacter jejuni* lipooligosaccharide causes Guillain-Barre syndrome. *Proc Natl Acad Sci U S A* 101:11404-11409.

Yuki N, Taki T, Inagaki F, Kasama T, Takahashi M, Saito K, Handa S, Miyatake T (1993b) A bacterium lipopolysaccharide that elicits Guillain-Barre syndrome has a GM1 ganglioside-like structure. *J Exp Med* 178:1771-1775.

Yuki N, Yamada M, Koga M, Odaka M, Susuki K, Tagawa Y, Ueda S, Kasama T, Ohnishi A, Hayashi S, Takahashi H, Kamijo M, Hirata K (2001) Animal model of axonal Guillain-Barre syndrome induced by sensitization with GM1 ganglioside. *Ann Neurol* 49:712-720.

Yuki N, Yoshino H, Sato S, Miyatake T (1990) Acute axonal polyneuropathy associated with anti-GM1 antibodies following *Campylobacter* enteritis. *Neurology* 40:1900-1902.

Yuki N, Yoshino H, Sato S, Shinozawa K, Miyatake T (1992b) Severe acute axonal form of Guillain-Barre syndrome associated with IgG anti-GD1a antibodies. *Muscle Nerve* 15:899-903.

Zhang Y, Bekku Y, Dzhashiashvili Y, Armenti S, Meng X, Sasaki Y, Milbrandt J, Salzer JL (2012) Assembly and maintenance of nodes of ranvier rely on distinct sources of proteins and targeting mechanisms. *Neuron* 73:92-107.

Zhu X, Meng G, Dickinson BL, Li X, Mizoguchi E, Miao L, Wang Y, Robert C, Wu B, Smith PD, Lencer WI, Blumberg RS (2001) MHC class I-related neonatal Fc receptor for IgG is functionally expressed in monocytes, intestinal macrophages, and dendritic cells. *J Immunol* 166:3266-3276.

Zitman FM, Todorov B, Verschuuren JJ, Jacobs BC, Furukawa K, Furukawa K, Willison HJ, Plomp JJ (2011a) Neuromuscular synaptic transmission in aged ganglioside-deficient mice. *Neurobiol Aging* 32:157-167.

Zitman FMP, Greenshields KN, Kuijf ML, Ueda M, Kaida KI, Broos LAM, Tio-Gillen AP, Jacobs BC, Kusunoki S, Willison HJ, Plomp JJ (2011b) Neuropathophysiological potential of Guillain-Barré syndrome anti-ganglioside-complex antibodies at mouse motor nerve terminals. *Clinical and Experimental Neuroimmunology* 2:59-67.

Zuckier LS, Rodriguez LD, Scharff MD (1989) Immunologic and pharmacologic concepts of monoclonal antibodies. *Semin Nucl Med* 19:166-186.

Zuo Y, Lubischer JL, Kang H, Tian L, Mikesh M, Marks A, Scofield VL, Maika S, Newman C, Krieg P, Thompson WJ (2004) Fluorescent proteins expressed in mouse transgenic lines mark subsets of glia, neurons, macrophages, and dendritic cells for vital examination. *J Neurosci* 24:10999-11009.